UNIVERSITÀ DEGLI STUDI DI TRIESTE

XXX CICLO DEL DOTTORATO DI RICERCA IN AMBIENTE E VITA

TRANSCRIPTOMICS AND METABARCODING APPROACHES FOR THE STUDY OF LICHEN SYMBIONTS

Settore scientifico-disciplinare: BIO/18 GENETICA

DOTTORANDA
ELISA BANCHI

COORDINATORE
PROF. GIORGIO ALBERTI

SUPERVISORE DI TESI
PROF. ALBERTO PALLAVICINI

CO-SUPERVISORE DI TESI
DR. SSA LUCIA MUGGIA

CO-SUPERVISORE DI TESI
PROF. MAURO TRETIACH

ANNO ACCADEMICO 2016/2017

To my family and Giorgio, my wonderwall.

Disinterested love for all living creatures,
the most noble attribute of man.
Charles Darwin

LIST OF CONTENT

RIASSUNTO

La mia ricerca si è concentrata su due principali aspetti della simbiosi lichenica: la caratterizzazione delle risposte allo stress in fotobionti lichenici e la diversità fungina presente all'interno del tallo.

Per lo studio dei meccanismi molecolari che sottendono alla tolleranza allo stress è stata analizzata una specie del genere più comune di alghe verdi lichenizzate, *Trebouxia gelatinosa*. I licheni possono far fronte a condizioni ambientali estreme e questa capacità è legata alla loro tolleranza al disseccamento, in particolare a quella dei fotobionti. In natura il tallo lichenico è continuamente sottoposto a cicli di disidratazione e reidratazione e nello stato disseccato è estremamente resistente. Il trascrittoma di *T. gelatinosa* è stato sequenziato e studiato in condizioni di controllo, nello stato disidratato e dopo la reidratazione. La disidratazione e la reidratazione hanno influenzato principalmente l'espressione genica di componenti dell'apparato fotosintetico, il sistema di scavenging delle specie reattive dell'ossigeno (ROS), le heat shock proteins (HSPs) e le desiccation related proteins (DRPs). I dati ottenuti sono stati utilizzati per indagare nel dettaglio la relazione tra l'espressione di geni di interesse e parametri fisiologici, importante per comprendere la risposta globale di *T. gelatinosa* agli stress ambientali. Sono stati analizzati sia lo stress ossidativo che il disseccamento. L'attività antiossidante del fotobionte è stata studiata tramite la quantificazione dell'espressione genica di enzimi ROS scavenging e correlati allo stress in campioni trattati con perossido di idrogeno (H_2O_2). I dati prodotti sono stati valutati in relazione all'analisi della fluorescenza della clorofilla a (Chl_aF). I trattamenti con H_2O_2 hanno prodotto effetti ossidativi dipendenti sia dalla dose che dal tempo di esposizione. È stata anche studiata l'espressione genica in relazione al contenuto di acqua cellulare durante la disidratazione. Il contenuto idrico relativo (RWC) e il potenziale idrico (Ψ) sono stati monitorati nella transizione tra stato idratato e disseccato. Il momento chiave che innesca il cambiamento nella trascrizione genica in *T. gelatinosa* è stato individuato nella perdita di turgore cellulare.

I licheni, poichè ospitano nei loro talli comunità fungine complesse formate da specie con strategie trofiche ed ecologiche divergenti, possono essere considerati micro-nicchie ecologiche. La complessità e la diversità dei micobiomi lichenici sono ancora in gran parte sconosciute, nonostante l'applicazione di approcci combinati di isolamenti e sequenziamenti ad alta resa (HTS). In questa ricerca è stata valutata la composizione tassonomica, tramite HTS della regione barcode ITS2, di una comunità di licheni epilitici alpini che comprendeva sia talli sintomaticamente infetti da funghi lichenicoli che talli privi di sintomi di infezione. La componente principale dei micobiomi osservati è rappresentata dall'ordine Chaetothyriales, mentre i basidiomiceti sono stati registrati in quantità ridotta. Sono state predette sequenze rappresentative di funghi lichenicoli morfologicamente caratterizzati e utilizzate per rilevarne la presenza asintomatica in altri talli.

ABSTRACT

This research has focused on two main aspects of lichen symbioses: the characterization of stress responses in lichen photobionts and the fungal diversity present inside the lichen thallus.

The study of the molecular mechanisms that underlie the stress tolerance considered a member of the most common genus of lichenized green algae, *Trebouxia gelatinosa*. Lichens can cope with extreme environmental conditions and this capacity is linked to the desiccation tolerance, in particular of their associated photobionts. In nature, lichen thalli continuously undergo cycles of dehydration and rehydration and in desiccated states they are extremely resistant. A transcriptome analysis on *T. gelatinosa* was performed under control conditions, in desiccated state and after rehydration. Desiccation and rehydration affected mainly the gene expression of components of the photosynthetic apparatus, the ROS-scavenging system, heat shock proteins (HSPs) and desiccation related proteins (DRPs). The obtained data were used to investigate in more detail the relationship between the expression of genes of interest and physiological parameters, important to understand the global response of *T. gelatinosa* under environmental stresses. Oxidative stress and desiccation were considered.

The antioxidant activity of the photobiont was studied by quantifying the gene expression of ROS scavenging and stress-related enzymes on samples treated with hydrogen peroxide (H_2O_2). The data produced have been evaluated in relation to the chlorophyll a fluorescence (Chl_aF) activity. H_2O_2 treatments produced dose and time dependent oxidative effects. The gene expression in dependence to the cell water content during desiccation was also evaluated. From the hydrated to the desiccated state, both relative water content (RWC) and water potential (Ψ) were monitored. The turgor loss point was found as a key moment that triggered changes in gene transcription.

Lichens are regarded as ecological microniches as their thalli harbor complex fungal communities (mycobiota) consisting of species with divergent trophic and ecological strategies. Complexity and diversity of lichen mycobiomes are still largely unknown, despite surveys combining culture-based and high throughput sequencing (HTS) have been applied. This research assessed the taxonomic composition (species diversity) of a well-characterized, alpine rock lichen community which included both thalli symptomatically infected by lichenicolous fungi and asymptomatic thalli. Taxonomic composition was assessed by HTS of the ITS2 barcode. Chaetothyriales was the major component of the observed lichen mycobiomes; Basidiomycota were recorded in the least amount. Sequences representative of morphologically characterized lichenicolous fungi were predicted and were used to assess whether there was an asymptomatic presence of these taxa in other thalli.

INTRODUCTION

The lichen symbioses

Lichens are symbiotic organisms, traditionally recognized as composed of a fungal partner, the mycobiont, and one or more populations of photosynthetic partners, the photobionts (Nash, 2008; Hawksworth and Honegger, 1994). Though, more recent investigations have highlighted the presence of bacteria and other fungi likely playing metabolic, key roles in the symbioses (Grube et al., 2009, 2015; Spribille et al., 2016). More than 90% of the 14,000 lichenized fungal species is represented by ascomycete (Eriksson et al., 2006); the mycobiont usually constitutes the majority (about 90%) of the biomass in the lichen body, the thallus (Dimijian et al., 2000). The photosynthetic partners (about 150 species described so far) are populations of green algae (85% of the lichens), cyanobacteria (10%), or even both (4%) can be part in the symbioses (tripartite lichens, Ahmadjian, 1993; Honegger, 2009).

The interdependent relationship between the two major symbionts is the basis of lichenization, which is required for both mycobiont and photobiont to preserve each other and receive mutual advantages (Ahmadjian, 1993; Wang et al., 2014), even if a predominant role of the fungal part has been proposed (Ahmadjian, 1993). In the thallus, the fungus receives photosynthetic products (carbohydrates) produced by the photobiont: green algal photobionts provide acyclic sugar alcohols (polyols) like ribitol and sorbitol, that are absorbed and used by the fungus as energy source (Richardson et al., 1967; Honegger, 1997). On the other hand, the fungal partner offers to the photosynthetic partner protection from the external environment, and provides water, moisture and nutrients (Nash, 2008). Green algal photobionts, whose cells are usually closely enveloped by the fungal hyphae, are protected from different biotic and abiotic stresses, such as drought, intense light radiations and mechanical damages (Wang et al., 2014).

Lichens are also ecologically important organisms; they present a remarkable biodiversity in terms of colors, forms, sizes, and biochemistry. They have a global distribution: over 10% of terrestrial ecosystems is dominated by lichens (Honegger, 2009). They are pioneers on bare rock, lava flows, cleared soil, and dead wood (Dimijian et al., 2000); they are also typically found in high alpine, polar, and desert habitats, where vascular plants cannot grow due to physiological limitations (Honegger, 2009).

Most of lichens are desiccation tolerant (DT, Kranner et al., 2008). Desiccation tolerance is the capacity of an organism to survive and recover metabolic activities even if its relative water content (RWC) decreases below 10%, corresponding to 0.1 g H_20 g^{-1} of dry mass (Farrant et al., 2012). Desiccation tolerance is a rare feature that appears in different animal and plant unrelated taxa

(Alpert, 2006), and usually occurs in organisms which colonize substrates or environments with little and unpredictable water availability (Berjak et al., 2006; Nardini et al., 2013). Despite numerous studies have been conducted (see Jenks and Wood, 2007 and Lüttge et al., 2011), the molecular mechanisms of this peculiar feature are still mostly unknown, especially in understudied organisms such as lichens.

The lichen thallus is devoid of any structure, such as stomata or cuticles, that allows a regulation of the water content (WC). As in poikilohydric (from the Greek "poikilo", meaning varied) organisms, the WC of lichens depends completely from the atmosphere; thalli can use different liquid water sources including rain, air humidity, fog, and dew (Büdel and Lange, 1991; Alpert et al., 2000; Lakatos, 2011).

During the day, the lichen thalli undergo cycles of dehydration and rehydration that can last even for few minutes (Alpert et al., 2000). In desiccated state, when they are metabolically inactive, most of lichens are highly resistant to environmental stresses (Dimijian et al., 2000) and can cope with severe conditions. Numerous field and laboratory studies have been conducted to test lichen responses to extreme environments (Gomez et al., 2012). Among them, desiccation (e. g. Lange et al., 2001; Candotto Carniel et al., 2015; Bertuzzi et al., 2017), oxidative stress (Kong et al., 1999; Català et al., 2010; del Hoyo et al., 2011), extreme temperatures, UV radiation and vacuum exposure (Bartàk et al., 2007). Lichens showed a remarkable resistance also in outer space (de la Torre et al., 2010) and Mars-like conditions (Brandt et al., 2015).

Despite the numerous studies, however, the ultrastructural, molecular and physiological bases that underlie the extraordinary capacity of lichen to tolerate environmental stresses are still not clarified.

Molecular characterization of stress responses in the lichen photobiont Trebouxia gelatinosa

The first part of my Ph.D. has focused on the characterization of stress responses in a representative lichen photobiont, the green alga *Trebouxia gelatinosa*. High-throughput-omic technologies, gene expression analysis and physiological parameters were combined in order to understand the global response of this species. Since photobionts, due to their photosynthetic activities, are more sensitive to environmental stresses and in general can be easily grown in cultures, studies on these organisms are the first step to understand the overall lichen response.

The genus *Trebouxia* belongs to the order Trebouxiales (Chlorophyta), which has been referred to as the "lichen algae group" (Leliaert et al., 2012). *Trebouxia* is the most common genus of lichenized algae, occurring in more than 50% of all lichen species (Ahmadjian, 1993). All

Trebouxias (c. 30 species; Friedl, 1989) are DT, and the mechanisms of their desiccation tolerance have not been entirely understood yet.

Beside lichens, green microalgae such as *Trebouxia* can be found on different substrates forming microfilms on soil, rocks, leaves, tree bark, and man-made substrata (Häubner et al., 2006; Lüttge and Büdel, 2010).

Trebouxia genus has long been investigated (Ahmadjian, 1960), and most of the studies has focused on taxonomy and ecophysiology (see Muggia et al., 2016a for a review). Researches on environmental stress responses and desiccation tolerance have also been conducted (Bačkor et al., 2006; Gasulla et al., 2009; del Hoyo et al., 2011; Sánchez et al., 2014; Candotto Carniel et al., 2015; Petruzzellis et al., 2017), but its molecular characterization is far form be completed.

The first work presented in this thesis is entitled "New features of desiccation tolerance in the lichen photobiont *Trebouxia gelatinosa* are revealed by a transcriptomic approach" (Candotto Carniel et al., 2016). Here, the first complete transcriptome of *T. gelatinosa* has been studied and changes in the gene expression have been analyzed in relation to dehydration and rehydration. Transcriptomics belongs to the high-throughput-omic technologies, of which the main purpose is the characterization and the quantification of the set of biological molecules which shape structures, functions and dynamics of cells and organisms (Simò et al., 2014). The transcriptome is the complete set of messenger RNA (mRNA) molecules generated by an organism in a given developmental stage or physiological condition (Wang et al., 2009). The main purpose in transcriptomics is to obtain a profile of global gene expression in relation to some conditions of interest (van der Spoel et al., 2015). In lichenology, transcriptomics has been mainly applied to study *i)* gene expression changes during the frequent drying and rewetting cycles experienced by lichens as poikilohydric organisms (Junttila and Rudd, 2012; Junttila et al., 2013), and *ii)* the air pollution tolerance (Nurhani et al., 2013).

From this first analysis, it emerged that *T. gelatinosa* mostly relies on constitutive mechanisms, but also inducible mechanisms play a role in its desiccation tolerance. Dehydration and rehydration affected mainly the gene expression of components of the photosynthetic apparatus, the ROS-scavenging system, heat shock proteins (HSPs) and desiccation related proteins (DRPs). With the purpose to understand the global response of *T. gelatinosa* under environmental stresses, the data acquired were further used to investigate in more detail the relationship between the expression of genes and physiological parameters in this species.

In this perspective, in the second work presented, "Relation between water status and desiccation-affected genes in the lichen photobiont *Trebouxia gelatinosa*" (Banchi et al., under

review), I assessed the gene expression in dependence to the cell water status during desiccation. Both the relative water content (RWC) and water potential (Ψ) were monitored during the transition from the hydrated into the desiccated state.

In the study on lichens and their symbionts, the water status is usually evaluated by RWC (Lange et al., 2007; Hartard et al., 2009), which prevents the discrimination of extra- and intracellular water loss. For this reason, Ψ was also considered, as it is used to assess the water status in terms of potential energy per unit volume. Ψ measurements are less applied because they are time-consuming and require dedicated laboratory equipment, but are essential for a precise description of the desiccation process (Nardini et al., 2013). Moreover, Ψ_{tlp} (the Ψ at which cells lose their turgor) was also assessed by the construction of pressure-volume (PV) curves (Tyree and Jarvis, 1982). Cell turgor loss, in fact, is considered the best indicator of water stress (McDowell, 2011; Dinakar et al., 2016). To date, few studies have been carried out on the turgor loss response in DT non-vascular plants such as green algae (Holzinger and Karsten, 2013), and an estimation of Ψ in relation to water status is important to understand if and how this feature is involved in desiccation tolerance of these organisms.

Regarding *Trebouxia*, a single work was performed considering both Ψ and RWC, showing that, at metabolomic level, water status mainly affects cell wall, extracellular polysaccharides (EPS), polyols, and antioxidant protection (Centeno et al., 2016).

Once that the water status of *T. gelatinosa* at different time points during desiccation was finely assessed by physiological parameters, my study aimed at identifying how water status triggered changes in the expression of stress- and desiccation-related genes. This was used to determine which were the key moments that activate the response of these important groups during water loss.

The third work presented, entitled "Effects of Graphene-Based Materials on the aeroterrestrial microalga *Trebouxia gelatinosa*: focus on internalization and oxidative stress" (Montagner et al., under review) aimed at detecting the effects that an exposure of Graphene-Based Materials (GBMs) and of the oxidant molecule hydrogen peroxide (H_2O_2) have on *T. gelatinosa*.

GBMs belong to the wide group of carbon-based nanomaterials and are widely researched (Novoselov et al., 2012) because of their potentials in the most diverse fields, such as electronics and biomedicine (Lalwani et al., 2016). Despite huge investments and wide applications at industrial level, the impact of GBMs on health and environment is not still clearly defined (Savolainen et al., 2013).

We tried to understand antioxidant activity of *T. gelatinosa* by quantifying the gene expression of ROS scavenging and stress-related enzymes on samples treated with two different GMBs and

different concentrations of H_2O_2. The data were evaluated in relation to the chlorophyll a fluorescence (Chl_aF), which was taken as a measure of photosynthetic activity. This is considered a proxy of cell vitality and is commonly applied in lichen and lichen symbionts studies, including *Trebouxia* (Tretiach et al., 2007; del Hoyo et al., 2011; Piccotto et al., 2011; Hájek et al., 2012). GBMs interaction with *T. gelatinosa* cell wall and their possible internalization were also investigated by the application of Confocal Laser Scanning Microscopy (CLSM) and Raman spectroscopy.

Fungal diversity within lichen thalli

The second part of my Ph.D. focused on the application of high-throughput-omic technologies for the characterization of lichen-associated fungi.

Under an ecological perspective, lichens can be regarded as miniature ecosystems or microniches (Nash, 2008), as their thalli harbor and are associated with complex bacterial and fungal communities, consisting of species with divergent trophic and ecological strategies (Arnold et al., 2009; Grube et al., 2009, 2015; Muggia and Grube, 2010; U'Ren et al., 2012; Muggia et al., 2016b; Spribille et al., 2016; Fernandez-Mendoza et al., 2017; Moya et al., 2017). In particular, lichen-inhabiting fungi are a successful and diversified ecological group of organisms. They have been distinguished into lichenicolous (Lawrey and Diederich, 2003) and endolichenic fungi (Arnold et al., 2009). Lichenicolous fungi, of which about 1800 species have been phenotypically described (Lawrey and Diederich, 2003; www.lichenicolous.net), colonize the lichen thalli symptomatically, showing characteristic phenotypes or reproductive structures and expressing different degrees of specificity and virulence towards their hosts. Endolichenic fungi occur asymptomatically inside the host thalli (Arnold et al., 2009; U'Ren et al., 2010, 2012), and their presence can be detected only through culture-based and molecular techniques.

Despite the application of surveys using different approaches including microscopy, cultures, and molecular analyses, the complexity and the diversity of lichen microbiomes and mycobiomes are still largely unknown.

For this reason, in the fourth part of this thesis, "ITS2 metabarcoding analysis complements data of lichen mycobiomes" (Banchi et al., under review), the fungal diversity present inside lichens of a well characterized alpine rock-dwelling community (Fleischhacker et al., 2015; Muggia et al., 2016b, 2017; Fernández-Mendoza et al., 2017) was studied. Lichen samples included both thalli symptomatically infected by lichenicolous fungi and uninfected thalli; fungal diversity and taxonomic composition was assessed by DNA metabarcoding, a particular application of metagenomics.

Metagenomics is the sequencing of the total DNA extracted from an environmental sample, which may contain many different organisms (Bohmann et al., 2014). Nowadays these massive sequencing efforts are feasible by the implementation of a high throughput sequencing (HTS) supported by next generation sequencing (NGS) technologies. They allow the automated identification of the species present in an environmental sample (Taberlet et al., 2012) and they are an important tool for understanding evolutionary history, functional and ecological biodiversity (Shokralla et al., 2012). The sequencing targets either a species-specific region in the genome, the so called 'DNA barcode' (Hebert et al., 2003; Taberlet et al., 2012), for taxonomic purposes, or the whole genome. DNA metabarcoding, in particular, combines NGS/HTS and the classical DNA barcoding.

In lichenology, these approaches allowed the exploration of lichen thalli as ecological niches, revealing the organization of complex symbiotic communities and, potentially, the presence of coherent patterns. The majority of the metagenomic studies on lichens refers to their associated bacteria (Sigurbjornsdottir et al., 2015; Grube et al., 2015; Cernava et al., 2017), but researches have extended also to the intrathalline fungal (U'Ren et al., 2012; Park et al. 2014; Fernández-Mendoza et al., 2017) and algal diversity (Moya et al., 2017).

Here, the taxonomic diversity of lichen-associated fungi was assessed targeting the ITS2 region as barcode, and special attention was driven to the identification of new fungal sequences potentially corresponding to lichenicolous fungi. The results were compared, in terms of amount and variation of shared, new, and missing taxa with data previously obtained by the analysis of the ITS1 region (Fernández-Mendoza et al., 2017).

Appendix I: DNA metabarcoding uncovers fungal diversity of mixed airborne samples

In my Ph.D., I applied DNA metabarcoding also to the study of fungi outside the lichen symbiosis. The work included in the Appendix I presents the results of a study entitled "DNA metabarcoding uncovers fungal diversity of mixed airborne samples" (Banchi et al., under review). The aim of the survey was to asses, by DNA metabarcoding, the fungal diversity present in airborne samples used for environmental and human health monitoring, which are routinely analyzed only by microscopical inspection. For this analysis, the ITS2 fungal barcode was sequenced, and the results compared with those obtained by microscopy analyses, with special focus to the identification of plant and human pathogenic taxa and alien invasive species.

REFERENCES

Ahmadjian V. (1960) Some new and interesting species of *Trebouxia*, a genus of lichenized algae. *Am. J. Bot.* 47: 677-683.

Ahmadjian, V. (1993). The lichen symbiosis. John Wiley & Sons.

Alpert P. (2000) The discovery, scope, and puzzle of desiccation tolerance in plants. *Plant Ecol.* 151(1): 5-17.

Alpert P. (2006) Constraints of tolerance: why are desiccation-tolerant organisms so small or rare? *J. Exp. Biol.* 209(9): 1575-1584.

Arnold AE, Miadlikowska J, Higgins KL, et al. (2009) A phylogenetic estimation of trophic transition networks for ascomycetous fungi: are lichens cradles of symbiotrophic fungal diversification? *Syst. Biol.* 58: 283-297.

Bačkor M, Gibalová A, Bud'ová J, et al. (2006) Cadmium-induced stimulation of stress-protein hsp70 in lichen photobiont *Trebouxia erici*. *Plant growth regul.* 50(2-3): 159-164.

Barták M, Váczi P, Hájek J, Smykla J. (2007) Low-temperature limitation of primary photosynthetic processes in Antarctic lichens *Umbilicaria antarctica* and *Xanthoria elegans*. *Polar Biol.* 31(1): 47-51.

Berjak P. (2006) Unifying perspectives of some mechanisms basic to desiccation tolerance across life forms. *Seed Sci. Res.* 16(1): 1-15.

Bertuzzi S, Pellegrini E, Candotto Carniel F, et al. (2017) Ozone and desiccation tolerance in chlorolichens are intimately connected: a case study based on two species with different ecology. *Environ. Sci. Pollut. Res*. 1-15.

Bohmann K, Evansn A, Gilbert MTP, et al. (2014) Environmental DNA for wildlife biology and biodiversity monitoring. *Trends Ecol. Evol.* 29(6): 358-367.

Brandt A, de Vera JP, Onofri S, Ott S. (2015) Viability of the lichen *Xanthoria elegans* and its symbionts after 18 months of space exposure and simulated Mars conditions on the ISS. *Int. J. Astrobiology* 14(3): 411-425.

Büdel B and Lange OL. (1991) Water status of green and blue-green phycobionts in lichen thalli after hydration by water vapor uptake: do they become turgid? *Plant Biol.* 104(5): 361-366.

Candotto Carniel F, Zanelli D, Bertuzzi S, Tretiach M. (2015) Desiccation tolerance and lichenization: a case study with the aeroterrestrial microalga *Trebouxia sp*. (Chlorophyta). *Planta* 242: 493-505.

Candotto Carniel F, Gerdol M, Montagner A, et al. (2016) New features of desiccation tolerance in the lichen photobiont *Trebouxia gelatinosa* are revealed by a transcriptomic approach. *Plant Mol. Biol.* 91(3): 319-339.

Catalá M, Gasulla F, del Real AEP, et al. (2010) Fungal-associated NO is involved in the regulation of oxidative stress during rehydration in lichen symbiosis. *BMC microbiol.* 10(1): 297.

Centeno DC, Hell AF, Braga MR, et al. (2016) Contrasting strategies used by lichen microalgae to cope with desiccation–rehydration stress revealed by metabolite profiling and cell wall analysis. *Environ. Microbiol.* 18(5): 1546-1560.

Cernava T, Erlacher A, Aschenbrenner IA, et al. (2017) Deciphering functional diversification within the lichen microbiota by meta-omics. *Microbiome* 5(1): 82.

de La Torre R, Sancho LG, Horneck G, et al. (2010) Survival of lichens and bacteria exposed to outer space conditions–Results of the Lithopanspermia experiments. *Icarus* 208(2): 735-748.

del Hoyo A, Álvarez R, del Campo EM, et al. (2011) Oxidative stress induces distinct physiological responses in the two *Trebouxia* phycobionts of the lichen *Ramalina farinacea. Ann. Bot.* 107: 109-18.

Dimijian GG. (2000) Evolving together: the biology of symbiosis, part 1. *Proc (Bayl Univ Med Cent)* 13(3): 217.

Dinakar C, Puthur JT, Bartels D. (2016) Surviving metabolic arrest: photosynthesis during desiccation and rehydration in resurrection plants. *Ann. N. Y. Acad. Sci.* 1365(1): 89-99.

Eriksson OE. (2006) Outline of Ascomycota. *Myconet* 12: 1-82.

Farrant JM, Cooper K, Nell H. (2012) Desiccation tolerance. In Plant stress physiology. CABI.

Fernández-Mendoza F, Fleischhacker A, Kopun T, et al. (2017) ITS1 metabarcoding highlights low specificity of lichen mycobiomes at a local scale. *Mol. Ecol.* doi:10.1111/mec.14244.

Fleischhacker A, Grube M, Kopun T, et al. (2015) Community analyses uncover high diversity of lichenicolous fungi in alpine habitats. *Microbial Ecol.* 70: 348-360.

Friedl T. (1989) Comparative ultrastructure of pyrenoids in *Trebouxia* (Microthamniales, Chlorophyta). *Plant Syst. Evol.* 164: 145-159.

Gasulla F, de Nova PG, Esteban-Carrasco A, et al. (2009) Dehydration rate and time of desiccation affect recovery of the lichenic algae *Trebouxia erici*: alternative and classical protective mechanisms. *Planta* 231: 195-208.

Gomez F, Barták M, Bell EM. (2012) Extreme environments on earth as analogues for life on other planets: astrobiology. In Life at extremes; environments, organisms and strategies for survival. CABI.

Grube M, Cardinale M, de Castro Jr JV, et al. (2009) Species-specific structural and functional diversity of bacterial communities in lichen symbioses. *ISME J.* 3: 1105.

Grube M, Cernava T, Soh J et al. (2015) Exploring functional contexts of symbiotic sustain within lichen-associated bacteria by comparative omics. *ISME J.* 9: 412.

Hájek J, Váczi P, Barták M, Jahnová L. (2012) Interspecific differences in cryoresistance of lichen symbiotic algae of genus *Trebouxia* assessed by cell viability and chlorophyll fluorescence. *Cryobiol.* 64(3): 215-222.

Hartard B, Cuntz M, Máguas C, Lakatos M. (2009) Water isotopes in desiccating lichens. *Planta* 231: 179-193.

Häubner N, Schumann R, Karsten U. (2006) Aeroterrestrial microalgae growing in biofilms on facades—response to temperature and water stress. *Microb. Ecol.* 51(3): 285-293.

Hawksworth DL, Honegger R. (1994) The lichen thallus: a symbiotic phenotype of nutritionally specialized fungi and its response to gall producers. In Plant galls: organisms, interactions, populations. Clarendon Press.

Hebert PD, Cywinska A, Ball SL. (2003) Biological identifications through DNA barcodes. *Proc R Soc Lond B Biol Sci.* 270(1512): 313-321.

Holzinger A, Karsten U. (2013) Desiccation stress and tolerance in green algae: consequences for ultrastructure, physiological and molecular mechanisms. *Front. Plant Sci.* 4: 327.

Honegger R. (2009) Lichen-forming fungi and their photobionts. In Plant relationships. Springer Berlin Heidelberg.

Honegger R. (1997) Metabolic interactions at the mycobiont-photobiont interface in lichens. In Plant relationships. Springer Berlin Heidelberg.

Jenks MA and Wood AJ. (2008) Plant desiccation tolerance. John Wiley & Sons.

Junttila S, Laiho A, Gyenesei A, Rudd S. (2013) Whole transcriptome characterization of the effects of dehydration and rehydration on *Cladonia rangiferina*, the grey reindeer lichen. *BMC genomics* 14: 1.

Junttila S and Rudd S. (2012) Characterization of a transcriptome from a non-model organism, *Cladonia Rangiferina*, the grey reindeer lichen, using high-throughput next generation sequencing and EST sequence data. *BMC Genomics* 13: 575.

Kong FX, Hu W, Chao SY, et al. (1999) Physiological responses of the lichen *Xanthoparmelia mexicana* to oxidative stress of SO_2. *Environ. Exp. Bot*. 42(3): 201-209.

Kranner I, Beckett R, Hochman A, Nash TH III. (2008) Desiccation-tolerance in lichens: a review. *Bryologist* 111: 576-593.

Lakatos M. (2011) Lichens and bryophytes: habitats and species. In Plant desiccation tolerance. Springer Berlin Heidelberg.

Lalwani G, D'Agati M, Khan AM, Sitharaman B. (2016) Toxicology of graphene-based nanomaterials. *Adv. Drug Delivery Rev.* 105: 109-44.

Lange OL, Green TA, Heber U. (2001) Hydration-dependent photosynthetic production of lichens: what do laboratory studies tell us about field performance? *J. Exp. Bot.* 52(363): 2033-2042.

Lange OL, Green TA, Meyer A, Zellner H. (2007) Water relations and carbon dioxide exchange of epiphytic lichens in the Namib fog desert. *Flora* 202(6): 479-487.

Lawrey JD and Diederich P (2003) Lichenicolous fungi: interactions, evolution, and biodiversity. *Bryologist* 106: 80-120.

Leliaert F, Smith DR, Moreau H, et al. (2012) Phylogeny and molecular evolution of the green algae. *Crit. Rev. Plant Sci.* 31: 1-46.

Lüttge U and Büdel B. (2010) Resurrection kinetics of photosynthesis in desiccation-tolerant terrestrial green algae (Chlorophyta) on tree bark. *Plant Biol.* 12: 437-444.

Lüttge U, Beck E, Bartels D. (2011) Plant desiccation tolerance. Springer Berlin Heidelberg.

McDowell NG. (2012) Mechanisms linking drought, hydraulics, carbon metabolism, and vegetation mortality. *Plant Physiol.* 155: 1051-1059.

Moya P, Molins A, Martínez-Alberola F, et al. (2017) Unexpected associated microalgal diversity in the lichen *Ramalina farinacea* is uncovered by pyrosequencing analyses. *PloS ONE* 12:e0175091.

Muggia L, Candotto Carniel F, Grube M. (2016a). The lichen photobiont *Trebouxia*: towards and appreciation of species diversity and molecular studies. In Algal and cyanobacteria symbioses. World Scientific.

Muggia L, Fleischhacker A, Kopun T, et al. (2016b) Extremotolerant fungi from alpine rock lichens and their phylogenetic relationships. *Fungal Div.* 76: 119-142.

Muggia L and Grube M. (2010) Fungal composition of lichen thalli assessed by single strand conformation polymorphism. *Lichenologist* 42: 461-473.

Muggia L, Kopun T, Grube M. (2017) Effects of growth media on the diversity of culturable fungi from lichens. *Molecules* 22: 824.

Nardini A, Marchetto A, Tretiach M. (2013) Water relations parameters of six *Peltigera* species correlate with their habitat preferences. *Fungal. Ecol.* 6: 397-407.

Nash TH III. (2008) Lichen Biology. Cambridge University Press.

Novoselov KS, Fal'ko VI, Colombo L, et al. (2012) A roadmap for graphene. *Nature* 490: 192-200.

Nurhani ARS, Munir AMA, Wahid SM, Diba ABF. (2013) A preliminary transcriptomic analysis of lichen *Dirinaria* sp. UKM FST Postgraduate Colloquium. In Proceedings of the University Kebangsaan Malaysia. AIP Publishing.

Park CH, Kim KM, Elvebakk A, et al. (2014) Algal and fungal diversity in antarctic lichens. *J. Eukaryot. Microbiol.* 196-205.

Petruzzellis F, Savi T, Bertuzzi S. et al. (2017) *Planta* https://doi.org/10.1007/s00425-017-2814-5

Piccotto M, Bidussi M, Tretiach M. (2011) Effects of the urban environmental conditions on the chlorophyll a fluorescence emission in transplants of three ecologically distinct lichens. *Environ. Exp. Bot.* 73: 102-107.

Richardson DHS, Hill DJ, Smith DC. (1968) Lichen physiology. *New Phytol.* 67(3): 469-486.

Sánchez FJ, Meeßen J, del Carmen Ruiz M, et al. (2014) UV-C tolerance of symbiotic *Trebouxia sp*. in the space-tested lichen species *Rhizocarpon geographicum* and *Circinaria gyrosa*: role of the hydration state and cortex/screening substances. *Int. J. Astrobiology* 13(1): 1-18.

Savolainen K, Backman U, Brouwer D, et al. (2013) Nanosafety in Europe 2015-2025: towards safe and sustainable nanomaterials and nanotechnology innovations. *Finnish Institute of Occupational Health*.

Shokralla S, Spall JL, Gibson JF, Hajibabaei M. (2012) Next-generation sequencing technologies for environmental DNA research. *Mol. Ecol.* 21(8): 1794-1805.

Sigurbjornsdottir MA, Andresson OS, Vilhelmsson O. (2015) Analysis of the *Peltigera membranacea* metagenome indicates that lichen-associated bacteria are involved in phosphate solubilization. *Microbiol.* 161(5): 989-996.

Simò C, Cifuentes A, García-Cañas V. (2014) Fundamentals of advanced omics technologies: from genes to metabolites. Elsevier.

Spribille T, Tuovinen V, Resl P et al. (2016) Basidiomycete yeasts in the cortex of ascomycete macrolichens. *Science* 353: 488-492.

Taberlet P, Coissac E, Pompanon F et al. (2012) Towards next-generation biodiversity assessment using DNA metabarcoding. *Mol. Ecol.* 21: 2045-2050.

Tretiach M, Piccotto M, Baruffo L. (2007) Effects of ambient NO_x on chlorophyll a fluorescence in transplanted *Flavoparmelia caperata* (Lichen). *Environ. Sci. Technol.* 41(8): 2978-2984.

Tyree MT and Jarvis PG. (1982) Water in tissues and cells. In Physiological plant ecology II. Springer.

U'Ren JM, Lutzoni F, Miadlikowska J, et al. (2010) Community analysis reveals close affinities between endophytic and endolichenic fungi in mosses and lichens. *Microb. Ecol.* 60: 340-353.

U'Ren JM, Lutzoni F, Miadlikowska J, et al. (2012) Host and geographic structure of endophytic and endolichenic fungi at a continental scale. *Am. J. Bot.* 99: 898-914.

van der Spoel E, Rozing MP, Houwing-Duistermaat JJ, et al. (2015) Association analysis of insulin-like growth factor-1 axis parameters with survival and functional status in nonagenarians of the Leiden Longevity Study. *Aging* (7).

Wang Z, Gerstein M, Snyder M. (2009) RNA-Seq: a revolutionary tool for transcriptomics. *Nat. Rev. Genet.* 10(1): 57-63.

Wang YY, Liu B, Zhang XY, et al. (2014) Genome characteristics reveal the impact of lichenization on lichen-forming fungus *Endocarpon pusillum* Hedwig (Verrucariales, Ascomycota). *BMC Genomics* 15(1): 34.

NEW FEATURES OF DESICCATION TOLERANCE IN THE LICHEN PHOTOBIONT *TREBOUXIA GELATINOSA* ARE REVEALED BY A TRANSCRIPTOMIC APPROACH

Fabio Candotto Carniel[1,2,‡], Marco Gerdol[1,‡,*], Alice Montagner[1], **Elisa Banchi**[1], Gianluca De Moro[1], Chiara Manfrin[1], Lucia Muggia[1], Alberto Pallavicini[1], Mauro Tretiach[1]

[1] Dipartimento di Scienze della Vita, Università degli Studi di Trieste, Trieste, Italy

[2] Institute of Botany, University of Innsbruck, Innsbruck, Austria

[‡] These authors contributed equally to this work

[*] Corresponding author: Marco Gerdol

Main abbreviations

DEG: differentially expressed genes

DRP: desiccation delated proteins

DT: desiccation tolerant

DUF: domain of unknown function

EXP: expansin

FC: fold change

GO: gene ontology

HSP: heat shock protein

LEA: late embryogenesis abundant protein

MnSOD: manganese superoxide dismutase

ORF: open reading frame

PFAM: protein family

PS: photosystem

qRT-PCR: quantitative real-time PCR

ROS: reactive oxygen species

RPL6: ribosomal protein L6

TPM: transcripts per million

WC: water content

Abstract

Trebouxia is the most common lichen-forming genus of aero-terrestrial green algae and all its species are desiccation tolerant (DT). The molecular bases of this remarkable adaptation are, however, still largely unknown. We applied a transcriptomic approach to a common member of the genus, *T. gelatinosa*, to investigate the alteration of gene expression occurring after dehydration and subsequent rehydration in comparison to cells kept constantly hydrated. We sequenced, *de novo* assembled and annotated the transcriptome of axenically cultured *T. gelatinosa* by using Illumina sequencing technology. We tracked the expression profiles of over 13,000 protein-coding transcripts. During the dehydration/rehydration cycle c. 92% of the total protein-coding transcripts displayed a stable expression, suggesting that the desiccation tolerance of *T. gelatinosa* mostly relies on constitutive mechanisms. Dehydration and rehydration affected mainly the gene expression for components of the photosynthetic apparatus, the ROS-scavenging system, Heat Shock Proteins, aquaporins, expansins, and Desiccation Related Proteins (DRPs), which are highly diversified in *T. gelatinosa*, whereas Late Embryogenesis Abundant Proteins were not affected. Only some of these phenomena were previously observed in other DT green algae, bryophytes and resurrection plants, other traits being distinctive of *T. gelatinosa*, and perhaps related to its symbiotic lifestyle. Finally, the phylogenetic inference extended to DRPs of other chlorophytes, embryophytes and bacteria clearly pointed out that DRPs of chlorophytes are not orthologous to those of embryophytes: some of them were likely acquired through horizontal gene transfer from extremophile bacteria which live in symbiosis within the lichen thallus.

Key Message: we investigated the gene expression patterns in *Trebouxia gelatinosa* subjected to dehydration and rehydration. This species relies on both constitutive and inducible mechanisms to cope with desiccation.

Key words: aero-terrestrial microalgae; Desiccation Related Proteins; gene expression; Illumina; lichenization; Trebouxiophyceae

Introduction

Poikilohydric organisms are able to colonize very harsh environments, such as hot and cold deserts, rock surfaces or tree barks, thanks to their ability to survive extreme desiccation states and to recover full metabolic activity within minutes to hours upon rewetting (Lidén et al. 2010). This ability is

commonly known as desiccation tolerance. It is documented in cyanobacteria (Büdel 2011), aeroterrestrial micro-algae (Trainor and Gladych 1995; Holzinger and Karsten 2013), intertidal algae (Büdel 2011), bryophytes (Richardson and Richardson 1981; Proctor 1990; Proctor et al. 2007), lichens (Mazur 1968; Kranner et al. 2008), and a few vascular plants, the so-called resurrection plants (Proctor and Tuba 2002). It also occurs among heterotrophs, such as tardigrades (Wright 2001), nematodes (Treonis and Wall 2005), and arthropods (Kikawada et al. 2005). This capability may be extended to the whole life cycle of the organism, or it may involve just some stages, as it happens in flowering plants, whose pollen grains and seeds are frequently desiccation tolerant (DT) (Hoekstra et al. 2001).

The desiccation tolerance in photo-autotrophic organisms involves several essential adaptations to withstand the anatomical, physiological and biochemical alterations caused by water loss. The recent comparative studies on DT vs. desiccation sensitive species allowed to identify the most important of these adaptations, which are: (*i*) the accumulation of non-reducing sugars (sucrose, trehalose, etc.) and Late Embryogenesis Abundant proteins (LEAs) which help to preserve the correct protein conformation and to avoid membrane fusion by replacing hydrogen bonds between water and other molecules (Hoekstra et al. 2001; Yobi et al. 2013); (*ii*) the production of molecular chaperones, such as Heat Shock Proteins (HSPs), to aid the correct refolding of proteins upon rehydration (Gechev et al. 2013; Oliver et al. 2009); (*iii*) the production of antioxidant substances (e.g. ascorbic acid, glutathione, etc.) and ROS scavenging enzymes, to maintain the intracellular redox homeostasis (Kranner et al. 2002; 2008); (*iv*) the involvement of mechanisms, such as the activity of expansins, to allow a safe cell shrinkage upon turgor-loss (Jones and McQueen-Mason 2004).

The analysis of transcriptome, proteome and metabolome have brought important advantages in the study of desiccation tolerance in phototrophic organisms, especially resurrection plants (Collett et al. 2003; Collett et al. 2004; Le et al. 2007; Rodriguez et al. 2010; Gechev et al. 2013; Mitra et al. 2013; Lyall et al. 2014; Ma et al. 2015), seeds (Farrant and Moore 2011; Maia et al. 2014), and mosses (Oliver et al. 2004; Oliver et al. 2009; Stark and Brinda 2015). The development of the so-called second-generation sequencing technologies, which allow to collect a very large amount of data in a single analysis, has extended the transcriptomic approach to non-model vascular plants (Wang et al. 2010; Fu et al. 2011; Garg et al. 2011), non-vascular plants (Xiao et al. 2011; Gao et al. 2015) and terrestrial algae. In particular, for the latter group, Holzinger et al. (2014) analysed the gene expression profile induced by dehydration in *Klebsormidium crenulatum*, a representative of Streptophytes, i.e. the ancestors of the land plants that were among the first organisms to colonize lands from aquatic environments (Becker 2013; Hori et al. 2014). Also Chlorophytes, the sister group of Streptophytes, experienced the transition to land. In some cases, as in some Trebouxiophyceae,

this passage led to the adoption of a symbiotic lifestyle. The most successful, in terms of both habitat extension and irradiative speciation, is lichenization, i.e. the capability of forming a stable extracellular symbiosis between one or more autotrophs (in this case green algae) and one heterotroph (fungi, mostly ascomycetes) (Lipnicki 2015). Intimately connected to this success was the acquisition of desiccation tolerance mechanisms, because lichens are *de facto* the prevailing organisms (in terms of biomass and species diversity) in several terrestrial macro- and micro-habitats where water is available in scarce and unpredictable quantities and/or soil is virtually absent (Nardini et al. 2013). Unfortunately, our knowledge on the desiccation tolerance mechanisms of lichen-forming algae is relatively poor, and they have never been investigated through a transcriptomic approach, notwithstanding some attempts made in the most recent years. Junttila and Rudd (2012), for instance, characterized the transcriptome of a lichen, *Cladonia rangiferina,* and bioinformatically assigned the expressed mRNAs either to the myco- or to the photobiont based on the comparison with sequence datasets obtained from separate axenic cultures. Later Junttila et al. (2013) also studied the effects of dehydration and rehydration on gene expression in the same lichen species. They discovered that these processes affect the expression of hundreds of genes, especially those related to short-chain and alcohol dehydrogenases, molecular chaperones and transporters. On the other hand, in the first and sole proteomic study on the desiccation tolerance of a lichen photobiont, the green alga *Asterochloris erici*, Gasulla et al. (2013) showed that this ability is mostly related to constitutive mechanisms, since only 11 and 13 proteins involved in glycolysis, cellular protection cytoskeleton, cell-cycle and targeting and degradation were up-regulated after dehydration and rehydration, respectively.

In this study we describe the *de novo* assembly of the first complete transcriptome of the axenically cultured lichen photobiont *Trebouxia gelatinosa* Archibald (Trebouxiophyceae, Chlorophyta), chosen as a member of the most widespread genus of lichenized algae. *Trebouxia* Puymaly is present in about half of the estimated 15,000 chlorolichens known so far, and therefore it is the most common aeroterrestrial micro-algal genus worldwide (Ahmadjian 2004). As in the lichen symbiosis, free-living *Trebouxia* spp. can withstand dehydrations to water contents below 10% of their dry weight, long periods in the desiccated conditions and recover metabolic activity within minutes upon rehydration (Kosugi et al. 2009; Candotto Carniel et al. 2015). The variation of gene expression profiles was studied in cultures kept fully hydrated, slowly dehydrated and subsequently rehydrated, with the aim of unravelling the key molecular processes involved in desiccation tolerance of lichen photobionts.

Materials and methods

Culture isolation of *Trebouxia* photobiont

Isolates of *T. gelatinosa* were obtained according to Yamamoto et al. (2002) from thalli of *Flavoparmelia caperata* (L.) Hale, collected in the Classic Karst plateau (NW Italy; 45°42'24.54"N; 13°45'21.70"E). The isolates were inoculated in sterile plastic tubes filled with c. 5 ml of slanted solid *Trebouxia* medium (TM) (1.5 % agar) (Ahmadjian 1973). The tubes were kept in a thermostatic chamber at 20 °C, under a light regime of 18□2 μmol photons m^{-2} sec^{-1} with a photoperiod of 14 h:10 h, light:dark until the colony reached a sufficient biomass. Cultures were re-inoculated every 30 days and were grown at the same conditions as the original inocula. The identity of the photobiont was checked by sequencing the nuclear ITS fragment (data available upon request) and by analysing the pyrenoid ultrastructure by TEM. Reference algal material was cryo-conserved according to Dahmen et al. (1983) and is available upon request.

Dehydration and rehydration treatments

Algal cultures were grown on hand-cut sterile filter paper discs (Whatman, 60±5 g m^{-2}, diam. 25 mm), laid on solid TM (1.5 % agar) inside Petri dishes. In each Petri dish four discs were inoculated with 100 μl of a water suspension of 3.5×10^6 cells mL^{-1}. The Petri dishes were kept in a thermostatic chamber at the same controlled condition described above. On the 30^{th} day of growth three discs representing the control samples (C) were randomly selected from the starting set of Petri dishes and promptly soaked in liquid nitrogen and stored at -80 °C. Six discs were slowly dehydrated on a thin layer of solid TM in a biological hood under air flow; complete dehydration took 10 hours. The time necessary to obtain a water content (WC, see below) of 0.1g H_2O g^{-1} DW was assessed in a preliminary experiment by following the weight loss of the discs with a precision balance.

After dehydration, three discs representing dehydrated samples (D), were soaked in liquid nitrogen and stored at -80 °C. The remaining three discs were wetted with a water drop and laid on solid TM inside a Petri dish for 12 hours to allow the full rehydration of the algae at the same, original growth conditions. After rehydration, the three discs representing rehydrated samples (R) were frozen in liquid nitrogen and stored at -80 °C.

The water content (WC) was measured on a different set of samples grown over acetate-cellulose discs at the same conditions. The cultures were harvested from the discs, weighed, freeze-dried and then weighed again. The WC of cultures was calculated as $(FW_t - DW)/DW \times 100$, where FW_t is the sample weight after each treatment (t: C, D, R) and DW is the sample weight after a freeze-drying of 72 h. The WC of the samples was 4.92 (C), 0.10 (D), 4.35 (R) g H_2O g^{-1} DW, respectively.

RNA sequencing and *de novo* transcriptome assembly

Total RNA was extracted from the frozen culture discs, each one comprising c. 40 mg DW algal colonies, accounting for several millions *T. gelatinosa* individuals, using the PowerPlant® RNA Isolation Kit (MO BIO Laboratories, Inc.). RNA quality was assessed with Agilent 2100 Bioanalyzer (Agilent Technologies). All samples achieved a RNA Integrity Number > 8 and the absence of RNA degradation in dehydrated samples was further evaluated, in a later stage, by an analysis of the 3' to 5' sequencing coverage drop on a subset of transcripts longer than 10 Kb (Online Resource 1). The RNA extracted from the three replicates prepared for each sample (C, D and R) were pooled together in equimolar quantities. The preparation of cDNA libraries and RNA-sequencing were carried out at the Institute of Applied Genomics (IGA) in Udine, Italy. Sequencing was performed on a single lane of an Illumina HiSeq2000 instrument, with a 100 cycles paired-end sequencing protocol. Raw sequencing reads were trimmed according to their base calling quality before proceeding with further analyses. Trimmed reads shorter than 60 bp were discarded.

Trimmed reads were used for a *de novo* transcriptome assembly by Trinity (Grabherr et al. 2011), selecting the Jaccard-clip option to allow the splitting of chimeric contigs resulting from overlapping genes. Minimum allowed contig length was set at 201 bp. The complete assembly obtained, containing the transcript variants produced from each of the predicted gene models, was processed as follows, prior to the annotation and gene expression analysis steps. Only the longest transcript of each gene was selected in order to reduce sequence redundancy and to obtain a set of transcripts suitable for a gene expression analysis. A minimum threshold of the mean coverage was set to discard all low quality transcripts which cumulatively contributed to the back mapping of just the 2 % of the reads (including poorly expressed and highly fragmented transcripts).

Contigs resulting from mitochondrial and plastidial mRNAs or from ribosomal RNA were detected by BLASTn search (Altschul et al. 1990) based on the Trebouxiophyceae sp. MX-AZ01 plastidial (GenBank: NC_018569) and mitochondrial (GenBank: NC_018568) genomes, and on the *Trebouxia arboricola* 5.8S, 18S and 26S rRNA genes (GenBank: Z68705.1) available at public databases. Matching sequences (e-value cut off = $1x10^{-30}$) were discarded prior to further analyses.

The entire RNA-seq experiment was deposited at the NCBI Sequence Read Archive database (SRA accessions: SRX330016 (C), SRX330011 (D) and SRX330015 (R); Bioproject: PRJNA213702).

Transcripts annotation and ORFeome definition

To overcome the technical issues linked with the high compactness of *T. gelatinosa* genome (see *infra*), in the non-redundant reference transcriptome we identified all the regions corresponding to Open Reading Frames (ORFs). ORFs were predicted based on their protein-coding potential, assessed

either by a significant BLASTx similarity (e-value cutoff $1x10^{-5}$) with the available complete proteomes of other Trebouxiophyceae, namely *Coccomyxa subellipsoidea* C-169 (v2.0, http://genome.jgi.doe.gov/Coc_C169_1/), *Chlorella variabilis* (v1.0, http://genome.jgi.doe.gov/ChlNC64A_1/) or *Asterochloris* sp. Cgr/Dha1pho (v.1.0, http://genome.jgi.doe.gov/Astpho1/), by the presence of PFAM domains (e-value cutoff $1x10^{-5}$) or by a length of at least 300 codons (if none of the previous criteria were met).

The resulting ORFs sequences were extracted from the assembled contigs and annotated with the Trinotate pipeline. Sequence similarities were identified by BLASTx (Altschul et al. 1990) performed against the UniProtKB/Swiss-Prot database; functional domains were detected by a HMMER (Finn et al. 2011) search against the PFAM domain database (Punta et al. 2012). ORFeome were also annotated based on eggNOG (Powell et al. 2012) and Gene Ontology (Ashburner et al. 2000) 'biological process', 'molecular function' and 'cellular component' functional categories. These annotations were automatically extracted from BLASTx matches and linked to the corresponding assembled transcripts by Trinotate.

The presence of orthologous sequences in the genomes of other representative Viridiplantae was assessed by reciprocal best BLASTp matches, comparing the proteins predicted from the *T. gelatinosa* transcriptome to the proteins encoded by those genomes. The e-value and identity cut-off used to consider two sequences as orthologous were set to $1x10^{-5}$ and 35%, respectively.

The selected species comprised the three Trebouxiophyceae mentioned above (*C. subellipsoidea*, *C. variabilis* and *Asterochloris* sp.), *Chlamydomonas reinhardtii* (v.4.0, http://genome.jgi.doe.gov/chlamy/), *Volvox carteri* (v.1.0, http://genome.jgi.doe.gov/Volca1/), *Klebsormidium flaccidum* (ASM70883v1), *Selaginella moellendorffii* (v.1.0, http://genome.jgi.doe.gov/Selmo1/), *Micromonas pusilla* (v.2.0, http://genome.jgi.doe.gov/MicpuC2/), *Ostreococcus tauri* (v.2.0, http://genome.jgi.doe.gov/Ostta4/), *Zea mays* (B73 RefGen_v3) and *Arabidopsis thaliana* (TAIR10).

Gene expression analysis

Trimmed reads obtained from the sequencing of the three samples (C, D and R *T. gelatinosa* cultures) were mapped on the annotated ORFeome with the RNA-seq tool included in the CLC Genomics Workbench v.8.0. Length and similarity fractions parameters were set to 0.75 and 0.95, respectively; the maximum number of matching contigs was set to 10. Paired reads distance was assumed, based on fragment length data, to be comprised between 100 and 500 bp.

We calculated gene expression levels as Transcript Per Million (TPM), a measure of RNA abundance which takes into account both transcript length and sequencing depth for normalization, thus being

proportional to the relative molar RNA concentration (Wagner et al. 2012). TPM values were used for the differential expression analysis using a Kal's Z-test on proportions (Kal et al. 1999) in the following comparisons: a) D vs C samples; b) R vs D samples; c) R vs C samples. Differentially expressed genes (DEGs) were identified with a False Discovery Rate-corrected p-value lower than 0.01, applied according to the Benjamini and Hochberg procedure (1995), and a proportions fold change (FC) value higher than 2 for up-regulated genes, or lower than -2 for down-regulated genes. TPM gene expression values were transformed by $\log_2$ for the graphical representation in the scatter plot.

Gene Ontology terms, PFAM domains and eggNOG functional categories over-represented in the subsets of differentially expressed genes were detected with a hypergeometric test on annotations. The sets of up-regulated and down-regulated genes were analysed separately. Significant over-representation was detected at p-value < 0.01 and observed - expected > 3. The over-representation of annotations displaying p-values lower than $1x10^{-5}$ was considered highly significant.

qRT-PCR analysis

To further validate the expression profiles obtained with RNA-seq and to take into account biological variation across replicates, a qRT-PCR analysis was carried out on the three non-pooled samples for each experimental condition (C, D and R), targeting six representative differentially expressed transcripts. Primers were designed with Primer3Plus (Untergasser et al. 2007) (Online Resource 2). For this analysis, cDNA was synthesized using the iScript cDNA synthesis kit (Bio-Rad).

Each reaction was performed in three technical replicates in a mix containing 1 µl cDNA (1:10 template dilution), 8 µl SSOAdvanced™ SYBR® Green Supermix (Bio-Rad) and 200 nM of each primer. The PCR amplifications were performed with CFX 96™ Real-Time PCR System (Bio-Rad) using the following cycle: 98 °C for 30' and 40 cycles at 95 °C for 10'and 60 °C for 20'. A melting curve analysis (65 °C to 95 °C, increment 0.5 °C each 5') was performed to verify the absence of non-specific amplification products. Transcript levels were calculated with Bio-Rad CFX Manager software, based on the comparative Ct method ($2^{-\Delta\Delta C_T}$ method) (Livak and Schmittgen 2001) and normalizing gene expression data using as housekeeping genes two transcripts showing steady expression levels in our RNA-seq experiment and frequently used for this purpose in literature: the ribosomal protein L6 (RPL6) and the translation elongation factor 1 beta (EF1b).

Phylogenetic analysis of Desiccation Related Proteins (DRPs)

Proteins pertaining to the Desiccation Related Proteins family (DRPs) predicted from *T. gelatinosa* and other 45 representative species of green algae, embryophytes and bacteria (Online Resource 3)

were aligned with MUSCLE (Edgar 2004) and the resulting alignment was trimmed to remove highly divergent and poorly informative regions with Gblocks v.0.91b (Castresana 2000). The Bayesian inference phylogenetic analysis was performed with MrBayes 3.2 (Ronquist et al. 2012) under a GTR+G+I model, identified by ProtTest 3.1 (Abascal et al. 2005) as the best-fitting our data, with two parallel runs with four chains each, for 1 million generations. Trees were sampled each 1,000 generations; a 25% burnin was adopted and the convergence of the analysis was reassured by a standard deviation of split frequencies lower than 0.01. Nodes with low statistical support (posterior probability < 0.5) were collapsed in the graphical tree representation.

Results

High throughput sequencing, *de novo* assembly and annotation of *T. gelatinosa* transcriptome

The output of the Illumina paired-end sequencing of the *T. gelatinosa* samples is summarized in Table 1. The overall *de novo* transcriptome assembly generated 19,601 contigs, with almost null sequence redundancy (Table 2).

Table 1 Sequencing and trimming statistics of *Trebouxia gelatinosa* transcriptomic analysis.

	Reads number	Average length (bp)	Sequenced data (Gbp)
Raw data			
Control	60,409,470	100	6.0
Dehydrated	92,783,850	100	9.3
Rehydrated	90,569,258	100	9.1
Total	243,762,578	100	24.4
After trimming			
Control	58,604,069	97.6	5.7
Dehydrated	90,464,518	97.6	8.8
Rehydrated	88,336,044	97.6	8.6
Total	237,404,631	97.6	23.0

Table 2 *De novo* assembly and annotation statistics of *Trebouxia gelatinosa* transcriptomic analysis.

Number of non-redundant assembled contigs	19,601
Total number of ORFs identified	13,648
Average contig length	1,605 nt
Contigs N50	3,594
Contigs longer than 5 Kb	1,261
Longest assembled contig	31,749 nt
Number of residual chimeric contigs*	3,509
Mapping rate** (contigs)	82.49%
Average ORF length	1,261 nt
Longest ORF	26,346 nt
Mapping rate** (ORFs)	47.17%
Sequence redundancy (non-specific matches)	0.57%
ORFs with BLAST matches (UniProtKB/SwissProt)	7,311 (53.6%)
ORFs with PFAM annotation	7,976 (58.4%)
ORFs with eggNOG annotation	5,941 (45.5%)
ORFs with Gene Ontology Cellular Component annotation	5,725 (41.9%)
ORFs with Gene Ontology Biological Process annotation	5,497 (40.3%)
ORFs with Gene Ontology Molecular Function annotation	5,576 (40.9%)

*chimeric contigs are identified as those comprising more than one ORF (Open Reading Frame). ** Mapping rate is defined as the percentage of reads that match contigs or ORFs with the CLC Genomic Workbench RNA-seq tool, based on 0.75 and 0.95 length and similarity fraction parameters. N50: this value is calculated by summing the lengths of the longest contigs until 50% of the total assembly length is reached. The minimum contig length in this set of contigs is the number that is usually used to report the N50 value of a *de novo* assembly.

The genomes of Trebouxiophyceae are highly compact with a relevant number of overlapping genes potentially leading to the *de novo* assembly of chimeric contigs (see Discussion section for details). This genomic peculiarity contributed to the generation of a high number of chimeric contigs in the assembly process of *T. gelatinosa* transcriptome (Online Resource 4). Non-directional sequencing reads originating from overlapping exons of different transcripts, either encoded by genes on the same or on the opposite DNA strand, were assembled *de facto* as belonging to a common transcript, generating chimeric contigs with multiple Open Reading Frames (ORFs). Despite the use of the

Jaccard-clip option of the Trinity assembler, we estimate that almost 2,000 assembled contigs included multiple transcripts originated from genes spatially close to each other (Online Resource 4). We therefore relied on predicted ORFs (see Materials and Methods) for the downstream gene expression analysis. Overall, we identified and annotated 13,648 ORFs, which likely correspond to c. 10,000 protein-coding genes. This set of protein-coding sequences is available as a multiFASTA file in Online Resource 5. This number is not far from those observed in the complete genome of other Trebouxiophyceae (Table 3), suggesting that the coverage applied in our RNA-sequencing was adequate to obtain a nearly-complete collection of *T. gelatinosa* transcripts.

Table 3 Number of three *Trebouxiophyceae* predicted protein models showing significant similarity (tBLASTn vs genome, cutoff =$1E^{-5}$) with *Trebouxia gelatinosa* and percentage.

	Total	similar to *T. gelatinosa*	Ratio (%)
Asterochloris sp.	7,159	6,233	87.1
Chlorella variabilis	9,791	7,426	75.8
Coccomyxa subellipsoidea	9,629	7,173	75.1

Overall, the *de novo* assembled transcriptome potentially provides a good reference for large-scale comparative analyses within Viridiplantae, as we could detect over 3,000 *bona fide* orthologous sequences even in largely divergent model vascular plants (Online Resource 6).

The annotation process permitted to assign a putative function to about 60% of the ORFs, due to the presence of conserved functional domains or significant BLAST similarity to proteins with known function deposited in the UniProtKB sequence database (Table 2).

Global effect of the dehydration/rehydration cycle on the transcriptional profiles

During the dehydration/rehydration cycle 12,533 protein-coding transcripts (91.83 % of the total) displayed a stable expression level (Fig. 1, group 5 in Online Resource 7), whereas 112 genes (0.82 % of the total) were perturbed in both processes (groups 1, 3, 7 and 9 in Online Resources 7, 8). Both dehydration and rehydration modified the gene expression of *T. gelatinosa*, with a perturbation of 7.01 % and 2.22 % of all genes respectively, with a more prominent effect triggered by dehydration (Fig. 1).

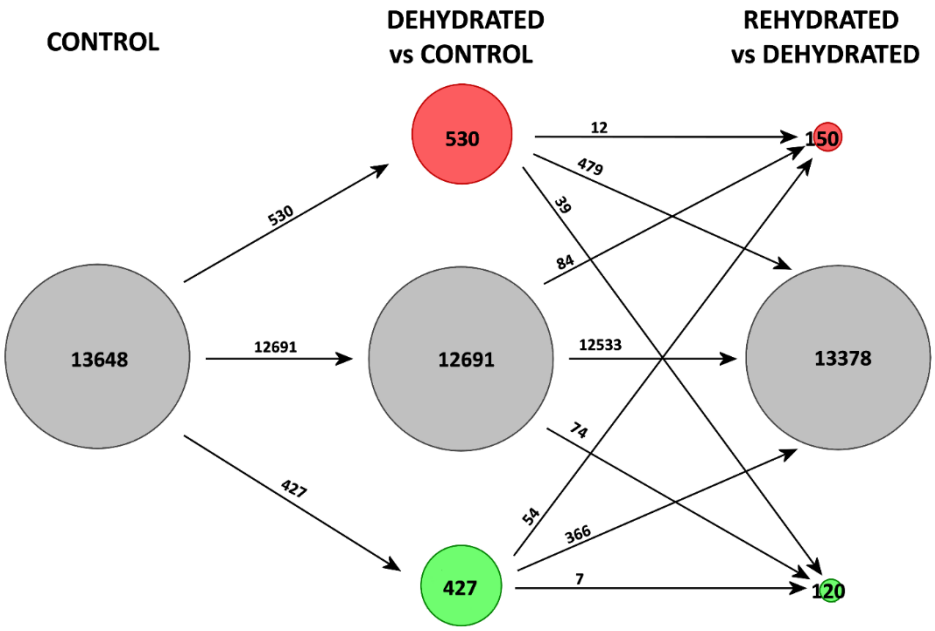

Fig. 1 Diagrams displaying the number of stable (grey), up-regulated (red) and down-regulated (green) transcripts in the dehydrated vs control and rehydrated vs dehydrated comparisons. The numbers displayed on the arrows indicate the number of transcripts. See Online Resources 7 and 8 for details.

The Kal's Z-test revealed 957 DEGs following dehydration: 530 DEGs were up-regulated and 427 down-regulated (Fig. 1 and Online Resource 9) *versus* the C sample. In R samples, 270 DEGs were identified, 150 genes being up-regulated and 120 down-regulated (Fig. 1 and Online Resource 9) *versus* the D sample. A significant overlap of gene expression profiles between D and R samples was observed (Fig. 2).

Fig. 2 Principal Component Analysis and Hierarchical Clustering of control, dehydrated and rehydrated samples of *Trebouxia gelatinosa*. Principal Component Analysis based on TPM expression values (a), Hierarchical Clustering based on Euclidean distance and average linkage on TPM, with the gradient colour scheme where blue and red stand for high or low expression levels respectively (b).

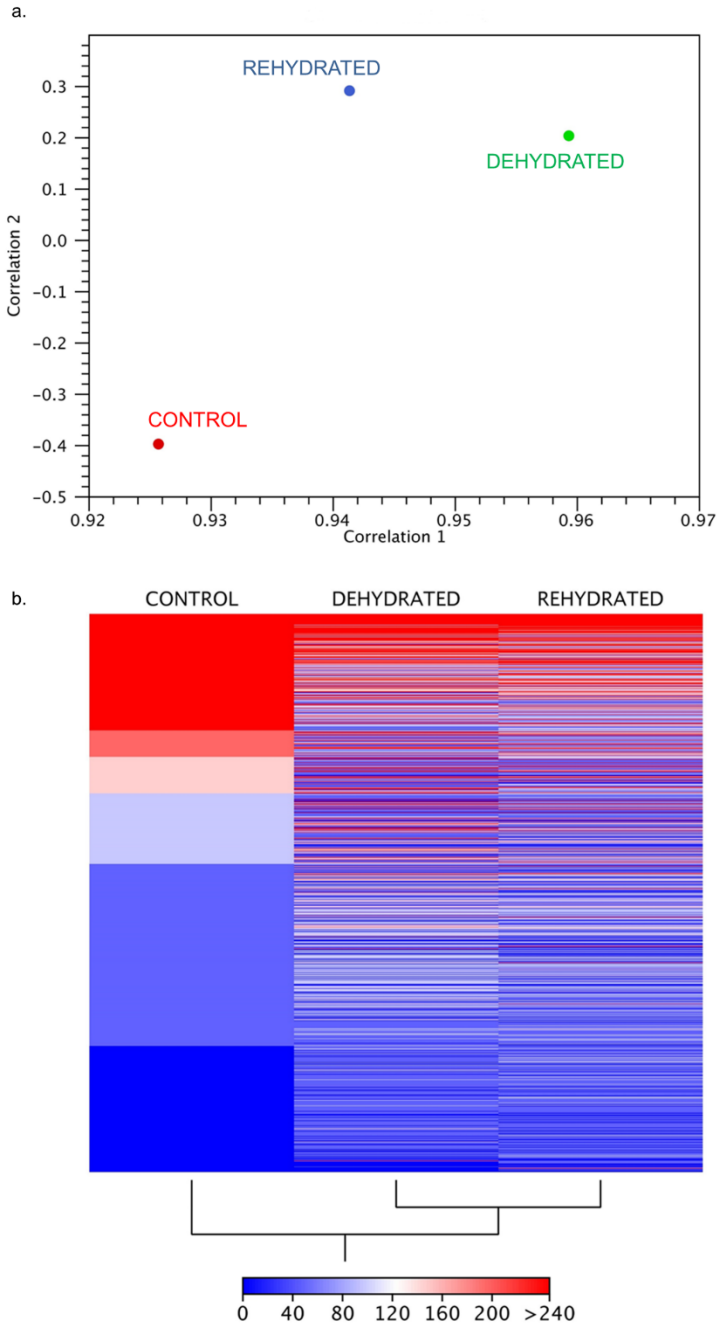

Compared to the control, 1,208 protein-coding genes were differentially expressed upon rehydration (Online Resource 9). Some genes, in particular during dehydration, experienced a highly significant induction by up to 100 folds (Online Resource 10).

qRT-PCR data validation

We confirmed the gene expression changes observed in the RNA-seq experiment by qRT-PCR, which was performed on the three non-pooled samples for each experimental condition (C, D and R). The trends of expression of all the genes analysed were consistent, with a Pearson correlation index of 0.77 (F-test of linear regression p-value = 0.01) (Fig. 3), although the FC values varied to some extent between qRT-PCR and RNA-Seq and among replicates. This slight discrepancy is compatible with the technical limitations and the differences of the two methodological approaches (SEQC/MAQC-III Consortium 2014).

Fig. 3 Comparison between the fold change of six differently expressed transcripts: Desiccation Related Protein 5 (DRP 5), Expansin 1 (EXP1), Expansin 2 (EXP2), Photosystem II (PSII), Heat Shock Protein 20 (HSP20) and Heat Shock Protein 90 (HSP90) obtained with RNA-seq (on three pooled biological replicates) and with qRT-PCR (on the three non-pooled biological replicates) in dehydrated (D) and rehydrated (R) samples of *Trebouxia gelatinosa*. Results of RT-PCR are given as the mean ±SD of three technical replicates.

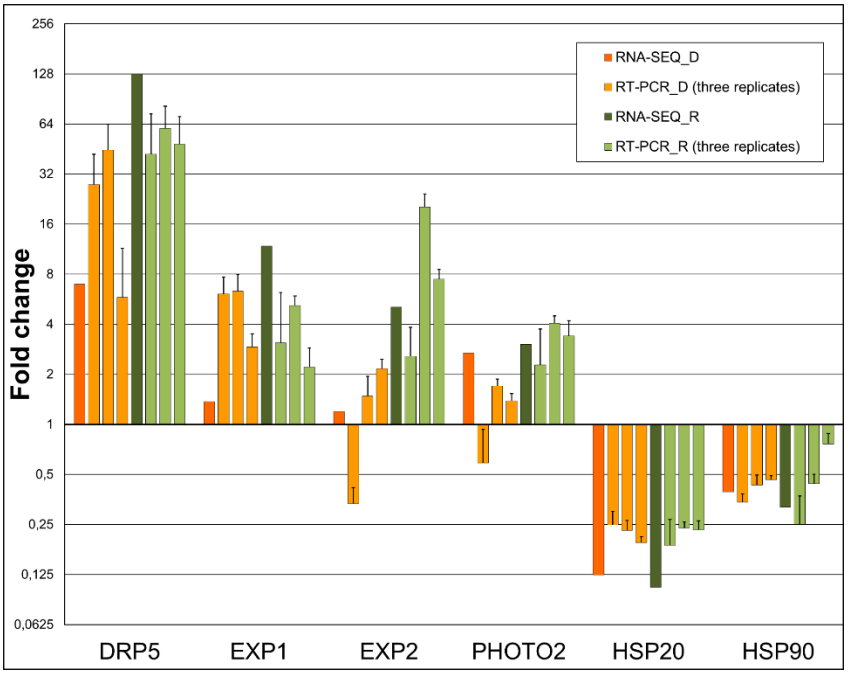

Gene set enrichment analysis

The information gathered from the annotation of the predicted gene models was used for the identification of the main gene categories influenced by dehydration and by the following rehydration. The eggNOG assignments, Gene Ontology (GO) terms and PFAM domains over-represented in each gene set are shown in Table 4 (D vs C and R vs D comparisons) and Online Resource 11 (R vs C comparison).

The GO terms related to the photosynthetic apparatus stand out as the largest group of up-regulated genes in response to dehydration. The GO terms with the best p-value score in the hypergeometric

test were light-harvesting complex (GO:0009765), chlorophyll binding (GO:0016168), PSI (GO:0009522), and PSII (GO:0009523). The 70% and 52% of the genes encoding for structural components of PSI and PSII, respectively, were strongly over-expressed, together with five out of the five detected genes encoding for components of the PSI reaction centre, chlorophyll a/b binding proteins and their transcriptional regulator Tbc2. The massive up-regulation of the photosynthetic machinery is graphically summarized in Fig. 4, according to the "photosynthesis" and "photosynthesis - antenna proteins" KEGG reference pathways (Kanehisa and Goto, 2000).

Fig. 4 Summary of the gene expression alterations which concern the photosynthetic machinery observed during dehydration. The KEGG reference pathway maps from "photosynthesis" and "photosynthesis - antenna proteins" are displayed. The genes involved are grouped in boxes below the figures and are coloured based on up- or down-regulation. Due to their very small size (< 100 aa) and high sequence divergence between the reference organism (*Arabidopsis thaliana*) and *T. gelatinosa*, several orthologous components, indicated by a gray colour, could not be identified.

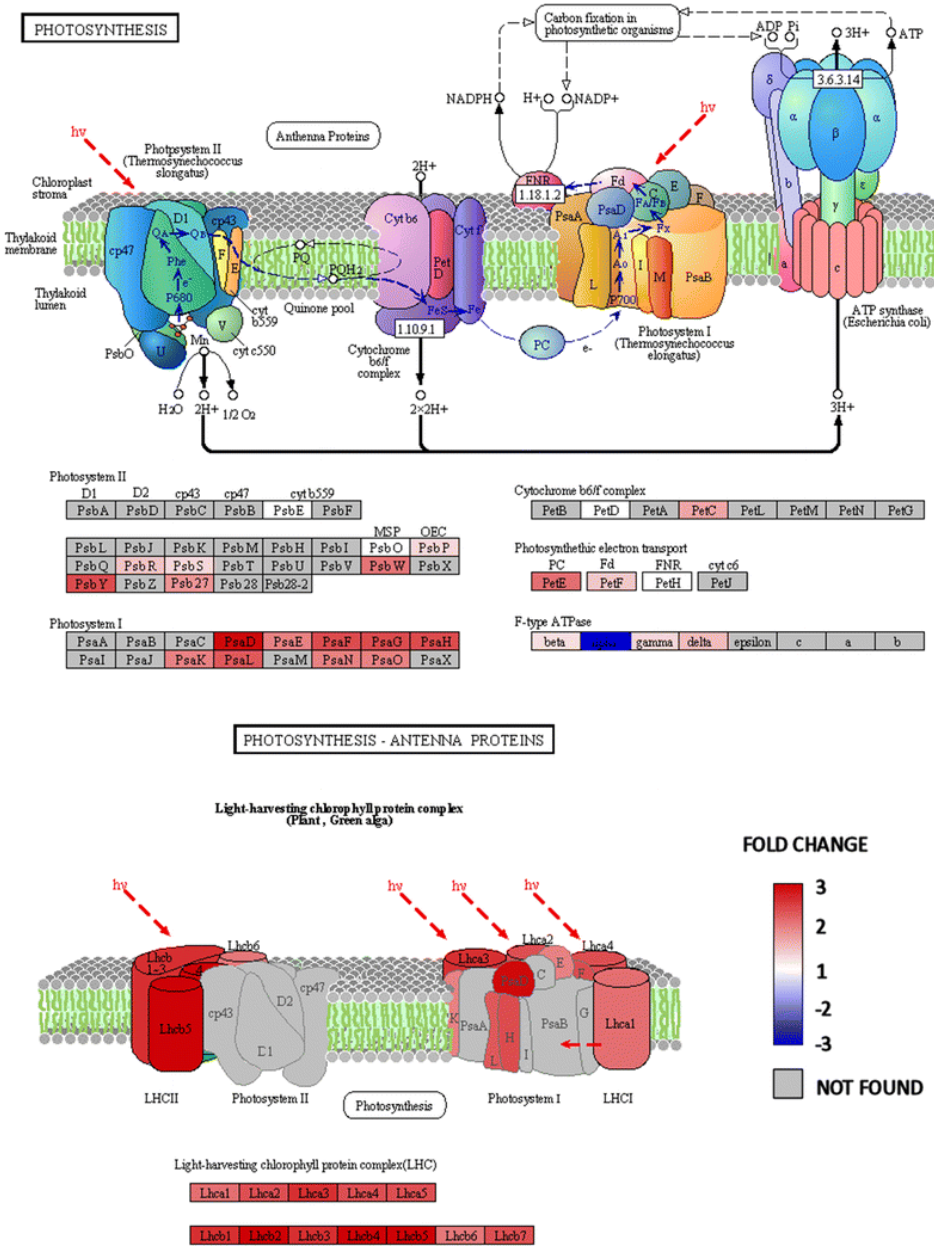

The Major Intrinsic Protein family (PF00230 and COG0580) was also significantly up-regulated upon dehydration; the five over expressed members of this protein family were all TIP (Tonoplast Intrinsic Proteins) or PIP (Plasma membrane Intrinsic Proteins) aquaporins. A remarkable protein family whose expression was induced by dehydration was MAPEG (Membrane-associated, eicosanoid/glutathione metabolism, PF01124), with three out of its four members being glutathione S-transferases. Another large class of enzymes induced by dehydration was represented by a series of short chain dehydrogenases with various functions (PF00106 and COG1029) with their associated domains (PF01370, PF08659) which include, among the others, two dihydroflavonol-4-reductases (DFRs). The ferritin-like domain (PF13668) was the most up-regulated Protein Family term and a highly significant p-value in the hypergeometric test, with seven out of thirteen genes up-regulated by the dehydration process (Table 4).

Table 4 Summary of the hypergeometric tests on annotations performed on the *Trebouxia gelatinosa* sets of differentially expressed genes in the dehydrated vs control and rehydrated vs dehydrated comparisons. *: significant; **: highly significant.

Category	ID	Description	P-value	Proportion
Dehydrated vs Control				
Up-regulated				
eggNOG	COG0580	Glycerol uptake facilitator and related permeases	3.91E-4*	4/9
eggNOG	COG1028	Dehydrogenases with different specificities	1.38E-3*	8/50
GO_BP	GO:0009765	photosynthesis, light harvesting	2.72E-14**	14/21
GO_BP	GO:0018298	protein-chromophore linkage	3.67E-12**	14/27
GO_BP	GO:0015979	photosynthesis	1.13E-5*	11/47
GO_BP	GO:0009736	cytokinin mediated signaling pathway	9.32E-4*	4/10
GO_BP	GO:0005975	carbohydrate metabolic process	1.09E-3*	10/65
GO_BP	GO:0006950	response to stress	4.39E-3*	10/78
GO_CC	GO:0009522	photosystem I	2.22E-16**	16/23
GO_CC	GO:0009523	photosystem II	3.87E-12**	14/27
GO_CC	GO:0009535	chloroplast thylakoid membrane	2.66E-10**	28/146
GO_CC	GO:0009538	photosystem I reaction center	2.75E-7**	5/5
GO_CC	GO:0016021	integral to membrane	8.95E-6**	96/1319
GO_CC	GO:0009543	chloroplast thylakoid lumen	5.31E-5*	8/29
GO_CC	GO:0009505	plant-type cell wall	9.95E-5*	5/11
GO_CC	GO:0005615	extracellular space	4.46E-3*	5/23
GO_MF	GO:0016168	chlorophyll binding	1.55E-15**	15/23
GO_MF	GO:0008242	omega peptidase activity	2.51E-4*	4/8
GO_MF	GO:0043169	cation binding	4.27E-3*	7/46
PFAM	PF00504	Chlorophyll A-B binding protein	7.48E-11**	14/32
PFAM	PF13668	Ferritin-like domain	1.61E-6**	7/14
PFAM	PF01124	MAPEG family	5.63E-6**	4/4
PFAM	PF00134	Cyclin, N-terminal domain	5.60E-5*	5/10
PFAM	PF00230	Major intrinsic protein	1.62E-4*	5/12
PFAM	PF01370	NAD dependent epimerase/dehydratase family	3.20E-4*	9/46
PFAM	PF00106	short chain dehydrogenase	3.55E-4*	13/89
PFAM	PF00168	C2 domain	3.81E-4*	6/21
PFAM	PF13561	Enoyl-(Acyl carrier protein) reductase	4.41E-4*	10/58
PFAM	PF08659	KR domain	2.47E-3*	10/72
Down-regulated				
GO_BP	GO:0006950	response to stress	1.14E-5*	12/78

GO_BP	GO:0009408	response to heat	1.38E-5*	10/55
GO_BP	GO:0016485	protein processing	2.42E-4*	4/10
GO_CC	GO:0005886	plasma membrane	6.14E-4*	33/575
GO_CC	GO:0000502	proteasome complex	2.41E-3*	5/30
GO_CC	GO:0009706	chloroplast inner membrane	7.70E-3*	5/39
GO_MF	GO:0017111	nucleoside-triphosphatase activity	3.35E-3*	7/61
GO_MF	GO:0043565	sequence-specific DNA binding	6.40E-3*	5/37
PFAM	PF00012	Hsp70 protein	4.56E-6**	6/14
PFAM	PF00320	GATA zinc finger	6.21E-4*	4/12
PFAM	PF00004	ATPase associated with various cellular activities (AAA)	3.88E-3*	8/72
Rehydrated vs Dehydrated				
Up-regulated				
GO_CC	GO:0005886	plasma membrane	7.99E-3*	11/575
Down-regulated				
GO_CC	GO:0005788	Endoplasmic reticulum lumen	3.80E-4*	4/41

Up- and down-regulated genes were analyzed separately. eggNOG: evolutionary genealogy of genes: Non-supervised Orthologous Groups; GO_BP: Gene Ontology Biological Process; GO_CC: Gene Ontology Cellular Component; GO_MF: Gene Ontology Molecular Function; PFAM: Protein Family. The proportion column indicates the number of differentially expressed genes with respect to the total number of genes annotated with the same term in the entire *Trebouxia gelatinosa* transcriptome.

These transcripts clearly belong to the same multigenic family, which displays remarkable sequence similarity with the Desiccation Related Proteins (DRPs) family previously described in some DT seed plants (Piatkowski et al. 1990; Zha et al. 2013). In total, 9 out of these 13 sequences were significantly responsive to at least one of the two treatments, either being up- or down-regulated. Most of them displayed a trend of expression that involved an increase during dehydration and a repression after rehydration. DRP1 and DRP2, however, followed a completely opposite trend, whereas the expression of DRP5 progressively increased during the experiment (Table 5).

Table 5 *Trebouxia gelatinosa* Desiccation Related Proteins (DRPs) with the respective expression values shown as normalized read counts, proportion fold change values in the dehydrated vs control and rehydrated vs dehydrated comparisons and predicted cellular localization according to TargetP.

ID	Normalized expression values			Fold Change		Cellular Localization
	Control	Dehydrated	Rehydrated	Dehydrated vs Control	Rehydrated vs Dehydrated	
*Trebouxia*_DRP1	4805.87	346.73	1647.46	-13.86*	4.75*	S
*Trebouxia*_DRP2	1893.78	79.53	420.01	-23.81*	5.28*	S
*Trebouxia*_DRP3	23.64	34.88	34.67	1.48	-1.01	S
*Trebouxia*_DRP4	69.03	257.4	333.66	3.73*	1.3	S
*Trebouxia*_DRP5	2.19	15.22	280.94	6.96*	18.45*	P
*Trebouxia*_DRP6	7.97	160.74	38.88	20.17*	-4.13*	S
*Trebouxia*_DRP7	483.62	1889.74	971.5	3.91*	-1.95	S
*Trebouxia*_DRP8	20.86	39.42	45.78	1.89	1.16	S
*Trebouxia*_DRP9	55.3	100.32	152.08	1.81	1.52	S
*Trebouxia*_DRP10	179.13	568.66	351.74	3.17*	-1.62	P
*Trebouxia*_DRP11	286.36	1325.71	667.34	4.63*	-1.99	T
*Trebouxia*_DRP12	145.44	208.69	210.09	1.43	1.01	S
*Trebouxia*_DRP13	2.02	17.73	4.77	8.78*	-3.71	M or S

* significant difference in the statistical expression analysis; S: secreted, P: plastidial, T: transmenbrane, M: mitochondrial.

Other categories significantly up-regulated by dehydration were cytokinin-mediated signaling pathway (GO:0009736), carbohydrate metabolic process (GO:0005975), cyclins (PF00134), omega peptidase activity (GO:0008242) and C2 domain-containing proteins (PF00168).
Due to the high similarity of the transcriptional profiles between rehydrated and dehydrated samples, just a few gene categories affected by the rehydration process were identified. However, their involvement remains questionable due to the low number of over-expressed genes compared to the total and to the poorly significant p-values (Table 4).

Desiccation Related Proteins (DRPs): structure and phylogeny

The ferritin-like domain denotes a taxonomically widespread structural fold, which characterizes different protein families including, among the others, ferritins, bacterioferritins and bacterial DNA-binding proteins from starved cells (DPS). However, DRPs show low sequence homology to *bona fide* ferritins and other ferritin-like protein families available in GenBank. Furthermore, they all present a ~100 aa long conserved C-terminal region, here named DUF1 (Domain of Unknown Function 1), which is absent in other ferritin-like proteins. The structural architecture of green algae DRPs is not uniform: they all present a ferritin-like domain followed by DUF1, but additional long N-terminal or C-terminal regions with unknown function are present in several cases (Fig. 5a).
A comparative genomic analysis revealed that DRPs are absent in most Chlorophyta genomes: no DRPs could be found in Ulvophyceae and they are present in a few Chlorophyceae (*Monoraphidium* spp. and *Chlamydomonas* spp.) as single-copy genes. However, the DRP gene family appears to have undergone expansion in some Trebouxiophyceae including, besides *T. gelatinosa*, other lichen photobionts, such as *Asterochloris* spp. and *Coccomyxa* spp. On the other hand, DRPs are absent in other genera of the same class (*Chlorella*, *Helicosporidium* and *Picochlorum*). The spread of DRPs within Charophyta, Chlorophyta's sister group within which the Embryophyta emerged, is difficult to address due to the limited sequence resources available; only a single DRP gene was actually found in *Klebsormidium flaccidum*. Among Embryophyta, DRPs are present in the genomes of all the species analysed so far, from those belonging to basal groups such as bryophytes (e.g. *Physcomitrella patens*) and lycophytes (e.g. *Selaginella moellendorffii*), to seed plants. Differently to what observed for Chlorophyta, Embryophyta DRPs share a similar length (~300 aa) and a more uniform protein architecture, with a N-terminal leader peptide, followed by the central ferritin-like domain and always ending with the C-terminal DUF1 domain (Fig. 5a). The taxonomic distribution of DRPs, however, is not limited to Viridiplantae, since this protein family is also present in several phylogenetically distant groups of Bacteria, but not in heterotrophic Eukaryota. All bacterial DRPs display a similar length and a protein architecture identical to that of most DRPs of green algae and higher plants.

Fig. 5 Structure characteristics of the 13 Desiccation Related Proteins (DRP1-13) found in the transcriptome of *Trebouxia gelatinosa* in comparison to those found in bacteria, other green microalgae and embryophytes. DUF1 and 2, Domains of Unknown Function 1 and 2. Proteins length not in scale (a). Bayesian phylogenetic tree of Desiccation-Related Proteins (DRPs). *Trebouxia gelatinosa* DRPs are indicated by empty circles, whereas the full circle indicates the DRP belonging to the streptophyte *Klebsormidium crenulatum* (b). The full list of the DRP sequences used for the phylogenetic analysis and their accession IDs is reported in Online Resource 3.

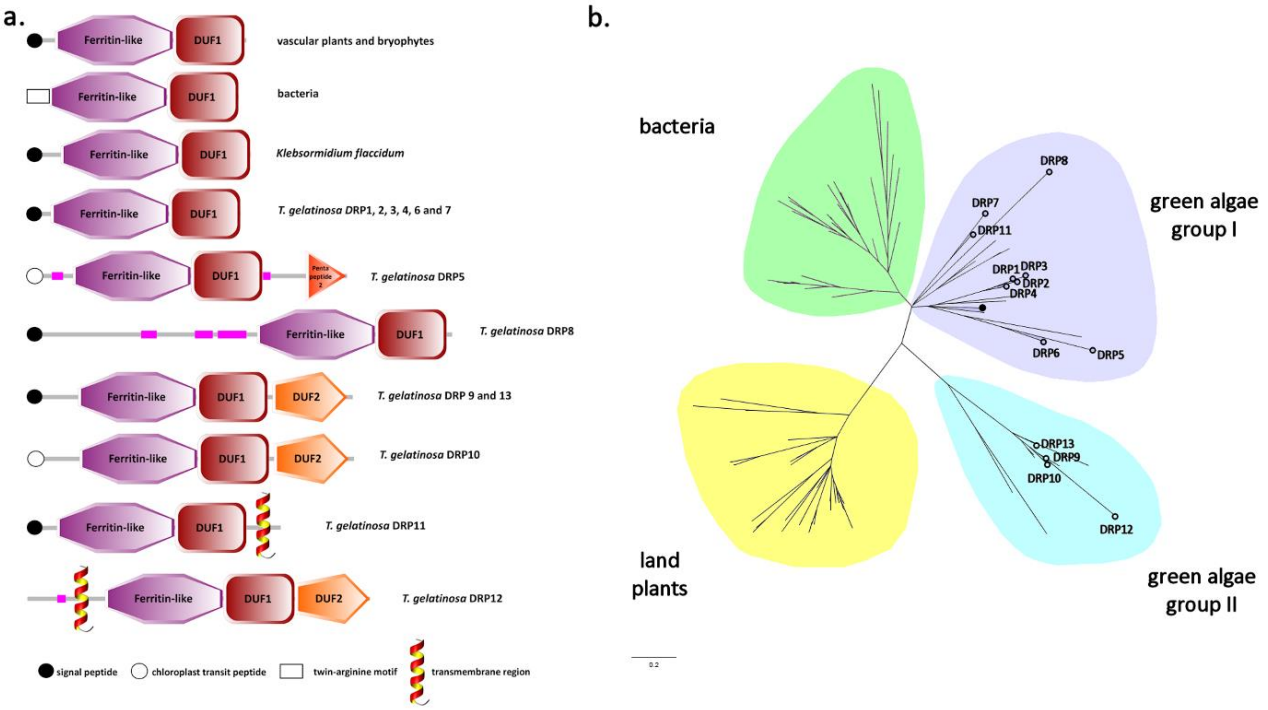

The Bayesian phylogenetic analysis divided higher plants and bacterial DRPs in two well distinct clades, but it surprisingly revealed that the DRPs of Chlorophyta are more closely related to bacterial proteins than they are to those of vascular plants. Although the remarkable sequence diversity did not permit to fully resolve the exact phylogenetic relationship among green algae DRPs, two major distinct subgroups could be identified. The first one is more closely related to bacterial DRPs and includes *T. gelatinosa* DRP1-DRP8 and DRP11, proteins with heterogeneous architecture and subcellular localization (Fig. 5b; Table 5). The second subgroup, which includes DRP9, DRP10, DRP12 and DRP13, is more distantly related to bacteria and comprises proteins characterized by a conserved C-terminal ~100 aa extension with unknown function (DUF2) located after DUF1 (Fig. 5a,b). While basal land plants (bryophytes and lycophytes) DRPs are clearly clustered within the same clade of vascular plants, the placement of the *K. flaccidum* DRP is enigmatic, as it shows marked similarity with bacterial and green algae DRPs.

Expression of genes and gene families related to stress response

We analysed in detail the expression profiles of specific genes or genes families which could be potentially involved in the responses to dehydration stress and rehydration, based on the recent literature concerning desiccation tolerance in Streptophyta and Embryophyta. This permitted us to comparatively investigate the regulation of molecular adaptive strategies to water stress. The comparison revealed that in *T. gelatinosa* there is a different regulation of genes included in the categories, "Aquaporins", "Cell wall modifications", "HSPs and other chaperones", "Late Embryogenesis Abundant proteins", "Oxidative stress response" and "Photosynthetic apparatus" (Table 6).

Table 6 Expression profiles during dehydration and rehydration of gene categories commonly associated to desiccation tolerance in the green alga *Trebouxia gelatinosa* (***Tg***), the Streptophyte *Klebsormidium crenulatum* (***Kc***) (Holzinger et al. 2014), the moss *Syntrichya ruralis* (***Sr***) (Oliver et al. 2004; Oliver et al. 2009), the club moss *Selaginella lepidophylla* (***Sl***) (Iturriaga et al. 2006), the dicots *Craterostigma plantagineum* (***Cp***) (Rodriguez et al. 2010; Mariaux at al. 1998; Jones and McQueen-Mason 2004), *Myrothamnus flabellifolia* (***Mf***) (Ma et al. 2015) and *Haberlea rhodopensis* (***Hr***) (Gechev et al. 2013), and in the monocot *Xerophyta humilis* (***Xh***) (Collet et al. 2004). ↑ up-regulated; ↓ down-regulated; ↑↓ contrasting results; = not affected. *the expression of most ROS-scavenging enzymes was not affected.

	Dehydration								Rehydration				
	Tg	***Kc***	***Sr***	***Sl***	***Cp***	***Mf***	***Hr***	***Xh***	***Tg***	***Sr***	***Cp***	***Mf***	***Hr***
Aquaporins	↑	=	=	↑	↑↓	=	=	↓	=	↑	↑	=	=
Cell wall modifications	=	=	=	=	↓↑	=	↓	=	↑	=	↑	=	↑
HSPs and other chaperones	↓	=	↑	↑	=	=	↑	=	↓	=	=	=	=
Late Embryogenesis Abundant proteins	=	↑	↑	↑	↑	↑	↑	↑	=	↑	↓	↓	↓
Oxidative stress response	↑*	↑	↑	↑	↓	↑	↑↓	↑	=	↑	↑	↓	↑↓
Photosynthetic apparatus	↑	↑	↓	↑	↓	↑	↓	↓	=	↑	↑	=	↑

Discussion

Features of *T. gelatinosa* transcriptome

The genomes of Trebouxiophyceae are generally small in size, with a 2C nuclear DNA content estimated between 0.01 and 1.06 pg (Kapraun 2007). For instance, the genome of *Asterochloris* sp.

has 56.1 Mbp (~0.06 pg, http://genome.jgi.doe.gov/Astpho1/), that of *Coccomyxa subellipsoidea* 49.0 Mbp (~0.05 pg) (Blanc et al. 2012), and that of *Helicosporidium* sp. only 10.5 Mbp (~0.01 pg), being one of the smallest genomes among free-living eukariotes (Pombert et al. 2014). The small genome size, however, is not due to a functional reduction (e.g. through massive loss of gene families) and therefore results in high genomic compactness (Pombert et al. 2014). *Asterochloris* sp. shows 128 gene models per Mbp, i.e. approximately 58% of its genome consists of coding genes, for the shrinkage of introns and non-coding intergenic regions. This is frequently associated to a transcriptional overlap (Williams et al. 2005), that potentially represents a problem in the *de novo* transcriptome assembly process. Unfortunately, the recently sequenced genome of a *T. gelatinosa* strain (ASM81890v1, see Bioproject PRJNA263654), with its 60.1 Mbp size, is not yet annotated. Furthermore, that strain differs genetically, on average, by 6.56% within ORFs from the isolate of this study, although the two strains have been given the same species name. This fact reflects the unsatisfactory taxonomy of the genus *Trebouxia* and the actual underestimation of genetic divergence within infrageneric taxa (Friedl 1989). The analysis of the nuclear ITS region have indeed already detected a high heterogeneity within other *Trebouxia* species (Piercey-Normore 2006; Leavitt et al. 2013; Muggia et al. 2014), and in the near future new infrageneric taxa will likely be recognized for lineages now gathered under the same name (O'Brien 2013; Muggia et al. unpublished data). Also *T. gelatinosa* is evidently heterogeneous and certainly deserves further study from this point of view.

Dehydration- and rehydration-induced gene expression changes in *T. gelatinosa* and comparison with other desiccation-tolerant (DT) photosynthetically active organisms

RNA-seq analyses can only provide information concerning the relative abundance of different mRNAs in a sample, so one should take into account that the TPM values we used do not represent an absolute measure of the actual abundance of mRNAs in a sample, but they are rather proportional to the ratio of their molar concentration over the sum of those of all transcripts in the pool of mRNAs (Musser and Wagner 2015).

The gene expression analysis showed that the D and R transcriptomes were unexpectedly very similar. This is an important feature which cannot be interpreted as a failure of the algae to recover from desiccation, which typically occurs within minutes or a few hours (Gasulla et al. 2009). The same conditions applied in this experiment should not be considered as particularly stressful for *T. gelatinosa,* for two reasons. First, *Trebouxia* species can withstand harsher conditions than those applied in this study, such as very long periods in the desiccated state (up to 45 days) under photo-oxidative conditions (Candotto Carniel et al. 2015; Candotto Carniel et al. 2016). Second, we could not detect any significant degradation of mRNAs caused by dehydration (D samples) in comparison

to the hydrated situations (C and R samples). Maintenance of RNA stability has been previously demonstrated to be a key protective strategy in DT plants (Dinakar and Bartels 2012). Interestingly, the transcripts obtained from D displayed a lower drop in the 3' to 5' end sequencing coverage, which suggests the presence of an unknown mRNA protection mechanism activated in response to dehydration (Online Resource 1). On the other side, the choice of keeping cultures at full hydration for a long period of time was essential to single out those genes which are expressed under the best conditions, although these rarely occur in nature (Lange and Green 2008), and usually only in a limited period of the year (Tretiach et al. 2013).

In *T. gelatinosa*, one of the major differences between C, D and R is the highly significant up-regulation of most genes related to the photosynthetic apparatus. Its maintenance is a priority in homoiochlorophyllous DT organisms because photosynthesis must fully recover as soon as possible upon rehydration to gain a positive CO_2 balance even when rehydration events are short and erratic. Several aeroterrestrial algae, all lichens and DT mosses can actually restore photosynthesis in a few minutes after rehydration (Veerman et al. 2007; Kosugi et al. 2009; Lüttge and Büdel 2010; Cruz de Carvalho et al. 2014; Holzinger and Karsten 2013; Candotto Carniel et al. 2015). The presence of abundant mRNA coding for components of the photosynthetic apparatus upon rehydration, such as photosystems (see Results session), may contribute to the fast re-establishment of photosynthesis. This pattern was also observed in the streptophyte *Klebsormidium crenulatum* by Holzinger et al. (2014), who argued that the up-regulation of genes related to the photosynthetic apparatus is aimed at preparing the organism for the next rehydration event. This hypothesis is supported by the findings of Aubert et al. (2007), who observed the increase of ribulose 1,5-diphospate to control levels after a few minutes upon rehydration of *Xanthoria elegans* (a lichen which has a species of *Trebouxia* as photobiont), meaning that the whole photosynthetic machinery is steadily maintained functional. Contrasting results have been collected in homoiochlorophyllous resurrection plants, displaying either a reduced (Rodriguez et al. 2010) or enhanced (Ma et al. 2015) production of photosynthesis-related mRNAs (Table 6). The immediate synthesis of structural components of the photosynthetic apparatus upon rehydration could also be interpreted as a strategy to reduce the damage caused by prolonged periods in the desiccated status under high light. At these conditions PSI and PSII are, in fact, potential sources of ROS (Veerman et al. 2007) which may damage the photosystems themselves and also membranes and nucleic acids (Smirnoff 1993; Kranner et al. 2008). This damaging action is usually countered by non-enzymatic antioxidant molecules coupled with the activity of ROS scavenging enzymes (Kranner and Birtić 2005). The expression of genes coding for these mechanisms is usually up-regulated in DT plants (Mowla et al. 2002; Iturriaga et al. 2006; Rodriguez et al. 2010; Gechev et al. 2013) (Table 6). In our case, the expression of most of the primary ROS

scavenging enzymes remained steady but two DFR homologs were over-expressed (with a FC ~2 times) in dehydrated samples. DFR is a crucial enzyme for the production of the flavonoid-like anthocyanins and proanthocyanidins, which is up-regulated in response to dehydration in drought-tolerant cowpea as well as in loblolly pine seedlings (Iuchi et al. 1996; Watkinson et al. 2003). Interestingly, flavonoids are thought to act as a secondary ROS-scavenging system in plants subject to high light stress, especially when the chloroplast antioxidants are depleted and the ROS are free to diffuse in the cytosol (Fini et al. 2011). Considering that the synthesis of flavonoids and the up-regulation of related enzymes have been reported in resurrection plants (Ma et al 2015; Moore et al. 2005) subjected to water stress we cannot exclude that this secondary ROS-scavenging system might play a role in the intracellular redox homeostasis in *Trebouxia*, especially when dehydration occurs under light regimes/levels that can induce ROS production.

Another important ROS source, especially upon metabolism reactivation, is the mitochondrion. We detected the over-expression of one mitochondrial manganese superoxide dismutase (MnSOD), an enzyme catalyzing the dismutation of superoxide anion to hydrogen peroxide. The up-regulation of this enzyme upon dehydration may be a way to build-up MnSOD mRNAs in preparation for rehydration, to replace the enzymes inactivated by ROS (Weissman et al. 2005). In addition, the up-regulation of three microsomal glutathione S-transferases pertaining to the MAPEG family could also be part of a mechanism to keep the intracellular redox state under control. Although the role of these trans-membrane enzymes has not been elucidated yet in plants, their role in cellular protection against ROS damage in animals has been clearly documented (Shi et al.2012).

In *Trebouxia* spp., loss and gain of water cause gross morphological modifications (Honegger 1995), with important effects on cell ultrastructure. Whenever cells experience dehydration, certain mechanisms need to be adopted to follow the shrinkage of the cell wall, avoiding the detachment of the plasma membrane. The regulation of expansins may possibly explain how this is achieved in *T. gelatinosa*. Expansins disrupt non-covalent polysaccharides bonds and are involved in cell wall flexibility (Cosgrove 2000). Their over-expression upon rehydration can thus be read as a preparation for the next dehydration event. Although their role in desiccation tolerance of the resurrection plant *C. plantagineum* has been recognized for a long time (Jones and McQueen-Mason 2004), this is the first evidence of their possible involvement in desiccation tolerance in an aero-terrestrial Chlorophyte. Gain of water can also be harmful since tearing of the membranes due to the sudden inrush of water is thought to be a cause of irreparable damage in many desiccation sensitive plants (Pammenter and Berjak 1999). The increase of membrane permeability to water can be seen as an adaptation to avoid damage to the membranes upon rehydration, especially if rehydration events are frequent. In *T. gelatinosa*, five TIP and PIP aquaporins were significantly up-regulated in dehydrated samples, but

their expression remained steady with rehydration. Plant aquaporins have been implicated in drought stress tolerance in several vascular plants, although their expression patterns largely vary depending on the isoform and tissue (Šurbanovski et al. 2013). For example, an enhanced expression of aquaporins has been observed in the desiccated resurrection plants *C. plantagineum*, *Reaumuria soongorica* and *Sporobolus stapfianus*, suggesting that they may have a regulatory role in maintaining cell turgor (Liu et al. 2014; Mariaux et al. 1998; Neale et al. 2000). More recent studies identified a Tonoplast Intrinsic Protein (TIP) in the small vacuoles of the bundle sheath cells of the resurrection grass *Eragrostis nindensis*, indicating that it may also cover an important role in the mobilization of solutes from the small vacuoles upon rehydration (Vander Willigen et al. 2004). On the other hand, aquaporins were strongly down-regulated in the dehydrated monocot resurrection plant *Xerophyta humilis* (Collett et al. 2004) (Table 6).

Beside morphological and ultrastructural modifications, loss and sudden gain of water cause the alteration of the structure and interactions of molecules. Interestingly HSPs, which prevent the denaturation of proteins and avoid their aggregation (Bartels and Sunkar 2005; Prieto-Dapena et al. 2008; Sun et al. 2001), seem not to be involved in the desiccation tolerance of *T. gelatinosa*. Indeed, the high expression level of several HSPs in the control samples (Online resource 12) was followed by a highly significant reduction during dehydration, which in many cases further decreased upon rehydration. On the contrary the *A. erici* HSP90 expression increased during dehydration, remaining higher than controls also during rehydration (Gasulla et al. 2013). The same trend, but for other HSPs, was observed in mosses (e.g. *Fontinalis antipyretica*, Wang et al. 2004; *Syntrichya ruralis*, Cruz de Carvalho et al. 2014), lycophytes (e.g. *Selaginella lepidophylla*, Iturriaga et al. 2006) and resurrection plants as well (e.g. *C. plantagineum*, Alamillo 1995) (Table 6). We are still unable to explain this peculiar behaviour, and certainly further analyses are needed to clarify this pattern and to understand the role of chaperones in the desiccation tolerance of *T. gelatinosa*.

Another unexpected result regards Late Embryogenesis Abundant proteins (LEAs). We found only few genes encoding for LEAs *sensu stricto* in *T. gelatinosa*: one dehydrin (group 2 LEAs) and two group 3 LEAs. More interestingly, the expression of these genes was constitutive and did not vary in relation to hydration. This expression pattern differs from those observed in other DT organisms (Table 6), where LEA proteins are commonly up-regulated during dehydration and/or rehydration. A constitutive expression of these proteins (i.e. in fully hydrated samples) was observed in the resurrection plant *H. rhodopensis* (Gechev et al. 2013), but in this case these genes were further up-regulated during dehydration. In vascular plants LEAs form a heterogeneous class that can be subdivided into at least five major groups (Cuming 1999), with several dozen genes (Hundertmark and Hincha 2008; Du et al. 2013; Lan et al. 2013), whose precise mechanism of action is still unclear

(Goyal et al. 2005; Tunnacliffe and Wise 2007). The low number of LEAs in *T. gelatinosa*, consistent with the situation observed in the genomes of other Trebouxiophyceae, suggests that the gene family expansion observed in vascular plants did not occur in this lineage. However, we found seven genes coding for proteins similar to the cold regulated LEA-like proteins of the Antarctic strain NJ-7 of *Chlorella vulgaris* (Liu et al. 2011). While it is certainly noteworthy that four out of these seven genes were constitutively expressed at very high levels and that the remaining three were over-expressed upon dehydration, the involvement of this poorly known gene family in desiccation-tolerance in *Trebouxia* remains to be investigated. Overall, LEAs activation does not seem to play a relevant role in response to dehydration in *T. gelatinosa*, further corroborating the idea that this organism mostly relies on alternative strategies to deal with the effects of dehydration.

The over-expression of cyclins (specifically of G2/mitotic-specific cyclins A) is a puzzling feature of the dehydration trascriptome of *T. gelatinosa*. Since the persistence of cyclin A prevents the stabilization of the kinetochore/microtubules complex (Kabeche and Compton 2013), this suggests that cell cycle progression has been blocked in dehydrated *T. gelatinosa* cells, similarly to what occurs in *K. crenulatum* (Holzinger et al. 2014).

The gene expression patterns described here for *T. gelatinosa* subjected to dehydration and a subsequent rehydration supports the idea that desiccation tolerance in *T. gelatinosa* is mostly achieved through: (*i*) constitutive mechanisms, which confer a background protection (Oliver et al. 2005), as already hypothesized by Junttila and Rudd (2012) for the lichen *C. rangiferina* and by Gasulla et al. (2013) for the alga *A. erici*; (*ii*) inducible mechanisms similar to those observed in mosses and resurrection plants, e.g. cell wall modifications and aquaporins; (*iii*) inducible mechanisms typical of *T. gelatinosa*, i.e. those mediated by DRPs, that will be further discussed in the next section.

DRPs: a peculiarity of *Trebouxia gelatinosa* transcriptome

The most intriguing feature of the *T. gelatinosa* trascriptome probably regards the gene family encoding for Desiccation Related Proteins (DRPs), whose diversification finds no parallelism in other DT organisms investigated so far. DRPs were firstly described in *C. plantagineum* (Bartels et al. 1990; Piatkowski et al. 1990) and later in other resurrection (Iturriaga et al. 1992; Collett et al. 2004; Ingle et al. 2007) and non-resurrection plants (Zha et al. 2013). However, although DRPs have been frequently implicated in desiccation tolerance (Bartels et al. 1990; Piatkowski et al. 1990; Battista et al. 2001), their mechanism of action is still unknown and several authors have pointed out that they may cover additional functions in higher plants (Zuo et al. 2005; Guo et al. 2008; Guo et al. 2011; Zha et al. 2013). As we have reported in the results section, DRPs are present also in several unrelated bacterial groups, including the *Deinococcus/Thermus* phylum, some sporigenous Actinobacteria,

Acidobacteria, some Betaproteobacteria (Burkholderiales) and some Alphaproteobacteria (mainly pertaining to Sphingomonadales and Rizhobiales). The function of DRPs has been unequivocally linked to DT in *Deinococcus radiodurans*, since the deletion of the locus DRB0118 determines a 75% loss in viability of desiccated cultures (Battista et al. 2001), and its expression is regulated by the crucial stress response regulator drRRA (Wang et al. 2008). Overall, it is certainly noteworthy that bacterial DRPs are mostly associated with taxa adapted to extreme environments or even tolerant to extreme desiccation (Mattimore and Battista 1996; Hiraishi et al. 2000; Farias et al. 2011; Quintana et al. 2013; Tatar et al. 2013).

Despite the lack of functional evidence, the presence of the ferritin-like domain suggests that DRPs might be involved in the protection mechanisms against oxidative stress, since other protein families containing the ferritin-like domain have been implicated in this function. For example, DPS prevent oxidative damage in bacteria, by either oxidizing iron to avoid the formation of oxidative radicals or by physically protecting DNA chains. This behaviour has also been specifically linked to desiccation tolerance in *Rhodococcus* sp. (Haikarainen and Papageorgiu 2010) and to photo-oxidative stress related to rehydration in the cyanobacterium *Nostoc flagelliforme* (Liang et al. 2012). There is clear evidence that classical ferritins themselves have a fundamental role in oxidative stress protection in various vascular plants, due to their potential to detoxify excess iron and dioxygen in mitochondria (Ravet et al. 2009; Briat et al. 2010). Moreover, the up-regulation of ferritins has previously been described in response to dehydration in mosses and red algae (Wang et al. 2009; López-Cristoffanini et al. 2015). The possibility that *Trebouxia* DRPs are similarly involved in protection from oxidative stress is particularly intriguing, considering that several ROS-scavenging enzymes were expressed at a steady level during the dehydration/rehydration experiment.

However, the sequence peculiarities of DPRs, including the presence of the DUF1 domain, leave their functional role still open to speculation. The 13 DRPs genes found in the *T. gelatinosa* transcriptome display a very different behavior in response to the water status of the alga (Table 5). This, together with their structural diversification (Fig. 5a) and different predicted subcellular localization, makes the understanding of the possible functions even more puzzling.

It is evident that the DRPs gene family has undergone relevant expansion in *T. gelatinosa.* Two other lichen chlorobionts belonging to Trebouxiophyceae, *Asterochloris* sp. and *C. subellipsoidea*, have only 5 and 7 DRPs, respectively. Alternatively, in most other green algae DRPs are usually absent or, as in few cases, they are present in just single copy. Bayesian phylogenetic inference clearly pointed out that DRPs of green algae are unlikely to be orthologous to those found in Embryophytes, as they share a surprising sequence similarity to those found in Bacteria (Fig. 5b). In particular, bacterial DRPs and those belonging to green algae group I are virtually indistinguishable, whereas those

belonging to group II are well recognizable due to the presence of the C-terminal DUF2 domain. This unexpected result suggests a bacterial origin for *Trebouxia* DRP genes, which may have been ancestrally acquired by horizontal gene transfer (HGT) from bacterial species associated with lichens. Indeed, the recognition of bacterial communities as a "third partner" in lichen symbioses shows how the traditional concept of lichens needs to be expanded (Grube et al. 2009; Erlacher et al. 2015), as originally proposed by Farrar (1976). Several metagenomic studies have identified Alphaproteobacteria (Rizhobiales, Rhodospirillales and Sphingomonadales in particular) as the dominant group in lichen-associated bacterial communities, usually followed by extremophile Acidobacteria (Bates et al. 2011; Printzen et al. 2012; Erlacher et al. 2015). The overlap between lichen-associated bacteria and those which have DRPs genes is striking and suggests that the possession of DRPs represents an evolutionary advantage for bacteria associated with lichens. On the other hand, beneficial genes could be theoretically passed by HGT between any of the three components of the lichen symbiosis (the bacterial community, the photobiont and the mycobiont), enabling long-term adaptation to specific environmental conditions or stresses (Tunjić and Korac 2013), possibly including water stress tolerance. HGT events between photobionts (including *Trebouxia* spp.) and fungi are well documented (Beck et al. 2014), as well as HGT from bacteria to fungi (Schmitt and Lumbsch 2009; McDonald et al. 2012). To the best of our knowledge, the acquisition of DRPs from symbiotic extremophile bacteria would be one of the first documented instances of HGT from bacteria to lichen photobionts.

Regardless of the evolutionary origin of DRPs, the investigation of their function and diversification in other species of the genus *Trebouxia* will be the next challenge.

Conclusions

Our transcriptomic analysis of the green aero-terrestrial alga/lichen photobiont *T. gelatinosa* shed some light on the molecular mechanisms which are activated or repressed by changes in the water status. Some of them are similar to those observed in other DT organisms, including the regulation of aquaporins and genes involved in the photosynthetic apparatus or the steady expression of most genes related to the primary antioxidant defenses. In particular, the latter behaviour highlights how constitutive mechanisms are used by *T. gelatinosa* to cope with unpredictable, sudden water loss. This could be an additional explanation on how *Trebouxia*-bearing lichens can face photo-oxidative conditions (Kranner et al. 2005; Candotto Carniel et al. 2015) and specific photochemical pollutants, such as ozone (Bertuzzi et al. 2013). On the other hand, the differences observed with DT vascular plants (Table 6) might be attributed to the remarkable differences existing between these organisms. *Trebouxia gelatinosa* and vascular plants are indeed phylogenetically very distant (they diverged

approximately 700 mya). This results in pronounced morphological differences, which in particular determine the different speed of dehydration these organisms are subjected to: in the pluricellular, histologically complex DT vascular plants dehydration is completed in days, whereas in the unicellular lichen photobiont dehydration can occur even in less than one hour. Constitutively expressed physiological mechanisms could thus help the organism to better cope with frequent and fast dehydration/rehydration cycles.

Our study also revealed novel, potentially important features of *T. gelatinosa* adaptation to water stress: the most relevant one is the expansion and diversification of the DRPs gene family, which finds no parallelism in other DT organisms investigated so far. Although the function of these proteins is currently unknown, their responsiveness to changes in the water status, and their similarity to proteins mostly found in extremophile bacteria offer important cues for future studies.

The high completeness of the assembled *T. gelatinosa* transcriptome here presented, represents now a valuable standard reference for RNA-seq based gene expression studies and a new tool to investigate in more detail the mechanisms at the base of desiccation tolerance of aero-terrestrial microalgae and lichens.

Acknowledgements

The study was funded by the Italian Ministry of Education, University, and Research under the PRIN 2010-11 project "TreeCity - Planning the green city in the global change era: urban tree functions and suitability for predicted future climates", and by University of Trieste ("Finanziamento di Ateneo per la Ricerca Scientifica 2011"), local resp. M. T. The activity of F. C. C. was partially funded by a DIANET post-doc outgoing fellowship grant. The activity of E. B. was funded by the Italian Government Commission with "Fondo Trieste". We thank Dr. Gabriele Leoni (Trieste) for technical help.

References

Abascal F, Zardoya R, Posada D (2005) ProtTest: selection of best-fit models of protein evolution. Bioinformatics 2:2104−2105

Ahmadjian V (1973) Methods of isolation and culturing lichen symbionts and thalli. In: Ahmadjian V, Hale ME (eds) The Lichens. Academic Press, New York, USA, pp 653−660

Ahmadjian V (2004) *Trebouxia*: reflections on a perplexing and controversial lichen photobiont. In: Seckbach J (ed) Symbiosis. Springer, Houten, Netherlands, pp 373−383

Alamillo J, Almoguera C, Bartels D, Jordano J (1995) Constitutive expression of small heat shock proteins in vegetative tissues of the resurrection plant *Craterostigma plantagineum*. Plant Mol Biol 29:1093−1099

Altschul SF, Gish W, Miller W, Myers EW, Lipman DJ (1990) Basic local alignment search tool. J Mol Biol 215:403−410

Ashburner M, Ball CA, Blake JA, Botstein D, Butler H, Cherry JM, Davis AP, Dolinski K, Dwight SS, Eppig JT, Harris MA, Hill DP, Issel-Tarver L, Kasarskis A, Lewis S, Matese JC, Richardson JE, Ringwald M, Rubin GM, Sherlock G (2000) Gene Ontology: tool for the unification of biology. Nat Genet 25:25−29

Aubert S, Juge C, Boisson AM, Gout E, Bligny R (2007) Metabolic processes sustaining the reviviscence of lichen *Xanthoria elegans* (Link) Th. Fr. in high mountain environments. Planta 226:1287−1297

Bartels D, Schneider K, Terstappen G, Piatkowski D, Salamini F (1990) Molecular cloning of abscisic acid-modulated genes which are induced during desiccation of the resurrection plant *Craterostigma plantagineum*. Planta 181:27−34

Bartels D, Sunkar R (2005) Drought and salt tolerance in plants. Crit Rev Plant Sci 24:23−58

Bates ST, Cropsey GWG, Caporaso JG, Knight R, Fierer N (2011) Bacterial communities associated with the lichen symbiosis. Appl Environ Microbiol 77:1309–1314

Battista JR, Park MJ, McLemore AE (2001) Inactivation of two homologues of proteins presumed to be involved in the desiccation tolerance of plants sensitizes *Deinococcus radiodurans* R1 to desiccation. Cryobiology 43:133−139

Beck A, Divakar PK, Zhang N, Molina MC, Struwe L (2014) Evidence of ancient horizontal gene transfer between fungi and the terrestrial alga *Trebouxia*. Org Divers Evol 15:235−248

Becker B (2013) Snow ball earth and the split of Streptophyta and Chlorophyta. Trends Plant Sci 18:180−183

Benjamini Y, Hochberg Y (1995) Controlling the False Discovery Rate: a practical and powerful approach to multiple testing. J Roy Stat Soc B Met 57:289−300

Bertuzzi S, Davies L, Power SA, Tretiach M (2013) Why lichens are bad biomonitors of ozone pollution? Ecol Indic 34:391−397

Blanc G, Agarkova I, Grimwood J, Kuo A, Brueggeman A, Dunigan D, Gurnon J, Ladunga I, Lindquist E, Lucas S, Pangilinan J, Pröschold T, Salamov A, Schmutz J, Weeks D, Yamada T, Lomsadze A, Borodovsky M, Claverie JM, Grigoriev IV, Van Etten JL (2012) The genome of the polar eukaryotic microalga *Coccomyxa subellipsoidea* reveals traits of cold adaptation. Genome Biol 13:R39

Briat JF, Ravet K, Arnaud N, Duc C, Boucherez J, Touraine B, Cellier F, Gaymard F (2010) New insights into ferritin synthesis and function highlight a link between iron homeostasis and oxidative stress in plants. Ann Bot 105:811–822

Büdel B (2011) Cyanobacteria: habitats and species. In: Lüttge U, Beck E, Bartels D (eds) Plant Desiccation Tolerance, Vol. 215, Ecological Studies. Springer, Heidelberg, Germany, pp 45–63

Candotto Carniel F, Zanelli D, Bertuzzi S, Tretiach M (2015) Desiccation tolerance and lichenization: a case study with the aeroterrestrial microalga *Trebouxia* sp. (Chlorophyta). Planta 242:493−505

Candotto Carniel F, Arc E, Craighero T, Fernández-Marín B, José Manuel Laza JM, Tretiach M, Kranner I (2016) Transition to the glassy state and molecular mobility in the lichen *Flavoparmelia caperata* (L.) Hale. 7th International Workshop on Desiccation Sensitivity and Tolerance across Life Forms, p. 46

Castresana J (2000) Selection of conserved blocks from multiple alignments for their use in phylogenetic analysis. Mol Biol Evol 17:540−552

Collett H, Butowt R, Smith J, Farrant JM, Illing N (2003) Photosynthetic genes are differentially transcribed during the dehydration-rehydration cycle in the resurrection plant, *Xerophyta humilis*. J Exp Bot 54:2593−2595

Collett H, Shen A, Gardner M, Farrant JM, Denby KJ, Illing N (2004) Towards transcript profiling of desiccation tolerance in *Xerophyta humilis*: construction of a normalized 11 k *X. humilis* cDNA set and microarray expression analysis of 424 cDNAs in response to dehydration. Physiol Planta 122:39−53

Cosgrove DJ (2000) Loosening of plant cell walls by expansins. Nature 407:321−326

Cruz de Carvalho R, Berndardes da Silva A, Soares R, Almeida AM, Coelho AV, Marques da Silva J, Branquinho C (2014) Differential proteomics of dehydration and rehydration in bryophytes: evidence towards a common desiccation tolerance mechanism. Plant Cell Environ 37:1499−1515

Cuming A (1999) LEA Proteins. In: Shewry P, Casey R (eds) Seed Proteins. Springer, Houten, Netherlands, pp 753−780

Dahmen H, Staub T, Schwinn FJ (1983) Technique for long-term preservation of phytopathogenic fungi in liquid nitrogen. Phytopathology 73:241–246

Dinakar C, Bartels D (2012) Light response, oxidative stress management and nucleic acid stability in closely related Linderniaceae species differing in desiccation tolerance. Planta 236:541–555

Du D, Zhang Q, Cheng T, Pan H, Yang W, Sun L (2013) Genome-wide identification and analysis of late embryogenesis abundant (LEA) genes in *Prunus mume*. Mol Biol Rep 40:1937−1946

Edgar RC (2004) MUSCLE: Multiple sequence alignment with high accuracy and high throughput. Nucleic Acids Res 32:1792−1797

Erlacher A, Cernava T, Cardinale M, Soh J, Sensen CW, Grube M, Berg G (2015) Rhizobiales as functional and endosymbiontic members in the lichen symbiosis of *Lobaria pulmonaria* L. Front Microbiol 6:53

Farias ME, Revale S, Mancini E, Ordoñez O, Turjanski A, Cortez N, Vazquez MP (2011) Genome sequence of *Sphingomonas* sp. S17, isolated from an alkaline, hyperarsenic, and hypersaline volcano-associated lake at high altitude in the Argentinean Puna. J Bacteriol 193:3686–3687

Farrant JM, Moore JP (2011) Programming desiccation-tolerance: from plants to seeds to resurrection plants. Curr Opin Plant Biol 14:340−345

Farrar JF (1976) The lichen as an ecosystem: observation and experiment. In: Brown DH, Hawksworth DL, Bailey RH (eds) Lichenology: Progress and Problems. Academic Press, London, United Kingdom, pp 385−406

Fini A, Brunetti C, Di Ferdinando M, Ferrini F, Tattini M (2011) Stress-induced flavonoid biosynthesis and the antioxidant machinery of plants. Plant Signaling & Behavior 6(5):709-711

Finn R, Clements J, Eddy SR (2011) HMMER web server: interactive sequence similarity searching. Nucleic Acids Res 39:29−37

Friedl T (1989) Comparative ultrastructure of pyrenoids in *Trebouxia* (Microthamniales, Chlorophyta). Plant Syst Evol 164:145−159

Fu CH, Chen YW, Hsiao YY, Pan ZJ, Liu ZJ, Huang YM, Tsai WC, Chen HH (2011) OrchidBase: a collection of sequences of the transcriptome derived from orchids. Plant Cell Physiol 52:238−243

Gao B, Zhang D, Li X, Yang H, Zhang Y, Wood AJ (2015) De novo transcriptome characterization and gene expression profiling of the desiccation tolerant moss *Bryum argenteum* following rehydration. BMC Genomics 16:416

Garg R, Patel RK, Tyagi AK, Jain M (2011) De novo assembly of chickpea transcriptome using short reads for gene discovery and marker identification. DNA Res 18:53−63

Gasulla F, Jain R, Barreno E, Guéra A, Balbuena TS, Thelen JJ, Oliver MJ (2013) The response of *Asterochloris erici* (Ahmadjian) Skaloud et Peksa to desiccation: a proteomic approach. Plant Cell Environ 36:1363−1378

Gechev TS, Benina M, Obata T, Tohge T, Sujeeth N, Minkov I, Hille J, Temanni MR, Marriott AS, Bergström E, Thomas-Oates J, Antonio C, Mueller-Roeber B, Schippers JH, Fernie AR, Toneva V (2013) Molecular mechanisms of desiccation tolerance in the resurrection glacial relic *Haberlea rhodopensis*. Cell Mol Life Sci 70:689−709

Goyal K, Walton L, Tunnacliffe A (2005) LEA proteins prevent protein aggregation due to water stress. Biochem J 388:151−157

Grabherr MG, Haas BJ, Yassour M, Levin JZ, Thompson DA, Amit I, Adiconis X, Fan L, Raychowdhury R, Zeng Q, Chen Z, Mauceli E, Hacohen N, Gnirke A, Rhind N, di Palma F, Birren BW, Nusbaum C, Lindblad-Toh K, Friedman N, Regev A (2011) Full-length transcriptome assembly from RNA-Seq data without a reference genome. Nat Biotechnol 29:644−652

Grube M, Cardinale M, de Castro JV, Müller H, Berg G (2009) Species-specific structural and functional diversity of bacterial communities in lichen symbioses. ISME J 3:1105–1115

Guo B, Chen X, Dang P, Scully BT, Liang X, Holbrook CC, Yu J, Culbreath AK (2008) Peanut gene expression profiling in developing seeds at different reproduction stages during *Aspergillus parasiticus* infection. BMC Dev Biol 8:12

Guo B, Fedorova ND, Chen X, Wan CH, Wang W, Nierman WC, Deepak B, Yu J (2011) Gene expression profiling and identification of resistance genes to *Aspergillus flavus* infection in peanut through EST and microarray strategies. Toxins 3:737−753

Haikarainen T, Papageorgiou AC (2010) Dps-like proteins: structural and functional insights into a versatile protein family. Cell Mol Life Sci 67:341-351

Hiraishi A, Matsuzawa Y, Kanbe T, Wakao N (2000) *Acidisphaera rubrifaciens* gen. nov., sp. nov., an aerobic bacteriochlorophyll-containing bacterium isolated from acidic environments. Int J Syst Evol Microbiol 50:1539–1546

Hoekstra FA, Golovina EA, Buitink J (2001) Mechanisms of plant desiccation tolerance. Trends Plant Sci 6:431–438

Holzinger A, Karsten U (2013) Desiccation stress and tolerance in green algae: consequences for ultrastructure, physiological and molecular mechanisms. Front Plant Sci 4:1

Holzinger A, Kaplan F, Blaas K, Zechmann B, Komsic-Buchmann K, Becker B (2014) Transcriptomics of desiccation tolerance in the streptophyte green alga *Klebsormidium* reveal a land plant-like defense reaction. PloS One 9(10):e110630

Honegger R (1995) Experimental studies with foliose macrolichens: fungal responses to spatial disturbance at the organismic level and to spatial problems at the cellular level during drought stress events. Can J Bot 73:569−578

Hori K, Maruyama F, Fujisawa T, Togashi T, Yamamoto N, Seo M, Sato S, Yamada T, et al. (2014) *Klebsormidium flaccidum* genome reveals primary factors for plant terrestrial adaptation. Nature Commun 5:3978

Hundertmark M, Hincha DK (2008) LEA (Late Embryogenesis Abundant) proteins and their encoding genes in *Arabidopsis thaliana*. BMC Genomics 9:118

Ingle RA, Schmidt UG, Farrant JM, Thomson JA, Mundree SG (2007) Proteomic analysis of leaf proteins during dehydration of the resurrection plant *Xerophyta viscosa*. Plant Cell Environ 30:435−446

Iturriaga G, Schneider K, Salamini F, Bartels D (1992) Expression of desiccation-related proteins from the resurrection plant *Craterostigma plantagineum* in transgenic tobacco. Plant Mol Biol 20:555−558

Iturriaga G, Cushman MAF, Cushman JC (2006). An EST catalogue from the resurrection plant *Selaginella lepidophylla* reveals abiotic stress-adaptive genes. Plant Sci 170:1173−1184

Iuchi S, Yamaguchi-Shinozaki K, Urao T, Terao T, Shinozaki K (1996) Novel Drought-Inducible Genes in the Highly Drought-Tolerant Cowpea: Cloning of cDNAs and Analysis of the Expression of the Corresponding Genes. Plant Cell Physiol 37(8):1073-1082

Jones L, McQueen-Mason S (2004) A role for expansins in dehydration and rehydration of the resurrection plant *Craterostigma plantagineum*. FEBS Lett 559:61−65

Junttila S, Rudd S (2012) Characterization of a transcriptome from a non-model organism, *Cladonia rangiferina*, the grey reindeer lichen, using high-throughput next generation sequencing and EST sequence data. BMC Genomics 13:575

Junttila S, Laiho A, Gyenesei A, Rudd S (2013) Whole transcriptome characterization of the effects of dehydration and rehydration on *Cladonia rangiferina*, the grey reindeer lichen. BMC Genomics 14:870

Kabeche L, Compton DA (2013) Cyclin A Regulates Kinetochore-Microtubules to Promote Faithful Chromosome Segregation. Nature 502(7469):110–113

Kanehisa M, Goto S (2000) KEGG: kyoto encyclopedia of genes and genomes. Nucleic Acids Res 28:27–30

Kal AJ, van Zonneveld AJ, Benes V, van den Berg M, Koerkamp MG, Albermann K, Strack N, Ruijter JM, Richter A, Dujon B, Ansorge W, Tabak HF (1999) Dynamics of gene expression revealed by comparison of serial analysis of gene expression transcript profiles from yeast grown on two different carbon sources. Mol Biol Cell 10:1859−1872

Kapraun DF (2007) Nuclear DNA content estimates in green algal lineages: Chlorophyta and Streptophyta. Ann Bot 99:677−701

Kikawada T, Minakawa N, Watanabe M, Okuda T (2005) Factors inducing successful anhydrobiosis in the African chironomid *Polypedilum vanderplanki*: significance of the larval tubular nest. Integr Comp Biol 45:710−714

Kosugi M, Arita M, Shizuma R, Moriyama Y, Kashino Y, Koike H, Satoh K (2009) Responses to desiccation stress in lichens are different from those in their photobionts. Plant Cell Physiol 50: 879–888

Kranner I, Beckett R, Wornik S, Zorn M, Pfeifhofer HW (2002) Revival of a resurrection plant correlates with its antioxidant status. The Plant Journal 31:13–24

Kranner I, and Birtić S (2005) A modulating role for antioxidants in desiccation tolerance. Integr Comp Biol 45:734−740

Kranner I, Cram WJ, Zorn M, Wornik S, Yoshimura I, Stabentheiner E, Pfeifhofer HW (2005) Antioxidants and photoprotection in a lichen as compared with its isolated symbiotic partners. P Natl Acad Sci USA 102:3141−3146

Kranner I, Beckett R, Hochman A, Nash TH III (2008) Desiccation-tolerance in lichens: a review. Bryologist 111:576−593

Lan T, Gao J, Zeng QY (2013) Genome-wide analysis of the LEA (Late Embryogenesis Abundant) protein gene family in *Populus trichocarpa*. Tree Genet Genomes 9:253−264

Lange OL, Green TGA (2008) Diel and seasonal courses of ambient carbon dioxide concentration and their effect on productivity of the epilithic lichen *Lecanora muralis* in a temperate, suburban habitat. Lichenologist 40:449−462

Leavitt SD, Nelsen MP, Lumbsch HT, Johnsonm LA, St. Clair LL (2013) Symbiont flexibility in subalpine rock shield lichen communities in the Southwestern USA. Bryologist 116:149–161

Le TN, Blomstedt CK, Kuang J, Tenlen J, Gaff DF, Hamill JD, Neale AD (2007) Desiccation-tolerance specific gene expression in leaf tissue of the resurrection plant *Sporobolus stapfianus*. Funct Plant Biol 34:589−600

Liang W, Zhou Y, Wang L, You X, Zhang Y, Cheng CL, Chen W (2012) Ultrastructural, physiological and proteomic analysis of *Nostoc flagelliforme* in response to dehydration and rehydration. J Proteomics 75:5604−5627

Lidén M, Jonsson Čabrajič AV, Ottoson-Löfvenius M, Palmqvist K, Lundmark T (2010) Species-specific activation time-lags can explain habitat restrictions in hydrophilic lichens. Plant Cell Environ 33:851−862

Lipnicki LI (2015) The role of symbiosis in the transition of some eukaryotes from aquatic to terrestrial environments. Symbiosis 65:39−53

Liu X, Wang Y, Gao H, Xu X (2011) Identification and characterization of genes encoding two novel LEA proteins in Antarctic and temperate strains of *Chlorella vulgaris*. Gene 482(1):51-58

Liu Y, Liu M, Li X, Cao B, Ma X (2014) Identification of Differentially Expressed Genes in Leaf of *Reaumuria soongorica* under PEG-Induced Drought Stress by Digital Gene Expression Profiling. PLoS ONE 9(4):e94277

Livak KJ, Schmittgen TD (2001) Analysis of relative gene expression data using real-time quantitative PCR and the 2(-Delta Delta C(T)) method. Methods 25:402–408

Lyall R, Ingle RA, Illing N (2014) The window of desiccation tolerance shown by early-stage germinating seedlings remains open in the resurrection plant, *Xerophyta viscosa*. PLoS one 9(3):e93093

López-Cristoffanini C, Zapata J, Gaillard F, Potin P, Correa JA, Contreras-Porcia L (2015) Identification of proteins involved in desiccation tolerance in the red seaweed *Pyropia orbicularis* (Rhodophyta, Bangiales). Proteomics doi:10.1002/pmic.201400625

Lüttge U, Büdel B (2010) Resurrection kinetics of photosynthesis in desiccation-tolerant terrestrial green algae (Chlorophyta) on tree bark. Plant Biol 12:437−444

Ma C, Wang H, Macnish AJ, Estrada-Melo AC, Lin J, Chang Y, Reid MS, Jiang CZ (2015) Transcriptomic analysis reveals numerous diverse protein kinases and transcription factors involved in desiccation tolerance in the resurrection plant *Myrothamnus flabellifolia*. Horticulture Research 2:15034

Maia J, Dekkers BJW, Dolle MJ, Ligterink W, Hilhorst HWM (2014) Abscisic acid (ABA) sensitivity regulates desiccation tolerance in germinated *Arabidopsis* seeds. New Phytol 203:81–93

Mariaux JB, Bockel C, Salamini F, Bartels D (1998) Desiccation-and abscisic acid-responsive genes encoding major intrinsic proteins (MIPs) from the resurrection plant *Craterostigma plantagineum*. Plant molecular biology 38(6):1089−1099

Mattimore V, Battista JR (1996) Radioresistance of *Deinococcus radiodurans*: functions necessary to survive ionizing radiation are also necessary to survive prolonged desiccation. J Bacteriol 178:633–637

Mazur P (1968) Survival of fungi after freezing and desiccation. Fungi 3:325−394

McDonald TR, Dietrich FS, Lutzoni F (2012) Multiple horizontal gene transfers of ammonium transporters/ammonia permeases from Prokaryotes to Eukaryotes: toward a new functional and evolutionary classification. Mol Biol Evol 29:51–60

Mitra J, Xu G, Wang B, Li M, Deng X (2013) Understanding desiccation tolerance using the resurrection plant *Boea hygrometrica* as a model system. Front Plant Sci 4:446

Moore JP, Hearshaw M, Ravenscroft N, Lindsey GG, Farrant JM, Brandt WF (2007) Desiccation-induced ultrastructural and biochemical changes in the leaves of the resurrection plant *Myrothamnus flabellifolia*. Australian Journal of Botany 55:482–491

Mowla SB, Thomson JA, Farrant JM, Mundree SG (2002) A novel stress-inducible antioxidant enzyme identified from the resurrection plant *Xerophyta viscosa* Baker. Planta 215:716–726

Muggia L, Perez-Ortega S, Kopun T, Zellnig G, Grube M (2014) Photobiont selectivity leads to ecological tolerance and evolutionary divergence in a polymorphic complex of lichenized fungi. Ann Bot 114:463–475

Musser JM, Wagner GP (2015) Character trees from transcriptome data: Origin and individuation of morphological characters and the so-called "species signal". J. Exp. Zool. (Mol. Dev. Evol.) 324B:588–604

Nardini A, Marchetto A, Tretiach M (2013) Water relations parameters of six *Peltigera* species correlate with their habitat preferences. Fungal Ecol 6:397–407

Neale AD, Blomstedt CK, Bronson P, Le TN, Guthridg K, Evans J, Gaff DF, Hamill JD (2000) The isolation of genes from the resurrection grass *Sporobolus stapfianus* which are induced during severe drought stress. Plant, Cell & Environment 23:265–277

O'Brien H. (2013) Trebouxia update. http://www.photobiontdiversity.org/. Accessed 24 May 2015

Oliver MJ, Dowd SE, Zaragoza J, Mauget SA, Payton PR (2004) The rehydration transcriptome of the desiccation-tolerant bryophyte *Tortula ruralis*: transcript classification and analysis. BMC Genomics 5:89

Oliver MJ, Velten J, Mishler BD (2005). Desiccation tolerance in bryophytes: a reflection of the primitive strategy for plant survival in dehydrating habitats? Integr Comp Biol 45:788–799

Oliver MJ, Hudgeons J, Dowd SE, Payton PR (2009) A combined subtractive suppression hybridization and expression profiling strategy to identify novel desiccation response transcripts from *Tortula ruralis* gametophytes. Physiol Plant 136:437−460

Pammenter NW, Berjak P (1999) A review of recalcitrant seed physiology in relation to desiccation-tolerance mechanisms. Seed Science Research 9(01):13-37

Piatkowski D, Schneider K, Salamini F, Bartels D (1990) Characterization of five abscisic acid-responsive cDNA clones isolated from the desiccation-tolerant plant *Craterostigma plantagineum* and their relationship to other water-stress genes. Plant Physiol 94:1682−1688

Piercey-Normore MD (2006) The lichen-forming ascomycete *Evernia mesomorpha* associates with multiple genotypes of *Trebouxia jamesii*. New Phytol 169:331–344

Pombert JF, Blouin NA, Lane C, Boucias D, Keeling PJ (2014) A lack of parasitic reduction in the obligate parasitic green alga *Helicosporidium*. PLoS Genet 10(5):e1004355

Powell S, Szklarczyk D, Trachana K, Roth A, Kuhn M, Muller J, Arnold R, Rattei T, Letunic I, Doerks T, Jensen LJ, von Mering C, Bork P (2012) eggNOG v3.0: orthologous groups covering 1133 organisms at 41 different taxonomic ranges. Nucleic Acids Res 40:284–289

Prieto-Dapena P, Castaño R, Almoguera C, Jordano J (2008) The ectopic overexpression of a seed-specific transcription factor, HaHSFA9, confers tolerance to severe dehydration in vegetative organs. Plant J 54:1004−1014

Printzen C, Fernández-Mendoza F, Muggia L, Berg G, Grube M (2012) Alphaproteobacterial communities in geographically distant populations of the lichen *Cetraria aculeate*. FEMS Microbiol Ecol 82:316–325

Proctor MCF (1990) The physiological basis of bryophyte production. Bot J Linn Soc 104:61−77

Proctor MCF, Tuba Z (2002) Poikilohydry and homoiohydry: antithesis or spectrum of possibilities? New Phytol 156:327−349

Proctor MCF, Oliver MJ, Wood AJ, Alpert P, Stark LR, Cleavitt NL, Mishler BD (2007) Desiccation-tolerance in bryophytes: a review. Bryologist 110:595−621

Punta M, Coggill PC, Eberhardt RY, Mistry J, Tate J, Boursnell C, Pang N, Forslund K, Ceric G, Clements J, Heger A, Holm L, Sonnhammer ELL, Eddy SR, Bateman A, Finn RD (2012) The Pfam protein families database. Nucleic Acids Res 40:290−301

Quintana ET, Badillo RF, Maldonado LA (2013) Characterisation of the first actinobacterial group isolated from a Mexican extremophile environment. Antonie Van Leeuwenhoek 104:63–70

Ravet K, Touraine B, Boucherez J, Briat JF, Gaymard F, Cellier F (2009) Ferritins control interaction between iron homeostasis and oxidative stress in Arabidopsis. The Plant Journal 57:400–412

Richardson DH, Richardson D (1981) The biology of mosses. Blackwell Scientific Publications, Oxford, United Kingdom

Rodriguez MCS, Edsgärd D, Hussain SS, Alquezar D, Rasmussen M, Gilbert T, Nielsen BH, Bartels D, Mundy J (2010) Transcriptomes of the desiccation-tolerant resurrection plant *Craterostigma plantagineum*. Plant J 63:212−228

Ronquist F, Teslenko M, van der Mark P, Ayres DL, Darling A, Höhna S, Larget B, Liu L, Suchard MA, Huelsenbeck JP (2012) MrBayes 3.2: efficient Bayesian phylogenetic inference and model choice across a large model space. Syst Biol 61:539−542

Seqc/Maqc-Iii Consortium (2014) A comprehensive assessment of RNA-seq accuracy, reproducibility and information content by the Sequencing Quality Control Consortium. Nature biotechnology 32(9):903−914

Schmitt I, Lumbsch HT (2009) Ancient horizontal gene transfer from bacteria enhances biosynthetic capabilities of fungi. PloS One 4(2):e4437

Shi J, Karlsson HL, Johansson K, Gogvadze V, Xiao L, Li J, Burks T, Garcia-Bennett A, Uheida A, Muhammed M, Mathur S, Morgenstern R, Kagan VE, Fadeel B (2012) Microsomal glutathione transferase 1 protects against toxicity induced by silica nanoparticles but not by zinc oxide nanoparticles. ACS Nano 6(3):1925–1938

Smirnoff N (1993) The role of active oxygen in the response of plants to water deficit and desiccation. New Phytol 125:27−58

Stark LR, Brinda JC (2015) Developing sporophytes transition from an inducible to a constitutive ecological strategy of desiccation tolerance in the moss *Aloina ambigua*: effects of desiccation on fitness. Ann Bot 115:593–603

Sun W, Bernard C, van Cotte BD, van Montagu M, Verbruggen N (2001) At-HSP17.6A, encoding a small heat-shock protein in *Arabidopsis*, can enhance osmotolerance upon overexpression. Plant J 27:407−415

Šurbanovski N, Sargent DJ, Else MA, Simpson DW, Zhang H, Grant OM (2013) Expression of *Fragaria vesca* PIP Aquaporins in Response to Drought Stress: PIP Down-Regulation Correlates with the Decline in Substrate Moisture Content. PLoS ONE 8(9):e74945

Tatar D, Sazak A, Guven K, Cetin D, Sahin N (2013) *Amycolatopsis cihanbeyliensis* sp. nov., a halotolerant actinomycete isolated from a salt mine. Int J Syst Evol Microbiol 63:3739–3743

Trainor FR, Gladych R (1995) Survival of algae in a desiccated soil: a 35-year study. Phycologia 34:191−192

Treonis AM, Wall DH (2005) Soil nematodes and desiccation survival in the extreme arid environment of the Antarctic dry valleys. Integr Comp Biol 45:741−750

Tretiach M, Bertuzzi S, Candotto Carniel F, Virgilio D (2013) Seasonal acclimation in the epiphytic lichen *Parmelia sulcata* is influenced by change in photobiont population density. Oecologia 173:649−663

Tunjić M, Korac P (2013) Vertical and horizontal gene transfer in lichens. Period Biol 115:321–329

Tunnacliffe A, Wise MJ (2007) The continuing conundrum of the LEA proteins. Naturwissenschaften 94:791−812

Untergasser A, Nijveen H, Rao X, Bisseling T, Geurts R, Leunissen JAM (2007) Primer3Plus, an enhanced web interface to Primer3. Nucleic Acids Res 35:71−74

Vander Willigen C, Pammenter NW, Mundree SG, Farrant JM (2004) Mechanical stabilization of desiccated vegetative tissues of the resurrection grass *Eragrostis nindensis*: does a TIP3; 1 and/or compartmentalization of subcellular components and metabolites play a role? Journal of Experimental Botany 55:651–661

Veerman J, Vasil'ev S, Paton GD, Ramanauskas J, Bruce D (2007) Photoprotection in the lichen *Parmelia sulcata*: the origins of desiccation-induced fluorescence quenching. Plant Physiol 145:997−1005

Wang W, Vinocur B, Shoseyov O, Altman A (2004) Role of plant heat-shock proteins and molecular chaperones in the abiotic stress response. Trends Plant Sci 9:244–252

Wang L, Xu G, Chen H, Zhao Y, Xu N, Tian B, Hua Y (2008) DrRRA: a novel response regulator essential for the extreme radioresistance of *Deinococcus radiodurans*. Molecular Microbiology 67:1211–1222

Wang XQ, Yang PF, Liu Z, Liu WZ, Hu Y, Chen H, Kuang TY, Pei ZM, Shen SH, He YK (2009) Exploring the mechanism of *Physcomitrella patens* desiccation tolerance through a proteomic strategy. Plant Physiol 149:1739–1750

Wang Z, Fang B, Chen J, Zhang X, Luo Z, Huang L, Chen X, Li Y (2010) De novo assembly and characterization of root transcriptome using Illumina paired-end sequencing and development of cSSR markers in sweet potato (*Ipomoea batatas*). BMC Genomics 11:726

Wagner GP, Koryu K, Lynch VJ (2012) Measurement of mRNA abundance using RNA-seq data: RPKM measure is inconsistent among samples. Theory in Biosciences 131.4:281–285

Watkinson JI, Sioson, AA, Vasquez-Robinet C, Shukla M, Kumar D, Ellis M, Heath LS, Ramakrishnan N, Chevone B, Watson LT, van Zyl L, Egertsdotter U, Sederoff RR, Grene R (2003) Photosynthetic Acclimation Is Reflected in Specific Patterns of Gene Expression in Drought-Stressed Loblolly Pine. Plant Physiology 133(4):1702–1716

Weissman L, Garty J, Hochman A (2005) Rehydration of the lichen *Ramalina lacera* results in production of reactive oxygen species and nitric oxide and a decrease in antioxidants. Appl Environ Microb 71:2121−2129

Williams BAP, Slamovits CH, Patron NJ, Fast NM, Keeling PJ (2005) A high frequency of overlapping gene expression in compacted eukaryotic genomes. P Natl Acad Sci USA 102:10936−10941

Wright JC (2001) Cryptobiosis 300 years on from Van Leeuwenhoek: What have we learned about Tardigrades? Zool Anz 240:563−582

Xiao L, Wang H, Wan P, Kuang T, He Y (2011) Genome-wide transcriptome analysis of gametophyte development in *Physcomitrella patens*. BMC Plant Biol 11:117

Yamamoto Y, Kinoshita Y, Yoshimura I (2002) Photobiont Culturing. In: Kranner I, Beckett RP, Varma AK (eds) Protocols in Lichenology. Culturing, Biochemistry, Ecophysiology and Use in Biomonitoring. Springer, Heidelberg, Germany, pp 34−42

Yobi A, Wone BWM, XuW, Alexander DC, Guo L, Ryals JA, Oliver MJ, Cushman JC (2013). Metabolic profiling in *Selaginella lepidophylla* at various hydration states provides new insights into the mechanistic basis of desiccation tolerance. Mol Plant 6:369–385

Zha HG, Liu T, Zhou JJ, Sun H (2013) MS-desi, a desiccation-related protein in the floral nectar of the evergreen velvet bean (*Mucuna sempervirens* Hemsl): molecular identification and characterization. Planta 238:77−89

Zuo K, Wang J, Wu W, Chai Y, Sun X, Tang K (2005) Identification and characterization of differentially expressed ESTs of *Gossypium barbadense* infected by *Verticillium dahliae* with suppression subtractive hybridization. Mol Biol (Mosk) 39:191−199

Online resources

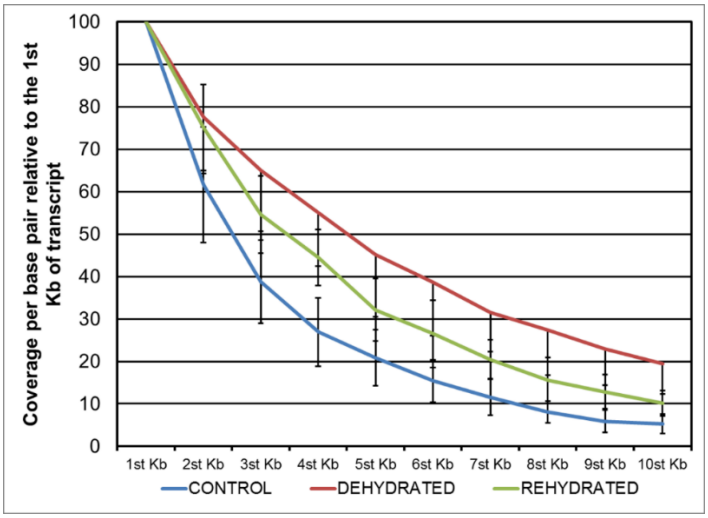

Online Resource 1 We assessed the possibility that dehydration may have increased RNA degradation, introducing possible biases in the analysis, by evaluating the sequencing coverage of long mRNA (> 10 Kb). In this case, a much higher drop in sequencing coverage from the 3' to the 5' end would have been expected in dehydrated samples compared to control and rehydrated samples. On the contrary, we can report that not only the mRNAs of desiccated samples did not appear to be more subject to 5' to 3' degradation, but that the intensity of degradation was lower compared to controls.

Online Resource 2 Primers used for qRT-PCR analysis.

Gene	Primer ID	Forward sequence	Reverse sequence
Desiccation related protein 5	DRP5	GGAGGCTTCTTCCCTAATGG	TCTGCAGTCACCTGAGATGG
Expansin 1	EXP1	GACAGGACTCCAGCTTTTGC	CTGAGGGGAGATGACGTTGT
Expansin 2	EXP2	CTGCAACATGGTGATGGAAC	GAGGCCATTACTCCACGGTA
Photosystem II	PSII	CTGATGACCCAGATGCCTTT	GGTCCTTTGCCTGTCACAAT
Heat shock protein 20	HSP20	GCTGAGCATCAGTGGTGAAA	GAATGTGCCAAACCGTCTTT
Heat shock protein 90	HSP90	AGCACAATGATGACGAGCAG	GGAGATGGGGTAGCTGATGA
Ribosomal protein L6	RPL6	AGGAGCTAGCTAGGGGCATC	TCTCGTGCTTTGGGAACTCT
Elongation factor1-beta	EF1b	CAAGAAAAGGCCAAGCTGAC	TTGGATTGACCCCAGAGAAG

Online Resource 3 Full list of the DRP sequences used for the phylogenetic analysis and their accession IDs.

GREEN ALGAE
Asterochloris sp. (pg00051, pg00071, pg00133)
Auxenochlorella protothecoides (XP_011399816.1, XP_011395871.1)
Chlamydomonas_acidophila (GBAH01011280.1)
Chlamydomonas reinhardtii (XP_001689614.1)
Coccomyxa subellipsoidea (XP_005651445.1, XP_005645257.1, XP_005645325.1, XP_005651481.1, XP_005651480.1, XP_005645326.1)
Monoraphidium neglectum (KIZ05609.1)

CHAROPHYTAE
Klebsormidium flaccidum (JO255866.1)

LAND PLANTS
Arabidopsis thaliana (NP_564518.1, NP_191832.1)
Craterostigma plantagineum (P22242.1)
Glycine max (XP_003533131.1, NP_001241405.1, XP_003546306.2, XP_006597690.1, XP_003528608.1, XP_003528610.1, XP_006587989.1)
Macuna sempervirens (AFD10411.1)
Medicago truncatula (XP_003594696.1, XP_003594692.1, XP_003594693.1, KEH32354.1)
Oryza sativa (EAY93988.1, NP_001050089.1, NP_001054671.2, AAU44142.1)
Physcomitrella patens (XP_001771514.1, XP_001760386.1)
Selaginella moellendorffii (XP_002977644.1, XP_002972030.1, XP_002965677.1)
Sorghum bicolor (XP_002447761.1, XP_002465286.1, XP_002440607.1)
Zea mays (NP_001150304.1, NP_001149373.1, XP_008663177.1, NP_001142402.1)

BACTERIA
Acidisphaera rubrifaciens (WP_048861735.1)
Actinoplanes sp.N902109 (WP_041833689.1)
Amycolatopsis azurea (WP_005154953.1)
Amycolatopsis orientalis (WP_044854273.1)
Comamonas sp.B9 (WP_021026695.1)
Deinococcus deserti (WP_012692797.1)
Deinococcus ficus (WP_027462050.1)
Deinococcus frigens (WP_029479228.1)
Deinococcus geothermalis (WP_011530456.1)
Deinococcus misasensis (WP_034344700.1)
Deinocossus pimensis (WP_045233845.1)
Delftia tsuruhatensis (WP_047327845.1)
Granulicella mallensis (WP_044178539.1)
Granulicella tundricola (ADW70652.1)
Kirrobacter mercurialis (WP_039097173.1)
Kribbella catacumbae (WP_026162498.1)
Massilia sp.9096 (WP_036177468.1)
Meiothermus ruber (WP_013013224.1)
Nocardiopsis synnemataformans (WP_017567992.1)
Rhodococcus sp.AW25M09 (WP_008712540.1)
Salinisphaera hydrothermalis (KEZ79181.1)
Sinorhizobium meliloti (WP_028054988.1)
Skermanella aerolata (WP_044435321.1)
Sphingobium sp.C100 (WP_024019515.1)
Sphingomonas echinoides (WP_010406016.1)
Sphingomonas phyllosphaerae (WP_022685724.1)

Sphingomonas taxi (WP_038664756.1)
Terriglobus roseus (AFL87044.1)

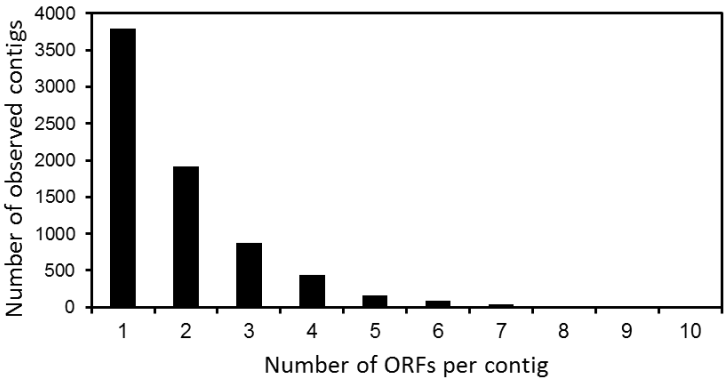

Online Resource 4 Chimeric contigs report relative to *Trebouxia gelatinosa* transcriptomic analysis; the number of ORFs annotated on each contig is shown on the x axis and the number of contigs observed for each category is indicated on the y axis.

Online Resource 5 Summary of the *Trebouxia gelatinosa* genes expression trends during dehydration and rehydration; genes were classified into 9 groups based on their up- or down-regulation in the dehydrated vs control and rehydrated vs dehydrated comparisons.

Group	Dehydrated vs Control	Rehydrated vs Dehydrated	Number of genes	% of the total
1	↑	↑	12	0.09
2	↑	=	479	3.50
3	↑	↓	39	0.28
4	=	↑	84	0.62
5	=	=	12533	91.83
6	=	↓	74	0.54
7	↓	↑	54	0.40
8	↓	=	366	2.68
9	↓	↓	7	0.05

↑: up-regulated; ↓ : down-regulated; = : stable

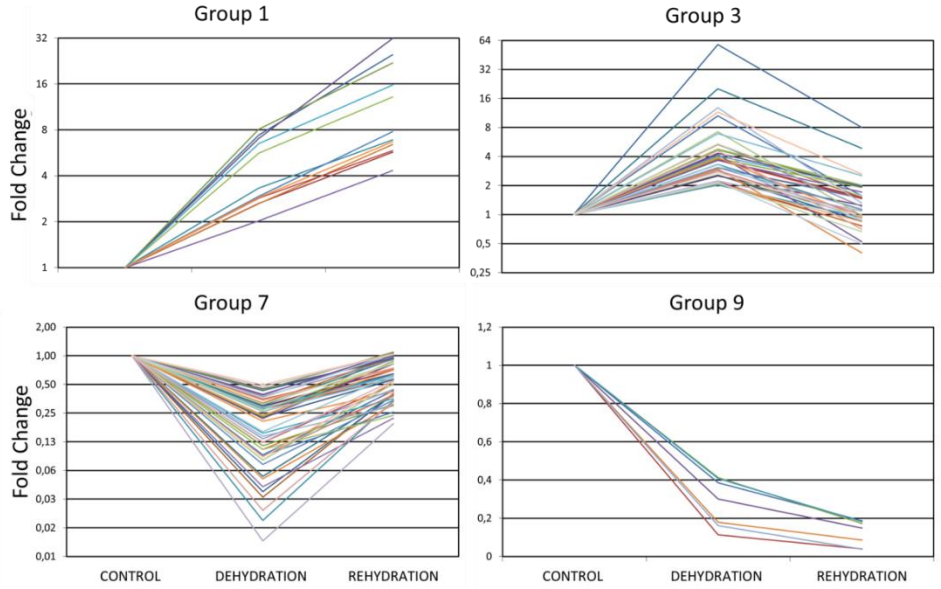

Online Resource 6 Spaghetti plot showing the transcriptional signature of *Trebouxia gelatinosa* selected genes pertaining to gene expression trends 1, 3, 7, 9 (see Online Resource 3). Fold change values relative to the control sample are shown on the y axis.

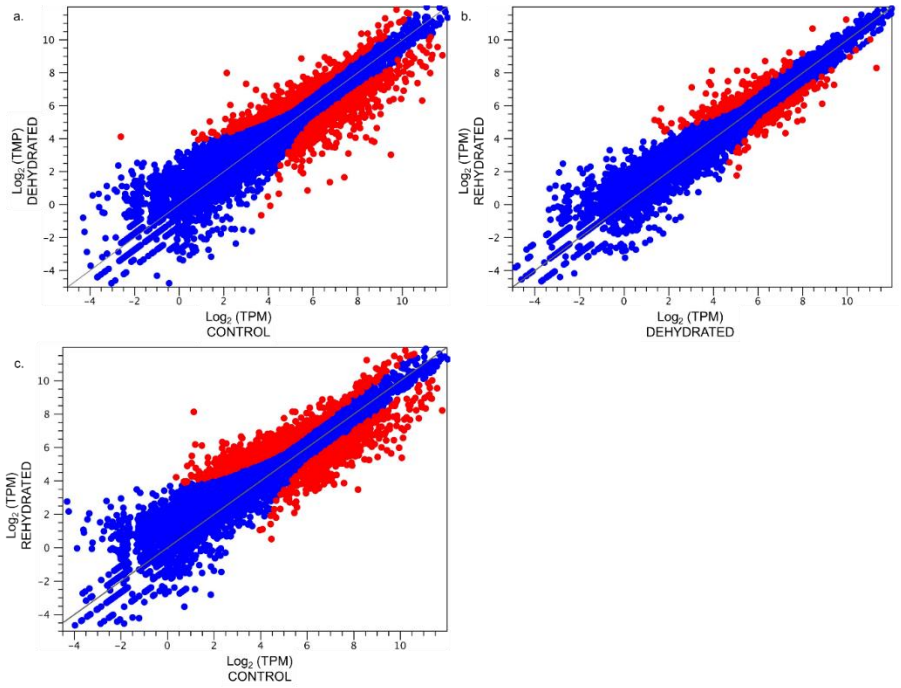

Online Resource 7 Scatter-plot summarizing the comparison of control vs dehydrated (a), dehydrated vs rehydrated (b) and control vs rehydrated (c) expression profiles of *Trebouxia gelatinosa*. Log_2 TPM expression values are plotted on the x and y axis. Differentially expressed genes identified by the Kal's Z-test on proportions (FDR corrected p-value < 0.01 and proportion fold change > ±2) are marked by red dots. Over-expressed genes following rehydration are located above the bisector line; down-regulated ones are located below.

Online Resource 8 List of the 10 *Trebouxia gelatinosa* genes showing the highest proportion fold change (FC) values in the dehydrated vs control and rehydrated vs dehydrated comparison.

Description	Proportion FC
Dehydrated vs Control	
Over-expressed	
Unknown (DUF1254 domain containing)	106.89
PRLI-interacting factor L (cobalamin biosyntheis related protein)	58.10
DRP6	20.17
PurA ssDNA and RNA-binding protein	13.50
Abscisic acid mediated signaling pathway	13.04
GDSL-like Lipase/Acylhydrolase	12.79
Unknown	11.52
Unknown	10.53
Histone H2A	9.24
Unknown	8.79
Under-expressed	
Unknown	-87.90
Glycosyltransferase-like protein (DUF604 domain containing)	-53.54
Unknown	-41.83
T-complex protein 11	-30.44
Unknown	-29.66
T-complex protein 11	-26.72
Unknown	-23.81
Unknown	-22.34
Unknown	-19.94
Unknown	-19.54
Rehydrated vs Dehydrated	
Over-expressed	
DRP5	18.45
Glycosyltransferase-like protein (DUF604 domain containing)	18.09
Unknown	17.00
Unknown	13.66
T-complex protein 11-like	12.31
Unknown	11.50
Expansin-like protein	8.59
Unknown	8.45
Proton phosphate symporter	8.38
3-oxoacyl ACP synthase	7.16
Under-expressed	
GDSL-like Lipase/Acylhydrolase	-9.66
Cold-regulated protein	-8.03
Unknown	-7.41
Beta-lactamase like	-7.39
PRLI-interacting factor L (cobalamin biosyntheis related protein)	-7.25
Unknown	-6.71
Unknown	-6.51
Glycosyl hydrolase catalytic core	-4.44
Subtilase family	-4.39
Unknown	-4.39

Online Resource 9 Summary of the hypergeometric test on annotations performed on the *Trebouxia gelatinosa* sets of differentially expressed genes in the rehydrated vs control comparison.

Category	ID	Description	P-value	Proportion
Rehydration vs Control				
Up-regulated				
eggNOG	COG1523	Type II secretory pathway, pullulanase PulA and	1.47E-5	4/4
GO_CC	GO:000952	photosystem I	1.11E-16	19/23
GO_CC	GO:000952	photosystem II	8.87E-13	16/27
GO_CC	GO:000953	chloroplast thylakoid membrane	1.49E-11	35/146
GO_CC	GO:000587	microtubule	1.01E-6	24/120
GO_CC	GO:000581	microtubule organizing center	3.14E-3	7/30
GO_CC	GO:003028	dynein complex	4.27E-3	5/17
GO_CC	GO:000592	cilium	6.34E-3	9/51
GO_MF	GO:001616	chlorophyll binding	3.33E-16	17/23
GO_MF	GO:004316	cation binding	4.97E-7	14/46
GO_MF	GO:000377	motor activity	1.62E-5	7/15
GO_MF	GO:000389	DNA primase activity	4.80E-4	4/7
GO_MF	GO:000028	magnesium ion binding	4.56E-3	13/91
GO_MF	GO:001711	nucleoside-triphosphatase activity	4.60E-3	10/61
GO_BP	GO:000976	photosynthesis, light harvesting	0.00	17/21
GO_BP	GO:001829	protein-chromophore linkage	2.18E-12	16/27
GO_BP	GO:005130	cell division	5.14E-8	31/151
GO_BP	GO:000706	mitosis	6.05E-7	23/103
GO_BP	GO:000627	DNA replication initiation	5.24E-6	7/12
GO_BP	GO:005125	protein polymerization	2.11E-5	6/10
GO_BP	GO:003017	regulation of DNA-dependent DNA replication initiation	1.21E-4	4/5
GO_BP	GO:000626	DNA unwinding involved in replication	1.21E-4	4/5
GO_BP	GO:001925	starch biosynthetic process	1.43E-4	6/13
GO_BP	GO:000598	starch catabolic process	2.36E-4	6/14
GO_BP	GO:001597	photosynthesis	3.60E-4	11/47
GO_BP	GO:000688	exocytosis	4.11E-3	5/16
GO_BP	GO:000597	carbohydrate metabolic process	5.78E-3	11/65
GO_BP	GO:000631	DNA recombination	7.05E-3	9/49
GO_BP	GO:000626	DNA replication	7.91E-3	12/77
GO_BP	GO:003024	cellulose catabolic process	9.16E-3	5/19
PFAM	GO:001616	chlorophyll binding	3.33E-16	17/23
PFAM	GO:004316	cation binding	4.97E-7	14/46
PFAM	GO:000377	motor activity	1.62E-5	7/15
PFAM	GO:000389	DNA primase activity	4.80E-4	4/7
PFAM	GO:000028	magnesium ion binding	4.56E-3	13/91
PFAM	GO:001711	nucleoside-triphosphatase activity	4.60E-3	10/61
Down-regulated				
eggNOG	COG2217	Cation transport ATPase	4.27E-4	4/11
eggNOG	COG5021	Ubiquitin-protein ligase	6.23E-4	4/12
GO_BP	GO:000695	response to stress	1.28E-6	14/78
GO_BP	GO:000940	response to heat	3.91E-5	10/55
GO_BP	GO:006000	copper ion export	1.36E-4	4/8
GO_BP	GO:000675	ATP biosynthetic process	2.36E-4	6/24
GO_BP	GO:001648	protein processing	3.83E-4	4/10
GO_BP	GO:000645	protein folding	1.79E-3	13/133
GO_BP	GO:000650	proteolysis	3.14E-3	17/211
GO_CC	GO:000588	plasma membrane	2.90E-3	34/575
GO_CC	GO:000050	proteasome complex	4.18E-3	5/30
GO_CC	GO:000953	chloroplast thylakoid membrane	6.79E-3	12/146
GO_MF	GO:000400	copper-exporting ATPase activity	1.15E-4	4/8
GO_MF	GO:000425	serine-type endopeptidase activity	8.53E-4	8/55
GO_MF	GO:001688	carbon-nitrogen ligase activity	1.06E-3	5/22
GO_MF	GO:001711	nucleoside-triphosphatase activity	1.70E-3	8/61
PFAM	PF00012	Hsp70 protein	3.96E-7	7/14

PFAM	PF02374	Anion-transporting ATPase	3.45E-5	4/6
PFAM	PF01425	Amidase	7.05E-4	5/19
PFAM	PF00004	ATPase family associated with various cellular activities	2.07E-3	9/72

Up- and down-regulated genes were analyzed separately. eggNOG: evolutionary genealogy of genes: Non-supervised Orthologous Groups; GO_BP: Gene Ontology Biological Process; GO_CC: Gene Ontology Cellular Component; GO_MF: Gene Ontology Molecular Function; PFAM: Protein Family. The proportion column indicates the number of differentially expressed genes in respect with the total number of genes annotated with the same term in the entire *Trebouxia gelatinosa* transcriptome.

Online Resource 10 List of the 30 most expressed genes in the control, dehydrated and rehydrated samples of *Trebouxia gelatinosa*. The rank of expression per sample, ordered by decreasing values from the most to the least expressed, is displayed.

	Description	Normalized means
Control		
1	HSC70	12461.15
2	Unknown Glycine-rich protein	7159.14
3	C2-domain containing protein_1	6364.77
4	HSP90	5778.33
5	HSP20_1	5156.20
6	Unknown protein_1	4942.85
7	Unknown protein_2	4938.49
8	Elongation factor 1-alpha	4878.50
9	Oxygen evolving enhancer protein 1	4872.42
10	DRP1	4805.87
11	Cold regulated protein_1	4610.81
12	DNAJ protein homolog	4340.36
13	HSP20_2	4294.05
14	Ribosomal protein S20	4178.63
15	Elongation factor 3	3912.00
16	Cyclophilin	3820.11
17	Chaperon-protein ClpB	355.009
18	Chlorophyll a/b binding protein_1	3413.93
19	Ribosomal protein S8	3411.92
20	RUBISCO small subunit	3305.77
21	Cold shock protein_1	3267.37
22	Unknown protein_3	3265.03
23	Ribosomal protein S6	3223.03
24	Polyubiquitin	3053.03
25	Ribosomal protein L26	3017.48
26	Ribosomal protein L15	3005.49
27	Ribosomal protein S3A	2917.57
28	Ribosomal protein S7	2868.57
29	Ribosomal protein S19	2724.38
30	Ribosomal protein L4	2699.97
Dehydrated		
1	Chlorophyll a/b binding protein_1	6832.96
2	Cold regulated protein_1	5277.19
3	Elongation factor 1-alpha	4847.59
4	Unknown Glycine-rich protein	4186.83
5	RUBISCO small subunit	4184.43
6	Plastocyanin	4049.36
7	Unknown protein_3	3958.44
8	C2-domain containing protein_1	3920.50
9	MnSOD	3641.60
10	Cyclophilin	3576.73

11	Elongation factor 3	3275.34
12	Chlorophyll a/b binding protein_2	3189.53
13	Photosystem I reaction center subunit 2	3091.57
14	Oxygen evolving enhancer protein 1	3031.50
15	Photosystem II reaction center W protein	2951.80
16	HSC70	2861.11
17	Tubulin alpha chain	2741.22
18	Cold regulated protein_2	2712.48
19	Unknown protein_4	2674.84
20	GAPDH	2613.38
21	Ribosomal protein S20	2608.67
22	Cold shock protein_2	2595.60
23	C2-domain containing protein_2	2527.03
24	Chlorophyll a/b binding protein_3	2430.70
25	Oxygen evolving enhancer protein 2	2425.39
26	Photosystem I reaction center subunit XI	2417.85
27	Ribosomal protein S8	2351.25
28	Glutharedoxin	2291.79
29	HSP90	2270.06
30	Ribosomal protein L19	2261.68
Rehydrated		
1	Chlorophyll a/b binding protein_1	10853.68
2	RUBISCO small subunit	6605.84
3	Elongation factor 3	5302.69
4	Elongation factor 1-alpha	5257.89
5	Unknown Glycine-rich protein	5254.13
6	Cold regulated protein_1	4986.01
7	Tubulin alpha chain	4104.74
8	Plastocyanin	3840.00
9	Chlorophyll a/b binding protein_2	3589.22
10	GAPDH	3499.78
11	C2-domain containing protein_1	3415.71
12	Cold shock protein_1	3139.78
13	C2-domain containing protein_2	3100.00
14	Unknown protein 3	3065.82
15	Carbonic anhydrase_1	2950.85
16	MnSOD	2860.31
17	Chlorophyll a/b binding protein_3	2857.11
18	Unknown protein_1	2815.44
19	Cyclophilin	2786.76
20	Fructose-bisphosphate aldolase	2754.13
21	Oxygen evolving enhancer protein 1	2680.95
22	Chlorophyll a/b binding protein_4	2617.73
23	Cold shock protein_2	2552.25
24	Ribosomal protein S8	2520.30
25	Ribosomal protein S20	2500.20
26	Carbonic anhydrase_2	2457.34
27	Chlorophyll a/b binding protein_5	2406.58
28	Ferredoxin	2378.67
29	Unknown protein_2	2347.22
30	Ribosomal protein S3A	2286.08

RELATION BETWEEN WATER STATUS AND DESICCATION-AFFECTED GENES IN THE LICHEN PHOTOBIONT *TREBOUXIA GELATINOSA*

Elisa Banchi[a]*, Fabio Candotto Carniel[a], Alice Montagner[a], Francesco Petruzzellis[a], Valentino Giarola[b], Dorothea Bartels[b], Alberto Pallavicini[a], Mauro Tretiach[a]

[a] *Department of Life Sciences, University of Trieste, Via Giorgieri 10,34127 Trieste, Italy*

[b] *Institute of Molecular Physiology and Biotechnology of Plants (IMBIO), University of Bonn, Kirschallee 1, D-53115 Bonn, Germany*

*Corresponding author: Elisa Banchi

Main abbreviations

APX: ascorbate peroxidase

CAT: catalase

DRP: desiccation related protein

DT: desiccation tolerant

DW: dry weight

EXP: expansin

FW: fresh weight

HSP: heat shock protein

LHCII: chlorophyll a-b binding protein of the light harvesting complex II

MnSOD: manganese superoxide dismutase

P_t: turgor pressure

qRT-PCR: quantitative real-time PCR

ROS: reactive oxygen species

RWC: relative water content

TLP: turgor loss point

WC: water content

Ψ: water potential

Ψ_{tlp}: water potential at turgor loss point

Highlights

- In *T. gelatinosa* gene expression is modulated by cell water potential
- The down-regulation of the HSP70 transcript is not reflected on the protein level
- Desiccation related proteins are involved in *T. gelatinosa* response to desiccation
- Turgor loss is a key time point for *T. gelatinosa* gene expression

Abstract

The relation between water status and expression profiles of stress- and desiccation-related genes has been studied in the desiccation tolerant (DT) aeroterrestrial green microalga *Trebouxia gelatinosa*, a common lichen photobiont. Algal colonies were desiccated in controlled condition. During desiccation, the water status was assessed by measuring water content, relative water content (RWC) and water potential (Ψ), and identifying the turgor loss point (Ψ_{tlp}). On a subset of samples, selected on the basis of their Ψ, Ψ_{tlp} and/or RWC, quantitative real-time PCR was performed to measure the expression of ten different transcripts related to photosynthesis, antioxidant defense, expansins, heat shock proteins (HSPs), and desiccation related proteins (DRPs). The HSP70 protein expression was also evaluated by immunodetection. Our analysis showed that the moments just before and after Ψ_{tlp} were key time points for *T. gelatinosa* gene expression. Each cell water potential stimulated a different response in terms of significant genes up- or down-regulation, and this implies a finely regulated perception of water stress. The strong down-regulation of HSP70 gene expression observed during desiccation was not reflected at the protein level. The study provides the first experimental evidence of the central involvement of DRPs in *T. gelatinosa* desiccation tolerance.

Key words

Water potential, relative water content, HSP70, DRPs, turgor loss.

1. Introduction

Desiccation tolerance [1] is the ability to survive and recover metabolism after drying to 0.1 g H_2O g^{-1} of dry mass [2]. This corresponds to the loss of more than 90 % of the relative water content (RWC) and to a water potential (Ψ) of ~ -100 MPa or even lower [3]. Desiccation tolerance implies the capacity of an organism to survive in this state for ecologically relevant periods of time, resuming a normal metabolism in a relatively short time (from minutes to days) as soon as water becomes

available again. Desiccation tolerance can be found in phylogenetically distant taxa, from lichens and bryophytes to nematodes, rotifers, and tardigrades [4] and is typical of organisms which colonize substrates or environments with little and unpredictable water availability [5]. Desiccation tolerant (DT) photoautotrophs include aero-terrestrial micro-algae, lichens, bryophytes, several clubmosses and ferns and a few hundred adult angiosperms plus most of the angiosperms at the embryo stage (as seeds) [4]. Aero-terrestrial microalgae, in particular, have a global distribution and typically occur in biofilms on soil, rocks, leaves, tree bark, and man-made substrata [6]. Some taxa form long-living, stable symbiosis with fungi, i.e. are lichen photobionts, including *Trebouxia* (Chlorophyta), which is the most common and widespread genus of lichen photobionts [7]. All Trebouxias (c. 30 species; [8]) are DT, and the mechanisms of their desiccation tolerance are not yet understood.

To cope with the effects derived by water loss, DT photoautotrophs apply multiple strategies. In most DT vascular plants, in which desiccation usually occurs in terms of days, the protection/repair mechanisms are activated by desiccation itself [9, 10]. On the other hand, DT non-vascular plants are subjected to frequent cycles of desiccation/rehydration that can last even a few minutes and thus they mostly rely on constitutive protection mechanisms [3, 4, 11]. In DT non-vascular plants, the influence of the water status and desiccation on molecular, physiological and morphological responses is far from being completely understood [12].

When desiccation is moderate, DT photoautotrophs accumulate compatible osmolytes (i.e. amino-acids, sugars, polyols) that allow osmotic adjustments [3]. Furthermore, an increased expression and accumulation of dehydrins, late embryogenesis abundant proteins (LEA), and heat shock proteins (HSPs) is commonly observed [13].

As desiccation is known to cause impairment of redox equilibrium, both vascular and non-vascular DT photoautotrophs must avoid oxidative damage derived from the accumulation of reactive oxygen species (ROS) [14]. ROS are harmful to cellular components like nucleic acids, polysaccharides, proteins and lipids [14]. Anti-oxidant defenses include protective enzymes like superoxide dismutase, catalase, peroxidases, and non-enzymatic molecules like glutathione and ascorbic acid [15]. An effective antioxidant system seems to be one of the most important prerequisites for desiccation tolerance [16].

During desiccation, one of the major threats for photoautotrophs is the loss of cell turgor. With turgor loss, the cell membrane progressively detaches from the cell wall [17], and the cell is thus subjected to mechanical and biochemical injuries that impair its functionality [3, 18]. This causes strong morphological modifications to the cell ultrastructure that can lead to irreversible damage to organelles and possibly to cell death [3, 18]. For these reasons, cell turgor loss is considered the best indicator of water stress in plant science [18].

Turgor loss can be monitored by measuring the water potential (Ψ), a parameter used to assess the water status in terms of potential energy per unit volume. Ψ measurements are not regularly applied (e. g. in lichenological studies; [19, 20]) as they are more time consuming than weight measurements to quantify the water content. However, Ψ measurements are definitely more informative, because they allow a description of the water status derived on irreversible thermodynamics, and the discrimination between extra- and intracellular water loss [5].

Ψ of distilled water is 0 MPa, and the potential of cells in equilibrium is slightly negative due to the solutes [21]. When the cells lose water during desiccation, the decrease of turgor pressure (P_t, MPa) and/or the increase of solutes concentration cause a drop in the water potential [21]. When P_t reaches 0, cell turgor is lost and the water potential is mostly determined by the osmotic potential (i.e. cell solutes concentration). This point, known as water potential at turgor loss point (Ψ_{tlp}), reflects the ability of an organism to maintain cell turgor in the face of fluctuating water supply [22]. Turgor maintenance during desiccation might extend time available to perform metabolic activities, including photosynthesis [23], and thus Ψ_{tlp} has been widely measured in vascular plants and recently also in poikilohydric organisms, such as lichens and algae [5, 23]. Water potential isotherms (pressure/volume curves, PV-curves), that take into account -1/Ψ and water loss (or RWC), are commonly used to measure different cell parameters, including Ψ_{tlp} [24, 25]. Lower Ψ_{tlp} values have been linked to higher water deficit tolerance in organisms adapted to arid environments, as seen in vascular plants [26] and lichens [5].

Generally, Ψ_{tlp} of vascular plants is between -1 MPa and -3 MPa [22, 27, 28], and the Ψ value at which non-DT species can be dried without triggering irreversible damage, also known as the critical water potential, occurs between -5 and -10 MPa, corresponding to ~ 20-30 % RWC [29]. The critical water potential of DT species is far lower than that of non-DT species. In DT vascular plants, it can reach values as low as ~ -200 MPa [30] whereas in lichens and their symbionts [31, 32] and in DT bryophytes [33] the critical Ψ can reach values below ~ -600 MPa. To date, few studies have been conducted on the turgor loss response in DT non-vascular plants [12], and an estimation of Ψ in relation to water status would be important to understand if and how this feature is involved in desiccation tolerance of these organisms.

Up to date, a single work was performed considering both Ψ and RWC in the lichen photobiont, *Trebouxia sp.* TR9 [34], showing that, at metabolomic level, water status affects mainly cell wall, extracellular polysaccharides (EPS), polyols and antioxidant protection. Candotto Carniel et al. [11] showed that desiccation tolerance of a further *Trebouxia* species, *T. gelatinosa* Archibald, mostly relies on constitutive mechanisms, but desiccation and rehydration affect also the gene expression of components of the photosynthetic apparatus, the ROS-scavenging system, HSPs,

expansins, and desiccation related proteins (DRPs) [11]. DRPs were first described in the resurrection plant *Craterostigma plantagineum* and have purportedly been linked to desiccation tolerance [35]. One of these DRPs, predicted to exist as small gene family (pcC13-62, [36]), presents similarities with *T. gelatinosa* DRPs. In *T. gelatinosa* the DRP family is highly expanded, exhibits high diversification in terms of cellular localization and structure, and the response to the water status is heterogeneous [11], a fact that asks for further investigations.

In this study, we monitored the response of *T. gelatinosa* during desiccation describing the water status in terms of water content (WC), relative water content (RWC) and Ψ. We aimed to identify how the water status of *T. gelatinosa* triggers changes in the expression of stress- and desiccation-related genes, i.e. which are the key moments that activate the transcription of these important genes during water loss.

1. Materials and methods

1.1.Cultures of Trebouxia *photobiont*

Trebouxia gelatinosa was isolated following Yamamoto et al. [37] from thalli of *Flavoparmelia caperata* (L.) Hale collected in the Classical Karst plateau (NW Italy). The algal cultures were subcultured on solid Trebouxia Medium (TM; 1.5 % agar) [38] every 30-45 days and kept in a thermostatic chamber at 18 ± 1 °C and 20 ± 2 μmol photons m^{-2} s^{-1} with a light/dark regime of 14/10 hours and a relative humidity of 53 %.

Axenic cultures of *T. gelatinosa* were inoculated with 100 μl of a water suspension of approximately 3.5×10^6 cells mL^{-1} on cellulose acetate membranes (25 mm diameter, pore size 0.45 μm, Sartorius Lab Holding GmbH), which were laid on 25 mL of solid TM (1.5 % agar) [38] at the bottom of Microbox Junior 40 vessels (Duchefa Biochemie), equipped with a micro-filter strip on the cover which allows gas exchange while keeping the internal volume in sterile conditions. The vessels, each containing six membranes, were kept in the thermostatic chamber at the same conditions reported above. On the 30th day of growth, a number of colonies (4 and 63 respectively) were used for Ψ_{tlp} assessment and desiccation treatment.

*1.2.*Trebouxia gelatinosa Ψ_{tlp} *assessment*

Four 30-days-old colonies (weight 0.22 ± 0.01 g) were taken from the vessels and used for the PV-curve measurements. Fresh colonies were progressively desiccated on a laboratory bench while maintained in the dark, at 21 ± 1 °C and with relative humidity ranging between 40 % and 55 %. Water potential (Ψ) measurements were performed using a dew point water potential meter (WP4,

Decagon Devices, Inc.) as the average of three subsequent values in the range below the error of the instrument (0.1 MPa), and coupled with measurements of sample fresh weight (FW). The experiment continued until the relationship between 1/Ψ and the cumulative amount of water loss by samples became linear ($r^2 > 0.98$). PV-curves were finally processed according to Tyree and Hammel [24] to obtain Ψ_{tlp}.

1.3.Desiccation treatment

Sixty-three 30-days-old *T. gelatinosa* colonies (weight 0.22 ± 0.01 g) were randomly (Lehmer Pseudo random number generator) selected from the vessels and placed in groups of seven along the border of single filter paper discs (Whatman, 60±5 g m^{-2}, 25 mm diameter) wetted with 100 µl of distilled water inside plate lids and left to desiccate at the air of the thermostatic chamber, at the same conditions described above.

During desiccation, 9 sampling points were selected as defined in a preliminary experiment performed at the same conditions, in which the decreasing weight of fully-hydrated *T. gelatinosa* colonies was followed over time with a precision balance. In the final experiment, at each sampling point (T0-T8), one plate lid with seven colonies was randomly selected and one of its colonies was placed in a dew point water potential meter (WP4, Decagon Devices, Inc.) to measure the water potential (Ψ), calculated as the average of three subsequent values in the range below the error of the instrument (0.1 MPa). Then the colony was gently transferred from the membrane to a pre-weighed labeled 1.5 mL tube, soaked in liquid nitrogen and freeze-dried for 48 h. After freeze-drying, the tube was weighed on a precision balance to obtain the dry weight (DW) of the colony.

Just before finishing the Ψ measurement, the other six colonies were transferred on the plate lid from the membrane to pre-weighed labeled 1.5 mL tubes, weighed on a precision balance for water content (WC) estimation, soaked in liquid nitrogen and stored at -80 °C. For the last time point (T8), colonies were kept in silica-gel for 24 h. The six colonies of each plate lid represent six replicates of the same sampling point (sample), which were referred to the specific Ψ measured on the seventh replicate.

The water content (WC) was expressed as g H_2O g^{-1} dry weight and calculated as WC = [(FW – DW) / DW], where the fresh weight (FW) was the weight at the sampling point, and the dry weight (DW) was the average weight of the freeze-dried colonies. The relative water content was calculated as RWC = [(FW – DW) / (IFW - DW)] × 100 following Nardini et al. [5], where the water lost until the decline of Ψ was interpreted as extracellular, and subtracted from the T0 fresh weight to get the initial fresh weight (IFW), which was considered the weight at full turgor Nardini et al. [5].

Subsequent analyses, i.e. quantitative real-time PCR (qRT-PCR) of ten genes and immunodetection of HSP70, were performed on a subset of samples, selected on the basis of their Ψ, Ψ_{tlp} and/or RWC.

This subset consisted of samples in the fully-hydrated state (T0), after loss of most extracellular water (T1), before (T4) and after (T5) turgor loss, and immediately before (T7) and after (T8) reaching the desiccated state (RWC <10 %).

1.4.RNA isolation and cDNA synthesis

RNA was extracted with PowerPlant® RNA Isolation Kit (MO BIO Laboratories Inc.) from three out of six random chosen replicates of all the selected samples. RNA quality was verified with NanoDrop® 2000 (Thermo Fisher Scientific), followed by a denaturing 1 % agarose gel. cDNA was synthesized using IScript cDNA synthesis kit (Bio-Rad).

1.5.Quantitative real-time PCR (qRT-PCR)

qRT-PCR was performed to measure the expression of ten different transcripts, five encoding stress-related proteins and five desiccation-related proteins. The former were ascorbate peroxidase (APX), expansin I (EXPI), manganese superoxide dismutase (MnSOD), heat shock protein 70 (HSP70) and the chlorophyll a-b binding protein of the light harvesting complex II (LHCII); the latter were the desiccation related proteins 1 (DRP1), 2 (DRP2), 6 (DRP6), 11 (DRP11) and 13 (DRP13).

Primers (Table A.1) were chosen following Candotto Carniel et al. [11], Montagner et al. [39], or custom-designed with Primer3Plus [40]. Each reaction was performed in three technical replicates in a mix containing 1 µL cDNA (1:10 template dilution), 8 µL SSOAdvanced™ SYBR® Green Supermix (Bio-Rad) and 200 nM of each primer. The PCR amplifications were performed with CFX 96™ real-time PCR System (Bio-Rad) using the following cycle: 98 °C for 30 minutes and 40 cycles at 95 °C for 10 minutes and 60 °C for 20 minutes. A melting curve analysis (65 °C to 95 °C increment 0.5 °C for 5 minutes) was performed to verify the absence of non-specific amplification products. Transcript levels were calculated with Bio-Rad CFX Manager software (Bio-Rad), based on the comparative Ct method ($2^{-\Delta\Delta}$ Ct method) [41] and gene expression data were normalized using as housekeeping gene the ribosomal protein L6 (RPL6) [11, 39].

1.6.Proteins isolation

Three out of six random chosen replicates of all the selected samples were grinded in liquid nitrogen, transferred to 1.5 mL tubes and resuspended in 100 µL of 1× Laemmli buffer [62.5 mM Tris–HCl pH 6.8, 10 % (v/v) glycerol, 2 % (w/v) SDS, 0.2M dithiothreitol (DTT) and 0.1 % (w/v) bromophenol blue [42]. Samples were then vortexed and incubated at 95 °C for 5 minutes. After a 3 minutes centrifugation at 14000 r.p.m., protein extracts were recovered from the upper phase of the tube and transferred to a new tube. Samples were stored at -20 °C and incubated 5 minutes at 95 °C

before loading on the gel, when not immediately used for the analysis. To check the quality and quantity of the total proteins extracted, 12 % sodium dodecyl sulphate - polyacrylamide gel electrophoresis (SDS-PAGE) was performed according to Laemmli [42] and the gel was stained with Coomassie brilliant blue R250 [43].

1.7.HSP70 immunodetection

To perform 12 % SDS-PAGE, 15 µg of proteins were used. Proteins were then transferred on a Hybond™ nitrocellulose membrane (Amersham) using the Criterion™ blotter apparatus (Bio-Rad, USA) [44]. The transfer of the proteins was obtained after 1 hour at 70 V with pre-chilled buffer. Before immunodetection, the membrane was stained for 30 minutes with Ponceau S red to check equal protein transfer. The membrane was incubated at 4°C overnight in blocking solution [3 % (w/v) skimmed milk in Tris-buffered saline] to prevent unspecific binding of antibodies. The membranes were incubated for 1 hour with HSP70/HSC70 primary antibody ([45], 1:1000 dilution), and for 45 minutes with secondary antibody (anti-rabbit IgG-peroxidase, 1:5000 dilution, Sigma-Aldrich). Antigen-antibody complexes were detected with the ECL kit (Amersham) and a lumi-imager (LAS 1000, Fujifilm). Densitometry of protein bands was done with Image J software 1.37 V (National Institute of Health).

1.8.Statistics

Statistics were performed with R version 3.2.0 [46]. A one-way Anova followed by a Fisher's LSD post-hoc test was applied to verify significant differences between the relative abundancy of transcripts and HSP70 protein content among samples. Figures were produced with Sigmaplot 10.0 (Systat Software).

2. Results

2.1.Water relations

Complete desiccation of the *T. gelatinosa* colonies (RWC ~ 1 %) occurred in approximately 10 hours (Fig. 1, Table A.2). Water loss was faster at the beginning of the desiccation: after the first four hours (T1), WC was halved (Fig. 1, Table A.2) and reached 0.01 g H_2O g^{-1} DW in T8.

Water potential decreased slowly from T0 to T4, and strongly decreased between T4 and T5 (Fig. 1, Table A.2). Ψ_{tlp} assessed trough PV-curves measurement was ~ -3.62 ± 0.62 MPa, corresponding to a point between T4 and T5 of the desiccation process (Fig. 1).

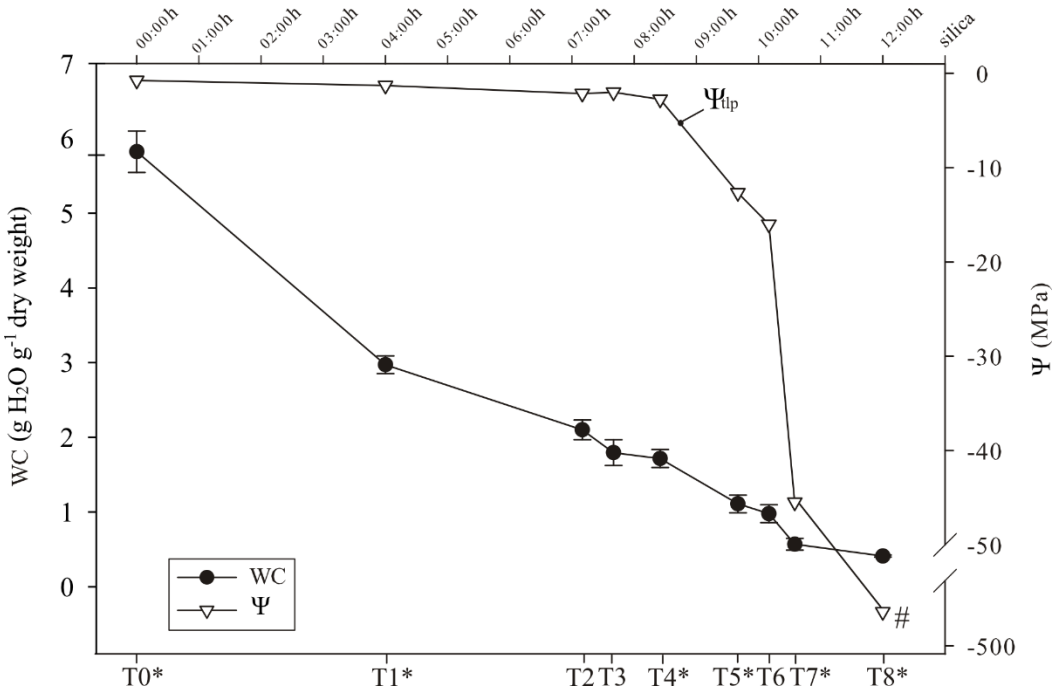

Fig. 1. Water content (WC, n = 6) and water potential (Ψ) during desiccation in *Trebouxia gelatinosa* colonies (T0-T8). Those marked with an asterisk were used for the subsequent analyses. Ψtlp according to PV-curves. #according to Candotto Carniel et al. [32].

2.2. Effects of desiccation on genes expression at transcript level

Significant changes in the expression of all tested genes were observed during desiccation. Regarding anti-oxidant enzymes, both APX and MnSOD increased their expression at T1 (~ 40 % and 100 %, respectively), then decreased (from ~ 110 % to ~ 180 %) from T4 to T6 and increased again at T8 around initial levels (Fig. 2). EXP1 had an opposite expression pattern; it increased four times from T0 to T4, remaining high at T5 and then it decreased to less than one tenth of the T0 level at T7 and T8 (Fig. 2). HSP70 and LHCII had a different expression pattern as well: they remained stable until T2, to significantly decrease between T4 and T7 (~ 90 %) and increase again to the T0 levels between T7 and T8 (Fig. 2).

The expression of DRP1 significantly increased to 40 % between T0 and T4, then it decreased back to T0 levels between T4 and T5 and increased again between T7 and T8 (Fig. 2). DRP2 and DRP6 shared a similar pattern, with the major increase (~ 50 %) of their expression at T4 and then a decrease of ~ 20 % from T5 to T8 (Fig. 2). DRP11 had the major increase at T4 (~ 40 %), then the expression decreased to the initial level from T5 to T8 (Fig. 2). DRP13 had also a major increase at T4 (~ 60 %), then it returned to initial levels at T5, decreased ~ 30 % at T7 and then it returned to initial levels at T8 (Fig. 2).

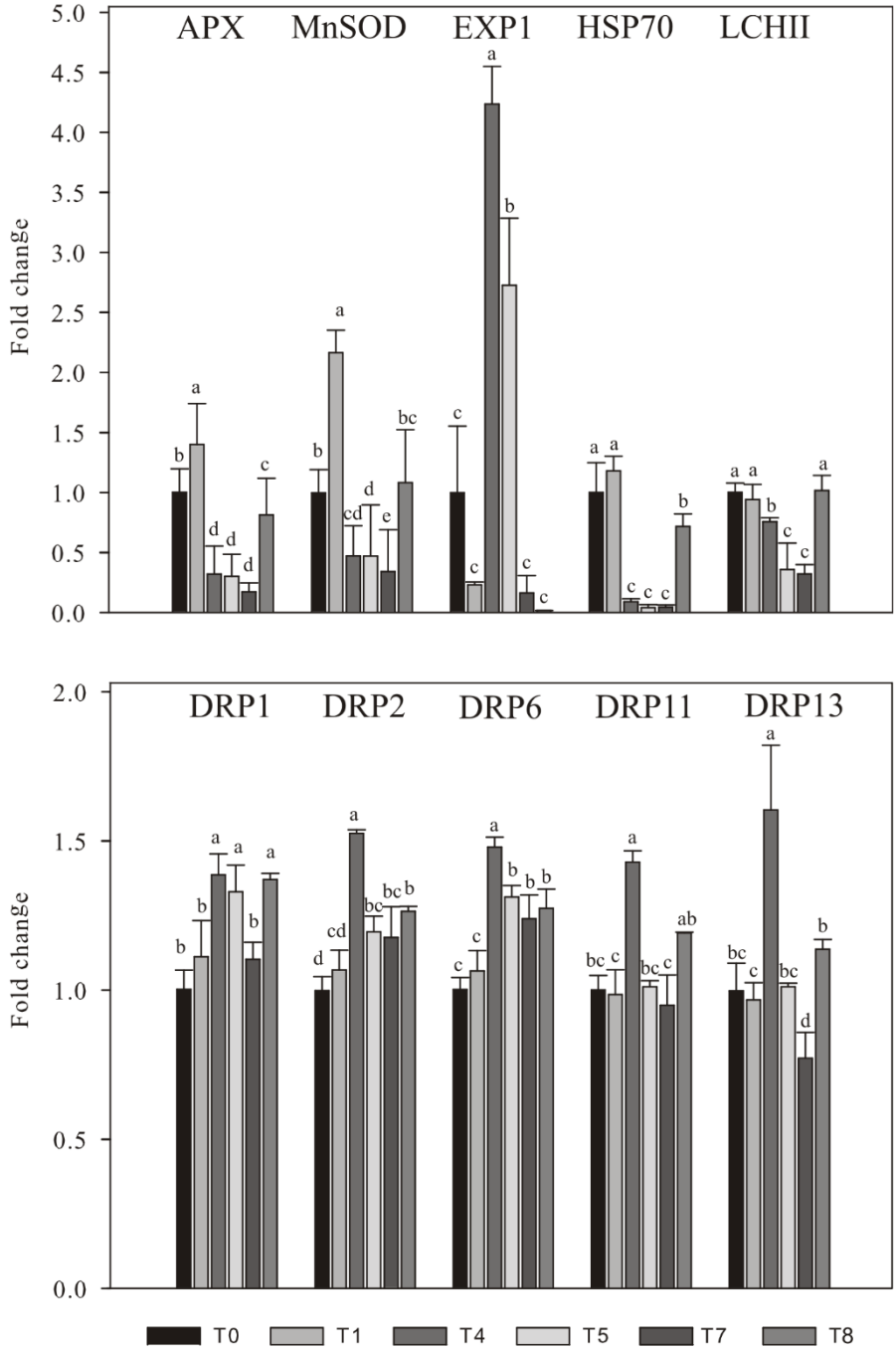

Fig. 2. Fold change in the expression of the 10 selected transcripts. Gene expression was determined using qRT-PCR for RNA of colonies of *Trebouxia gelatinosa* during desiccation. Different letters on the top of the bars indicate significant differences among samples ($p < 0.05$, $n = 3$). APX: ascorbate peroxidase; EXP1: expansin 1; MnSOD: manganese superoxide dismutase; HSP70: heat shock protein 70; LHCII: chlorophyll a-b binding protein of the light harvesting complex II; DRP: desiccation related protein.

2.3. Effects of desiccation on the HSP70 protein level

Desiccation did not affect the HSP70 protein level: no significant differences were found among the sampling points (Fig. 3).

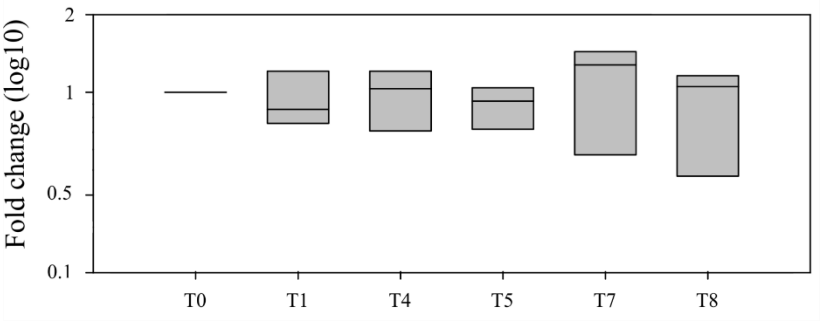

Fig. 3. Fold change in the level of HSP70 protein. The level was assessed using immunodetection on 15 µg of proteins extracted from colonies of *Trebouxia gelatinosa* during desiccation. No significant differences were found among samples ($p < 0.05$, $n = 3$).

3. Discussion

Transcriptional activation or repression in plant cells involves a stress-sensor at the cell wall or plasma membrane, the generation and release of second messengers (including calcium ions, Ca^{2+}) and the activation/inhibition of protein kinases (PKs) and phosphatase (PPs) [47]. A possible signal for the activation of the cascade of messengers is the modification of the environment surrounding the cells and/or a mechanical modification of the cell wall. Such stimuli might be the trigger for a gene expression change connected to the inducible mechanisms at the basis of *Trebouxia gelatinosa* response to desiccation. The aim of this study was to deepen the knowledge on *T. gelatinosa* desiccation tolerance.

In studying plant responses to desiccation, the assessment of the water status is essential as most of the anatomical, physiological and biochemical alterations occur when the water content decreases below a certain level. Hence, in this work, WC, RWC and Ψ were used to describe the water status of the *T. gelatinosa* cells. WC provides a measurement of the quantity of water available per unit of dry mass [48], RWC expresses WC in % at a given time as related to the WC at full turgor [49], while Ψ is important for the assessment of the water deficit and turgor loss point [29].

Part of the WC of fully hydrated *T. gelatinosa* is extracellular/apoplastic [50]; a similar water storage is commonly found in lichens [51] and in *Trebouxia sp.* [32]. In these organisms, considerable water can be lost before the water potential falls sufficiently to affect metabolism [52]. Based on the PV curves, Ψ_{tlp} of *T. gelatinosa* was ~ -4 MPa, a value also recorded by Petruzzellis et al. [23], when studying the lichen *Flavoparmelia caperata* and its isolated photobiont, i.e. the same alga studied here. The authors suggested that the turgor state influences the functionality of photosynthetic process in lichens and algae, and thus it might have a role also in the desiccation tolerance of *T. gelatinosa*.

In this work, ten and eight out of ten genes showed significant expression changes right before and after the turgor loss, respectively. Seven and five out of ten genes showed significant expression changes right before and after reaching the desiccated state (RWC ~ 1 %), respectively.

Regarding the turgor loss, the major change in terms of up-regulation in the proximity of this moment was recorded in the expression of the gene coding for the cell wall protein expansin. When a plant cell loses water, the most evident result is a reduction of cell volume [53]: this can lead to a mechanical stress [53], due to the tension between the cell wall and the plasma membrane, occurring when turgor pressure is lost [54]. Tackling this stress efficiently seems to be decisive for DT plants [55]. Cell wall features, like composition, thickness, and presence of extracellular polysaccharides (EPS), are found to play a significant role in the desiccation tolerance of green algae, *Trebouxia* included [34, 56], as they avoid or retard desiccation [52]. When a cell shrinks, cell wall plasticity has a crucial role for the maintenance of its integrity. Cell wall extensibility depends on the underlying structure and on the activity of wall-modifying proteins, like expansins [57]. These proteins disrupt the bonds between non-covalent wall polysaccharides and have a role in the loosening of the cell wall [54, 58]. Expansin genes in general have been found to be up-regulated by abiotic stress conditions such as desiccation, osmotic stress and salinity [59]; an up-regulation of expansin expression was found in the DT plant *C. plantagineum* during both desiccation and rehydration [58]. Candotto Carniel et al. [11] proposed that expansins have a key role also in desiccation tolerance of *T. gelatinosa*, since they found a significant up-regulation in rehydrated *T. gelatinosa* colonies, while in the desiccated state the expression was stable. The flexibility of the cell wall is particularly important to prevent the mechanical stress at turgor loss [60]. The connection between water loss and cell wall has been investigated both in higher plants (see [54] and reference within) and in green algae [61]. In green algae desiccation leads to a shrinkage process, which is particularly spectacular in the sub-spherical cells of *Trebouxia* with important effects on cell ultrastructure [12].

In the alga investigated here, the major down-regulation before turgor loss occurred for the HSP70 gene. The expression of HSP70 significantly increased when RWC diminished under the threshold of 10 %. In higher eukaryotes, including plants, HSP70s are stress-inducible proteins [62]. They have a crucial role in protecting living organisms from environmental stresses and support correct protein folding under stress conditions [63]. A down-regulation of HSP70 gene expression in desiccated *T. gelatinosa* was already documented [11]. Decreased expression of members of the HSP70 gene family was also recorded during desiccation in the DT moss *Physcomitrella patens* [64], and for oxidative stress and heavy metal exposure in *Trebouxia sp.* [39, 65, 66]. Although the mechanisms of HSP70 function under stress conditions are not fully understood [62], the up-regulation of HSP70 genes generally determines higher tolerance to abiotic stress in plants [62, 67]:

for this reason, HSP70 down-regulation as observed in *T. gelatinosa* still needs to be clarified. A change in plant HSP70 expression has been linked to the induction of Ca^{2+}/calmodulin (CaM) genes [68]. Another pathway could include mitogen activated protein kinases (MAPK) that are involved in signal transduction and in signaling of plant abiotic stress [69]. Despite significant changes in mRNA level, the HSP70 protein levels remained stable during desiccation (Fig. 3): it is known that mRNA abundance and protein level may have a low correlation [70]. The accumulation/reduction of mRNA during water deficit may indicate gene induction or repression, but further regulatory mechanisms, such as translational and post-translational modifications, could be necessary [71]. Moreover, while it has been shown that in DT dry seeds low WC does not inhibit transcription, for translation contrasting results have been obtained [72]. Further investigations are required to clarify the role of molecular chaperones in *T. gelatinosa*; however, the constitutive protein expression of HSP70 seems to be required during water stress.

Generally, in plants and green algae photosynthesis is suppressed by desiccation as a protective mechanism [12]. A decrease in photosynthesis was recorded in *Trebouxia sp.* at low (15-3 %) RWC [32]. Furthermore, Petruzzellis et al. [23] found that in *T. gelatinosa* desiccation, photosynthesis decreased more markedly after Ψ_{tlp}. At transcriptomic level, however, an increase of photosynthesis-related transcripts (including LCHII) in the desiccated state was detected in *T. gelatinosa* [11]. In our study, LCHII was down-regulated before turgor loss, and in the desiccated state it returned to the T0 level (Fig. 2). This different behavior could be due to the different desiccation rate, which is important for the recovery of photosynthesis in another lichen photobiont species, *Asterochloris erici* [73], taxonomically near to the genus *Trebouxia*.

In both vascular and non-vascular plants including green algae, one of the most important effects of desiccation is the oxidative burst related to reactive oxygen species (ROS) production, which damage cellular structures [1, 12]. In *Trebouxia sp.,* an increased ROS production during desiccation was demonstrated by histochemical localization [44, 74]. In lichens and their photobionts, the anti-oxidant protection seems to be constitutive [1, 11]. In our work, the transcript level, both MnSOD and APX were up-regulated at the beginning of desiccation, when extracellular water was still present, but then they were down-regulated immediately before and after turgor loss. Interestingly, the expression increased when the RWC had reached ~ 1 % (Fig. 2). A decrease of antioxidant enzyme activities including SOD, catalase (CAT), and APX was recorded during desiccation in both lichens [75] and their photobionts [73].

Among the numerous and highly diversified DRPs found in *T. gelatinosa* [11], here we analyzed the most desiccation-responsive ones in terms of fold change. The response of these genes showed all the same trend, as all the five analyzed transcripts (DRP1, DRP2, DRP6, DRP11, DRP13)

remained stable at the beginning of desiccation and had a peak of expression before turgor loss (Fig. 2). DRP1 and DRP2 expression profiles differ from the one found in Candotto Carniel et al. [11], as their expression was not down- but up-regulated in the desiccated state. It could be possible that in Candotto Carniel et al. [11] these genes were early and transiently up-regulated; DRPs and other stress-induced genes can show highest expression in partial desiccation stages. Furthermore, as the predicted cellular localization of these proteins is "secreted" [11], the secretory pathways involved could have a role in the different regulation of these DRPs. DRPs in plants are involved in numerous processes, including drought tolerance [35, 36], and their transcripts are frequently up-regulated during desiccation [76]. Even if a clear explanation for the role of DRPs during desiccation is still missing, the presence of the ferritin-like domain suggests a relation with oxidative stress protection [77]. Expression of DRPs in *T. gelatinosa* was not responsive to oxidative stress caused by hydrogen peroxide (H_2O_2; [51]); the hypothesis of a stress specific response is intriguing, and deserves more investigations. If the role of the *T. gelatinosa* DRPs is at the cell wall or apoplast level, early activation of gene expression should permit the protein to accumulate in the apoplastic space to carry out biochemical functions, such as the protection of cell wall from mechanical stress generated late during desiccation.

Conclusions

Plants respond to stress with specific changes in gene expression, metabolism, and physiology, and this indicates the ability to sense environmental stress conditions [78]. From our analysis it is clear that the time points just before and after the turgor loss and the desiccated state (RWC ~ 1 %) are key points in terms of gene expression in the response of *T. gelatinosa*. Each of them induced a response in terms of up- or down-regulation of specific genes, which implies a finely regulated perception of water stress. The study provides important evidence for the involvement of DRPs in desiccation tolerance of the green microalga, which is one of the most common lichen photobionts.

Acknowledgements

The activity of E.B. was partially funded by the Italian Government Commission with "Fondo Trieste". We thank Dr. S. Bertuzzi (Trieste, I) for help in the laboratory and Prof. Dr. Höhfeld (University of Bonn, D) for HSP70 antiserum.

Appendix A. Supplementary data

Supplementary data associated with this article can be found in the on line version.

References

[1] I. Kranner, R. Beckett, A. Hochman, TH III Nash, Desiccation-tolerance in lichens: a review, Bryologist 111 (2008) 576-593.
[2] J.M. Farrant, K. Cooper, H. Nell, Desiccation tolerance, in: S. Shabala (Ed.), Plant Stress Physiology, CABI Publishing, Cambridge, 2012, pp. 238-226.
[3] B. Fernàndez-Marin, A. Holzinger, J.I. Garcia-Plazaola, Photosynthetic strategies of desiccation-tolerant organisms, in M. Pessarakli (Ed.), Handbook of Photosynthesis, CRC Press, Boca Raton, Florida, USA, pp. 719-737.
[4] P. Alpert, Commentary constraints of tolerance: why are desiccation-tolerant organisms so small or rare? J. Exp. Biol. 209 (2006) 1575-1584.
[5] A. Nardini, A. Marchetto, M. Tretiach, Water relations parameters of six *Peltigera* species correlate with their habitat preferences, Fungal Ecol. 6 (2013) 397-407.
[6] U. Lüttge, B. Büdel, Resurrection kinetics of photosynthesis in desiccation-tolerant terrestrial green algae (Chlorophyta) on tree bark, Plant Biol. 12 (2010) 437-444.
[7] D.L. Hawksworth, P.M. Kirk, B.C. Sutton, D.N. Pegler, Ainsworth & Bisby's Dictionary of the Fungi, CAB International Eds., Wallingford, 1995.
[8] T. Friedl, Comparative ultrastructure of pyrenoids in *Trebouxia* (Microthamniales, Chlorophyta), Plant Syst. Evol. 164 (1989) 145-159.
[9] I. Kranner, R.P. Beckett, S. Wornik, M. Zorn, H.W. Pfeifhofer, Revival of a resurrection plant correlates with its antioxidant status, Plant J. 31 (2002) 13-24.
[10] F. Gasulla, K. Dorp, I. Dombrink, U. Zähringer, N. Gisch, P. Dörmann, D. Bartels, The role of lipid metabolism in the acquisition of desiccation tolerance in *Craterostigma plantagineum*: a comparative approach, Plant J. 75 (2013) 726-741.
[11] F. Candotto Carniel, M. Gerdol, A. Montagner, E. Banchi, G. De Moro, C. Manfrin, L. Muggia, A. Pallavicini, M. Tretiach, New features of desiccation tolerance in the lichen photobiont *Trebouxia gelatinosa* are revealed by a transcriptomic approach, Plant Mol. Biol. 91 (2016) 319-339.
[12] A. Holzinger, U. Karsten, Desiccation stress and tolerance in green algae: consequences for ultrastructure, physiological and molecular mechanisms, Front. Plant Sci. 4 (2013).
[13] T.S. Gechev, C. Dinakar, M. Benina, V. Toneva, D. Bartels, Molecular mechanisms of desiccation tolerance in resurrection plants, Cell Mol. Life Sci. 69 (2012) 3175-3186.
[14] C. Dinakar, D. Djilianov, D. Bartels, Photosynthesis in desiccation tolerant plants: energy metabolism and antioxidative stress defense, Plant Sci. 182 (2012) 29-41.
[15] I. Kranner, W.J. Cram, M. Zorn, S. Wornik, I. Yoshimura, E. Stabentheiner, H.W. Pfeifhofer, Antioxidants and photoprotection in a lichen as compared with its isolated symbiotic partners, P. Nat. Acad. Sci. USA 102 (2005) 3141-3146.
[16] A. Holzinger, C. Lütz, U. Karsten, Desiccation stress causes structural and ultra-structural alterations in the aeroterrestrial green alga *Klebsormidium crenulatum* (Klebsormidiophyceae, Streptophyta) isolated from an alpine soil crust, J. Phycol. 47 (2011) 591-602.
[17] I. Lang, S. Sassmann, B. Schmitt, G. Komis, Plasmolysis: loss of turgor and beyond, Plants. 3 (2014) 583-593.
[18] C. Dinakar, J.T. Puthur, D. Bartels, Surviving metabolic arrest: photosynthesis during desiccation and rehydration in resurrection plants, Ann. N. Y. Acad. Sci. 1365 (2016) 89-99.

[19] O.L. Lange, T.A. Green, A. Meyer, H. Zellner, Water relations and carbon dioxide exchange of epiphytic lichens in the Namib fog desert, Flora 202 (2007) 479-487.
[20] B. Hartard, M. Cuntz, C. Máguas, M. Lakatos, Water isotopes in desiccating lichens, Planta 231 (2009) 179-193.
[21] L. González, Determination of water potential in leaves, in M.J. Reigosa Roger (Ed.), Handbook of Plant Ecophysiology Techniques, Kluwer Academic Publishers, Dordrecht, 2001, pp. 193-206.
[22] T.I. Lenz, I.J. Wright, M. Westoby, Interrelations among pressure–volume curve traits across species and water availability gradients, Physiol. Plant. 127 (2006) 423-433.
[23] F. Petruzzellis, T. Savi, S. Bertuzzi, A. Montagner, M. Tretiach, A. Nardini, Relationships between water status and photosystem functionality in a chlorolichen and its isolated photobiont, Planta (2017) 1-10.
[24] M.T. Tyree, H.T. Hammel, The measurement of the turgor pressure and the water relations of plants by the pressure-bomb technique, J. Exp. Bot. 23 (1972) 267-282.
[25] Y. Ding, Y. Zhang, Q.S. Zheng, M.T. Tyree, Pressure–volume curves: revisiting the impact of negative turgor during cell collapse by literature review and simulations of cell micromechanics, New Phytol. 203 (2014) 378-387.
[26] M.K. Bartlett, C. Scoffoni, R. Ardy, Y. Zhang, S. Sun, K. Cao, L. Sack, Rapid determination of comparative drought tolerance traits: using an osmometer to predict turgor loss point, Methods Ecol. Evol. 3 (2012) 880-888.
[27] A. Nardini, G. Pedà, G., N.L. Rocca, Trade-offs between leaf hydraulic capacity and drought vulnerability: morpho-anatomical bases, carbon costs and ecological consequences, New Phytol. 196 (2012) 788-798.
[28] I. Maréchaux, M.K. Bartlett, L. Sack, C. Baraloto, J. Engel, E. Joetzjer, J. Chave, Drought tolerance as predicted by leaf water potential at turgor loss point varies strongly across species within an Amazonian forest, Funct. Ecol. 29 (2015) 1268-1277.
[29] M.J. Oliver, J.C. Cushman, Dehydration tolerance in plants, in R. Sunkar (Ed.), Plant Stress Tolerance: Methods and Protocols, Humana Press, 2010, pp. 3-24.
[30] M. Black, H.W. Pritchard, Desiccation and Survival in Plants: Drying Without Dying, Cabi, Wallingford, 2002.
[31] R.P. Beckett, F.V. Minibayeva, Rapid breakdown of exogenous extracellular hydrogen peroxide by lichens, Physiol. Plant. 129 (2007) 588-596.
[32] F. Candotto Carniel, D. Zanelli, S. Bertuzzi, M. Tretiach, Desiccation tolerance and lichenization: a case study with the aeroterrestrial microalga *Trebouxia* sp. (Chlorophyta), Planta 242 (2015) 493-505.
[33] M.J. Oliver, J. Velten, B.D. Mishler, Desiccation tolerance in bryophytes: a reflection of the primitive strategy for plant survival in dehydrating habitats? Integr. Comp. Biol. 45 (2005) 788-799.
[34] D.C. Centeno, A.F. Hell, M.R. Braga, E.M. Del Campo, L.M. Casano, Contrasting strategies used by lichen microalgae to cope with desiccation–rehydration stress revealed by metabolite profiling and cell wall analysis, Environ. Microb. 18 (2016) 1546-1560.
[35] D. Bartels, K. Schneider, G. Terstappen, D. Piatkowski, F. Salamini, Molecular cloning of abscisic acid-modulated genes which are induced during desiccation of the resurrection plant *Craterostigma plantagineum*, Planta 181 (1990) 27-34.
[36] D. Piatkowski, K. Schneider, F. Salamini, D. Bartels, Characterization of five abscisic acid responsive cDNA clones isolated from the desiccation-tolerant plant *Craterostigma plantagineum* and

their relationship to other water-stress genes, Plant Physiol. 94 (1990) 1682-1688.
[37] Y. Yamamoto, Y. Kinoshita, I. Yoshimura, Photobiont Culturing, in: I. Kranner, R.P. Beckett, A.K. Varma (Eds.), Protocols in Lichenology. Culturing, Biochemistry, Ecophysiology and Use in Biomonitoring, Springer, Heidelberg, Germany, 2002, pp 34-42.
[38] V. Ahmadjian, Methods of isolation and culturing lichen symbionts and thalli, in: V. Ahmadjian, M.E. Hale (Eds.), The Lichens, Academic Press, New York, USA, 1973, pp. 653-660.
[39] A. Montagner, Ecotoxicological effects of Graphene-Based Materials, Ph.D. thesis, University of Trieste (2017).
[40] A. Untergasser, H. Nijveen, X. Rao, T. Bisseling, R. Geurts, J.A.M. Leunissen, Primer3Plus, an enhanced web interface to Primer3, Nucleic Acids Res. 35 (2007) 71-74.
[41] K.J. Livak, T.D. Schmittgen, Analysis of relative gene expression data using real-time quantitative PCR and the 2(-Delta Delta C(T)) method, Methods 25 (2001) 402-408.
[42] U.K. Laemmli, Cleavage of structural proteins during the assembly of the head of bacteriophage T4, Nature 227 (1970) 680-685.
[43] B.D. Zehr, T.J. Savin, R.E. Hall, A one-step, low background Coomassie staining procedure for polyacrylamide gels, Anal. Biochem. 182 (1989) 157-159.
[44] C. Dinakar, D. Bartels, Light response, oxidative stress management and nucleic acid stability in closely related Linderniaceae species differing in desiccation tolerance, Planta 236 (2012) 541-555.
[45] A. Ulbricht, F.J. Eppler, V.E. Tapia, P.F.M. van der Ven, N. Hampe, N. Hersch, P. Vakeel, D. Stadel, A. Haas, P. Saftig, C. Behrends, D.O. Fürst, R. Volkmer, B. Hoffmann, W. Kolanus, J. Höhfeld, Cellular mechanotransduction relies on tension-induced and chaperone-assisted autophagy, Curr. Biol. 23 (2013) 430-435.
[46] R Development Core Team, R: A language and environment for statistical computing, R Foundation for Statistical Computing, Vienna, Austria, 2015.
[47] S.J. Neill, E.C. Burnett, Regulation of gene expression during water deficit stress, Plant Growth Regul. 29 (1999) 23-33.
[48] D. Mullan, J. Pietragalla, Leaf relative water content, in: A.J.D. Pask, J. Pietragalla, D. Mullan, M. Reynolds (Eds.), Physiological breeding II: A field guide to wheat phenotyping, CIMMYT, Mexico, 2012, pp. 25-27.
[49] L. González, M. González-Vilar, Determination of relative water content, in: M.J. Reigosa Roger (Ed.), Handbook of plant ecophysiology techniques, Springer, Netherlands, 2001, pp. 207-212.
[50] M.C.F. Proctor, Physiological ecology, in: B. Goffinet, A.J. Shaw (Eds.), Bryophyte biology. Cambridge University Press, Cambridge, 2008, pp. 237-268.
[51] T.G.A. Green, O.L. Lange, Photosynthesis in poikilohydric plants: a comparison of lichens and bryophytes, in: E.D. Schulze, M.M. Caldwell (Eds.), Ecophysiology of photosynthesis, Springer, Berlin Heidelberg, 1995, pp. 319-341.
[52] M.C.F. Proctor, Z. Tuba, Poikilohydry and homoiohydry: antithesis or spectrum of possibilities? New Phytol. 156 (2002) 327-349.
[53] J.M. Farrant, A comparison of mechanisms of desiccation tolerance among three angiosperm resurrection plant species, Plant Ecol. 151 (2000) 29-39.
[54] J.P. Moore, M. Vicré-Gibouin, J.M. Farrant, A. Driouich, Adaptations of higher plant cell walls to water loss: drought vs desiccation, Physiol. Plant. 134 (2008) 237-245.
[55] W.S. Iljin, Drought resistance in plants and physiological processes, Ann. Rev. Plant Biol. 8 (1957) 257-274.

[56] Z.A. Popper, M.C. Ralet, D.S. Domozych, Plant and algal cell walls: diversity and functionality, Ann. Bot. 114 (2014) 1043-1048.
[57] S. McQueen-Mason, D.M. Durachko, D.J. Cosgrove, Two endogenous proteins that induce cell wall extension in plants, Plant Cell. 4 (1992) 1425-1433.
[58] L. Jones, S. McQueen-Mason, A role for expansins in dehydration and rehydration of the resurrection plant *Craterostigma plantagineum*, FEBS Lett 559 (2004) 61-65.
[59] R. Tenhaken, Cell wall remodeling under abiotic stress, Front. Plant Sci. 5 (2015) 771.
[60] M.R. Zhao, F. Li, Y. Fang, Q. Gao, W. Wang, Expansin-regulated cell elongation is involved in the drought tolerance in wheat, Protoplasma 248 (2011) 313-323.
[61] A. Holzinger, M. Pichrtová, Abiotic stress tolerance of charophyte green algae: new challenges for omics techniques, Front. Plant Sci. 7 (2016).
[62] W. Wang, B. Vinocur, O. Shoseyov, A. Altman, Role of plant heat-shock proteins and molecular chaperones in the abiotic stress response, Trends Plant Sci. 9 (2004) 244-252.
[63] A. Yu, P. Li, T. Tang, J. Wang, Y. Chen, L. Liu, Roles of Hsp70s in stress response of microorganisms, plants, and animals. Biomed Res. Int. (2015) 510319.
[64] T. Tang, A. Yu, P. Li, H. Yang, G. Liu, L. Liu, Sequence analysis of the Hsp70 family in moss and evaluation of their functions in abiotic stress responses, Sci. Rep. 6 (2016).
[65] M. Bačkor, A. Gibalová, J. Bud'ová, J. Mikeš, P. Solár, Cadmium-induced stimulation of stress-protein hsp70 in lichen photobiont *Trebouxia erici*, Plant Growth Regul. 50 (2006) 159-164.
[66] A. del Hoyo, R. Álvarez, E.M. del Campo, F. Gasulla, E. Barreno, L.M. Casano, Oxidative stress induces distinct physiological responses in the two *Trebouxia* phycobionts of the lichen *Ramalina farinacea*. Ann. Bot. 107 (2010) 109-118.
[67] D. Bartels, R. Sunkar, Drought and salt tolerance in plants, Crit. Rev. Plant Sci. 24 (2005) 23-58.
[68] J.H. Wu, L.C. Hong, Y.Y. Tsai, H.W. Chen, W.X. Chen, T.S. Wu, Mitogen activated protein kinase (MAPK) signalling pathways in HepG2 cells infected with a virulent strain of *Klebsiella pneumoniae*, Cell. microbiol. 8 (2006) 1467-1474.
[69] A.K. Sinha, M. Jaggi, B. Raghuram, N. Tuteja, Mitogen activated protein kinase signaling in plants under abiotic stress, Plant Signal. Behav. 6 (2011) 196-203.
[70] D.A. Day, M.F. Tuite, Post-transcriptional gene regulatory mechanisms in eukaryotes: an overview, J. Endocrinol. 157 (1998) 361-371.
[71] E.A. Bray, Plant responses to water deficit, Trends Plant Sci. 2 (1997) 48-54.
[72] B. Fernández-Marín, I. Kranner, M.S. Sebastián, U. Artetxe, J.M. Laza, J.L. Vilas, H.W. Pritchard, J. Nadajaran, F. Mìguez, J.M. Becerril, J.I. García-Plazaola, Evidence for the absence of enzymatic reactions in the glassy state. A case study of xanthophyll cycle pigments in the desiccation-tolerant moss *Syntrichia ruralis*, J. Exp. Bot. 64 (2013) 3033-3043.
[73] F. Gasulla, P.G. de Nova, A. Esteban-Carrasco, J.M. Zapata, E. Barreno, A. Guéra, Dehydration rate and time of desiccation affect recovery of the lichenic algae *Trebouxia erici*: alternative and classical protective mechanisms, Planta 231 (2009) 195-208.
[74] M. Catalá, F. Gasulla, A.E.P. del Real, F. García-Breijo, L. Reig-Armiñana, E. Barreno, Fungal-associated NO is involved in the regulation of oxidative stress during rehydration in lichen symbiosis, BMC microbiol. 10 (2010) 297.
[75] N. Mayaba, R.P. Beckett, The effect of desiccation on the activities of antioxidant enzymes in lichens from habitats of contrasting water status, Symbiosis 31 (2001) 113-121.

[76] H.G. Zha, T. Liu, J.J. Zhou, H. Sun, MS-desi, a desiccation-related protein in the floral nectar of the evergreen velvet bean (*Mucuna sempervirens* Hemsl): molecular identification and characterization, Planta 238 (2013) 77-89.
[77] W. Liang, Y. Zhou, L. Wang, X. You, Y. Zhang, C.L. Cheng, W. Chen, Ultrastructural, physiological and proteomic analysis of *Nostoc flagelliforme* in response to dehydration and dehydration, J. Proteomics 75 (2012) 5604-5627.
[78] J.K. Zhu, Abiotic stress signalling and responses in plants, Cell, 167 (2016) 313-324.

Supplementary material

Table A.1. Primers for quantitative real-time PCR analysis.

Gene	Primers	Forward sequence	Reverse sequence	Reference
Ascorbate peroxidase	APX	CAGGGTTCACAAGGACAGGT	TCAGCAAACAGGCACTCATC	[39]
Desiccation related protein 1	DPR1	CAAAATGGCGATGTTGTCAC	CAACGTTGAAGATGCCAATG	This study
Desiccation related protein 2	DPR2	AAATTGCCCACGTCAACTTC	GAGGAGCAGCACCCTTGTAG	This study
Desiccation related protein 6	DPR6	CCAGATCGACCTCTCTGCTC	GCCAACAGGGTCTTGTCAGT	This study
Desiccation related protein 11	DPR11	CATATGGCGAGGGTATTGCT	TGTGCGATTTCATTCTCAGC	[39]
Desiccation related protein 13	DPR13	AGGACATCAGACAGGGATGG	AATTGCCAACAAAGCCAAAC	This study
Expansin 1	EXP1	GACAGGACTCCAGCTTTTGC	CTGAGGGGAGATGACGTTGT	[11]
Heat shock protein 70	HSP70	CAGTCACCACTGCCTTCTCA	CAAGTCAGCCAATGCAAAGA	[39]
Light harvesting complex II	LHCII	CTGATGACCCAGATGCCTTT	GGTCCTTTGCCTGTCACAAT	[11]
Mn-superoxide dismutase	MnSOD	CACCCAGCTTGCTGACTACA	GGTCAAACTGTGCCTGGAAT	[39]
Ribosomal protein L6	RPL6	AGGAGCTAGCTAGGGGCATC	TCTCGTGCTTTGGGAACTCT	[11]

EFFECTS OF GRAPHENE-BASED MATERIALS ON THE AEROTERRESTRIAL MICROALGA *TREBOUXIA GELATINOSA*: FOCUS ON INTERNALIZATION AND OXIDATIVE STRESS

Alice Montagner[1†], **Elisa Banchi**[1†], Fabio Candotto Carniel[2], Cristina Martín[3,4], Susanna Bosi[2], Alberto Pallavicini[1], Ester Vázquez[3,4], Mauro Tretiach[1*] and Maurizio Prato[2,5,6]

[1]Dipartimento di Scienze della Vita, Università degli Studi di Trieste, 34127, Trieste, Italy
[2]Dipartimento di Scienze Chimiche e Farmaceutiche, Università degli Studi di Trieste, 34127, Trieste, Italy
[3]Departamento de Química Orgánica, Facultad de Ciencias y Tecnologías Químicas, Universidad de Castilla-La Mancha, 13071, Ciudad Real, Spain
[4]Instituto Regional de Investigación Científica Aplicada (IRICA), Universidad de Castilla-La Mancha, 13071, Ciudad Real, Spain
[5]Carbon Nanobiotechnology Laboratory, CIC biomaGUNE, 20009, San Sebastian (Spain)
[6]Basque Fdn Sci, Ikerbasque, 48013, Bilbao, Spain

[†]These authors contributed equally to this work.

*Corresponding author: Mauro Tretiach

Main abbreviations

APX: ascorbate peroxidase
CAT: catalase
Chl_aF: chlorophyll a fluorescence
CLSM: confocal laser scanning microscopy
DRP: desiccation related protein
FLG: few-layers graphene
F_v/F_m: maximum quantum yield of PSII photochemistry
GBM: graphene-based material
GO: graphene oxide
GR: gluthatione reductase
H_2O_2: hydrogen peroxide
HSC: heat shock cognate
HSP: heat shock protein

LHCII: chlorophyll a-b binding protein of the light harvesting complex II
Mn-SOD: manganese superoxide dismutase
PS: photosystem
qRT-PCR: quantitative real-time PCR
ROS: reactive oxygen species
RPL6: ribosomal protein L6

Key words: graphene, green algae, internalization, oxidative stress, ecotoxicity, HSP70, cell wall.

Originality – Significance Statement

This work contributes new knowledge on the interaction between Graphene-Based Materials (GBMs) and aeroterrestrial green microalgae. It is the first to assess the effects on GBMs on a lichen photobiont, *Trebouxia gelatinosa*, integrating different disciplines and approaches. The work is significant, as it demonstrates non-harmful interaction between *T. gelatinosa* and both few-layers graphene (FLG) and graphene oxide (GO). Our results are important in the view of the environmental safety assessment and management of GBMs in terrestrial ecosystems.

Summary

The exposure effects of two Graphene-Based Materials (GBMs), few-layers graphene (FLG) and graphene oxide (GO), have been studied in the aeroterrestrial green microalga *Trebouxia gelatinosa*. Algal suspensions without GBMs and with FLG or GO at the concentration of 50 μg mL^{-1} were shaken for 10 and 30 minutes. After exposure, GBMs internalization was investigated with confocal microscopy and Raman spectroscopy. Potential oxidative effects of GBMs in comparison to H_2O_2, used as positive controls, were studied analyzing (*i)* the quantum yield of primary photochemistry in the dark-adapted state (F_v/F_m), (*ii)* changes of gene expression of eight genes of interest, and (*iii)* quantification of heat shock protein 70 (HSP70). GO was not clearly detected inside the cells, despite it was observed in close contact with them, whereas FLG was detected within the cells when different laser power densities were used. While H_2O_2 treatments produced dose- and time-dependent oxidative effects, GO was ineffective, and FLG caused the down-regulation of a single gene (HSP70). However, this did not correspond to a decrease in the quantity of HSP70 protein. The results suggest that harmless interactions occurred between GBMs and plasma membrane inside the algal cell wall, which were more intense for FLG than for GO.

Introduction

In the recent years, the rapid advancement in the field of nanomaterials has increased their development and consequently their production and commercialization. Among nanomaterials, the carbon-based ones are the most widely researched because of their potential on the most diverse fields (Lalwani *et al.*, 2016), with a predominant role occupied by Graphene-Based Materials (GBMs) (Novoselov *et al.*, 2012). Graphene is a two-dimensional crystal composed of monolayers of carbon atoms arranged in a honeycombed network with six-membered rings (Geim and Novoselov, 2007). Since its discovery, the attention of researchers was focused on its unique and exceptional properties, such as mechanical stiffness, strength, elasticity, very high electrical and thermal conductivity. This led to the development of multiple applications in electronics, photonics, composite materials, energy generation and storage, sensors and metrology and biomedicine (Novoselov *et al.*, 2012). The huge investments brought to an incredible advancement in the industrial field, unfortunately accompanied by a slower progress in the understanding of the impact on human health and the environment, hence making nanosafety a priority (Savolainen *et al.*, 2013).

So far, the effects of GBMs have been evaluated mostly on animal and bacterial model organisms (Montagner *et al.*, 2017), highlighting that GBMs toxicity seems to depend on various physiochemical properties such as shape, size, oxidative state and presence of functional groups (Sanchez *et al.*, 2011; Jastrzębska *et al.*, 2012; Seabra *et al.*, 2014). In particular, these properties affect also the graphene ability to cross cell membranes.

In animal cells, GBMs were frequently observed being internalized through many different endocytosis pathways. For example, graphene oxide (GO) sheets were found either surrounded by membranes into endosome-like structures or free in the cytoplasm (Russier *et al.*, 2013). Furthermore, internalization of graphene quantum dots (GQD) by caveolae-mediated endocytosis have been observed in breast cancer MCF-7 cells (Wu *et al.*, 2013). Despite GBMs uptake in both the previously mentioned studies led to toxicity, a carboxyl functionalization allowed graphene to enter the cells without causing any toxic effect (Sasidharan *et al.*, 2011). For this reason, GBMs could also be successfully used as nano-carriers for selective drug delivery (Bitounis *et al.*, 2013).

Differently from animals, bacteria, fungi and plants have cells surrounded by a cell wall of different nature which is the first site of interaction with GBMs but also the primary barrier preventing GBMs uptake (Navarro *et al.*, 2008).

The most widely used species for studying GBMs and bacteria interactions is certainly *Escherichia coli* (Akhavan and Ghaderi, 2010; Akhavan and Ghaderi, 2012), although more recently also *Pseudomonas putida* (Combarros et *al.*, 2016) and *Staphylococcus aureus* (Palmieri *et al.*, 2017) have been investigated. During the interaction with GO, different inhibition levels are provoked

(Szunerits and Boukherroub, 2016). Physical interactions between bacteria and GBMs include surface adhesion and membrane piercing (Romero-Vargas Castrillón *et al.*, 2015). Cell internalization has been shown to be the key mechanism that leads to cell intoxication (Akhavan and Ghaderi, 2010; Kostarelos and Novoselov, 2014). GO characteristics, including concentration, incubation time, type of bacteria (Gram − or Gram +), influence the degree of inhibition (Combarros *et al.*, 2016). In general, bacterial inhibition caused by this GBM were mainly due to oxidative stress and/or damage of the cell membrane (Combarros *et al.*, 2016).

Regarding plants, it has been shown that nanoparticles smaller than the pore size of the cell wall are able to enter into the plant cell (Navarro *et al.*, 2008) and that GO with a lateral dimension of 500 nm is internalized in *Arabidopsis thaliana* T87 cells by a non-energy dependent endocytosis, while larger sheets of about 1 μm by phagocytosis (Begum and Fugetsu, 2013). In both cases, internalization caused decreased mitochondrial function and eventually cell death (Begum and Fugetsu, 2013). By contrast, in another research, GO internalization did not influence *A. thaliana* germination, seed development, shoot and root development of seedlings and flowering time (Zhao *et al.*, 2015). Obviously, GBMs internalization plays a key role in cell toxicity (Zhou and Gao, 2014), although in plant cells this phenomenon has not been investigated in detail.

Aeroterrestrial microalgae are a cosmopolitan cluster naturally occurring on a variety of substrates (wet soils, rocks, man-mane substrata, tree bark) (Lüttge and Büdel, 2010), colonizing the most diverse environments (Belnap *et al.*, 2001; Freystein and Reisser, 2010). Some of them (*e.g.* the genus *Trebouxia* - Chlorophyta) are able to form a stable symbiotic association with fungi (usually ascomycetes) through lichenization (Hawksworth *et al.*, 1995; Candotto Carniel *et al.*, 2015).

Microalgae in general have been broadly employed to study nanoparticles toxicity, turning out to be important organisms to study internalization and its effects. The cell walls of these organisms are very different in thickness and composition, often with peculiar species-specific characteristics (Domozych *et al.*, 2012). Some of them may have very thick cell walls, like that of *Apatococcus lobatus*, which can be more than 2 μm thick (Gärtner and Ingolić, 1989). Cell wall has an important role in the control of algal water status, and contributes in their desiccation tolerance (Popper *et al.*, 2011). So far, GBMs internalization has been reported in the green algae *Chlorella pyrenoidosa* (Zhao *et al.*, 2017) and *C. vulgaris* (Hu *et al.*, 2014; Hu *et al.*, 2015; Ouyang *et al.*, 2015). In the former study, the authors claimed that only multi-layer graphene (MG) and reduced graphene oxide (rGO) entered the cells, while GO did not. Some researchers demonstrated that internalization of GBMs in general is linked to the production of ROS or to the increase of oxidative stress (Ouyang *et al.*, 2015). Oxidative stress is one of the main toxic effects induced by GBMs on microorganisms (Zhang *et al.*, 2012; Yan *et al.*, 2013), together with mechanical damage (Akhavan and Ghaderi, 2010) and cell

wrapping by the GBMs flakes (Akhavan *et al.*, 2011; Hu *et al.*, 2015). Normal cellular redox homeostasis is a balance between ROS generation and their elimination or reduction by the antioxidative defences. Most stress factors have in common that they increase the ROS production/development in organisms, hence unbalancing the cell redox status. Thus, an uncontrolled ROS accumulation can cause membrane peroxidation, protein cleavage, and DNA strand breakage (Yan *et al.*, 2013), which in the worst case can lead to cell death. The studies conducted so far had showed that poikilohydric aeroterrestrial microalgae, *i.e.* those algae which are able to survive deep desiccation, resuming the normal metabolism in some minutes as soon as water becomes available again, possess a constitutive antioxidant machinery which is able to scavenge the "oxidative burst" in minutes after its insurgence (Weissman *et al.*, 2005; Candotto Carniel *et al.*, 2016); however, oxidative stress response on these ecological important organisms has been still poorly investigated.

The aim of the study was to analyze GBMs internalization and the effects on physiology and gene transcription of a short-term exposure to two GBMs, few-layers graphene (FLG) and graphene oxide (GO), selected as reference materials by the Working Package 4, Health and Environment, in the framework of the European Project Graphene-Flagship. Among photoautotrophic organisms, we selected the aeroterrestrial microalga *Trebouxia gelatinosa* Archibald, which is a member of the most widespread genus of lichenized algae (Ahmadjian, 2004), which can be found also living in the free state in complex algal biofilms on tree bark (Lüttge and Büdel, 2010), demonstrating its relevant ecological importance. *T. gelatinosa* proved to be a resistant organism towards several stresses including desiccation (Candotto Carniel *et al.*, 2016). Moreover, *T. gelatinosa* transcriptome was recently published (Candotto Carniel *et al.*, 2016), allowing to design specific primers for the analysis of gene expression. After a short-term exposure, we evaluated whether (*i*) GBMs are internalized by *T. gelatinosa* cells, (*ii*) GBMs exposure induces oxidative stress response and (*iii*) increases algal mortality, through confocal laser scanning microscopy (CLSM) observations, physiological measurements, gene expression analyses at transcript and protein level.

Results

Characterization of GBMs

Elemental analysis was performed to determine carbon, hydrogen, nitrogen and oxygen content in the two GBMs (Fig. 1c). The value of %N in FLG corresponds to a melamine content of 0.84 wt %. The results of the elemental analysis agree with those of the thermogravimetric analysis (TGA) for both materials: a weight loss of 6.4 % was observed in the case of FLG, corroborating the low quantity of oxygen groups generated by the exfoliation process, while a weight loss of 46 % was obtained from TGA analysis of GO (Fig. 1a). The differences between the Raman spectra of FLG and GO

evidence the contrast between these derivatives (Fig. 1b). The Raman spectrum of FLG shows the two most intense peaks of graphene, the G band and the 2D peak, which appear at around 1580 cm^{-1} and 2700 cm^{-1}, respectively. The average I(2D)/I(G) ratio is 0.49, proving the samples to be few-layer graphene, usually assigned for I(2D)/I(G) < 1 (Ferrari *et al.*, 2006; Mogera *et al.*, 2015). When graphene is affected by defects, a peak appears at around 1345 cm^{-1} (D band). In this case, the average spectrum of FLG shows an I(D)/I(G) ratio about 0.36, confirming a low level of defects which are attributed to the edges of the micrometer flakes (Torrisi *et al.*, 2012). The average Raman spectrum of GO, in contrast, shows broad D and G bands. In addition, a bump can be observed in this spectrum instead of the usual 2D band common to graphene structures. TEM analysis showed higher lateral dimensions for FLG sheets compared to GO sheets. Lateral size distributions of both GBMs are shown in Fig. 1d (n = 100), with representative TEM images of FLG and GO in Fig. 1e and Fig. 1f, respectively.

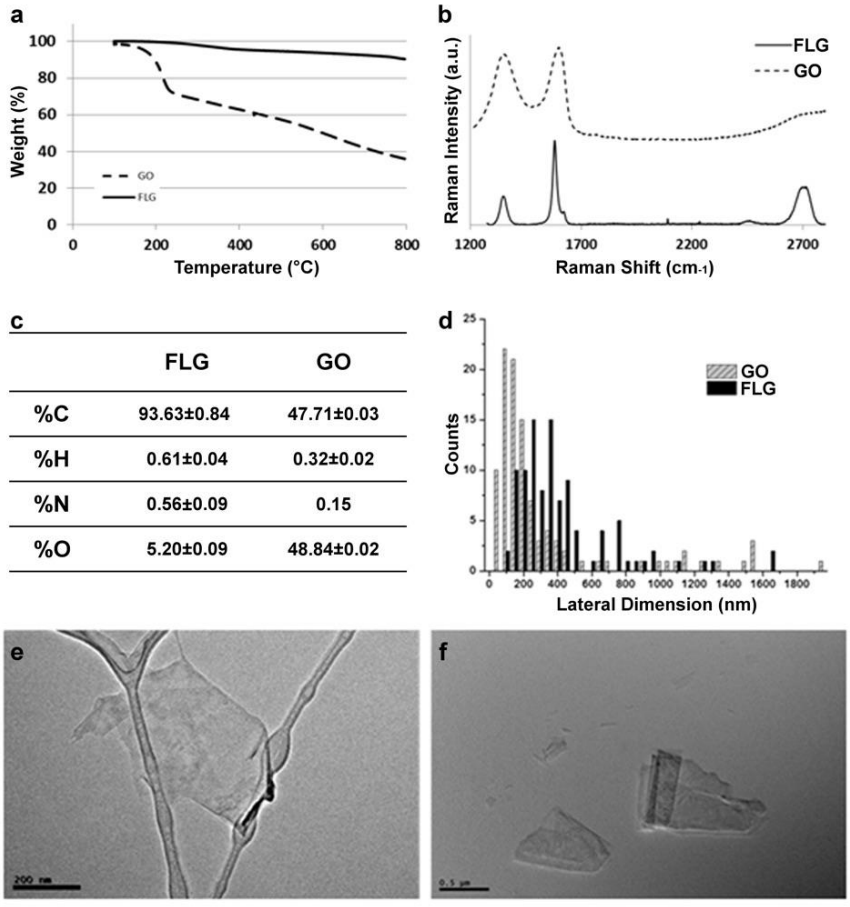

	FLG	GO
%C	93.63±0.84	47.71±0.03
%H	0.61±0.04	0.32±0.02
%N	0.56±0.09	0.15
%O	5.20±0.09	48.84±0.02

Figure 1. Thermogravimetric analysis of few-layer graphene (FLG), produced by ball milling, and graphene oxide (GO), produced by oxidation of carbon fibres (a); average Raman spectra of FLG and GO (b); elemental analysis of FLG and GO, (c); lateral size distribution (n = 100) of FLG and GO (d); representative TEM images of: FLG (e, scale bar = 200 nm) and GO (f, scale bar = 500 nm).

GBMs internalization assessment

The cell wall of *Trebouxia gelatinosa* observed at CLSM reflected a faint light when illuminated by the laser (Fig. 2a), especially with the setup used for the visualization of GO (Fig. 2b). In the autospores (diam. < 7 μm) light was reflected also from a single defined spot which was observed in both controls and treated samples (Figs. 2b, 2d), not present in adult cells. For this reason, it was impossible to distinguish very small GBMs flakes (c. 500 nm) from the light-reflecting spots of the cell walls. On the other hand, the GBMs flakes with a lateral dimension bigger than 1 μm were clearly distinguishable by the more intense light reflection (Figs. 2c, 2d) and they were observed adhering to the cell wall whenever they got in contact with the algae (Figs. 2c, 2d). FLG flakes were also observed within the cell wall (Fig. 3), but never in the cytoplasm of the cells.

GBMs internalization in *T. gelatinosa* was verified also by Raman spectroscopy. In the Raman spectrum of algae two peaks were observed, one at around 1200 cm^{-1} and a second at around 1525 cm^{-1} (Fig. 4a), both corresponding to β-carotene (Samek *et al.*, 2010), an accessory photosynthetic pigment typical of oxygenic photosynthetic organisms. In the samples exposed to GMBs, the typical Raman bands of FLG (Fig. 4b) were observed together with the peak of β-carotene, indicating the co-occurrence of both algae and graphene in the same measurement spot (Fig. 4c, α). The Raman bands of FLG became more prominent when the power density was increased up to 3 or 6 mW μm^{-2} in the same cell point (Fig. 4c, β, γ), which could mean that FLG was present at deeper levels within the cytoplasm. No typical Raman bands of GO (Fig. 4d) were observed at any power density in any part of the samples that had been treated with this nanomaterial, when properly rinsed in distilled water (Fig. 4e).

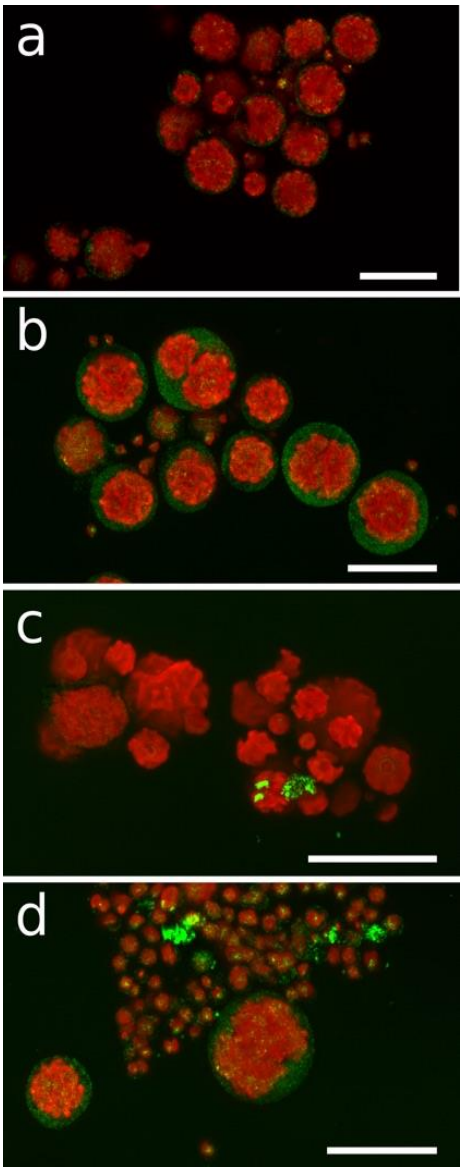

Figure 2. Cells of the green microalga *Trebouxia gelatinosa* observed with confocal laser scan microscopy in reflection mode. Cells before exposure observed with FLG setting (a) and GO setting (b); after exposure to FLG (c) or GO (d). Red signal emitted by chlorophyll *a*; weak green signal reflected by algal cell walls (b, d); strong green signal reflected by FLG (c) or GO (d).

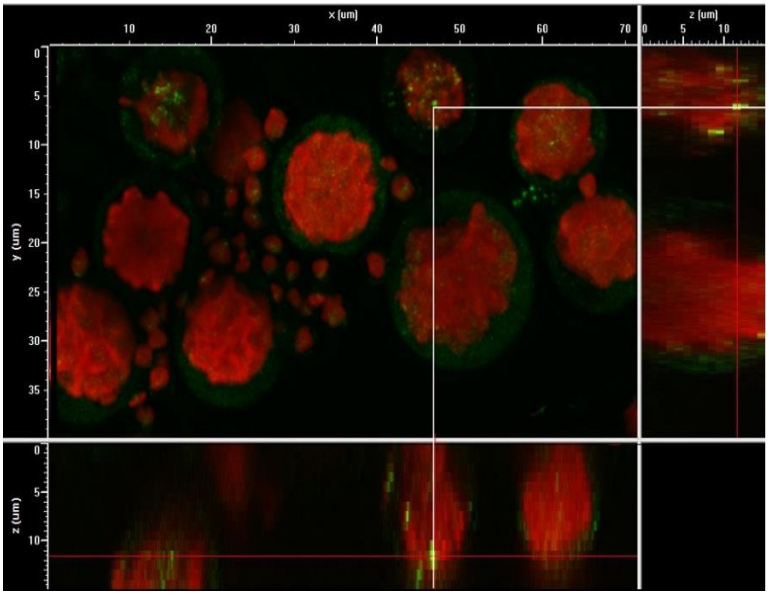

Figure 3. 3D reconstruction of cells of the green microalga *Trebouxia gelatinosa* observed with confocal laser scan microscopy in reflection mode after the exposure to FLG. Red signal emitted by chlorophyll *a*; weak green signal reflected by algal cell walls; strong green signal reflected by FLG.

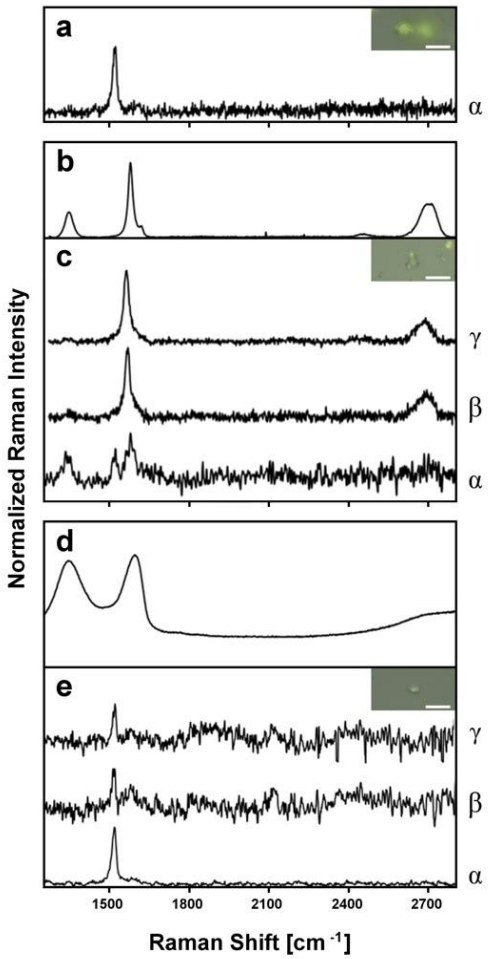

Figure 4. Raman spectra and respective Raman images (scale bars = 10 μm) of the green microalga *Trebouxia gelatinosa*. Representative Raman spectrum of GBMs-free algae (a); few-layers graphene (FLG) (b); water-washed, FLG exposed algae (c); graphene oxide (GO) (d); water-washed, GO exposed algae (e). Power density (mW μm^{-2}): $\alpha = 0.6$; $\beta = 3$; $\gamma = 6$.

Effects of GBMs and H_2O_2 on the quantum yield of primary photochemistry (F_v/F_m)

F_v/F_m values were consistent in pre-treatment and control samples, suggesting that the shaking treatment applied in the GBMs exposure treatment did not affect cell viability. F_v/F_m of pre-treatment samples was 0.514±0.068, which slightly increased to 0.522±0.075 and 0.518±0.079 in control samples after 10 and 30 minutes (Fig. 5), respectively. The samples exposed to H_2O_2 at concentrations higher than 0.05 M had significantly lower F_v/F_m. At 0.5 M and 0.8 M, after 10 minutes it decreased to 80 % (p = 0.00132) and to 50 % (p = 4.5e-06) of the control values, respectively, while after 30 minutes F_v/F_m further decreased to 50 % (p = 6.3e-06) in the former and to 30 % (p = 6.6e-09) in the latter. No significant differences were observed in samples exposed to FLG or GO with respect to control values

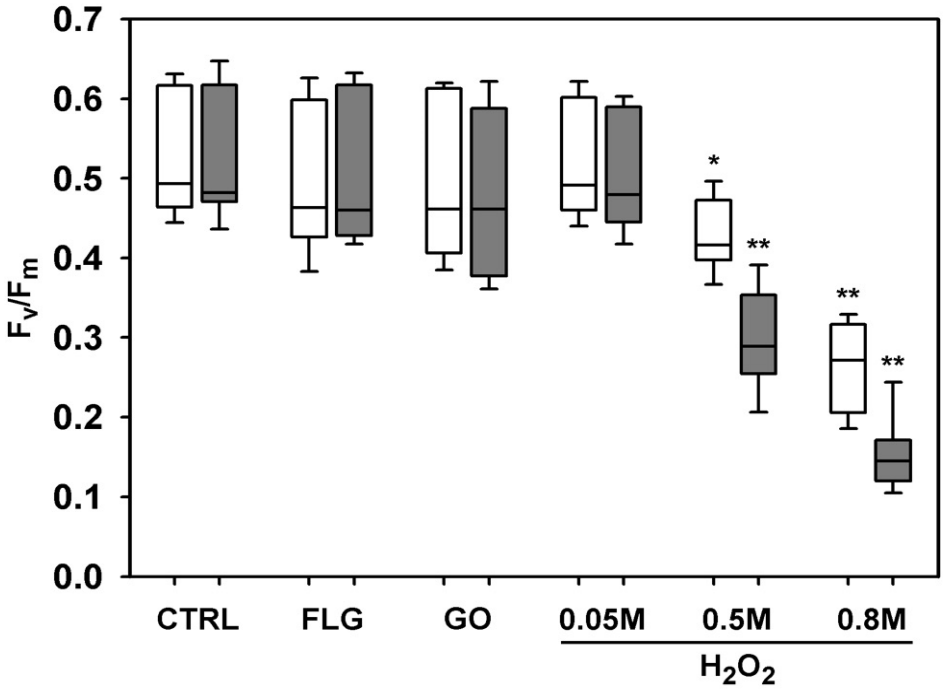

Figure 5. Maximum quantum yield of PSII photochemistry (F_v/F_m) measured in *Trebouxia gelatinosa* resuspended for 10 (a) and 30 (b) minutes in dH_2O (Ctrl), different H_2O_2 solutions (0.05 M, 0.5 M and 0.8 M) and GBMs suspensions (FLG or GO; 50 μg mL^{-1}). * $p \leq 0.05$, ** $p \leq 0.01$, non-parametric Kruskal-Wallis test and non-paired Wilcoxon post-hoc test (n = 18).

Effects of GBMs and H_2O_2 on stress-related genes expression at transcript level

Samples exposed to GBMs for 10 minutes did not modify the expression level of any of the genes considered (Fig. 6), whereas after 30 minutes the exposure to FLG significantly affected the transcription level of a single gene, heat shock protein 70 (HSP70), which was reduced to 35 % of the control value (Fig. 6).

Samples exposed to H_2O_2 had their ascorbate peroxidase (APX) and HSP70 transcripts levels significantly reduced after 10 minutes; the former transcript was reduced to ~35 % of its control value by the highest H_2O_2 concentration whereas the latter was significantly reduced to 50 % at 0.5 M and to 15% at 0.8 M H_2O_2. Transcripts levels of H_2O_2 treated samples further decreased after 30 minutes of exposure. Among antioxidant enzymes, APX transcription decreased to ~30 % and 15 % at 0.5 and 0.8 M H_2O_2, respectively (Fig. 6). At the same concentrations, the transcription level of catalase (CAT) was significantly reduced to 70 % and 65 % whereas that of gluthatione reductase (GR) remained steady independently of the H_2O_2 concentrations (Fig. 6). Differently, H_2O_2 had an inverse effect on the manganese superoxide dismutase (Mn-SOD) transcription levels, with the strongest decrease (down to ~25 %) observed at the lowest H_2O_2 concentration. Among the stress related proteins, the transcription levels of the desiccation related protein 11 (DRP11) and heat shock cognate (HSC70) remained steady throughout the experiment. Those of HSP70, instead, had the most severe decrease among all the transcripts, *i.e.* the highest H_2O_2 concentration completely inhibited the transcription of HSP70, reducing it to 1 %. Furthermore, the chlorophyll a-b binding protein of the light harvesting complex II (LHCII) transcript showed a significant dose-dependent reduction (to ~50 % up to ~20 %) in the expression.

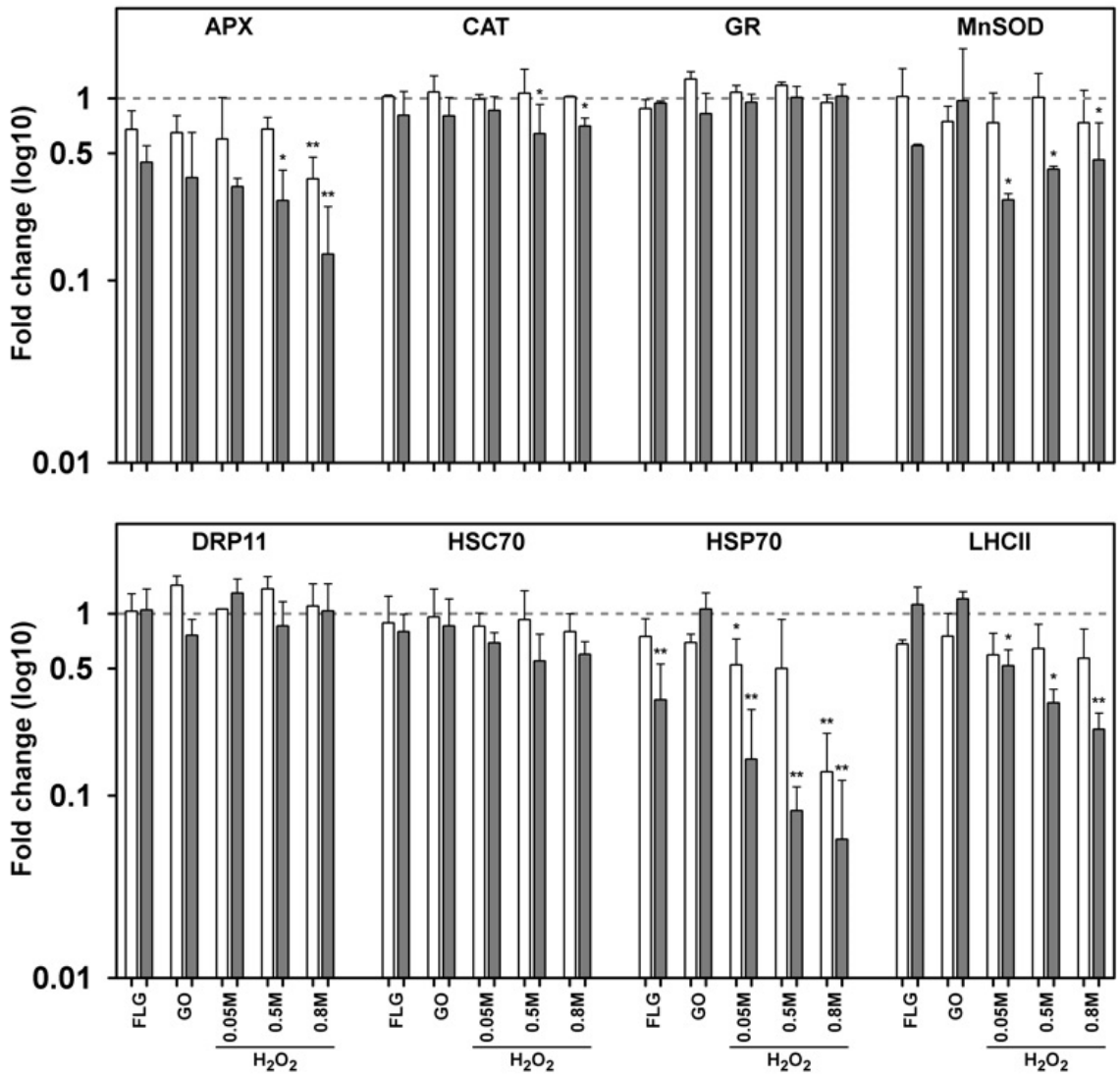

Figure 6. Fold change in the expression of 8 transcripts obtained with qRT-PCR in cultures of the green microalga *Trebouxia gelatinosa* treated with various concentrations of H_2O_2 and GBMs compared to the respective controls (dotted line) after 10 (a) and 30 (b) minutes of exposure. *$p \leq 0.05$, **$p \leq 0.01$ (n = 3).

Effects of GBMs and H_2O_2 on the HSP70 protein level

The HSP70 protein level was not affected by any GBMs treatment, while a significant decrease was detected at the highest H_2O_2 concentration after both exposure times (Fig. 7).

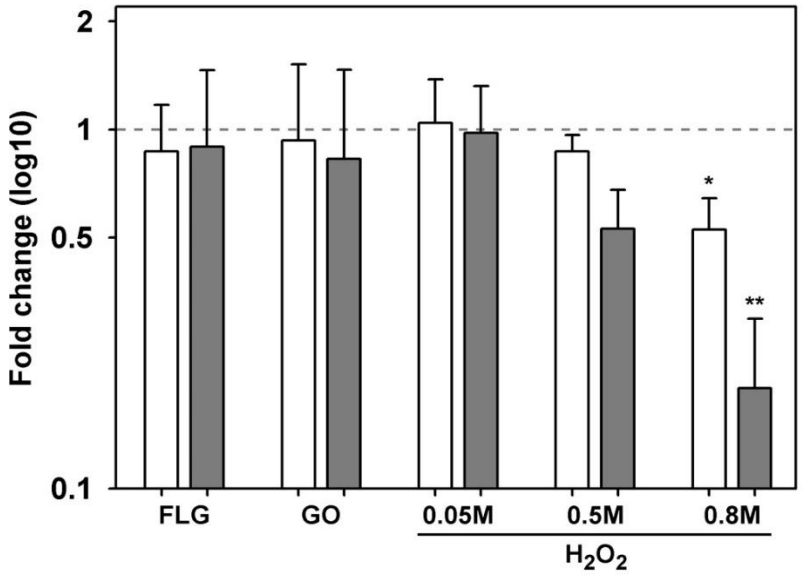

Figure 7. Levels of HSP70 protein in colonies of the green microalga *Trebouxia gelatinosa* exposed to various concentrations of H_2O_2 and GBMs compared to the respective controls after 10 (a) and 30 minutes (b) exposure. HSP70 bands of representative experiments after 10 (c) and 30 minutes (d) exposure. *$p \leq 0.05$, **$p \leq 0.01$ (n = 3).

Discussion

Internalization of GBMs is a controversial issue, depending both on the different characteristics of the material itself (Dallavalle *et al.*, 2015) and on the investigated organism. In our study, there are evidences suggesting a possible internalization of GBMs by the thick-walled cells of *T. gelatinosa*: small FLG flakes, but not GO, were observed by CLSM at the boundaries between cytoplasm – plasma membrane and plasma membrane – cell wall interfaces. The lateral size of these flakes observed by CLSM ranges around 1 μm, which is close to the limit of precise measurability of GBMs flakes (0.5 μm) with that technique (Fig. 3). The natural light reflection observed at the cell wall level, especially with the settings needed for the observations of GO (Figs. 2b, 2d), might have prevented the detection of the light reflected by the smaller flakes. Moreover, the small brilliant spots observed in the autospores, which reflect light more intensely than the surrounding cell wall, might be misleadingly recognized as GBMs flakes (Fig. 3). They are provisionally identified here, on the basis of observations in transmitted light microscopy, as the nucleolus. However, considering that both the GBMs batches tested in this study are made of graphene flakes with lateral dimensions that can be as small as 100 nm for FLG and 50 nm for GO (Fig. 1), it is possible that only the fractions of the graphene with the smallest sizes reached and/or crossed the plasma membrane.

These hypotheses are supported by the Raman spectroscopy observations (Fig. 4) since they allowed the detection of FLG flakes inside the algal cells. Raman spectroscopy is commonly used to determine the nature and the location of GBMs, *i.e.* if the flakes are inside a tissue or even a cell (Huang *et al.*, 2012).

The observation of the down-regulation of the HSP70 transcript (Fig. 6), which is interestingly the unique significant change in the gene expression induced by a 30 minutes FLG exposure, suggests that a functional interaction with the algae at the plasma membrane or even at the cytoplasm level might have been occurred. We hypothesize that the presence of FLG at the interface between the plasma membrane and the cell wall or in the cytoplasm could have activated/deactivated the signal pathways leading to changes in the HSP70 expression. HSP70 proteins can be activated by receptors at the plasma membrane level, starting a signal cascade involving intracellular changes in calcium ions (Ca^{2+}): the induction of Ca^{2+}/calmodulin (CaM) genes followed by transcriptional changes of different HSPs, including HSP70, were already recorded in plants (Liu *et al.*, 2003; Wu *et al.*, 2012). CaM genes can be regulated during abiotic stress by the activation of plasma membrane receptors like the cyclic nucleotide gated channels (CNGCs) (Virdi *et al.*, 2015), or by others, still unidentified (Liu *et al.*, 2003), that could respond to the interaction with GBMs at plasma membrane level. Furthermore, changes in HSP70 expression triggered by the presence of FLG inside the cell could involve the interaction of the nanomaterial with the filamentous proteins of the cytoskeleton, *i.e.* microtubules and actin filaments, causing deformation of cytoskeletal networks and the displacement in the cytoplasm fluid (Wu *et al.*, 2012). Molecular chaperones, as HSP70, have been proposed not only to facilitate the formation of the cytoskeleton and to regulate its function, but also to protect it during stress (Liang and MacRae, 1997). However, the reason why HSP70 was down-regulated is still unknown since HSP70 are considered stress-inducible proteins (Hartl and Hayer-Hartl, 2002; Wang *et al.*, 2004). As chaperones, they are important in protein stabilization, folding, assembly, translocation and degradation especially under stress conditions (Wang *et al.*, 2004) such as heat, drought, salinity, acidity, and cold (Yu *et al.*, 2015). Generally, the over-expression of HSP70 genes results in enhanced tolerance to abiotic stress in plants (Wang *et al.*, 2004; Bartels and Sunkar, 2015). Interestingly, a down-regulation of HSP70 at protein level was recorded after cumene hydroperoxide (CuHP) exposure in another member of the genus *Trebouxia*, the lichen photobiont TR1, while in TR9 (an alternative photobiont of the same lichen species, *Ramalina farinacea*), the oxidative treatment caused a strong increase in the amounts of this protein (del Hoyo *et al.*, 2011). In our case, instead, the down-regulation of the HSP70 gene expression did not correspond to a decrease in the quantity of the protein itself (Fig. 7); low correlations between mRNA abundance and protein level are common (Maier *et al.*, 2009), and are usually attributed to post-transcriptional regulations (Day and Tuite,1998).

Some authors demonstrated that internalization of GBMs in general is linked to the production of ROS (Sasidharan *et al.*, 2011) or to the increase of oxidative stress (Ouyang *et al.*, 2015), which eventually led to cell death. In our experimental design, we investigated the expression changes of

some gene of interest, among which antioxidant enzymes and proteins related to stress. Gene expression changes in general are a major component of stress responses, which in some cases are activate by intracellular signaling pathways. Interestingly, the control of gene expression has fast response kinetics, even within minutes in the presence of stress, and is able to return to basal state after the removal of the stress (de Nadal *et al.*, 2011).

The potential changes in gene expression after GBMs exposure were here compared to the ones induced by H_2O_2 treatments, a substance which is known to induce reactive oxygen species production (Russier *et al.*, 2013). From the gene expression analysis of antioxidant enzymes (Fig. 6), it can be concluded that these are not involved in the response to GBMs exposure. Interestingly, *Trebouxia* species are known to be oxidative stress tolerant because they own a strong constitutive antioxidant machinery which is able to scavenge an "oxidative burst" in minutes after his potential insurgence (Candotto Carniel *et al.*, 2016). However, H_2O_2 treatments produced dose- and time-dependent oxidative effects, evidenced by significant changes in the transcripts level of APX, CAT, and Mn-SOD. This response is in agreement with Chl*a*F measurements (Fig. 5), which showed a dose- and time- dependent decrease in F_v/F_m and therefore a corresponding algal vitality decrease after H_2O_2 treatments, while F_v/F_m after GBMs exposures was not impaired.

Studies focused on microalgae reported GBMs internalization, in particular in *Chlorella pyrenoidosa* and *C. vulgaris* (Hu *et al.*, 2014; Hu *et al.*, 2015; Ouyang *et al.*, 2015). Comparing these species with *T. gelatinosa,* the main differences are thickness and composition of the cell walls. In *T. gelatinosa* the cell wall is c. 1 μm thick (Archibald, 1975), while that of both *Chlorella* species is only c. 20 nm thick (Northcote *et al.*, 1958; Yamamoto *et al.*, 2004). In comparison, the latter is therefore considerably thinner, and represents a weaker barrier against GBMs, which may easily be internalized, also because the α-cellulose microfibrils are present as an irregular network over the cell wall, lying approximately in two directions at right angles to one another (Northcote *et al.*, 1958), although a wide variability has been documented in the cell wall composition of other members of the genus *Chlorella* (Loos and Meindl, 1982). The cell wall of *T. gelatinosa*, on the contrary, is relatively stable in composition, and highly differentiated (König and Peveling, 1984). It consists of five different layers, mostly composed by highly packed cellulosic fibrils, non-cellulosic species-specific polysaccharides and a three-dimensional web of sporopollenin, which is highly resistant and chemically stable. Moreover, *T. gelatinosa* develops a gelatinous sheath 1.5 – 2 μm thick outside the cell wall (Archibald, 1975), which is sticky, with species-specific sugar-acids, such as uronic acids, and proteins (Casano *et al.*, 2015), and may support a close contact with GBMs.

Hence, all these evidences reported herewith allow us to hypothesize that the interaction between FLG and *T. gelatinosa* cells which eventually occurs after 30 minutes of exposure is

harmless, as confirmed by further unpublished results concerning short-term K^+ release and long-term colonial growth. At this moment, we do not know, however, which pathway is involved in the reaction which led to the down-regulation of the HSP70 gene expression, caused interestingly only by FLG. GO, in respect to FLG, is considered to be more toxic, but no generalizations can be made because of the contradictory results available in the literature (Montagner *et al.*, 2017). In general, however, GO is more stable in suspension thanks to the carboxyl groups on the periphery, which make the sheets more hydrophilic, and probably also more prone to be immobilized by the outer gelatinous sheath of *T. gelatinosa*.

Experimental procedures

GBMs preparation and characterization

Two types of GBMs were used in this study, few-layers graphene (FLG) and graphene oxide (GO). FLG was prepared by ball-milling treatment, according to previous published procedures (León *et al.*, 2016). In general, a mixture of graphite and melamine (1,3,5-Triazine-2,4,6-triamine) (7.5 mg of SP-1 graphite powder, purchased from Bay Carbon, Inc. (USA), and 22.5 mg of melamine (Sigma-Aldrich, D) was ball-milled at 100 rpm for 30 minutes using a Retsch PM 100 (Retsch Technology GmbH, D) planetary mill under air atmosphere. The resulting solid mixture was dispersed in 20 mL of water and sonicated for 1 minute to produce a dark suspension. Melamine was afterwards eliminated by dialysis. The precipitate, consisting in poorly exfoliated graphene, was removed from the liquid fraction after stabilization for 5 days. The FLG water dispersions were lyophilized and the final graphene powder was thoroughly characterized.

GO was purchased from Grupo Antolin Ingeniería (Burgos, S), which produced it by oxidation of carbon fibers (GANF Helical-Ribbon Carbon Nanofibres, GANF®) and sodium nitrate in sulfuric acid at 0 °C.

TGA of FLG and GO were performed with a TGA Q50 (TA Instruments, USA) at 10 ºC per minute under nitrogen atmosphere, from 100 ºC to 800 ºC. In addition, the dispersions of both GBMs were drop-cast onto a Si wafer and dried on a hot plate in order to study the Raman spectra. At least 30 Raman measurements on both materials were collected in different locations using a inVia Raman Microscope (Renishaw plc, UK) at 532 nm with a 100× objective and an incident power of 1 % (1 mW μm^{-2}). Quantitative elemental analyses on FLG and GO were then performed with a LECO CHNS-932 (LECO Corporation, USA) elemental analyzer. Lateral dimension distribution of GBMs was calculated by using Fiji software. GBMs were studied by transmission electron microscopy (TEM). Stable dispersions of both materials were drop-cast on nickel grids (3.00 mm, 200 mesh) and

dried under vacuum. The samples were studied by a JEM 2100 (JEOL Ltd, JP) high-resolution transmission electron microscope (HRTEM) at an accelerating voltage of 200 kV.

Cultures of T. gelatinosa *apophotobiont*

Trebouxia gelatinosa Archibald was isolated following Yamamoto *et al*. (2002) from thalli of *Flavoparmelia caperata* (L.) Hale collected in the Classical Karst plateau (NW Italy). The algal cultures were subcultured on solid Trebouxia Medium (TM; 1.5 % agar) (Ahmadjian, 1973) every 30-45 days and kept in a thermostatic chamber at 18±1 °C and 20±2 μmol photons m^{-2} s^{-1} with a light/dark regime of 14/10 hours. Reference algal material has been cryo-conserved according to Dahmen *et al*. (1983) and is available upon request.

GBMs exposure and oxidative stress treatments

Algal cells of *T. gelatinosa* from 4 weeks-old colonies were resuspended in distilled water and gently pressed with a syringe through a filter net (mesh size = 40 μm). This procedure was used to disaggregate the clusters of cells in order to obtain a homogeneously dispersed algal suspension. Thirteen 1.5 mL Eppendorf tubes (with pierced lids) were filled with algal suspension (samples); one was left untreated representing the pre-treatment whereas the other twelve were spin-centrifuged to separate the cells from the supernatant, of which 1.3 mL were discarded. Thereafter, the treatments were conducted in the dark to induce the complete oxidation of the reaction centers, that allows to measure the maximum quantum efficiency of PSII immediately after the treatments. To the samples were then added, two by two, 1.3 mL of: distilled water (controls), distilled water plus aqueous suspensions of GBMs (FLG or GO) to reach the final concentration of 50 μg mL^{-1} and distilled water plus H_2O_2 to reach the final concentrations of 0.05 M, 0.5 M, 0.8 M. The samples were then placed on a shaker and one sample of each couple per treatment was taken for the analyses after 10 and 30 minutes, respectively. The procedure was repeated six times and for each repetition three biological replicates were processed. The exposure times were defined based on a preliminary experiment in which the effect of H_2O_2 on *T. gelatinosa* was evaluated in order to have an increasing oxidative effect. The experiment was implemented in the dark to prevent possible phototoxic effects.

In-vivo *GBMs internalization assessment by CLSM*

A sub-aliquot (10 μL) of the algal suspension for each treatment was put on Polysine™ Microscope Adhesion Slides (Thermo Fisher Scientific, USA) immediately after the GBMs treatments, covered with coverslips and then observed *in-vivo* with a CLSM Nikon C1-si (Nikon, JP). To visualize GBMs flakes, the microscope was used in reflection mode: samples were illuminated with a 514 nm laser

set at an intensity of 0.2 % and 0.5 % for the observation of FLG and GO, respectively, since they have different light reflection capacity, higher in the former than in the latter. Light reflected by GBMs was detected by a 525/50 band pass filter. Algal cells were visualized by illuminating samples with a 488 nm laser (12 % intensity) and acquiring the autofluorescence of chlorophylls with a 650 long pass filter ($\lambda > 650$ nm). One to three fields were acquired for each replicate (n = 4). A variable number of focal planes (stacks), depending on the algal abundance and the dimension of the GBMs flakes were acquired for each field. In total, more than 1300 cells were analysed. Acquisitions were elaborated with the Nikon EZ-C1 FreeViewer software (Nikon, JP) and with the freeware suite ImageJ 1.46r (NIH, USA). A unification algorithm (Z-projection) was applied to merge stacks into bi-dimensional images, and 3D reconstruction were obtained by using the ImageJ 3D viewer plugin.

GBMs internalization assessment by Raman spectroscopy

Algal samples without GBMs and with FLG or GO were prepared as explained above. After 30 minutes of shaking each suspension was vacuum filtered on a membrane (10 µm pore size), and the algae were gently washed with 50 mL of distilled water in order to remove the GBMs floating or attached outside the cells. Algal cells were then immediately resuspended with 500 µL of distilled water; three distinct drops of 40 µL each were put on Polysine™ Microscope Adhesion Slides (Thermo Fisher Scientific, USA) which were then put into a 50 mL Falcon tube and immediately frozen in liquid nitrogen. Thereafter, the samples were freeze-dried for 24 hours. Raman spectra were recorded with an inVia Raman Microscope (Renishaw plc, UK) equipped with a 532 nm point-based laser. At first, confocal mode was used to collect Raman spectra between defined X Y coordinates and at different depths within the samples. However, during the acquisition of a series of spectra on the same coordinates, cells were progressively destroyed by the laser. To overcome this issue, the operation mode was changed; samples were measured with a fixed exposure time of 1 second using the objective 50×, 10 accumulations and three different laser power densities (0.6, 3 and 6 mW μm^{-2}) in order to penetrate at different levels into the cell.

Chlorophyll a *fluorescence (Chl$_a$F) measurements*

After the treatments, each sample was collected by vacuum filtration on a cellulose acetate membrane (25 mm diameter, pore size 0.45 µm, Sartorius Lab Holding GmbH, D) and measurements of chlorophyll *a* fluorescence (Chl$_a$F) emission were taken with a photosynthetic efficiency analyzer fluorimeter Handy-PEA (Hansatech, UK). A modified clip was positioned right over the sample on the membrane. A saturating red light pulse of 1500 µmol photons m^{-2} s^{-1} for 1 second was emitted to obtain the Kautsky induction and thus F_m (transient maximum Chl$_a$F level). F_0 (minimal Chl$_a$F level),

which is needed to calculate F_v (variable Chl$_a$F level, *i.e.* $F_m - F_0$) and thus F_v/F_m (maximum quantum efficiency of PSII photochemistry), was calculated *a posteriori* by an algorithm that determines a line of best fit through the data points recorded immediately after the start of illumination. Afterwards, each sample was put inside an Eppendorf tube, soaked in liquid nitrogen and stored at -80 °C for downstream applications.

RNA isolation and cDNA synthesis

Three replicates per treatment from three distinct experiments were randomly selected and pooled together for three times to obtain three samples for RNA extraction. PowerPlant® RNA Isolation Kit (MO BIO Laboratories Inc., USA) was used to extract total RNA. RNA quality was verified with NanoDrop® 2000 (Thermo Fisher Scientific, USA), followed by a denaturing 1 % agarose gel. cDNA was synthesized using IScript cDNA synthesis kit (Bio-Rad, USA).

qRT-PCR

The expression of eight different transcripts, four coding for antioxidant enzymes and four for stress-related proteins was measured by qRT-PCR. The former were APX, CAT, GR, and Mn-SOD, the latter were DRP11, HSC70 and HSP70, and LHCII. Primers were designed with Primer3Plus (Untergasser *et al.*, 2007) (Table S1) or following Candotto Carniel *et al.* (2016). Each reaction was performed in three technical replicates in a mix containing 1 µL cDNA (1:10 template dilution), 8 µL SSOAdvanced™ SYBR® Green Supermix (Bio-Rad, USA) and 200 nM of each primer. The PCR amplifications were performed with CFX 96™ Real-Time PCR System (Bio-Rad, USA) using the following cycle: 98 °C for 30 minutes, 40 cycles at 95 °C for 10 minutes and 60 °C for 20 minutes. A melting curve analysis (65 °C to 95 °C increment 0.5 °C for 5 minutes) was performed to verify the absence of non-specific amplification products. Transcript levels were calculated with Bio-Rad CFX Manager software (Bio-Rad, USA), based on the comparative Ct method ($2^{-\Delta\Delta}$ Ct method) (Livak and Schmittgen, 2001) and gene expression data were normalized using as housekeeping gene the ribosomal protein L6 (RPL6) (Candotto Carniel *et al.*, 2016).

Proteins isolation

Three pooled samples of *T. gelatinosa* frozen cultures prepared as mentioned in the "*RNA isolation and cDNA synthesis*" section, were pulverized in liquid nitrogen, transferred in 1.5 mL Eppendorf tubes and resuspended in 100 µl of 1× Laemmli buffer (62.5 mM Tris–HCl pH 6.8, 10 % (v/v) glycerol, 2 % (w/v) SDS, 0.2M dithiothreitol (DTT) and 0.1 % (w/v) bromophenol blue) (Laemmli, 1970). Samples were then vortexed and incubated at 95 °C for 5 minutes. After a 3 minutes

centrifugation at 14000 r.p.m., protein extracts were recovered from the upper phase of the tube and transferred in a new Eppendorf. When not immediately used for analysis, the samples were stored at -20 °C and incubated 5 minutes at 95 °C before loading on the gel. To check quality and quantity of the total proteins extracted, 12 % sodium dodecyl sulphate - polyacrylamide gel electrophoresis (SDS-PAGE) was performed according to Laemmli (1970). The gel was stained with Coomassie brilliant blue R250 (Zehr *et al.*, 1989).

HSP70 immunodetection

To perform 12 % SDS-PAGE, 15 µg of proteins were used. Proteins were then transferred on a Hybond™ nitrocellulose membrane (Amersham, UK) using the Criterion™ blotter apparatus (Bio-Rad, USA) as explained in Dinakar and Bartels (2012). Transfer was obtained after 1 hour at 70 V with pre-chilled buffer. Before immunodetection, the membrane was stained for 30 minutes with Ponceau S red to visualize the samples and check their equal amount. 4 °C overnight incubation with blocking solution [3 % (w/v) skimmed milk in Tris-buffered saline] was performed to prevent unspecific binding of antibodies. The membranes were incubated for 1 hour with HSP70/HSC70 primary antibody (1:1000 dilution) (Ulbricht *et al.*, 2013), and for 45 minutes with secondary antibody (anti-rabbit IgG-peroxidase, 1:5000 dilution, Sigma-Aldrich, USA). Antigen-antibody complexes were detected with the ECL kit (Amersham, UK) and a lumi-imager (LAS 1000, Fujifilm, JP). Densitometry of protein bands was with Image J software 1.37 V (National Institute of Health, USA).

Statistics

Descriptive statistics were performed with R version 0.99.441 (The R Foundation for Statistical Computing, 2012). The non-parametric Kruskal-Wallis test and Wilcoxon non-paired test were applied to verify the significance of differences for Chl_aF measurements (Lazár and Nauš, 1998; Baruffo and Tretiach, 2007). A one-way ANOVA followed by a Fisher's LSD post-hoc test was applied to verify significant differences between the relative abundancy of transcripts and HSP70 protein content in treated versus control samples. Figures were produced with Sigmaplot 10.0 (Systat Software, USA).

Acknowledgements

The activity of E.B. was partially funded by the Italian Government Commission with "Fondo Trieste". We acknowledge financial support from the H2020-GRAPHENE Flagship Core 1 project (no. 696656) and from Spanish Ministerio de Economía y Competitividad (MINECO) under project

grant CTQ2014-53600-R. We gratefully thank Dr. Syrgiannis (University of Trieste, I) for helpful comments, Prof. Dr. Bartels (University of Bonn, D) for providing the laboratory facilities and for the support to western blot analysis and Prof. Dr. Höhfeld (University of Bonn, D) for HSP70 antiserum.

References

Ahmadjian, V. (1973) Methods of isolation and culturing lichen symbionts and thalli. In The Lichens. Ahmadjian, V. and Hale, M.E. (eds). New York: Academic Press, pp. 653–660.

Ahmadjian, V. (2004) *Trebouxia*: reflections on a perplexing and controversial lichen photobiont. In Symbiosis. Seckbach, J. (eds). Houten: Springer, pp. 373–383.

Akhavan, O., and Ghaderi, E. (2010) Toxicity of graphene and graphene oxide nanowalls against bacteria. *ACS Nano* **4:** 5731–5736.

Akhavan, O., and Ghaderi, E. (2012) *Escherichia coli* bacteria reduce graphene oxide to bactericidal graphene in a self-limiting manner. *Carbon* **50:** 1853–1860.

Akhavan, O., Ghaderi, E., and Esfandiar, A. (2011) Wrapping bacteria by graphene nanosheets for isolation from environment, reactivation by sonication, and inactivation by near–infrared irradiation. *J. Phys Chem B* **115:** 6279–6288.

Archibald, P.A. (1975) *Trebouxia* de Pulmaly (Chlorophyceae, Chlorococcales) and *Pseudotrebouxia* gen. nov. (Chlorophyceae, Chlorosarcinales). *Phycologia* **14:** 125–137.

Bartels, D., and Sunkar, R. (2005) Drought and salt tolerance in plants. *Crit Rev Plant Sci* **24:** 23–58.

Baruffo, L., and Tretiach, M. (2007) Seasonal variations of F_0, F_m, and F_v/F_m in an epiphytic population of the lichen *Punctelia subrudecta* (Nyl.) Krog. *Lichenologist* **39:** 555–565.

Begum, P., and Fugetsu, B. (2013) Induction of cell death by graphene in *Arabidopsis thaliana* (Columbia ecotype) T87 cell suspensions. *J Hazard Mater* **260:** 1032–1041.

Belnap, J., Budel, B., and Lange, O.L. (2001) Biological soil crusts: characteristics and distribution. In Biological soil crusts: structure, function, and management. Belnap, J. and Lange, O.L. (eds). Berlin: Springer-Verlag, pp. 3–30.

Bitounis, D., Ali-Boucetta, H., Hong, B.H., Min, D.H., and Kostarelos, K. (2013) Prospects and challenges of graphene in biomedical applications. *Adv Mater* **25:** 2258–2268.

Candotto Carniel, F., Gerdol, M., Montagner, A., Banchi, E., De Moro, G., Manfrin, C., Muggia, L., Pallavicini. A., and Tretiach, M. (2016) New features of desiccation tolerance in the lichen photobiont *Trebouxia gelatinosa* are revealed by a transcriptomic approach. *Plant Mol Biol* **91:** 319–339.

Candotto Carniel, F., Zanelli, D., Bertuzzi, S., and Tretiach, M. (2015) Desiccation tolerance and lichenization: a case study with the aeroterrestrial microalga *Trebouxia* sp. (Chlorophyta). *Planta* **242:** 493–505.

Casano, L.M., Braga, M.R., Álvarez, R., del Campo, E.M., and Barreno, E. (2015) Differences in the cell walls and extracellular polymers of the two *Trebouxia* microalgae coexisting in the lichen *Ramalina farinacea* are consistent with their distinct capacity to immobilize extracellular Pb. *Plant Sci* **236:** 195–204.

Combarros, R.G., Collado, S., and Diaz, M. (2016) Toxicity of graphene oxide on growth and metabolism of *Pseudomonas putida*. *J Hazard Mater* **310:** 246–252.

Dahmen, H., Staub, T., and Schwinn, F.J. (1983) Technique for long-term preservation of phytopathogenic fungi in liquid nitrogen. *Phytopathology* **73:** 241–246.

Dallavalle, M., Calvaresi, M., Bottoni, A., Melle-Franco, M., and Zerbetto, F. (2015) Graphene can wreak havoc with cell membranes. *ACS Appl Mater Interfaces* **7:** 4406–4414.

Day, D.A., and Tuite, M.F. (1998) Post-transcriptional gene regulatory mechanisms in eukaryotes: an overview. *J Endocrinol* **157:** 361–371.

de Nadal, E., Ammerer, G., and Posas, F. (2011) Controlling gene expression in response to stress. *Nat Rev Genet* **12:** 833–845.

del Hoyo, A., Álvarez, R., del Campo, E.M., Gasulla, F., Barreno, E., and Casano, L.M. (2011) Oxidative stress induces distinct physiological responses in the two *Trebouxia* phycobionts of the lichen *Ramalina farinacea*. *Ann Bot* **107:** 109–118.

Dinakar, C., and Bartels, D. (2012) Light response, oxidative stress management and nucleic acid stability in closely related Linderniaceae species differing in desiccation tolerance. *Planta* **236:** 541–555.

Domozych, D.S., Ciancia, M., Fangel, J.U., Mikkelsen, M.D., Ulvskov, P. and Willats, W.G.T. (2012) The cell walls of green algae: a journey through evolution and diversity. *Front Plant Sci* **3:** 82.

Ferrari, A.C., Meyer, J.C., Scardaci, V., Casiraghi, C., Lazzeri, M., Mauri, F., *et al*. (2006) Raman spectrum of graphene and graphene layers. *Phys Rev Lett* **97:** 187401.

Freystein, K., and Reisser, W. (2010) Green biofilms on tree barks: more than just algae. In Symbioses and stress: Joint ventures in biology. Seckbach, J. and Grube, M. (eds). Dordrecht: Springer, pp. 557–573.

Gärtner, G., and Ingolić, E. (1989) Ein Beitrag zur Kenntnis von *Apatococcus lobatus* (Chlorophyta, Chaetophorales, Leptosiroideae). *Plant Syst Evol* **164:** 133–143.

Geim, A.K., and Novoselov, K.S. (2007) The rise of graphene. *Nat Mater* **6:** 183–191.

Hartl, F.U., and Hayer-Hartl, M. (2002) Molecular chaperones in the cytosol: from nascent chain to folded protein. *Science* **295:** 1852–1858.

Hawksworth, D.L., Kirk, P.M., Sutton, B.C. and Pegler, D.N. (1995) Ainsworth & Bisby's Dictionary of the fungi. Wallingford: CAB International.

Hu, C., Wang, Q., Zhao, H., Wang, L., Guo, S., and Li, X. (2015) Ecotoxicological effects of graphene oxide on the protozoan *Euglena gracilis*. *Chemosphere* **128:** 184–190.

Hu, X., Lu, K., Mu, L., Kang, J., and Zhou, Q. (2014) Interactions between graphene oxide and plant cells: regulation of cell morphology, uptake, organelle damage, oxidative effects and metabolic disorders. *Carbon* **80:** 665–676.

Huang, J., Zong, C., Shen, H., Liu, M., Chen, B., Ren, B., and Zhang, Z. (2012) mechanism of cellular uptake of graphene oxide studied by surface-enhanced Raman spectroscopy. *Small* **8:** 2577–2584.

Jastrzębska, A.M., Kurtycz, P., and Olszyna, A.R. (2012) Recent advances in graphene family materials toxicity investigations. *J Nanopart Res* **14:** 1–21.

König, J., and Peveling, E. (1984) Cell walls of the phycobionts *Trebouxia* and *Pseudotrebouxia*: constituents and their localization. *Lichenologist* **16:** 129–144.

Kostarelos, K., and Novoselov, K.S. (2014) Exploring the interface of graphene and biology. *Science* **344:** 261–263.

Laemmli, U.K. (1970) Cleavage of structural proteins during the assembly of the head of bacteriophage T4. *Nature* **227:** 680–685.

Lalwani, G., D'Agati, M., Khan, A.M., and Sitharaman, B. (2016) Toxicology of graphene-based nanomaterials. *Adv Drug Delivery Rev* **105:** 109–144.

Lazár, D., and Nauš, J. (1998) Statistical properties of chlorophyll fluorescence induction parameters. *Photosynthetica* **35:** 121–127.

León, V., González–Domínguez, J.M., Fierro, J.L., Prato, M., and Vázquez, E. (2016) Production and stability of mechanochemically exfoliated graphene in water and culture media. *Nanoscale* **8:** 14548–14555.

Liang, P., and MacRae, T.H. (1997) Molecular chaperones and the cytoskeleton. *J Cell Sci* **110:** 1431–1440.

Liu, H.T., Li, B., Shang, Z.L., Li, X.Z., Mu, R.L., Sun, D.Y., and Zhou, R.G. (2003) Calmodulin is involved in heat shock signal transduction in wheat. *Plant Physiol* **132:** 1186–1195.

Livak, K.J., and Schmittgen, T.D. (2001) Analysis of relative gene expression data using real-time quantitative PCR and the $2^{-\Delta\Delta C_T}$ method. *Methods* **25:** 402–408.

Loos, E., and Meindl, D. (1982) Composition of the cell wall of *Chlorella fusca. Planta* **156:** 270–273.

Lüttge, U., and Büdel, B. (2010) Resurrection kinetics of photosynthesis in desiccation-tolerant terrestrial green algae (Chlorophyta) on tree bark. *Plant Biol* **12:** 437–444.

Maier, T., Güell, P., and Serrano, L. (2009) Correlation of mRNA and protein in complex biological samples. *FEBS Lett* **583:** 3966–3973.

Mogera, U., Dhanya, R., Pujar, R., Narayana, C., and Kulkarni, G.U. (2015) Highly decoupled graphene multilayers: turbostraticity at its best. *J Phys Chem Lett* **6:** 4437–4443.

Montagner, A., Bosi, S., Tenori, E., Bidussi, M., Alshatwi, A.A., Tretiach, M., Prato, M., and Syrgiannis, Z. (2017) Ecotoxicological effects of graphene–based materials. *2D Mater* **4:** 012001.

Navarro, E., Baun, A., Behra, R., Hartmann, N.B., Filser, J., Miao, A.J., *et al.* (2008) Environmental behavior and ecotoxicity of engineered nanoparticles to algae, plants, and fungi. *Ecotoxicology* **17:** 372–386.

Northcote, D.H., Goulding, K.J., and Horne, R.W. (1958) The chemical composition and structure of the cell wall of *Chlorella pyrenoidosa. Biochem J* **70:** 391–397.

Novoselov, K.S., Fal'ko, V.I., Colombo, L., Gellert, P.R., Schwab, M.G., and Kim, K. (2012) A roadmap for graphene. *Nature* **490:** 192–200.

Ouyang, S., Hu, X., and Zhou, Q. (2015) Envelopment-internalization synergistic effects and metabolic mechanism of graphene oxide on single-cell *Chlorella vulgaris* are dependent on the nanomaterial particle size. *ACS Appl Mater Interfaces* **7:** 18104–18112.

Palmieri, V., Bugli, F., Lauriola, M.C., Cacaci, M., Torelli, R., Ciasca, G., *et al.* (2017) Bacteria meet graphene: modulation of graphene oxide nanosheet interaction with human pathogens for effective antimicrobial therapy. *ACS Biomater Sci Eng* **3**: 619–627.

Romero-Vargas Castrillón, S., Perreault, F., De Faria, A.F., and Elimelech, M. (2015) Interaction of graphene oxide with bacterial cell membranes: insights from force spectroscopy. *Environ Sci Technol Lett* **2:** 112–117.

Russier, J., Treossi, E., Scarsi, A., Perrozzi, F., Dumortier, H., Ottaviano, L., Meneghetti, M., Palermo, V., and Bianco, A. (2013) Evidencing the mask effect of graphene oxide: a comparative study on primary human and murine phagocytic cells. *Nanoscale* **5:** 11234–11247.

Samek, O., Jonáš, A., Pilát, Z., Zemánek, P., Nedbal, L., Tříska, J., Kotas, P., and Trtílek, M. (2010) Raman microspectroscopy of individual algal cells: sensing unsaturation of storage lipids in vivo. *Sensors* **10:** 8635–8651.

Sanchez, V.C., Jachak, A., Hurt, R.H. and Kane, A.B. (2011) Biological interactions of graphene-family nanomaterials: an interdisciplinary review. *Chem Res Toxicol* **25:** 15–34.

Sasidharan, A., Panchakarla, L.S., Chandran, P., Menon, D., Nair, S., Rao, C.N.R., and Koyakutty, M. (2011) Differential nano-bio interactions and toxicity effects of pristine versus functionalized graphene. *Nanoscale* **3:** 2461–2464.

Savolainen, K., Backman, U., Brouwer, D., Fadeel, B., Fernandes, T., Kuhlbusch, T., Landsiedel, R., Lynch, I., and Pylkkänen, L. (2013) Nanosafety in Europe 2015-2025: towards safe and sustainable nanomaterials and nanotechnology innovations. Finnish Institute of Occupational Health.

Seabra, A.B., Paula, A.J., de Lima, R., Alves, O.L., and Durán, N. (2014) Nanotoxicity of graphene and graphene oxide. *Chem Res Toxicol* **27:** 159–168.

Szunerits, S., and Boukherroub, R. (2016) Antibacterial activity of graphene-based materials. *J. Mater. Chem. B* **4:** 6892-6912.

Torrisi, F., Hasan, T., Wu, W., Sun, Z., Lombardo, A., Kulmala, T.S., *et al.* (2012) Inkjet-printed graphene electronics. *ACS nano* **6:** 2992–3006.

Ulbricht, A., Eppler, F.J., Tapia, V.E., van der Ven, P.F., Hampe, N., Hersch, N., *et al.* (2013) Cellular mechanotransduction relies on tension-induced and chaperone-assisted autophagy. *Curr Biol* **23:** 430–435.

Untergasser, A., Nijveen, H., Rao, X., Bisseling, T., Geurts, R., and Leunissen, J.A.M. (2007) Primer3Plus, an enhanced web interface to Primer3. *Nucleic Acids Res* **35:** 71–74.

Virdi, A.S., Singh, S., and Singh, P. (2015) Abiotic stress responses in plants: roles of calmodulin-regulated proteins. *Front. Plant Sci* **6:** 809.

Wang, S.B., Hu, Q., Sommerfeld, M., and Chen, F. (2004) Cell wall proteomics of the green alga *Haematococcus pluvialis* (Chlorophyceae). *Proteomics* **4:** 692–708.

Weissman, L., Garty, J., and Hochman, A. (2005) Rehydration of the lichen *Ramalina lacera* results in production of reactive oxygen species and nitric oxide and a decrease in antioxidants. *Appl Environ Microbiol* **71:** 2121–2129.

Wu, C., Wang, C., Han, T., Zhou, X., Guo, S., and Zhang, J. (2013) Insight into the cellular internalization and cytotoxicity of graphene quantum dots. *Adv Healthcare Mater* **2:** 1613–1619.

Wu, H.C., Luo, D.L., Vignols, F., and Jinn, T.L. (2012) Heat shock- induced biphasic Ca^{2+} signature and OsCaM1-1 nuclear localization mediate downstream signalling in acquisition of thermotolerance in rice (*Oryza sativa* L.). *Plant Cell Environ* **35:** 1543–1557.

Yamamoto, M., Fujishita, M., Hirata, A., and Kawano, S. (2004) Regeneration and maturation of daughter cell walls in the autospore-forming green alga *Chlorella vulgaris* (Chlorophyta, Trebouxiophyceae). *J Plant Res* **117:** 257–264.

Yamamoto, Y., Kinoshita, Y., and Yoshimura, I. (2002) Culture of thallus fragments and redifferentiation of lichens. In Protocols in lichenology. Culturing, biochemistry, ecophysiology and use in biomonitoring. Kranner, I., Beckett, R., Varma, A. (eds) Heidelberg: Springer, pp. 34–42.

Yan, L., Gu, Z., and Zhao, Y. (2013) Chemical mechanisms of the toxicological properties of nanomaterials: generation of intracellular reactive oxygen species. *Chem Asian J* **8:** 2342–2353.

Yu, H.Y., Ziegelhoffer, T., Osipiuk, J., Ciesielski, S.J., Baranowski, M., Zhou, M., Joachimiak, A., and Craig, E.A. (2015) Roles of intramolecular and intermolecular interactions in functional regulation of the Hsp70 J-protein co-chaperone Sis1. *J Mol Biol* **427:** 1632–1643.

Zehr, B.D., Savin, T.J., and Hall, R.E. (1989) A one-step, low background Coomassie staining procedure for polyacrylamide gels. *Anal Biochem* **182:** 157–159.

Zhang, W., Wang, C., Li, Z., Lu, Z., Li, Y., Yin, J.J., *et al.* (2012) Unraveling stress-induced toxicity properties of graphene oxide and the underlying mechanism. *Adv Mater* **24:** 5391–5397.

Zhao, J., Cao, X., Wang, Z., Dai, Y., and Xing, B. (2017) Mechanistic understanding toward the toxicity of graphene-family materials to freshwater algae. *Water Res* **111:** 18–27.

Zhao, S., Wang, Q., Zhao, Y., Rui, Q., and Wang, D. (2015) Toxicity and translocation of graphene oxide in *Arabidopsis thaliana. Environ Toxicol Pharmacol* **39:** 145–156.

Zhou, R., and Gao, H. (2014) Cytotoxicity of graphene: recent advances and future perspective. *Wiley Interdiscip Rev: Nanomed Nanobiotechnol* **6:** 452–474.

Supplementary Information

Table S1. Primers custom designed for quantitative Real-Time PCR analysis.

Gene	Primer	Forward sequence	Reverse sequence
Ascorbate peroxidase	APX	CAGGGTTCACAAGGACAGGT	TCAGCAAACAGGCACTCATC
Glutathione reductase	GR	TTCGAACAGCAGACATCGAC	CCTCCAGTCTTTTCGTCAGC
Mn-superoxide dismutase	MnSOD	CACCCAGCTTGCTGACTACA	GGTCAAACTGTGCCTGGAAT
Catalase	CAT	ACTACTTCCCATCCCGCTTT	CCTGGTGATGAACCTGTCCT
Light Harvesting Complex	LHCII	CTGATGACCCAGATGCCTTT	GGTCCTTTGCCTGTCACAAT
Desiccation Related Protein	DPR11	CATATGGCGAGGGTATTGCT	TGTGCGATTTCATTCTCAGC
Heat Shock Protein 70	HSP70	CAGTCACCACTGCCTTCTCA	CAAGTCAGCCAATGCAAAGA
Heat Shock Cognate 70	HSC70	AGGAGCAGACCTTCTCCACA	GACCACAATTTGGGGAACAC
Ribosomal protein L6*	RPL6	AGGAGCTAGCTAGGGGCATC	TCTCGTGCTTTGGGAACTCT

*from Candotto Carniel *et al.* (2016)

ITS2 METABARCODING ANALYSIS COMPLEMENTS DATA OF LICHEN MYCOBIOME DIVERSITY

Elisa Banchi[1], David Stankovic[1,2], Fernando Fernández-Mendoza[3], Fabrizia Gionechetti[1], Alberto Pallavicini[1], Lucia Muggia[1, 3*]

[1]Department of Life Sciences, University of Trieste, Via Giorgieri 10, 34127 Trieste, Italy

[2] National Institute of Biology, Marine Biology Station, Fornače 41, 6330 Piran, Slovenia

[3]Institute of Plant Sciences, Karl-Franzens University of Graz, Holteigasse 6, 8010 Graz, Austria

*Corresponding author: Lucia Muggia

Main abbreviations

HTS: high-throughput sequencing

ITS: internal transcribed spacer

OTU: operational taxonomic unit

PCoA: principal coordinate analysis

Abstract

Lichen thalli harbor complex fungal communities (mycobiomes) of species with divergent trophic and ecological strategies. The complexity and diversity of lichen mycobiomes are still largely unknown, despite surveys combining culture-based methods and high-throughput sequencing (HTS). The results of such surveys are strongly influenced by the barcode locus chosen, its sensitivity in discriminating taxa, and the depth to which public sequence repositories cover the phylogenetic spectrum of fungi. Here, we use HTS of the ITS2 spacer to assess the taxonomic composition and diversity of a well-characterized, alpine rock lichen community that includes thalli symptomatically infected by lichenicolous fungi as well as asymptomatic thalli. Taxa belonging to the order Chaetothyriales are the major components of the observed lichen mycobiomes. We predict sequences representative of lichenicolous fungi characterized morphologically, and assess their asymptomatic presence in lichen thalli. We show how the estimation of species diversity widely differs when ITS1 or ITS2 are used as barcode, and particularly biases the detection of Basidiomycota. The complementary analysis of both ITS1 and ITS2 loci is therefore required to reliably estimate the diversity of lichen mycobiomes.

Keywords ascomycetes, basidiomycetes, endophytes, fungi, Ion Torrent, ITS1.

Introduction

The traditional view of lichens as mutualistic, symbiotic associations between one fungus, the mycobiont, and a population of algae, the photobionts (Hawksworth and Honegger 1994), has been reviewed in a more comprehensive and integrative context in which lichens act as microhabitats where multiple fungi (representing diverse classes of Dikarya), algae and bacteria coexist and likely contribute to the functions of the symbiotic system as a whole (Arnold et al. 2009; Grube et al. 2009; Muggia and Grube 2010; U'Ren et al. 2012; Grube et al. 2015; Spribille et al. 2016; Moya et al. 2017). The high diversity of lichen-associated fungi, and the fact that many species are found in different hosts and habitats, suggested that lichens act as "cradles of symbiotrophic fungal diversification" (Harutyunyan et al. 2008; Arnold et al. 2009; U'Ren et al. 2010, 2012). Recently, the diversity of lichen-associated fungi, hereafter referred to as lichen mycobiomes, has been emphasized by both culture-based methods and high-throughput amplicon sequencing techniques (U'Ren et al. 2010, 2012; Muggia et al. 2016; Fernández-Mendoza et al. 2017).

Multiple ecological guilds of fungi can be found growing associated with lichen thalli (Arnold et al. 2009; Bates et al. 2012; Fernández-Mendoza et al. 2017). One group of lichen-associated taxa are readily recognizable by their phenotypic characters and the conspicuous symptoms of infection shown by their hosts. Such taxa have long been referred to as lichenicolous fungi (Hawksworth 1979, 1981; Lawrey and Diederich 2003, 2016; Hafellner 2015). While the symptomatic occurrence of lichenicolous fungi is restricted to a few lichen hosts, we have recently observed that some lichenicolous fungi are present in other lichens without producing visible symptoms (Fernández-Mendoza et al. 2017). A second component of the lichen mycobiome is formed by species that cannot be detected morphologically, but are widely present within lichen thalli and are abundantly isolated using culture methods (Petrini et al. 1990; Girlanda et al. 1997; Harutyunyan et al. 2008; Muggia et al. 2016). These fungi have been collectively termed endolichenic fungi due to their relatedness to plant endophytes (Arnold et al. 2009); many others are also related to plant pathogens and rock-inhabiting fungi (RIF; Selbmann et al. 2015; Muggia et al. 2016). Finally, a third component is represented by extraneous fungi or fungal propagules found upon or incorporated within lichen thalli without playing any definite ecological role in the lichen community (Fernández-Mendoza et al. 2017). This third component can be derived from other lichen mycobionts present in the community under focus, or from fungi known from different niches. Lichens may act in this way as complex banks of spores and mycelia and would function as suboptimal habitats or reservoirs where the regeneration of local fungal communities can be potentially boosted (Fernández-Mendoza et al.

2017). In this regard, lichen thalli may serve as refuges where such fungi can remain in an immature state until an opportunity arises to occupy more favorable habitats (Muggia et al. 2010; Fernández-Mendoza et al. 2017).

The ITS region has been selected as formal DNA barcode for fungi due to its high interspecific variability, conserved primer sites and presence in multiple copies (Blaalid et al. 2013; Schoch et al. 2012). Its length, up to 800 base pairs (bp), is suitable for traditional (Sanger) DNA barcoding, but exceeds the read length required by most second-generation sequencing platforms for DNA metabarcoding, which averages 200-400 bp. For this reason, only one of the two spacers, either ITS1 or ITS2, has been sequenced so far. Even though diversity studies using these new technologies have become more and more common in the last years (Bellemain et al. 2013; Abdelfattah et al. 2015; Miller et al. 2016), it is still debated whether ITS1 or ITS2 has the best taxonomic resolution.

Few studies have dealt with the taxonomic resolution obtained using both the ITS1 and the ITS2 barcodes on the same dataset (Mello et al. 2011; Blaalid et al. 2013; Bazzicalupo et al. 2013; Monard et al. 2013; Orgiazzi et al. 2013). They have been carried out on both Ascomycota (Nilsson et al. 2009; Bellemain et al. 2013) and Basidiomycota (Badotti et al. 2017). Taxonomic bias can be introduced by the choice of primers, as these cause a higher number of mismatches in different taxa (Bellemain et al. 2013; Tedersoo et al. 2015; Tedersoo and Lindahl 2016). Some studies also reported that the two spacers are prone to preferential amplification at different level (Nilsson et al. 2009; Mello et al. 2011; Bellemain et al. 2013; Bazzicalupo et al. 2013; Monard et al. 2013). Basidiomycetes have on average longer amplicon sequences for the ITS2, and since the shorter sequences are preferentially sequenced with HTS, the use of ITS2 would favor the detection of ascomycetes (Bellemain et al. 2013). On the other hand, ITS1 often contains an intron that extends its sequence at the 5'-end (Martin and Rygiewicz 2005), thereby promoting an over-representation of those sequences that lack the intron (Bazzicalupo et al. 2013). Because ITS2 is more frequently represented in public databases, has a higher number of available sequences, and offers a better taxonomic resolution, it has been proposed as the better choice for parallel sequencing (Nilsson et al. 2009). In some cases, however, no substantial differences between ITS1 and ITS2 were recovered (Blaalid et al. 2013; Badotti et al. 2017). Finally, there are numerous studies that consider a single spacer, either the ITS1 or ITS2 (Bellemain et al. 2013; Langarica-Fuentes et al. 2014; U'Ren et al. 2014; Miller et al. 2016; Fernández-Mendoza et al. 2017).

As fungal metabarcoding studies have used different HTS platforms (see Cuadros-Orellana et al. 2013 for a review), different bioinformatic pipelines have been proposed (White et al. 2013; Bálint et al. 2014; Gweon et al. 2015). These have been developed based on experience gained from data analyses of prokaryote datasets (Hibbett 2016). However, no standard procedure has been established so far

for fungal sequence data. The analyses seem strongly dependent on the working hypotheses of each study and on the type of sequence at hand. As the majority of studies target fungal communities to uncover unknown diversity, an important and ongoing problem is the definition of those sequences lacking an assigned taxonomy (Nilsson et al. 2016). For this reason, many sequences still remain identified as "uncultured fungus". In addition, many fungi have not yet been sequenced and cannot offer reference sequences for ongoing studies (Hibbett 2016). Both cases emerge as main issues in investigations of lichen mycobiome(s) where unidentified fungi represent the largest proportion.

Previous studies processed high-throughput amplicon sequencing data from lichens, considering thalli of different growth forms and others infected by symptomatic lichenicolous fungi (Bates et al. 2012; U'Ren et al. 2012, 2014; Fernández-Mendoza et al. 2017). These studies demonstrated that lichens and their mycobiomes are suitable subjects for implementing bioinformatic analyses of fungal metabarcoding. Nonetheless, individual environmental specimens have rarely been used for the characterization of fungal assemblages (Yahr et al. 2016); this approach was initiated only recently by Fernández-Mendoza et al. (2017). The authors highlighted the suitability of single lichen thalli for reliable estimation of the mycobiome diversity within. Fernández-Mendoza et al. (2017) studied the mycobiome diversity by applying 454-pyrosequencing to a well characterized set of lichens (Fleischhacker et al. 2015; Muggia et al. 2016), comparing thalli visibly infected by lichenicolous fungi to others devoid of detectable infections. The authors expected fungal diversity within the lichen community and sought to determine whether lichenicolous fungi were asymptomatically present in typical and atypical lichen hosts, and whether the presence of symptomatic lichenicolous fungi correlated with the diversity of the other intrathalline, asymptomatically occurring fungi. They also attempted to gauge the potential specificity of thallus mycobiomes among different lichen hosts (Fernández-Mendoza et al. 2017).

As studies of lichen mycobiomes may fail to recover the complete taxonomic profile when using either the ITS1 or ITS2 regions individually, both regions should be examined to obtain more accurate estimates of species diversity. Here, we re-evaluate the fungal communities (Fig. 1) studied by Fernández-Mendoza et al. (2017) by sequencing the ITS2 fragment using the Ion Torrent (Thermo Fisher Scientific) platform. We assess the taxon diversity detected with the ITS2 barcode, focusing on new fungal sequences potentially corresponding to lichenicolous fungi, and compare the new ITS2 dataset with the previously analyzed ITS1 results. Because Fernández-Mendoza et al. (2017) used the 454-pyrosequencing method, we also evaluate the performance of high-throughput amplicon sequencing approaches in the analyses of lichen mycobiomes.

Material and methods

Sampling

Lichen samples and their DNA extractions correspond to those recently analyzed by Fernández-Mendoza et al. (2017) as part of a comprehensive study on fungi associated with lichens in alpine rock communities (Fleischhacker et al. 2015; Muggia et al. 2016, 2017). Samples (Table 1) were collected in ten plots (each about 300 m^2) at an altitude of 1800-1900 m on the Koralpe mountain range in Eastern Austria as reported in Fleischhacker et al. (2015). DNA was extracted from 26 samples, including 25 crustose and one foliose lichens, using the DNeasy Plant Mini Kit (Qiagen, Austria). Crustose lichens were predominant in the selected community; thalli consisted of contiguous areoles tightly adhering to the substrate. The single foliose thallus was represented by *Umbilicaria cylindrica*, which is attached to the substrate by a central holdfast (umbilicus). Half of the samples (13) were symptomatically infected by lichenicolous fungi, including, teleomorphic and anamorphic ascomycetes (Fig. 1 and Table 1). This means that lichenicolous fungi could be observed on the thallus and identified using light microscopy. The other 13 thalli were devoid of symptomatic fungal infections; we refer to them as 'asymptomatic samples,' without ruling out the cryptic presence of lichenicolous fungi within the thalli. The dataset includes a total of 10 species of symptomatic lichenicolous fungi and 13 species of lichen hosts (Table 1).

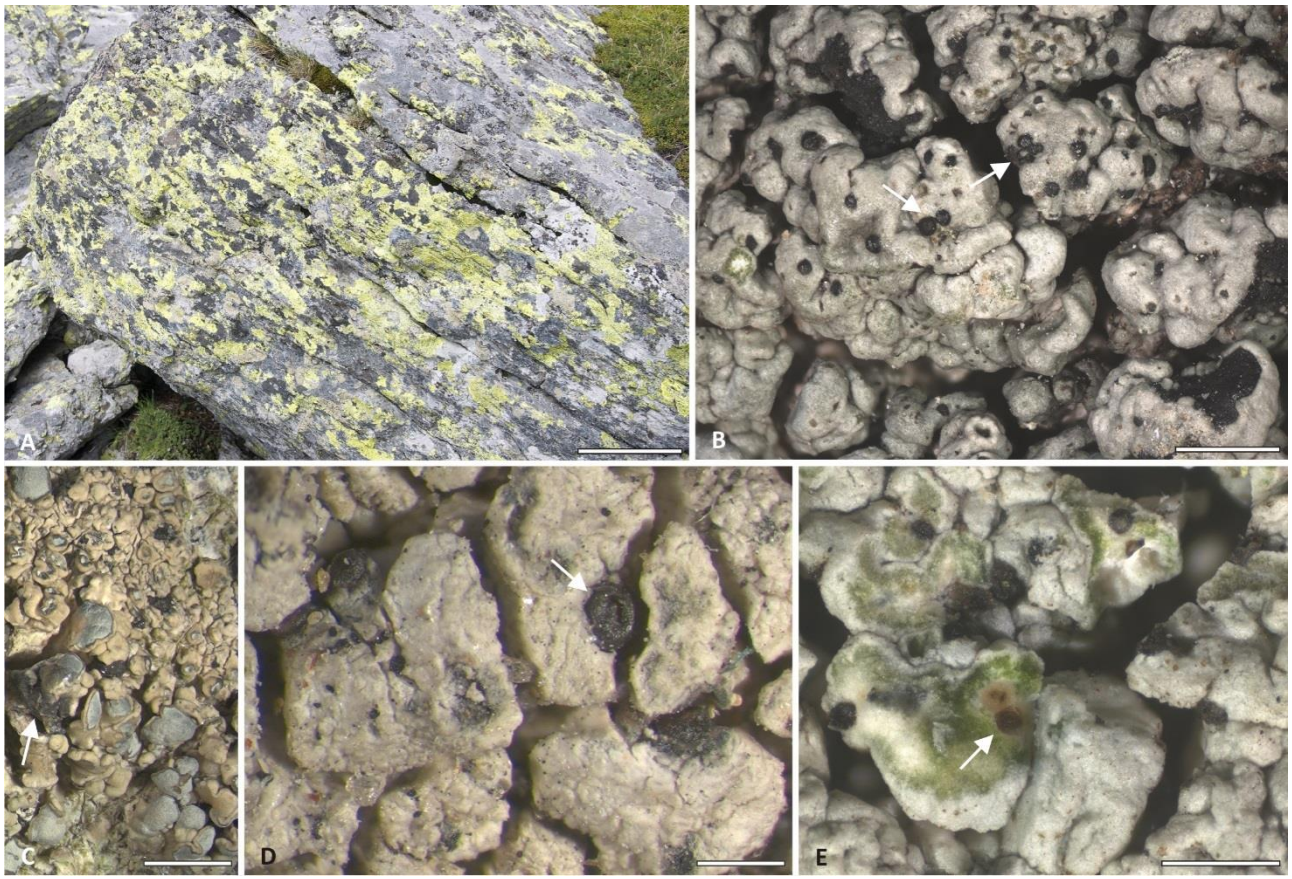

Figure 1. A) Alpine community of rock inhabiting lichens on siliceous boulders. B-E) Symptomatically infecting lichenicolous fungi on lichen host thalli: B) *Muellerella atricola* on *Tephromela atra*, C) *Sphaerellothecium atrinae* on *Lecanora swartzii*, D) *Sagediopsis fissurisedens* on *Aspilidea myrinii*. Arrows indicate the recognizable, phenotypic characters of the lichenicolous fungi: B, D) perithecia immerse at the margins of thallus areoles, C) dark, melanized discoloration in which perithecia are present, E) conidiomata (pycnidia) containing conidiospores immerse in the thallus areoles. Scale bars: A = 15 cm, B = 1 mm, C = 2 mm, D, E = 0.5 mm.

Table 1. Summary of dataset description and sequencing results. The table includes: sample numbers, name of the lichen host and of the symptomatic lichenicolous fungus, the total number of reads (Tot), the number of reads that passed quality filter (Qf), the number of reads (ITS2 extracted and chimera filtered) of the three datasets analyzed (complete, "no host", no myco"). The number of observed OTUs in each sample is given for the entire sample, whereas values of Chao1 and Shannon diversity indexes are calculated on datasets rarefied to 7133 for the complete, to 1073 for the "no host" and to 1060 reads for the "no myco". The diversity indexes are not reported where sequencing depth was not sufficient (/).

			Reads					OTUs			Chao1 estimate			Shannon diversity index		
Sample	**Lichen host**	**Infecting fungus**	Tot	Qf	Complete	"No host"	"No myco"	Complete	"No host"	"No myco"	Complete	"No host"	"No myco"	Complete	"No host"	"No myco"
A032	*Umbilicaria cylindrica*	-	16,964	13,049	11,898	217	166	111	35	19	111 ± 24	/	/	2.19 ± 0.05	/	/
A138	*Candelariella vitellina*	-	16,544	12,822	12,285	1,348	1,213	372	172	131	374 ± 57	185 ± 32	140 ± 24	3.6 ± 0.09	4.06 ± 0.67	3.57 ± 0.6
A172	*Rhizocarpon geographicum*	-	20,395	14,775	14,329	1,901	1,898	221	175	172	215 ± 44	177 ± 41	172 ± 36	2.67 ± 0.07	4.85 ± 0.72	4.85 ± 0.7
A194	*Rhizocarpon geographicum*	*Endococcus macrosporus*	18,682	15,256	14,643	1,073	1,060	229	117	109	224 ± 44	120 ± 23	116 ± 20	1.71 ± 0.07	3.97 ± 0.56	3.9 ± 0.55
A227	*Lecanora swartzii*	-	16,328	13,409	12,360	86	54	549	22	9	568 ± 75	/	/	3.32 ± 0.1	/	/
A229	*Psorinia conglomerata*	-	21,095	15,997	14,283	3,453	160	417	332	64	414 ± 107	299 ± 99	/	2.99 ± 0.07	4.21 ± 0.57	/
A243	*Lecanora polytropa*	-	16,726	13,489	13,176	224	40	135	64	18	137 ± 29	/	/	0.58 ± 0.04	/	/
A280	*Tephromela atra*	*Skyttea tephromelarum*	11,074	7,805	7,140	863	854	201	90	87	242 ± 54	/	/	2.6 ± 0.05	/	/
A360	*Lecanora intricata*	-	18,643	13,619	12,329	5,671	5,326	179	127	77	183 ± 41	90 ± 38	57 ± 37	1.89 ± 0.06	1.29 ± 0.27	0.83 ± 0.17
A361	*Tephromela atra*	-	13,883	11,180	11,040	44	43	141	26	25	161 ± 49	/	/	1.14 ± 0.03	/	/
A368	*Lecanora bicincta*	-	14,797	12,120	11,836	36	4	220	17	2	223 ± 54	/	/	1.52 ± 0.07	/	/
A405	*Rhizocarpon geographicum*	*Muellerella pygmaea-Rg*	18,630	11,455	10,963	1,377	1,363	265	232	228	267 ± 40	235 ± 31	238 ± 26	1.96 ± 0.08	6.16 ± 1.02	6.14 ± 1.02
A418	*Lecanora polytropa*	*Lichenoconium lecanorae*	17,149	13,200	12,196	588	305	208	147	80	215 ± 53	/	/	2.75 ± 0.05	/	/
A420	*Aspilidea myrinii*	-	13,490	8,955	8,147	593	435	295	61	51	313 ± 45	/	/	3.43 ± 0.06	/	/
A434	*Lecanora polytropa*	*Lichenoconium lecanorae*	16,335	12,172	11,296	7,370	7,223	557	526	491	579 ± 73	426 ± 148	400 ± 158	5.06 ± 0.11	4.53 ± 0.59	4.46 ± 0.62

A440	*Tephromela atra*	*Muellerella atricola*	14,501	11,034	9,276	1,371	1,321	215	129	114	244 ± 60	139 ± 35	128 ± 31	2.06 ± 0.07	4.14 ± 0.52	3.95 ± 0.49
A476	*Psorinia conglomerata*	-	16,627	13,164	12,803	2,939	655	417	352	132	456 ± 117	325 ± 98	/	2.98 ± 0.09	4.64 ± 0.7	/
A482	*Lecanora polytropa*	*Cercidospora epipolytropa*	11,479	9,472	9,171	471	446	166	79	67	168 ± 28	/	/	1.28 ± 0.06	/	/
	Aspilidea myrinii	*Sagediopsis fissurisedens*	16,780	13,002	12,326	7,964	7,858	362	158	146	370 ± 71	105 ± 51	105 ± 60	2.52 ± 0.07	0.76 ± 0.19	0.65 ± 0.2
A622	*Varicellaria lactea*	*Stigmidium eucline*	25,805	12,400	12,068	5,296	4,822	326	204	143	323 ± 61	149 ± 64	107 ± 45	3.84 ± 0.06	2.57 ± 0.37	2.06 ± 0.33
A623	*Acarospora fuscata*	-	19,532	16,069	15,939	38	32	96	19	13	97 ± 34	/	/	1.1 ± 0.03	/	/
A636	*Lecidea lapicida*	*Muellerella pygmaea s.s.*	3,499	496	454	230	230	52	37	37	/	/	/	/	/	/
A670	*Lecanora polytropa*	*Muellerella pygmaea-Lp*	12,531	9,404	8,923	6,447	6,192	360	308	277	361 ± 49	247 ± 92	228 ± 81	3.41 ± 0.1	2.33 ± 0.47	2.1 ± 0.4
A792	*Lecidea lapicida*	-	17,241	13,683	12,326	863	79	184	128	27	183 ± 38	/	/	1.38 ± 0.06	/	/
A809	*Tephromela atra*	*Taeniolella atricerebrina*	24,994	20,106	19,353	7,980	7,964	304	198	190	290 ± 81	181 ± 114	143 ± 68	1.99 ± 0.06	0.94 ± 0.22	0.91 ± 0.25
A832	*Lecanora bicincta*	*Arthonia varians*	9,016	7,403	7,133	85	68	164	23	9	216 ± 54	/	/	1.11 ± 0.05	/	/
Symptomatically infected samples			200,475	143,205	134,942	41,115	39,706	3,409	2,248	1,978	244 ± 95	238 ± 125	215 ± 118	2.56 ± 1.10	3.46 ± 1.88	3.29 ± 1.93
Uninfected samples			222,265	172,331	162,751	17,413	10,105	3,337	1,530	740	216 ± 115	259 ± 120	133 ± 43	2.25 ± 0.99	4.14 ± 1.40	3.34 ± 1.84
Total			422,740	315,536	297,693	58,528	49,811	6,746	3,778	2,718	229 ± 107	246 ± 123	193 ± 110	2.40 ± 1.06	3.72 ± 1.74	3.31 ± 1.91

Molecular analysis and sequencing

The fungal nuclear ribosomal ITS2 region was amplified with the forward primer ITS3 and the reverse primer ITS4 (White et al. 1990). The amplicons for HTS were obtained by performing two PCR amplifications. The first PCR amplification used the forward and the reverse primers ITS3 and ITS4 modified with GC rich universal tails on the 5'-end (Carew et al. 2013). The 5'-end tail was identical to the tail applied on the 3'-end of the barcodes used in the second PCR. The first PCR reaction mix contained 3 µl DNA template (10-20 ng), 3 µl HotMasterMix (5PRIME, Fisher Scientific), 0.5 µl BSA 10X (Sigma-Aldrich), 0.75 µl EvaGreen™ 20X (Biotium), 0.5 µl forward primer ITS3 (10 µM), 0.5 µl reverse primer ITS4 (10 µM) in a final volume of 15 µl. The PCR amplifications were performed with CFX 96™ PCR System (Bio-Rad) with the following cycling profile: 94 °C for 2 min and 30 cycles at 94 °C for 20 sec, 55 °C for 20 sec, 65 °C for 40 sec followed by a final extension at 65 °C for 2 min. A negative control was used to verify the absence of non-specific amplification products along the whole amplification and sequencing process.

The second PCR amplification (switch PCR) was required for the multiplex sequencing and the attachment of the barcodes. It used primers modified with an 'A' adaptor and a sample-specific 10 bp barcode to the 5'-end of the forward primer, and a P1 adaptor to the 5'-end of the reverse primer. The reaction was performed in a mix containing 5 µl of the first PCR product, 20 µl HotMasterMix (5PRIME), 2.5 µl EvaGreen™ 20X (Biotium), 1.5 µl forward primer (10 µM), and 1.5 µl reverse primer (10 µM) in a final volume of 50 µl. PCR conditions were the same as for the first PCR amplification but were repeated for 8 cycles. All the amplicons were checked for their quality and size by agarose gel electrophoresis and normalized using Mag-Bind® Normalizer Kit (Omega Biotek). Product concentrations were checked with NanoDrop® 2000 (Thermo Fisher Scientific). The amplicons of the different samples were pooled together in equimolar amounts and the resulting barcoded library was measured with Qubit™ Fluorimeter (Thermo Fisher Scientific) and sequenced with an Ion Torrent Personal Genome Machine™ (PGM, Thermo Fisher Scientific) using a 314™ chip (Thermo Fisher Scientific) for a maximum read length of 400 bp.

Data analysis

QIIME v.1.8.1 (Caporaso et al. 2010) was used to process the sequence data (Fig. 2).

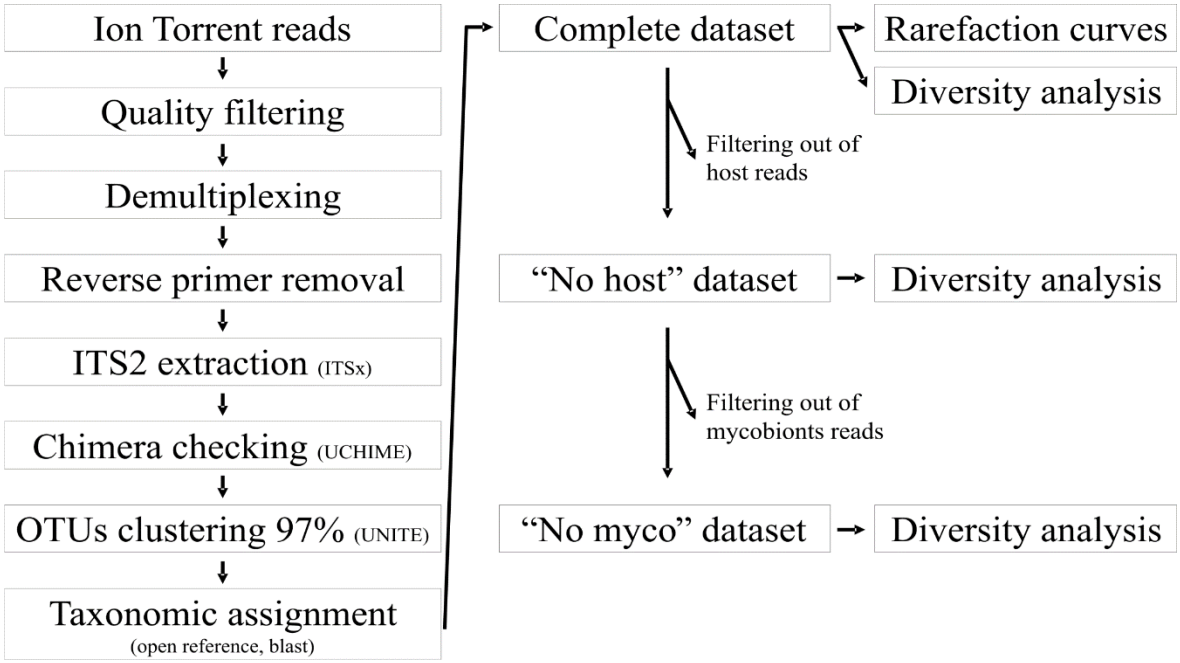

Figure 2. Flowchart of the analytical pipeline implemented in QIIME and performed for the analyses of the fungal ITS2 dataset. The programs used are reported in parentheses.

High quality sequences were demultiplexed (minimum length 150 bp, maximum length of homopolymer 8, maximum number of primer mismatches 3). Minimum average quality score was set to 20 (Kemler et al. 2013; Tang et al. 2015). Reverse primers and barcodes were removed, and reads that did not pass through the filtering were discarded. In order to retain only fungal reads, the ITS2 region was extracted with ITSx v.1.0.11 (Bengtsson-Palme et al. 2013) selecting the fungal (F) profile option. Chimeric reads were identified and filtered out with UCHIME v.4.0 algorithm using the reference dataset updated on 01.01.2016 (Edgar et al. 2011; Nilsson et al. 2015) to obtain the final, high quality dataset, here referred as complete dataset. Operational Taxonomic Units (OTUs) were picked at 97% similarity with open reference strategy and UNITE database, updated on November 2016 (Kõljalg et al. 2013). OTUs taxonomy was assigned using NCBI public nucleotide database implemented with the blastn algorithm (max E-value $1e^{-30}$). Singletons, intended as reads present once in the entire sequence dataset (Zhang et al. 2015; Fernández-Mendoza et al. 2017; Moya et al. 2017) were removed. Our workflow (Fig. 2) was organized into three steps in which we analyze progressively more reduced datasets of reads. All the reads representing the mycobiont hosts of each samples at genus level (e.g. *Lecanora*, *Rhizocarpon*) were subtracted from the initial complete dataset. This reduced second dataset was named 'no host'. From the 'no host' dataset, all reads corresponding to lichen mycobionts (i.e. *Caloplaca*, *Parmelia*), independently from their presence in

the lichen community under study, were further filtered out and the obtained third dataset was named 'no myco'.

Due to the lack or the limited number of reference sequences in the NCBI database for certain lichen host species, such as *Aspilidea myrinii*, *Psorinia conglomerata* and *Varicellaria lactea*, the automatic blast search resulted in an incorrect taxonomic assignment of these taxa. They matched with sequences of the genera *Cladonia, Lecania* and *Mycosphaerella*, respectively. Furthermore, the automatic blast search resulted in "no blast hit, unclassified" for a number of OTUs corresponding to the lichen host *Rhizocarpon*; these biases were manually corrected. Our dataset included 13 samples that were symptomatically infected by ten species of lichenicolous fungi (Fig. 1, Table 1 and Table 2). However, ITS reference sequences were available in NCBI database for only four genera, *Arthonia*, *Endococcus*, *Skyttea* and *Taeniolella*, and corresponded to the following hits: *Arthonia sardoa* (AF138813), *Endococcus fusigera* (FJ645262), *Skyttea gregaria* (KJ559537), *S. radiatilis* (KJ559536, KJ559538), *S. lecanorae* (KJ559539), *S. cismonicae* (KP984783), *Taeniolella stilbospora* (AY843127), *T. phialosperma* (GU966521, KF703925, LC053497) and *T. rudis* (JQ429152). Read identity of the three lichenicolous fungi *Endococcus macrosporus*, *Skyttea tephromelarum* and *Taeniolella atricerebrina* in the respective symptomatically infected samples (Table 2) could be confirmed according to the reference sequences.

Statistics and ecological indices were performed with QIIME (Caporaso et al. 2010). The alpha and beta diversity analyses were conducted on the three datasets (i.e. complete dataset, 'no host', 'no myco') each rarefied to the lowest reads count, considering samples with at least 1000 reads. Alpha diversity was calculated using Chao1 (Chao et al. 2009) and Shannon indices (Spellerberg and Fedor 2003). The non-parametric Kruskal-Wallis test was applied to verify the significance of differences in alpha diversity between symptomatically infected and asymptomatic samples with R v.3.2.0 (R Core Team 2015). The distribution of beta diversity was explored using Principal Coordinate Analysis (PCoA) on Bray-Curtis distance matrices; the uncertainty in PCoA plots was estimated using jackknife replicates. Rarefaction was applied by taking a random subset of reads for each sample, corresponding to the 80% of the total read number of those samples with the lowest number of reads in each dataset. The PCoA axes were visualized with EMPeror (Vazquez-Baeza et al. 2013) in two-dimensional plots. Spearman's correlation on the samples was performed using the software package Statistica v.10 (StatSoft Inc.) to verify the linear relationship between the taxonomic composition detected by ITS1 (Fernández-Mendoza et al. 2017) and by ITS2 (this study) barcodes.

Shared OTUs were visualized using the software Circos v.0.63-9 (Krzywinski et al. 2009). We compared: *i)* the amount of shared OTUs among samples, considering the complete, the 'no host' and the 'no myco' datasets; *ii)* the mycobiomes in the 'no myco' dataset among samples of the same lichen

host genus or species (*Lecanora* spp., *Rhizocarpon geographicum* and *Tephromela atra*) which were either symptomatically infected by different lichenicolous fungi or asymptomatic; *iii)* the presence of the main orders of lichen-associated fungi in symptomatically infected and asymptomatic samples.

DNA extraction, amplification and sequencing of fungal isolates

To determine whether any fungus isolated in culture from lichen samples within the same community was also detected in the amplicon dataset, we selected ten fungal isolates available from the previous analyses of Muggia et al. (2016). The ten isolates (A572, A899, A923, A930, A931, A951, A985, A993, A1022, A1033) represent those strains of Dothideomycetes and Eurotiomycetes which were most frequently isolated from the studied lichen community. The DNA was extracted with the Plant DNeasy Kit (Qiagen) following manufactures instructions. The fungal nuclear ribosomal ITS2 region was amplified with the forward primer ITS3 and the reverse primer ITS4 (White et al. 1990). The PCR reaction mix contained 3 µl DNA template (10-20 ng), 5 µl Taq Buffer A (10X, Kapa Biosystems), 0.2 µl Taq DNA Polymerase (5 U/µl, Kapa Biosystems), 1 µl dNTPs (10 mM), 2 µl forward primer ITS3 (10 µM), 2 µl reverse primer ITS4 (10 µM) in a final volume of 50 µl. The PCR amplifications were performed with the following cycling profile: 95 °C for 3 min and 38 cycles at 95 °C for 30 sec, 55 °C for 30 sec, 72 °C for 1 min followed by a final extension at 72 °C for 1 min. A negative control was used to verify the absence of non-specific amplification products along the whole amplification and sequencing process. Sanger sequencing of PCR products (one for each culture) was performed at the Applied Genomic Institute (IGA) in Udine (Italy).

Results

DNA sequencing and data analysis

A total of 422,740 raw reads with an average length of 342 bp were generated after quality filtering (Table 1); raw data can be accessed at the NCBI short reads repository under the accession number SRR5750451. After the extraction of ITS2 and checking for chimera sequences, 297,693 reads were retained to constitute the complete dataset. The sequencing depth was not even among samples, ranging between 7,133 to 19,353 reads, with only one sample with less than 1000 reads (Table 1). After excluding reads belonging to the mycobiont host in each sample, 58,528 reads were retained to constitute the 'no host' dataset. The subsequent exclusion of reads belonging to any lichen mycobionts from all the samples, retained 49,811 reads to form the 'no myco' dataset (Fig. 2, Table 1).

Rarefaction curves of the three datasets showed large variation in the total number of OTUs among samples; not all of them leveled off and approached saturation, indicating that detection of additional OTUs may be possible (Supplementary Fig.1).

Comparison between symptomatically infected and asymptomatic samples

The complete dataset was rarified to 7133, the 'no host' to 1073 and the 'no myco' to 1060 reads. This led to the progressive exclusion of one (A636), thirteen (A032, A227, A243, A280, A361, A368, A418, A420, A482, A623, A636, A792 and A832) and fourteen samples (A032, A227, A243, A280, A361, A368, A418, A420, A476, A482, A623, A636, A792 and A832) from the three datasets, respectively. Sample A434 (*Lecanora polytropa* infected with *Lichenoconium lecanorae*) presented the highest fungal diversity in all three datasets (579±73, 426±148 and 400±158 in the complete, 'no host' and 'no myco' dataset, respectively) according to the Chao1 index, and the highest diversity only in the complete dataset, according to the Shannon diversity index (5.06 ± 0.11). No significant differences between infected and asymptomatic samples were found in the three datasets (Chao1 p-values: 0.302, 0.685, 0.540; Shannon p- values: 0.625, 0.306, 0.882 for the complete, 'no host' and 'no myco' datasets respectively; Table 1) when the indexes were compared with the Kruskal-Wallis test.

The beta diversity analysis showed that, in the complete dataset, samples were grouped mostly according to the lichen host species. Here, samples of *Psorinia conglomerata* and *Tephromela atra* distinctly separate from the other samples (Supplementary Fig. 2). In the PCoA analyses of the 'no host' (Fig. 3A) and 'no myco' (Fig. 3B) datasets the maximum percentage of variation explained by PC1 axis was 15.4% and 13.7%, respectively (Fig. 3 and Supplementary Fig. 3). The two dimensional plots in both datasets do not separate the samples according to the lichen host, the lichen associated fungi, or the symptomatic fungal infection.

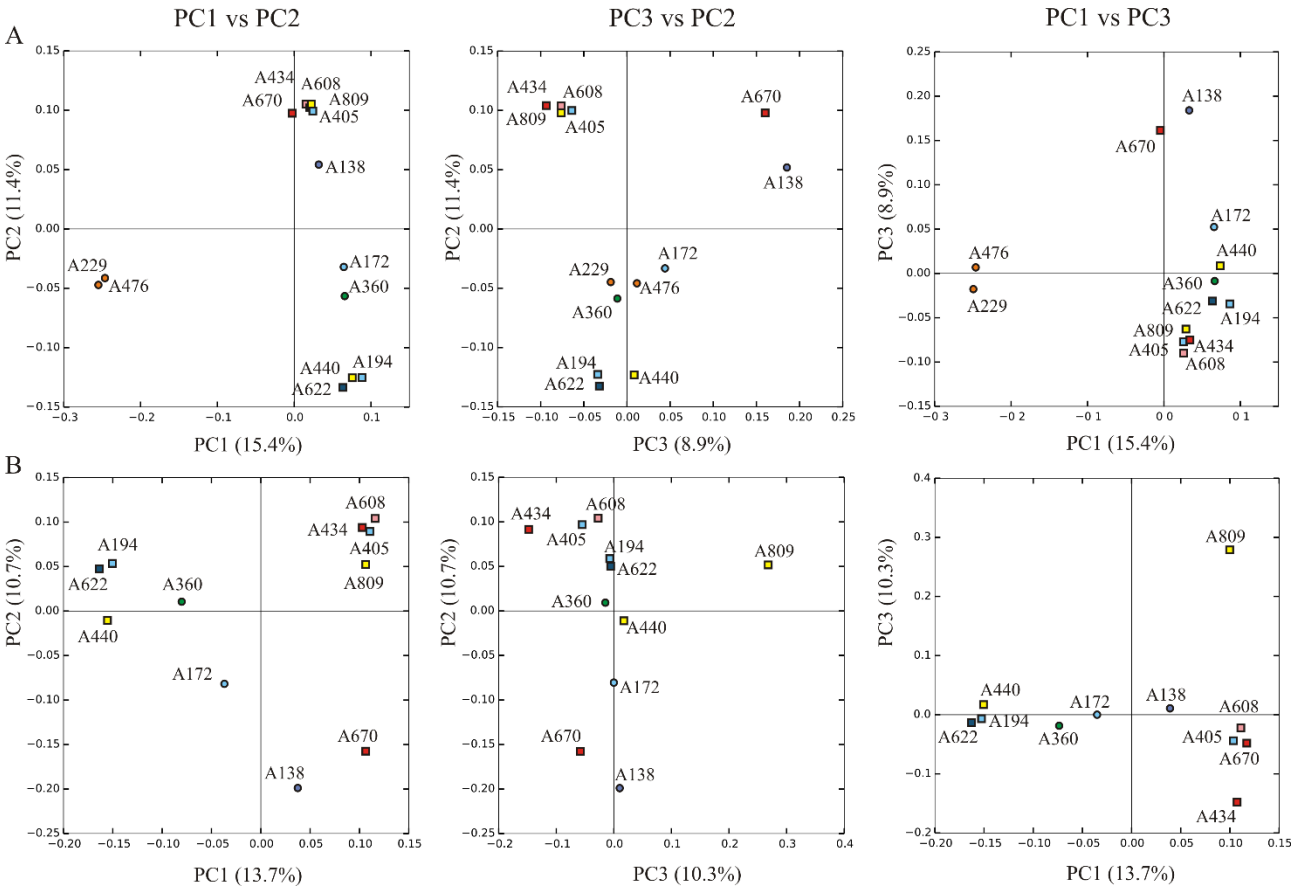

Figure 3. Principal Coordinate Analysis (PCoA) plots of Bray-Curtis distances based on the rarefied datasets of "no host" (A) and "no myco" (B). Symptomatically infected samples are represented by squares, asymptomatic samples are represented by circles. The percentage of variation explained by each axis is reported in parentheses. The colors indicate different lichen hosts: *Aspilidea myrinii* (pink), *Candelariella vitellina* (violet), *Lecanora intricata* (green), *L. polytropa* (red), *Psorinia conglomerata* (orange), *Rhizocarpon geographicum* (light blue), *Tephromela atra* (yellow) and *Varicellaria lactea* (blue).

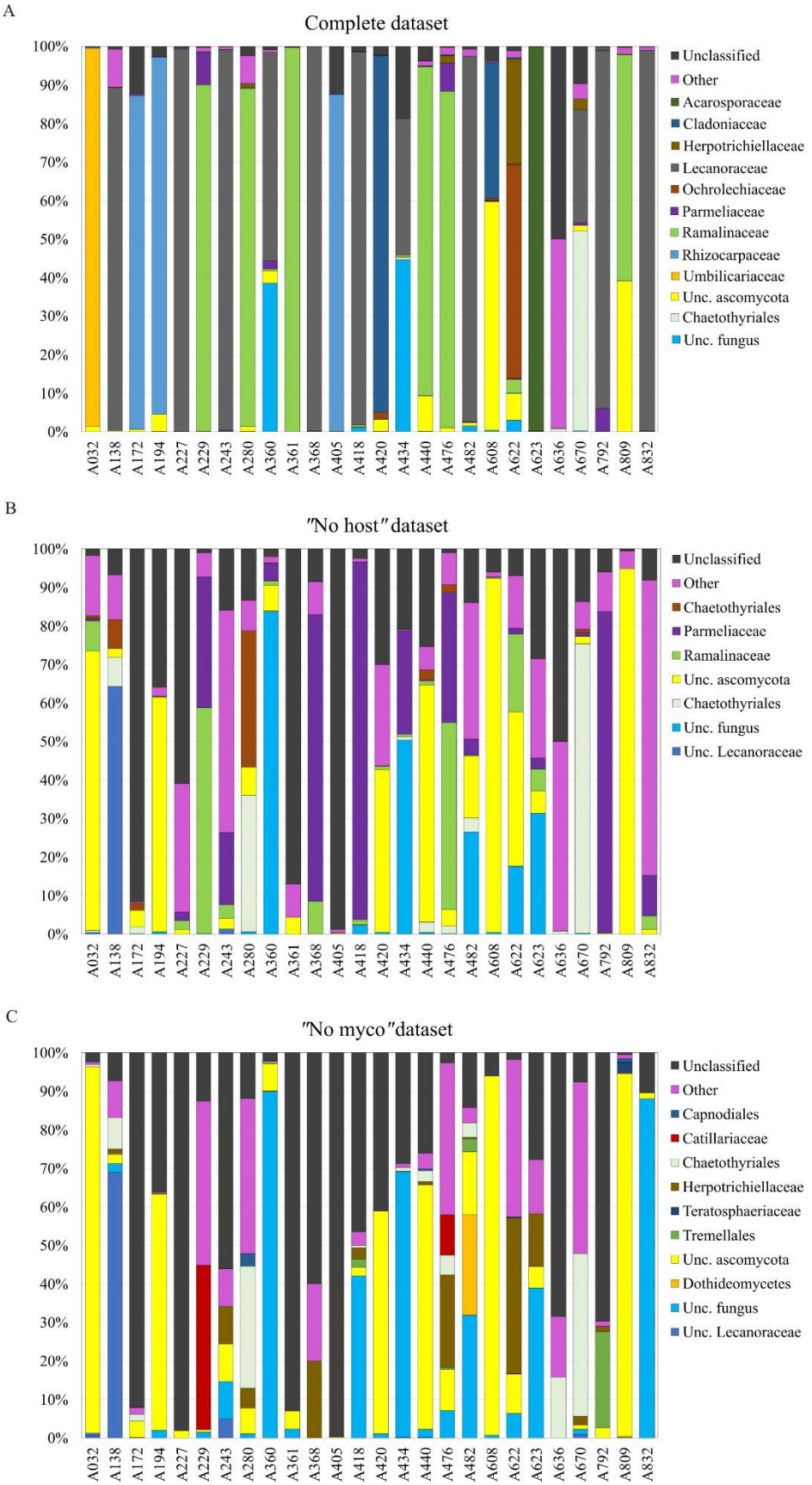

Figure 4. Summary of the taxonomic assignment up to family level of the complete (A), the "no host" (B) and the "no myco" (C) datasets. Taxa accounting for <1% (in A and B) and <0.1% (in C) of reads are grouped as "Other". "Unc." stays for "uncultured". Bars reflect the proportion of reads from the ITS2 dataset for each sample.

Detection of fungal diversity: lichen mycobionts and lichen-associated fungi

Almost all the reads assigned at kingdom level were ascomycetes (99.9%, Fig. 4); basidiomycetes (mostly Tremellomycetes) were detected in a very low proportion and in 12 samples only. In 12 samples, over 90% of the reads corresponded to the lichen mycobiont (Fig. 4A, Table 1 and Table 2). The three samples that were symptomatically infected by lichenicolous fungi (A434, A608 and A670) also had the lowest proportion of mycobionts reads (<35%). In each sample, multiple OTUs were found to correspond to the same mycobiont host (as similarly recovered by Fernández-Mendoza et al. 2017), whereas for the lichenicolous fungi this was the case only for *Taeniolella atricerebrina*, for which three OTUs were recovered (Table 2).

Table 2. Number of OTUs and corresponding number of reads identified as the lichen host and the symptomatic lichenicolous fungi (in bold). (°) Samples in which reads corresponding to more than one lichenicolous fungus were recovered. (#) Samples without reads corresponding to any lichenicolous fungi. (*) Lichenicolous fungi for which the identity was confirmed with GenBank BLAST search.

Sample	**Lichen host**	**OTUs (reads)**	**Infecting fungus**	*A.varians**	*C. epipolytropa*	*E. macrosporus**	*L. lecanorae*	*M. atricola*	*M. pygmaea*	*S. eucline*	*S. fissurisedens*	*S. tephromelarum**	*T. atricerebrina**
A032#	*Umbilicaria cylindrica*	76 (11,681)	-										
A138	*Candelariella vitellina*	200 (10,937)	-										OTU52 (3)
A172#	*Rhizocarpon geographicum*	46 (12,428)	-										
A194	*Rhizocarpon geographicum*	112 (13,570)	*Endococcus macrosporus*			**OTU6656 (48)**							
A227	*Lecanora swartzii*	527 (12,274)	-										OTU52 (1)
A229	*Psorinia conglomerata*	85 (10,830)	-								OTU43 (2)		
A243#	*Lecanora polytropa*	71 (12,952)	-										
A280°	*Tephromela atra*	111 (6,277)	*Skyttea tephromelarum*								OTU43 (1)	**OTU3878 (2)**	
A360	*Lecanora intricata*	52 (6,658)	-	-									OTU52 (4)
A361#	*Tephromela atra*	115 (10,996)	-										
A368	*Lecanora bicincta*	203 (11,800)	-							OTU45 (1)			
A405	*Rhizocarpon geographicum*	33 (9,586)	*Muellerella pygmaea-Rg*						-	OTU45 (1)			
A418°	*Lecanora polytropa*	52 (11,608)	*Lichenoconium lecanorae*				**OTU15 (36)**				OTU43 (2)		

A420	*Aspilidea myrinii*	234 (7,554)	-								OTU43 (238)		
A434°	*Lecanora polytropa*	22 (3,926)	*Lichenoconium lecanorae*				**OTU15 (1,208)**				OTU43 (1)		OTU52 (1)
A440°	*Tephromela atra*	86 (7,905)	*Muellerella atricola*					**OTU4764 (111)**					OTU52 (7)
A476	*Psorinia conglomerata*	65 (9,864)	-							OTU45 (1)			
A482	*Lecanora polytropa*	87 (8,700)	*Cercidospora epipolytropa*		**OTU8283 (123)**								
A608	*Aspilidea myrinii*	204 (4,362)	*Sagediopsis fissurisedens*								**OTU43 (7312)**		
A622°	*Varicellaria lactea*	122 (6,772)	*Stigmidium eucline*							**OTU45 (3,288)**			OTU52 (3)
A623	*Acarospora fuscata*	77 (15,901)	-										OTU52 (1)
A636	*Lecidea lapicida*	15 (224)	*Muellerella pygmaea s.s.*						**OTU38 (40)**				
A670°	*Lecanora polytropa*	52 (2,476)	*Muellerella pygmaea-Lp*						**OTU38 (4,633)**				OTU52 (1)
A792	*Lecidea lapicida*	56 (11,463)	-								OTU43 (1)		
A809	*Tephromela atra*	106 (11,373)	*Taeniolella atricerebrina*										**OTU52 (7,093), OTU3 (214), OTU1403 (49)**
A832	*Lecanora bicincta*	141 (7,048)	*Arthonia varians*	-									

Taeniolella atricerebrina was detected asymptomatically in samples of the same lichen host (*Tephromela atra* A440) symptomatically infected by the lichenicolous fungus *Muellerella atricola*, and in other four lichen hosts (*Acarospora*, *Candelariella*, *Lecanora*, *Varicellaria*; Table 2). *Taeniolella atricerebrina* was identified by three OTUs, the most abundant represented by 7,093 reads (OTU52), the second and the third most abundant ones by 214 and 49 reads (OTU3 and OTU1403), respectively. All three OTUs were present in the symptomatically infected sample *Tephromela atra* A809, while only the most abundant OTU52 was recovered in the other samples, though with a number of reads ranging from 1 to 7 (Table 2).

Based on the abundance and taxonomic assignment, we predicted the identity of the reads corresponding to the symptomatically infecting lichenicolous fungi *Cercidospora epipolytropa* (A482), *Stigmidium eucline* (A622), *Lichenoconium lecanorae* (A418, A434), *Sagediopsis fissurisedens* (A608) and *Muellerella atricola* (A440). For each of these fungi, a blast search recovered a single OTU matching with "uncultured Ascomycota" or "unclassified". The OTUs corresponding to *Sagediopsis fissurisedens* (OTU43) and *Stigmidium eucline* (OTU45) were also found in lichen samples other than their known hosts (Table 2). The lichenicolous fungus *Muellerella pygmea* was symptomatically present in three lichen samples (A405, A636, A670); however, OTU38, which we tentatively assigned to *M. pygmaea* because it matched with Chaetothyriales in a blast search, was found only in two of them (in A636 with 40 reads, 9%; in A670 with 4633 reads, 52%). This result suggests that the identification of *Muellerella* could be correct, as previous studies reported the fungus in this order (Muggia et al. 2015; Triebel and Kainz 2004). In the single case of the sample *Lecanora bicincta* A832 infected by *Arthonia varians*, we could not detect any OTU assignable to the lichenicolous fungus. Finally, we did not recover any OTU assignable to lichenicolous fungi in four specimens (A032, A172, A243, A361) whereas we recovered OTUs of different lichenicolous fungi co-occurring in seven specimens, of which six were symptomatically infected (A280, A418, A434, A440, A622, A670) and one was without visible infection (A360; Table 2).

In the 'no host' dataset, 23% of the reads belonged to the orders Chaetothyriales (Eurotiomycetes, Ascomycota) and Lecanorales (Lecanoromycetes, Ascomycota) (Fig. 4B). The most represented families were Herpotrichiellaceae (Chaetothyriales), Parmeliaceae and Ramalinaceae (Lecanorales); 30% of the reads could be assigned up to the kingdom level (Fig. 4B). Reads blasting as "uncultured fungi" and "unclassified" represented 13% and 15% of the dataset, respectively.

In the 'no myco' dataset (Fig. 4C) up to 37% of the reads could be assigned to the order level within Ascomycota and they belonged again to Chaetothyriales (Eurotiomycetes), Capnodiales (Dothideomycetes) and Lecanorales (Lecanoromycetes). The most represented families were

Herpotrichiellaceae (Chaetothyriales) and Catillariaceae (Lecanorales). About 0.12% belonged to Tremellales (Basidiomycota), 22% to "uncultured fungi" and 17% remained unclassified (Fig. 4C).

The relative abundances of Ascomycota and Basidiomycota among the lichen-associated fungi was compared (Fig. 5) between the ITS1 (Fernández-Mendoza *et al*. 2017) and ITS2 datasets (this study). Spearman's correlation was calculated for the most represented orders Capnodiales, Chaetothyriales and Tremellales. The relative abundances were 0.24, 0.07 and -0.036 respectively, and indicated no significant ($P<0.05$) linear relationship between ITS1 and ITS2 datasets. The relative abundance of these orders differs between the two barcodes, being 25.6% and 0.3% for Capnodiales, 10.1% and 9.6% for Chaetothyriales and 44.5% and 0.2% for Tremellales in the ITS1 and ITS2 datasets, respectively.

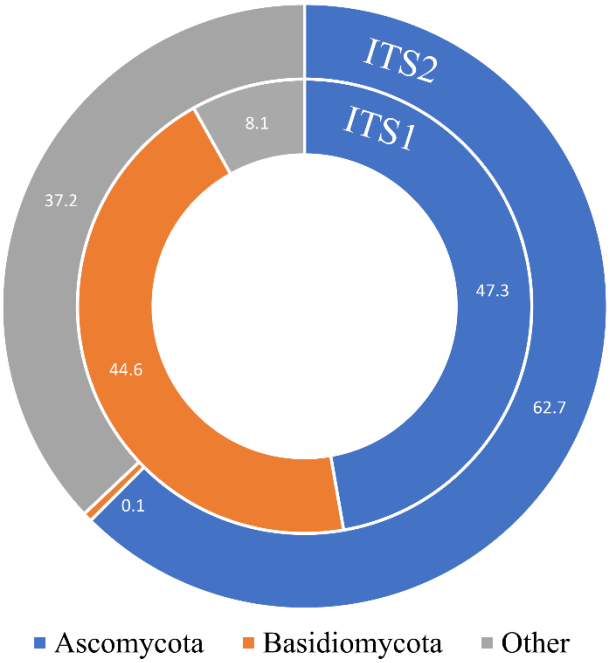

Figure 5. Comparison between the taxonomic composition of ITS1 (Fernández-Mendoza *et al.* 2017) and ITS2 based on the most recovered fungal orders in Ascomycota (Capnodiales and Chaetothyriales) and Basidiomycota (Tremellales). Bars reflect the proportion of reads assigned to the respective taxa in the two datasets. "Other" comprehends other fungal divisions, uncultured and unidentified fungi.

Shared OTUs among samples

Though each sample is characterized overall by a high proportion of sample-specific OTUs, lichen mycobiomes are quite interconnected due to many shared OTUs (Fig. 6; Supplementary Tables 1-9). The main orders of lichen-associated fungi in which shared OTUs are recovered are Capnodiales, Chaethotyriales and Tremellales (Fig. 7; Supplementary Tables 7-9).

In the complete dataset (Fig. 6A; Supplementary Table 1) and in the 'no host' dataset (Fig. 6B; Supplementary Table 2), the two samples A229 and A476 of *Psorinia conglomerata* share a maximum of 307 and 250 OTUs, respectively. The 250 shared OTUs in *P. conglomerata* belong mainly to mycobiont genera of Ramalinaceae and Parmeliaceae, and are responsible for the strong similarity of the two samples (as in Fig. 3A). No OTUs were shared by 26 pairs of samples in the complete dataset, nor by 102 pairs of samples in the 'no host' dataset.

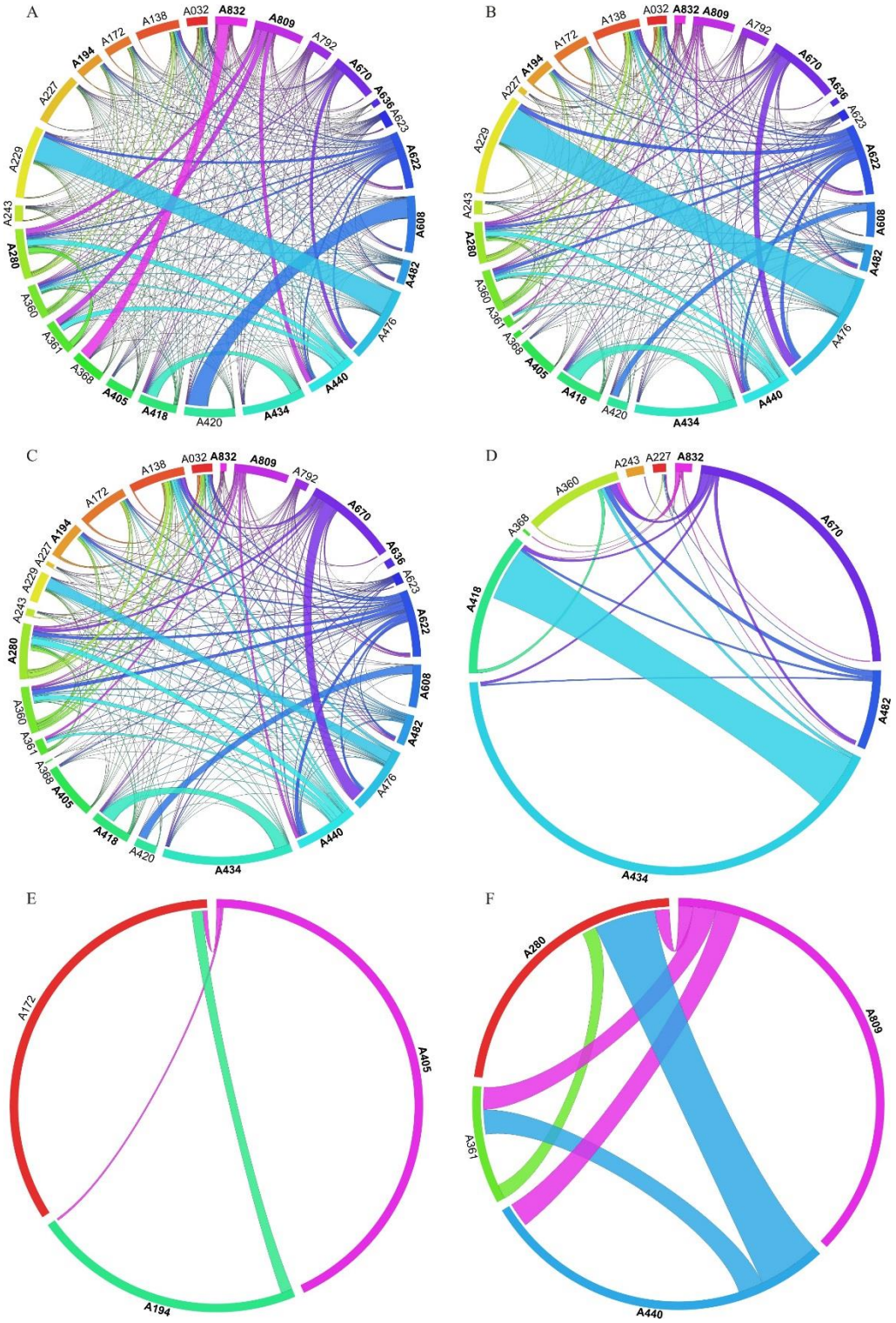

Figure 6. Circos plots showing shared OTUs among lichen mycobiomes. Symptomatically infected samples (as in Table 1) are in bold. The length of the sample-ribbons is directly proportional to the number of OTUs identified in each sample. The width of each connector between two samples is directly proportional to the number of shared OTUs. Shared OTUs among all samples in the complete dataset (A), "no host" (B) and "no myco" (C) dataset are presented. Shared OTUs calculated on the "no myco" dataset among samples of the same mycobiont genus or same species are shown for the lichens *Lecanora* spp. (D), *Rhizocarpon geographicum* (E) and *Tephromela atra* (F).

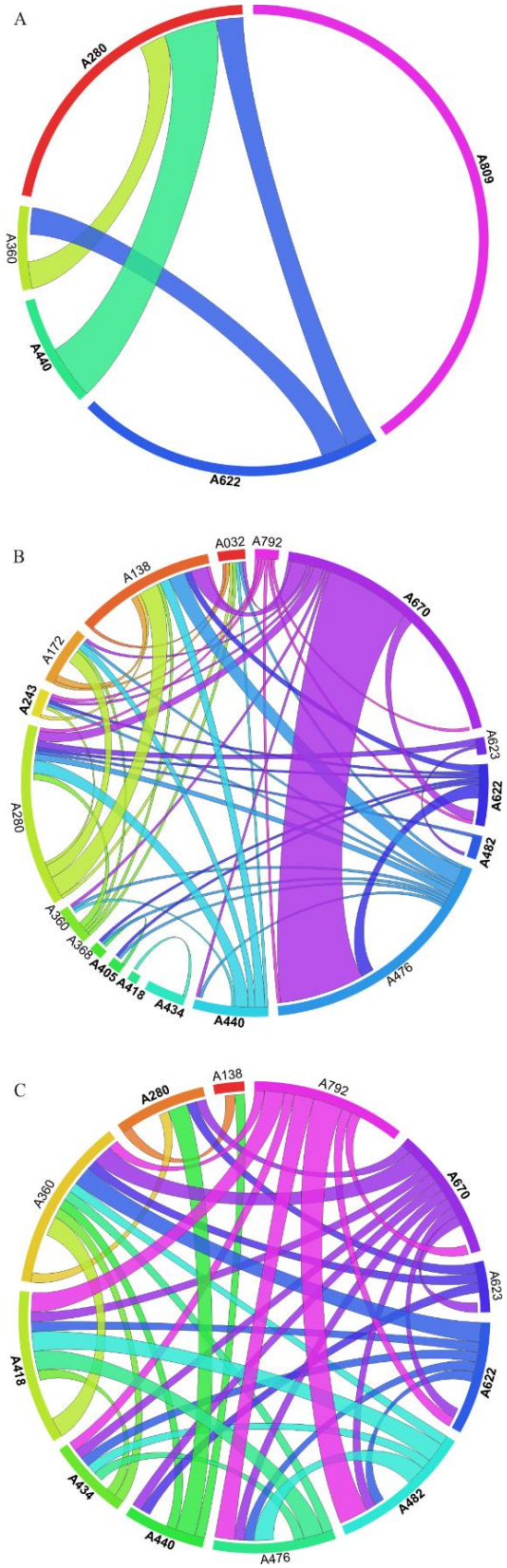

Figure 7. Circos plots showing shared OTUs among lichen mycobiomes. Symptomatically infected samples (as in Table 1) are in bold. The length of the sample-ribbons is directly proportional to the number of OTUs identified in each sample. The width of each connector between two samples is directly proportional to the number of shared OTUs: (A) Capnodiales, (B) Chaetothyriales and (C) Tremellales.

In the 'no myco' dataset (Fig. 6C; Supplementary Table 3), a maximum of 60 shared OTUs between the two samples A418 and A434 of *Lecanora polytropa* was recorded. This redundancy was seen also in the analysis comparing the OTUs diversity among *Lecanora* spp. samples only (Fig. 6D). The 60 OTUs belong mostly to unclassified and uncultured fungi, and include reads that we predict to be the lichenicolous fungus *Lichenoconium lecanorae* (Table 2; Supplementary Table 4). This is supported by the symptomatic presence of *Lichenoconium lecanorae* on both A418 and A434 *L. polytropa* samples. In the 'no myco' dataset, no OTUs were shared by 132 pairs of samples.

In the three samples of *Rhizocarpon geographicum* (Fig. 6E), the asymptomatic sample A172 shared two OTUs with sample A405 symptomatically infected by *M. pygmaea*, and five OTUs with sample A194 symptomatically infected by *E. macrosporus*. The two symptomatically infected samples A194 and A405 shared only one OTU (Supplementary Table 5).

Tephromela atra A361 without symptomatic infection shared OTUs with all the other symptomatically infected thalli of *T. atra* (Fig. 6F): seven OTUs with sample A280 infected by *S. tephromelarum*, 12 OTUs with sample A440 infected by *M. atricola*, and 11 OTUs with A809 infected by *T. atricebrina*. The three symptomatically infected *T. atra* were connected with a minimum of 7 and a maximum of 30 shared OTUs. Samples A280 and A809 shared the same OTU of *T. atricebrina*, which is therefore detected as asymptomatic in A280 (Table 2). Samples A280 and A440 share 30 OTUs mostly belonging to “uncultured Ascomycota” (Supplementary Table 6).

Capnodiales (Fig. 7A) were present in five samples, of which five infected symptomatically and two asymptomatically. No more than two shared OTUs were detected between the two symptomatically infected samples A280 (*T. atra* infected by *S. tephromelarum*) and A440 (*T. atra* infected by *M. atricola*).

Chaethotyriales (Fig. 7B) were present in 17 samples (eight symptomatically infected and nine asymptomatic) and a maximum of 26 OTUs were recorded between samples A476 (*P. conglomerata*) and A670 (*L. polytropa* infected by *M. pygmaea*).

Tremelalles (Fig. 7C) were present in 12 samples (seven symptomatically infected and five asymptomatic) and a maximum of 3 OTUS were shared between the symptomatically infected sample A482 (*L. polytropa* infected by *C. epipolytropa*) and the asymptomatic sample A792 (*Lecidea lapicida*).

Amplicon sequencing vs fungal isolates results

The ten selected fungal strains were all amplified for the ITS fragment; however, ITS2 sequences could be successfully obtained only for four of them (NCBI accessions MF276907-MF276910), and were queried against the complete dataset. ITS2 sequences of the strains A930 and A1022 successfully matched (≥ 97%) with a total of five OTUs (Supplementary Table 10). The cultured strain A923 is a Dothideomycete (Lichenostigmatales; Muggia et al. 2016) isolated from a thallus of *T. atra* symptomatically infected by *M. atricola*; it matched with two OTUs of "uncultured Ascomycota" in 14 samples. These included both multiple lichen hosts and the sample A440, which represents the same combination of mycobiont-lichenicolous fungus (*T. atra* infected by *M. atricola*) of the thallus used for the isolation of this fungus. The strain A1022 is an Eurotiomycete (Chaetothyriomycetidae; Muggia et al. 2016), and was isolated from a thallus of *R. geographicum* symptomatically infected by *E. macrosporus*. The three matching OTUs were assigned to the group of "fungal endophyte" and were present in two samples (Supplementary Table 10). In this case, however, there is no correspondence with the lichen used for the isolation, as the detected OTUs came from two *Lecanora* spp. specimens (A360 and A832).

Discussion

Lichen mycobiome diversity

Though the comparison between ITS1 and ITS2 barcoding markers is not novel for fungal communities, it has not been tested for lichens yet, and it gives here pioneering insights for methodological approaches in studying lichen mycobiomes.

Because the two datasets of the ITS1 and the ITS2 were gained independently, using two different sequencing approaches and clustering algorithms, we have refrained from comparing them more closely. Alternatively, we opted to compare the taxonomic diversity as far as possible and to comment on the differential detection of taxa. Our approach, which considers the lichen thallus as distinctive and still largely unexplored niche for unknown fungal assemblages, further strengthens the perception that diversity estimates based on metabarcoding are limited by the barcode locus selected (Tedersoo et al. 2015; Tedersoo and Lindahl 2016).

Our workflow (Fig. 2) was organized into three steps that analyzed a progressively more reduced dataset of reads. With this method, we succeeded in reliably assessing the fungal diversity of each sample at different taxonomic levels, and in predicting which reads potentially correspond to

the symptomatically infecting lichenicolous fungi. This enabled comparison of symptomatically infected and asymptomatic samples using alpha and beta diversity indexes.

Alpha diversity in symptomatically infected samples is not higher than that in lichens devoid of fungal infections. Beta diversity was characterized by the low percentage of variation explained by the three major axes (around 35% in total for both 'no host' and 'no myco' datasets). Moreover, due to the rarefaction of the datasets, the results are impaired by the number of retained samples. Indeed, symptomatically infected and asymptomatic samples are unequally represented, being the asymptomatic samples only three out of 11 samples in the 'no myco' dataset. Overall, the beta diversity analyses showed no tendency among samples to group according to presence/absence of symptomatic infection nor according to lichen host species. This observation is in congruence with the results presented by Fernández-Mendoza et al. (2017).

The presence of different haplotypes derived from different fungal individuals could explain why multiple OTUs for the same mycobiont species were recovered. On rocks, lichen thalli develop side by side, and hyphae from one mycelium could penetrate into neighboring thalli. The multicopy nature of the ITS region (Schoch et al. 2012) may also result in overestimation of diversity if divergent paralogs or non-orthologous gene copies are sequenced (Simon and Weiß 2008). However, this intragenomic variation does not compromise the taxonomic identification value of the ITS region (Hollingsworth 2011). Another, more parsimonious explanation that cannot be ruled out in any sequencing approach is that errors may be introduced by sequencing.

The main orders of lichen-associated fungi detected by the ITS2 barcode were Capnodiales, Chaethotyriales and Tremellales (Basidiomycetes), which closely agrees with the results obtained previously by analyzing the ITS1 fragment. The order Capnodiales includes endophytes, pathogens and, like Tremellales, parasites of fungi (Crous et al. 2009; Lindgren et al. 2015). Chaethotyriales are saprobic, rock-inhabiting, lichenicolous and epiphytic fungi (Réblová et al. 2013; Lawrey and Diederich 2016). In our dataset, these orders are distributed differently among the samples and do not show any correlation with the lichen host species or the presence of symptomatic infections. The same pattern is observed for the relevant fraction of unidentified taxa (i.e. uncultured Ascomycota, uncultured fungus, unidentified), which could belong to parasymbiontic or commensal fungi occurring incidentally on lichen thalli, as hypothesized by Fernández-Mendoza et al. (2017).

ITS barcodes capture unequal taxon diversity in lichen mycobiomes

Lichen mycobiomes are still uncharted terrains for investigating patterns of fungal specificity and ecological adaptations, and have recently become the subjects of metabarcoding analyses (Bates et al. 2012; U'Ren et al. 2014; Zhang et al. 2015; Mark et al. 2016). In our sequencing of the ITS2 locus,

the proportion of reads belonging to the lichen hosts is higher (min 27.7%, max 99.8%) than when those obtained previously from ITS1 (min 3.5%, max 97.7%; Fernández-Mendoza et al. 2017). Although we could not assign any reads to two lichenicolous fungal species, *M. pygmaea* and *A. varians*, using either ITS1 (Fernández-Mendoza et al. 2017) or ITS2, with ITS2 we were able to detect reads assignable to other lichenicolous taxa in asymptomatic thalli. Chaetothyriales and Capnodiales are the most highly represented orders detected in lichen mycobiomes using both ITS1 and ITS2 barcodes.

Basidiomycetes are known to be common partners in lichen symbioses (Spribille et al. 2016; Oberwinkler 2017). The previous study, performed with 454 pyrosequencing and based on the ITS1 barcode, demonstrated a high proportion of Tremellomycetes in the samples, with basidiomycetes present in 23 and representing the main component of 11 samples (Fernández-Mendoza et al. 2017). On the other hand, basidiomycetes were the least detected in our dataset: they were represented by less than 1% of all the reads and were found in only 12 samples. Other studies reported a variable fraction of basidiomycetes in lichen mycobiomes: about 15% of the complete dataset in arctic lichens (Zhang et al. 2015; analyzing the whole ITS region), less than 1% of rock-inhabiting foliose lichens (Bates et al. 2012; 18S rRNA) and less than 3% among endolichenic fungi in a comprehensive study (U'Ren et al. 2012; analyzing the complete ITS region). It is important to note that these studies considered lichens with growth forms (foliose and fruticose) different from those in the community we studied (epilithic and crustose thalli). Implicitly, lichen growth forms likely influence the presence of certain fungal taxa within the thalli.

ITS1 vs. ITS2 as barcode for lichenicolous fungi

Given that the selected samples harbored symptomatic lichenicolous fungi and a high proportion of other asymptomatic fungi (Fleischhacker et al. 2015; Fernández-Mendoza et al. 2017; Muggia et al. 2016), particular attention was paid in predicting which sequences, based on their read abundance and taxonomic assignment, could represent the symptomatic lichenicolous fungi. Fernández-Mendoza et al. (2017) succeeded in identifying three taxa also found in our analyses.

We identified sequences of potentially five additional lichenicolous fungi (Table 2). We also could detect the same OTUs of three lichenicolous fungal species (*T. atricebrina*, *S. eucline* and *S. fissurisedens*) in other samples which did not correspond with the known lichen host and occurred asymptomatically. The corresponding reads were found in the samples devoid of symptoms in a much smaller fraction (<10 reads) than in the symptomatically infected thalli (Table 2); the exception is the high number of reads of *S. fissurisedens* on the asymptomatic host *A. myrinii*. Furthermore, it seems that many lichenicolous fungi can be present in a thallus where only one of them is symptomatically

detectable. In this case, the lichenicolous fungus, recognized within the first group of lichen-associated taxa (*sensu* Fernández-Mendoza et al. 2017) in the symptomatic sample, could be part of the third fungal fraction (*sensu* Fernández-Mendoza et al. 2017) when its corresponding reads are recovered in the mycobiome of any asymptomatic samples.

Interestingly, the number of reads for each OTUs recovered for lichenicolous fungi using ITS2 as barcode is much higher than those recovered using ITS1. As reported by Fernández-Mendoza et al. (2017), also in our analyses the presence of symptomatic lichenicolous fungi does not affect the composition of the individual lichen mycobiomes in general, but it still remains unexplained if the presence of a lichenicolous fungus may inhibit the symptomatic development of a second one.

The differences in taxonomic composition that emerge when data for either ITS region are analyzed separately suggests that both ITS1 and ITS2 barcodes should be considered together for a more reliable estimation of lichen mycobiome diversity. Monard et al. (2013) reached a similar conclusion for other fungal communities. The application of sequencing platforms that allow analysis of larger fragments, such as PacBio (Pacific Bioscience) or MinION (Oxford Nanopore Technologies), are likely to make the metabarcode sequencing of the whole ITS region feasible in the near future.

HTS platforms for the analyses of lichen mycobiomes

In the most common environmental samples, such as those from soil or water, the DNA detected and amplified usually contributes evenly to the overall taxonomic composition, regardless of whether animal, plant, fungal or bacterial barcodes are used (Taberlet et al. 2012; Bálint et al. 2014; Sunagawa et al. 2015; Bell et al. 2016; Vences et al. 2016). Lichen thalli, however, consist mainly of one fungus; when fungal barcodes are analyzed, a high fraction of the reads belong to the lichen mycobiont (Bates et al. 2012; Zhang et al. 2015; Fernández-Mendoza et al. 2017), affecting the sampling depth of the other fungi. This shallow and uneven sampling depth of lichen-associated fungi causes a substantial loss of information, and biases the interpretation of species diversity patterns. This is clearly exemplified by the alpha and beta diversity analyses in our study. About half of the samples in the 'no host' and 'no myco' datasets had to be excluded due to the low number of reads (<1000), and the remaining samples did not always approach saturation. This condition is independent from the HTS platform used, and could be partially prevented by increasing the complete sampling depth of the analysis, for example with use of larger PGM chips such as 318^{TM}. However, the fraction of lichen mycobiont reads is never predictable. One potential solution would be the use of species-specific blocking primers, which prevent the amplification of non-target DNA. This strategy would substantially increase the cost of the analyses, especially when multiple lichen hosts are excluded

from the amplifications. Using multiple blocking primers might further bias the library preparation, as specific blocking oligonucleotides can block closely related non-target sequences at the same time (Leray et al. 2013a; Piñol et al. 2015). This approach has already been used in DNA metabarcoding dietary studies (Deagle et al. 2010; Leray et al. 2013b), where samples are often enriched with the DNA of the host organism (Piñol et al. 2015). If the sequencing depth of the lichen-associated fungi could be selectively increase in metabarcoding studies, it will allow us to significantly deepen the taxonomic and functional analysis of lichen mycobiomes.

Acknowledgments

This research was supported by the project FRA-2014 (Finanziamenti di Ateneo per progetti di Ricerca scientifica) by the University of Trieste and by the Austrian Science Fund (FWF project P24114-B16) assigned to LM. The activity of EB was partially funded by the Italian Government Commission with "Fondo Trieste". We thank Sergio Stefanni for his advice during data analysis, Fiorella Florian and Theodora Kopun for technical help in the lab.

References

Abdelfattah A, Li Destri Nicosia MG, Cacciola SO et al (2015) Metabarcoding analysis of fungal diversity in the phyllosphere and carposphere of olive (*Olea europaea*). PloS ONE 10:1–19

Arnold AE, Miadlikowska J, Higgins KL et al (2009) A phylogenetic estimation of trophic transition networks for ascomycetous Fungi: Are lichens cradles of symbiotrophic Fungal diversification? Syst Biol 58:283–297

Badotti F, De Oliveira FS, Garcia CF et al (2017) Effectiveness of ITS and sub-regions as DNA barcode markers for the identification of Basidiomycota (Fungi). BMC Microbiol 17:42

Bálint M, Schmidt, PA, Sharma R et al (2014) An Illumina metabarcoding pipeline for fungi. Ecol Evol 4:2642–2653

Bates ST, Donna BL, Lauber CL et al (2012) A preliminary survey of lichen associated eukaryotes using pyrosequencing. Lichenologist 44:137–146

Bazzicalupo AL, Bálint M, Schmitt I (2013) Comparison of ITS1 and ITS2 rDNA in 454 sequencing of hyperdiverse fungal communities. Fungal Ecol 6:102–109

Bell KL, de Vere N, Keller A et al (2016) Pollen DNA barcoding: current applications and future prospects. Genome 59:629–640

Bellemain E, Davey ML, Kauserud H et al (2013) Fungal palaeodiversity revealed using high-throughput metabarcoding of ancient DNA from arctic permafrost. Environ Microbiol 15:1176–1189

Bengtsson-Palme J, Ryberg M, Hartmann M et al (2013) Improved software detection and extraction of ITS1 and ITS2 from ribosomal ITS sequences of fungi and other eukaryotes for analysis of environmental sequencing data. Methods Ecol Evol 4:914–919

Blaalid R, Kumar S, Nilsson RH et al (2013) ITS1 versus ITS2 as DNA metabarcodes for fungi. Mol Ecol Resour 13:218–224

Caporaso GJ, Kuczynski J, Stombaugh J et al (2010) QIIME allows analysis of high-throughput community sequencing data. Nat Methods 7:335–336

Carew ME, Pettigrove VJ, Metzeling L et al (2013) Environmental Monitoring Using Next Generation Sequencing: Rapid Identification of Macroinvertebrate Bioindicator Species. Front Zool 10:45

Chao A, Colwell RK, Lin CW et al (2009) Sufficient sampling for asymptotic minimum species richness estimators. Ecology 90:1125–1133

Crous PW, Schoch CL, Hyde KD et al (2009) Phylogenetic lineages in the Capnodiales. Stud Mycol 64:17–47

Cuadros-Orellana S, Leite LR, Smith A et al (2013) Assessment of Fungal Diversity in the Environment using Metagenomics: a Decade in Review. Fungal Genom Biol 3:1–13

Deagle BE, Chiaradia A, McInnes J et al (2010) Pyrosequencing faecal DNA to determine diet of little penguins: is what goes in what comes out? Conserv Genet 11:2039–2048

Edgar RC, Haas BJ, Clemente JC et al (2011) UCHIME improves sensitivity and speed of chimera detection. Bioinformatics 27:2194–2200

Fernández-Mendoza F, Fleischhacker A, Kopun T et al (2017) ITS1 metabarcoding highlights low specificity of lichen mycobiomes at a local scale. Mol Ecol. doi:10.1111/mec.14244

Fleischhacker A, Grube M, Kopun T et al (2015) Community analyses uncover high diversity of lichenicolous fungi in alpine habitats. Microbial Ecol 70:348–360

Girlanda M, Isocrono D, Bianco C et al (1997) Two foliose lichens as microfungal ecological niches. Mycologia 531–536

Grube M, Cardinale M, de Castro Jr JV et al (2009) Species-specific structural and functional diversity of bacterial communities in lichen symbioses. ISME J 3:1105

Grube M, Cernava T, Soh J et al (2015) Exploring functional contexts of symbiotic sustain within lichen-associated bacteria by comparative omics. ISME J 9:412

Gweon HS, Oliver A, Taylor J et al (2015) PIPITS: An automated pipeline for analyses of fungal internal transcribed spacer sequences from the Illumina sequencing platform. Methods Ecol Evol 6:973–980

Hafellner J (2015) Lichenicolous Biota (Nos 201–230). Fritschiana 80:24–41

Harutyunyan S, Muggia L, Grube M (2008) Black fungi in lichens from seasonally arid habitats. Stud Mycol 61:83–90.

Hawksworth DL, Honegger R (1994) The lichen thallus: a symbiotic phenotype of nutritionally specialized fungi and its response to gall producers. In: Williams MAJ (ed) Systematics Association Special Volume, Oxford, Clarendon Press, pp 77–98

Hawksworth DL (1979) The lichenicolous Hyphomycetes. Bull br Mus nat Hist Bot 6:183–300

Hawksworth DL (1981) The lichenicolous Coleomycetes. Bull br Mus nat Hist Bot 9:1–98

Hibbett D (2016) The invisible dimension of fungal diversity. Science 351:1150–1151

Hollingsworth PM (2011) Refining the DNA barcode for land plants. PNAS 108:19451–19452

Kemler M, Garnas J, Wingfield MJ et al (2013) Ion Torrent PGM as Tool for Fungal Community Analysis: A Case Study of Endophytes in Eucalyptus grandis Reveals High Taxonomic Diversity. PLoS ONE 8(12):e81718

Kõljalg U, Nilsson RH, Abarenkov K et al (2013) Towards a Unified Paradigm for Sequence-Based Identification of Fungi. Mol Ecol 22:5271–5277

Krzywinski M, Schein J, Birol I et al (2009) Circos: an information aesthetic for comparative genomics. Genome Res19:1639–1645

Langarica-Fuentes A, Zafar U, Heyworth A et al (2014) Fungal succession in an in-vessel composting system characterized using 454 pyrosequencing. FEMS Microbiol Ecol 88:296–308

Lawrey JD, Diederich P (2003) Lichenicolous Fungi: Interactions, Evolution, and Biodiversity. Bryologist 106:80–120

Lawrey JD, Diederich P (2016) Lichenicolous fungi – worldwide checklist, including isolated cultures and sequences available. http://www.lichenicolous.net Accessed 1 March 2017

Leray M, Agudelo N, Mill SC et al (2013a) Effectiveness of Annealing Blocking Primers versus Restriction Enzymes for Characterization of Generalist Diets: Unexpected Prey Revealed in the Gut Contents of Two Coral Reef Fish Species. PloS ONE 8:e58076

Leray M, Yang JY, Meyer CP et al (2013b) A new versatile primer set targeting a short fragment of the mitochondrial COI region for metabarcoding metazoan diversity: application for characterizing coral reef fish gut contents. Front Zool 10:34

Lindgren H, Diederich P, Goward, T et al (2015) The phylogenetic analysis of fungi associated with lichenized ascomycete genus *Bryoria* reveals new lineages in the Tremellales including a new species *Tremella huuskonenii* hyperparasitic on *Phacopsis huuskonenii*. Fungal Biol 119:844856

Mark K, Cornejo C, Keller C et al (2016) Barcoding lichen-forming fungi using 454 pyrosequencing is challenged by artifactual and biological sequence variation. Genome 59:685–704

Martin KJ, Rygiewicz PT (2015) Fungal-specific PCR primers developed for analysis of the ITS region of environmental DNA extracts. BMC Microbiol 5:28

Mello A, Napoli C, Murat C et al (2011) ITS-1 versus ITS-2 pyrosequencing: a comparison of fungal populations in truffle grounds. Mycologia 103:1184–93

Miller KE, Hopkins K, Inward DJ et al (2016) Metabarcoding of fungal communities associated with bark beetles. Ecol Evol 6:1590–1600

Monard C, Gantner S, Stenlid J (2013) Utilizing ITS1 and ITS2 to study environmental fungal diversity using pyrosequencing. FEMS Microbiol Ecol 84:165–175

Moya P, Molins A, Martínez-Alberola F et al (2017) Unexpected associated microalgal diversity in the lichen *Ramalina farinacea* is uncovered by pyrosequencing analyses. PloS ONE 12:e0175091

Muggia, L, Kopun T, Grube M (2017) Effects of Growth Media on the Diversity of Culturable Fungi from Lichens. Molecules 22:824

Muggia L, Fleischhacker A, Kopun T et al (2016) Extremotolerant fungi from alpine rock lichens and their phylogenetic relationships. Fungal Div 76:119–142

Muggia L, Grube M (2010) Fungal composition of lichen thalli assessed by single strand conformation polymorphism. Lichenologist 42:461–473

Muggia L, Kopun T, Ertz D (2015) Phylogenetic placement of the lichenicolous, anamorphic genus *Lichenodiplis* and its connection to *Muellerella*-like teleomorphs. Fungal Biol 119:1115–1128

Nilsson RH, Ryberg M, Abarenkov K et al (2009) The ITS region as a target for characterization of fungal communities using emerging sequencing technologies. FEMS Microbiol Lett 296:97–101

Nilsson RH, Wurzbacher C, Bahram M et al (2016) Top 50 most wanted fungi. MycoKeys 12:29–40

Nilsson RH, Tedersoo L, Ryberg M et al (2015) A comprehensive, automatically updated fungal ITS sequence dataset for reference-based chimera control in environmental sequencing efforts. Microbes Environ 30:145–150

Oberwinkler F (2017) Yeasts in Pucciniomycotina. Mycol. Prog. 1–26

Orgiazzi A, Bianciotto V, Bonfante P et al (2013) 454 Pyrosequencing Analysis of Fungal Assemblages from Geographically Distant, Disparate Soils Reveals Spatial Patterning and a Core Mycobiome. Diversity 5:73–98

Petrini O, Hake U, Dreyfuss MM (1990) An analysis of fungal communities isolated from fruticose lichens. Mycologia 1990;444–451

R Development Core Team (2015) R: A Language and Environment for Statistical Computing, 2.15.1 Eds. 2012 Vienna, Austria: R Foundation for Statistical Computing

Piñol J, Mir G, Gomez–Polo P et al (2015) Universal and blocking primer mismatches limit the use of high–throughput DNA sequencing for the quantitative metabarcoding of arthropods. Mol Ecol Res 15:819–830

Réblová M, Untereiner WA, Réblová K (2013) Novel evolutionary lineages revealed in the Chaetothyriales (Fungi) based on multigene phylogenetic analyses and comparison of ITS secondary structure. PloS ONE 8:e63547

Schoch CL, Seifert KA, Huhndorf S et al (2012) Nuclear ribosomal internal transcribed spacer (ITS) region as a universal DNA barcode marker for Fungi. Proc Natl Acad Sci USA 109:1–6

Selbmann L, Zucconi L, Isola D et al (2015) Rock black fungi: excellence in the extremes, from the Antarctic to space. Curr Genet 61:335–345

Simon UK, Weiß M (2008) Intragenomic variation of fungal ribosomal genes is higher than previously thought. Mol biol evol 25:2251–2254

Spellerberg IF, Fedor PJ (2003) A tribute to Claude Shannon (1916–2001) and a plea for more rigorous use of species richness, species diversity and the 'Shannon–Wiener' Index. Glob Ecol Biogeogr 12:177–179

Spribille T, Tuovinen V, Resl P et al (2016) Basidiomycete yeasts in the cortex of ascomycete macrolichens. Science 353:488–492

Sunagawa S, Coelho LP, Chaffron S et al (2015) Structure and function of the global ocean microbiome. Science 348:1261359

Taberlet P, Coissac E, Pompanon F et al (2012) Towards next-generation biodiversity assessment using DNA metabarcoding. Mol Ecol 21:2045–2050

Tang J, Iliev ID, Brown J et al (2015) Mycobiome: approaches to analysis of intestinal fungi. J Immunol Methods 421:112–121

Tedersoo L, Anslan S, Bahram M, Polme S, Riit T, Liiv I et al (2015) Shotgun metagenome and multiple pair-barcode combinations of amplicons reveal biases in metabarcoding analyses of Fungi. MycoKey 10:1–43

Tedersoo L, Lindahl B (2016) Fungal identification biases in microbiome projects. Environ Microbiol Rep 8:774–779

Triebel D, Kainz C (2004) Muellerella. In: Nash TH, Ryan BD, Diederich P, Gries C, Bungartz F (ed) Lichen Flora of the Greater Sonoran Desert Region, Vol. 2. Arizona State University, Tempe, Arizona: Lichens Unlimited, pp 673–675

U'Ren JM, Lutzoni F, Miadlikowska J et al (2010) Community analysis reveals close affinities between endophytic and endolichenic fungi in mosses and lichens. Microb Ecol 60:340–353

U'Ren JM, Lutzoni F, Miadlikowska J et al (2012) Host and geographic structure of endophytic and endolichenic fungi at a continental scale. Am J Bot 99:898–914

U'Ren, JM, Riddle JM, Monacell JT et al (2014) Tissue storage and primer selection influence pyrosequencing-based inferences of diversity and community composition of endolichenic and endophytic fungi. Mol Ecol Resour 14:1032–1048

Vazquez-Baeza Y, Pirrung M, Gonzalez A et al (2013) EMPeror: a tool for visualizing high-throughput microbial community data. Gigascience 2:16

Vences M, Lyra ML, Perl RGB et al (2016) Freshwater vertebrate metabarcoding on Illumina platforms using double-indexed primers of the mitochondrial 16S rRNA gene. Conserv Genet Resour 8:323–327

White JR, Maddox C, White O et al (2013) CloVR-ITS: Automated internal transcribed spacer amplicon sequence analysis pipeline for the characterization of fungal microbiota. Microbiome 1:6

White TJ, Bruns T, Lee SJWT, Taylor JW (1990) Amplification and direct sequencing of fungal ribosomal RNA genes for phylogenetics. In: Innis MA, Gelfand DH, Sninsky JJ, White TJ (ed) PCR protocols: a guide to methods and applications. New York: Academic Press Inc, 1990, pp 315–322

Yahr R, Schoch CL, Dentinger BT (2016) Scaling up discovery of hidden diversity in fungi: impacts of barcoding approaches. Phil. Trans. R. Soc. B 371:20150336

Zhang T, Wei XL, Zhang YQ et al (2015) Diversity and distribution of lichen-associated fungi in the Ny-Ålesund Region (Svalbard, High Arctic) as revealed by 454 pyrosequencing. Sci Rep 5:14850

Supplementary material

Supplementary Fig. 1 Rarefaction curves of the complete (A), “no host” (B) and “no myco” (C) datasets.

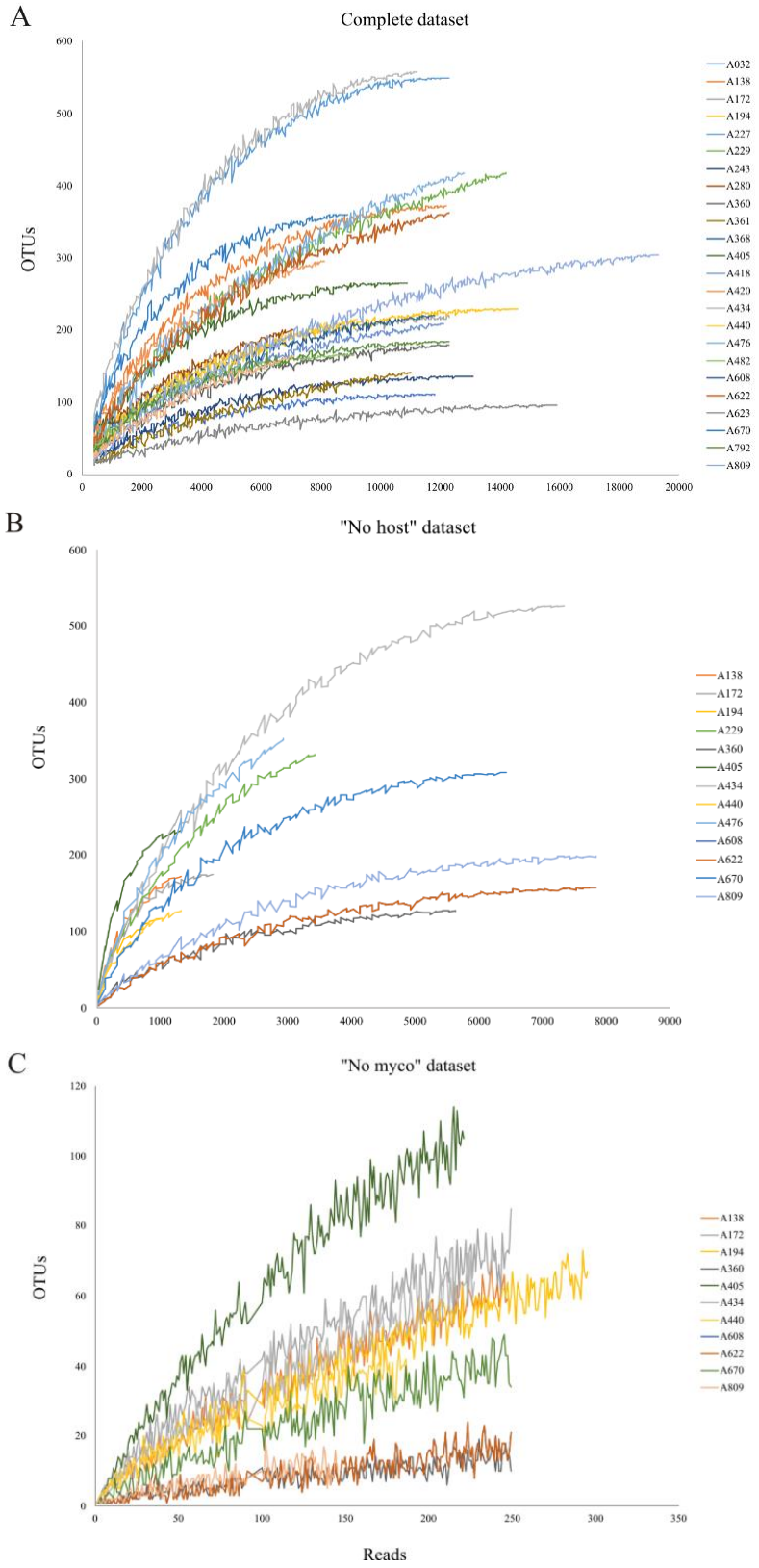

Supplementary Fig. 2 Principal Coordinate Analysis (PCoA) plots of Bray-Curtis distances calculated among the lichen mycobiomes considering the complete dataset.

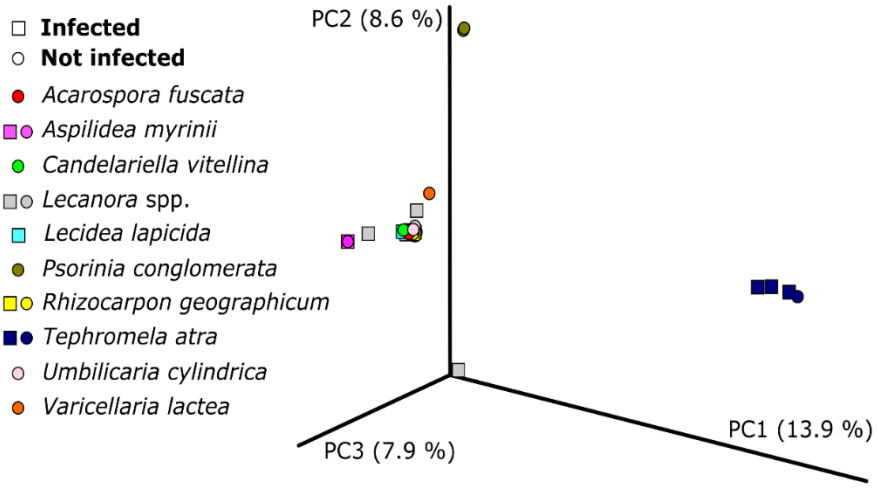

Supplementary Fig. 3 Jackknifed Principal Coordinate Analysis (PCoA) plots of Bray-Curtis distances based on the "no host" (A) and "no myco" (B) datasets. The statistical confidence of the results is presented by ellipsoids around the samples.

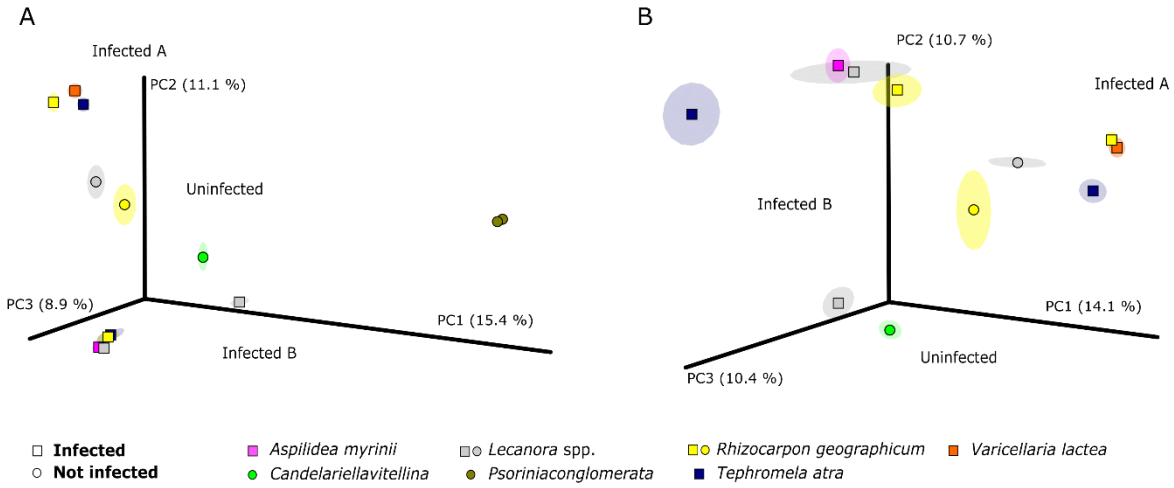

Supplementary Table 1 Matrix of the shared OTUs among samples in the complete dataset used for Fig. 6A.

	A229	**A138**	**A792**	**A194**	**A440**	**A361**	**A280**	**A809**	**A032**	**A360**	**A622**	**A172**	**A227**	**A832**	**A405**	**A670**	**A418**	**A636**	**A623**	**A482**	**A476**	**A434**	**A243**	**A608**	**A368**	**A420**
A229	417	0	5	3	7	5	8	3	3	10	41	4	4	3	3	3	6	2	3	3	307	4	2	5	1	4
A138	0	372	3	3	13	3	20	5	7	12	14	5	1	2	1	17	2	0	4	7	14	2	7	0	2	1
A792	5	3	184	1	5	1	9	3	3	4	6	1	1	2	2	7	11	1	8	6	4	6	3	7	1	5
A194	3	3	1	229	8	1	6	2	6	10	13	7	1	1	2	3	2	0	6	6	1	0	0	1	0	0
A440	7	13	5	8	215	69	73	60	14	27	29	8	2	5	3	8	10	1	5	8	7	4	3	4	0	2
A361	5	3	1	1	69	141	66	76	3	9	8	1	1	1	1	1	1	1	1	3	3	1	0	1	0	1
A280	8	20	9	6	73	66	201	58	12	19	23	11	4	6	3	17	9	1	6	7	8	7	6	4	3	4
A809	3	5	3	2	60	76	58	304	8	10	12	2	5	3	2	3	4	1	5	5	2	3	1	1	3	3
A032	3	7	3	6	14	3	12	8	111	12	16	9	2	5	4	6	3	1	3	4	3	1	2	1	5	2
A360	10	12	4	10	27	9	19	10	12	179	30	10	4	7	4	9	9	1	6	9	10	5	2	1	3	2
A622	41	14	6	13	29	8	23	12	16	30	326	9	4	7	9	11	7	3	5	15	42	4	4	17	4	18
A172	4	5	1	7	8	1	11	2	9	10	9	221	3	3	5	4	4	1	4	2	2	0	1	0	0	0
A227	4	1	1	1	2	1	4	5	2	4	4	3	549	3	4	3	7	1	4	2	0	2	2	1	2	1
A832	3	2	2	1	5	1	6	3	5	7	7	3	3	164	2	4	7	2	3	3	1	2	1	5	131	4
A405	3	1	2	2	3	1	3	2	4	4	9	5	4	2	265	4	4	1	3	3	1	0	1	0	1	1
A670	3	17	7	3	8	1	17	3	6	9	11	4	3	4	4	360	10	2	5	7	55	6	2	2	3	2
A418	6	2	11	2	10	1	9	4	3	9	7	4	7	7	4	10	208	2	5	5	3	120	2	9	1	7
A636	2	0	1	0	1	1	1	1	1	1	3	1	1	2	1	2	2	52	1	0	0	0	0	1	0	0
A623	3	4	8	6	5	1	6	5	3	6	5	4	4	3	3	5	5	1	96	5	1	6	1	2	1	3
A482	3	7	6	6	8	3	7	5	4	9	15	2	2	3	3	7	5	0	5	166	8	3	2	4	2	5
A476	307	14	4	1	7	3	8	2	3	10	42	2	0	1	1	55	3	0	1	8	417	1	2	0	1	0
A434	4	2	6	0	4	1	7	3	1	5	4	0	2	2	0	6	120	0	6	3	1	557	1	4	1	6
A243	2	7	3	0	3	0	6	1	2	2	4	1	2	1	1	2	2	0	1	2	2	1	135	2	3	2
A608	5	0	7	1	4	1	4	1	1	1	17	0	1	5	0	2	9	1	2	4	0	4	2	362	3	231
A368	1	2	1	0	0	0	3	3	5	3	4	0	2	131	1	3	1	0	1	2	1	1	3	3	220	2
A420	4	1	5	0	2	1	4	3	2	2	18	0	1	4	1	2	7	0	3	5	0	6	2	231	2	295

Supplementary Table 2 Matrix of the shared OTUs among samples in the "no host" dataset used for Fig. 6B.

	A032	A138	A172	A194	A227	A229	A243	A280	A360	A361	A368	A405	A418	A420	A434	A440	A476	A482	A608	A622	A623	A636	A670	A792	A809	A832
A032	35	7	8	6	1	2	0	9	9	1	0	1	2	1	0	10	3	4	0	11	1	0	5	2	4	3
A138	7	172	5	3	1	0	4	19	10	2	0	1	2	1	2	13	13	7	0	13	3	0	16	3	4	2
A172	8	5	175	5	1	1	0	8	6	0	0	2	1	0	0	6	1	2	0	7	1	0	3	0	0	3
A194	6	3	5	117	0	1	0	5	8	0	0	1	1	0	0	6	0	6	1	11	4	0	3	1	0	1
A227	1	1	1	0	22	2	0	0	1	0	0	0	0	0	1	1	0	1	0	1	1	0	1	0	1	2
A229	2	0	1	1	2	332	0	2	5	2	0	1	2	2	2	3	250	1	2	33	0	0	1	2	1	1
A243	0	4	0	0	0	0	64	3	1	0	2	0	1	0	0	3	2	0	0	3	1	0	1	2	0	0
A280	9	19	8	5	0	2	3	90	14	7	0	1	5	2	3	31	8	5	1	18	4	0	14	5	8	3
A360	9	10	6	8	1	5	1	14	127	2	1	1	5	0	4	21	6	7	0	24	3	0	8	2	3	4
A361	1	2	0	0	0	2	0	7	2	26	0	0	0	0	0	12	2	2	0	3	0	0	0	0	11	0
A368	0	0	0	0	0	0	2	0	1	0	17	1	0	0	0	0	1	0	0	4	0	0	0	0	1	6
A405	1	1	2	1	0	1	0	1	1	0	1	232	1	0	0	1	1	2	0	5	1	0	2	0	0	1
A418	2	2	1	1	0	2	1	5	5	0	0	1	147	4	94	7	2	4	5	5	2	0	6	5	0	3
A420	1	1	0	0	0	2	0	2	0	0	0	0	4	61	3	1	0	2	44	3	1	0	1	3	2	1
A434	0	2	0	0	1	2	0	3	4	0	0	0	94	3	526	2	1	2	1	3	5	0	3	2	1	0
A440	10	13	6	6	1	3	3	31	21	12	0	1	7	1	2	129	5	7	3	23	3	0	7	4	12	3
A476	3	13	1	0	0	250	2	8	6	2	1	1	2	0	1	5	352	7	0	38	0	0	55	4	2	0
A482	4	7	2	6	1	1	0	5	7	2	0	2	4	2	2	7	7	79	0	12	4	0	6	5	5	2
A608	0	0	0	1	0	2	0	1	0	0	0	0	5	44	1	3	0	0	158	2	1	0	1	1	1	1
A622	11	13	7	11	1	33	3	18	24	3	4	5	5	3	3	23	38	12	2	204	3	1	10	4	8	6
A623	1	3	1	4	1	0	1	4	3	0	0	1	2	1	5	3	0	4	1	3	19	0	3	1	2	1
A636	0	0	0	0	0	0	0	0	0	0	0	0	0	0	0	0	0	0	0	1	0	37	0	0	0	0
A670	5	16	3	3	1	1	1	14	8	0	0	2	6	1	3	7	55	6	1	10	3	0	308	5	1	2
A792	2	3	0	1	0	2	2	5	2	0	0	0	5	3	2	4	4	5	1	4	1	0	5	128	1	1
A809	4	4	0	0	1	1	0	8	3	11	1	0	0	2	1	12	2	5	1	8	2	0	1	1	198	1
A832	3	2	3	1	2	1	0	3	4	0	6	1	3	1	0	3	0	2	1	6	1	0	2	1	1	23

Supplementary Table 3 Matrix of the shared OTUs among samples in the "no myco" dataset used for Fig. 6C.

	A032	A138	A172	A194	A227	A229	A243	A280	A360	A361	A368	A405	A418	A420	A434	A440	A476	A482	A608	A622	A623	A636	A670	A792	A809	A832
A032	19	6	6	6	0	0	0	8	9	1	0	1	2	0	0	10	2	3	0	9	1	0	5	1	3	1
A138	6	131	5	3	1	0	4	18	10	2	0	1	2	0	2	12	13	6	0	12	3	0	16	2	3	1
A172	6	5	172	5	0	0	0	8	6	0	0	2	1	0	0	6	1	2	0	6	1	0	3	0	0	1
A194	6	3	5	109	0	0	0	5	8	0	0	1	1	0	0	6	0	5	1	10	3	0	3	0	0	1
A227	0	1	0	0	9	0	0	0	1	0	0	0	0	0	1	1	0	1	0	1	1	0	1	0	1	1
A229	0	0	0	0	0	64	0	2	3	2	0	1	2	1	2	3	51	0	1	3	0	0	1	1	1	0
A243	0	4	0	0	0	0	18	3	0	0	0	0	0	0	0	2	1	0	0	1	1	0	1	2	0	0
A280	8	18	8	5	0	2	3	87	14	7	0	1	4	1	3	30	8	4	1	16	4	0	14	4	7	1
A360	9	10	6	8	1	3	0	14	77	2	0	1	4	0	4	21	4	6	0	21	3	0	8	2	3	4
A361	1	2	0	0	0	2	0	7	2	25	0	0	0	0	0	12	2	2	0	3	0	0	0	0	11	0
A368	0	0	0	0	0	0	0	0	0	0	2	1	0	0	0	0	1	0	0	1	0	0	0	0	0	1
A405	1	1	2	1	0	1	0	1	1	0	1	228	1	0	0	1	1	2	0	5	1	0	2	0	0	1
A418	2	2	1	1	0	2	0	4	4	0	0	1	80	3	60	4	2	3	1	2	1	0	4	4	0	1
A420	0	0	0	0	0	1	0	1	0	0	0	0	3	51	3	0	0	0	38	1	0	0	0	1	0	0
A434	0	2	0	0	1	2	0	3	4	0	0	0	60	3	491	2	1	2	1	3	5	0	3	2	1	0
A440	10	12	6	6	1	3	2	30	21	12	0	1	4	0	2	114	5	6	2	21	3	0	6	3	12	2
A476	2	13	1	0	0	51	1	8	4	2	1	1	2	0	1	5	132	6	0	14	0	0	55	3	2	0
A482	3	6	2	5	1	0	0	4	6	2	0	2	3	0	2	6	6	67	0	9	4	0	4	3	4	1
A608	0	0	0	1	0	1	0	1	0	0	0	0	1	38	1	2	0	0	146	1	0	0	0	1	0	0
A622	9	12	6	10	1	3	1	16	21	3	1	5	2	1	3	21	14	9	1	143	2	1	8	2	6	1
A623	1	3	1	3	1	0	1	4	3	0	0	1	1	0	5	3	0	4	0	2	13	0	3	0	1	1
A636	0	0	0	0	0	0	0	0	0	0	0	0	0	0	0	0	0	0	0	1	0	37	0	0	0	0
A670	5	16	3	3	1	1	1	14	8	0	0	2	4	0	3	6	55	4	0	8	3	0	277	4	1	1
A792	1	2	0	0	0	1	2	4	2	0	0	0	4	1	2	3	3	3	1	2	0	0	4	27	0	0
A809	3	3	0	0	1	1	0	7	3	11	0	0	0	0	1	12	2	4	0	6	1	0	1	0	190	0
A832	1	1	1	1	1	0	0	1	4	0	1	1	1	0	0	2	0	1	0	1	1	0	1	0	0	9

Supplementary Table 4 Matrix of the shared OTUs among samples of *Lecanora* spp. in the "no myco" dataset used for Fig. 6D.

	A227	**A243**	**A360**	**A368**	**A418**	**A434**	**A482**	**A670**	**A832**
A227	9	0	1	0	0	1	1	1	1
A243	0	18	0	0	0	0	0	1	0
A360	1	0	77	0	4	4	6	8	4
A368	0	0	0	2	0	0	0	0	1
A418	0	0	4	0	80	60	3	4	1
A434	1	0	4	0	60	491	2	3	0
A482	1	0	6	0	3	2	67	4	1
A670	1	1	8	0	4	3	4	277	1
A832	1	0	4	1	1	0	1	1	9

Supplementary Table 5 Matrix of the shared OTUs among samples of *Rhizocarpon geographicum* in the "no myco" dataset used for Fig. 6E.

	A172	**A194**	**A405**
A172	172	5	2
A194	5	109	1
A405	2	1	228

Supplementary Table 6 Matrix of the shared OTUs among samples of *Tephromela atra* in the "no myco" dataset used for Fig. 6F.

	A280	**A361**	**A440**	**A809**
A280	87	7	30	7
A361	7	25	12	11
A440	30	12	114	12
A809	7	11	12	190

Supplementary Table 7 Matrix of the shared OTUs belonging to Capnodiales in the complete dataset used for Fig. 7A.

	A280	**A360**	**A440**	**A622**	**A809**
A280	7	1	2	1	0
A360	1	1	0	1	0
A440	2	0	2	0	0
A622	1	1	0	9	0
A809	0	0	0	0	21

Supplementary Table 8 Matrix of the shared OTUs belonging to Chaetothyriales in the complete dataset used for Fig. 7B.

	A032	A138	A172	A243	A280	A360	A368	A405	A418	A434	A440	A476	A482	A622	A623	A670	A792
A032	1	1	1	0	1	1	0	0	0	0	1	1	0	0	0	1	0
A138	1	14	2	1	6	1	0	0	0	0	3	5	0	2	0	5	1
A172	1	2	5	0	4	1	0	0	0	0	2	1	0	0	0	1	0
A243	0	1	0	2	1	0	0	0	0	0	0	1	0	1	0	1	1
A280	1	6	4	1	25	2	0	0	0	0	4	2	1	1	2	3	1
A360	1	1	1	0	2	3	0	0	0	0	1	1	0	0	0	1	0
A368	0	0	0	0	0	0	1	1	0	0	0	1	0	1	0	0	0
A405	0	0	0	0	0	0	1	1	0	0	0	1	0	1	0	0	0
A418	0	0	0	0	0	0	0	0	2	1	0	0	0	0	0	0	0
A434	0	0	0	0	0	0	0	0	1	11	0	0	0	0	0	0	0
A440	1	3	2	0	4	1	0	0	0	0	9	1	0	0	0	1	0
A476	1	5	1	1	2	1	1	1	0	0	1	28	0	4	0	26	1
A482	0	0	0	0	1	0	0	0	0	0	0	0	5	0	1	0	0
A622	0	2	0	1	1	0	1	1	0	0	0	4	0	4	0	3	1
A623	0	0	0	0	2	0	0	0	0	0	0	0	1	0	2	0	0
A670	1	5	1	1	3	1	0	0	0	0	1	26	0	3	0	36	1
A792	0	1	0	1	1	0	0	0	0	0	0	1	0	1	0	1	1

Supplementary Table 9 Matrix of the shared OTUs belonging to Tremellales in the complete dataset used for Fig. 7C.

	A138	A280	A360	A418	A434	A440	A476	A482	A608	A622	A623	A670	A792
A138	1	1	0	0	0	1	0	0	0	0	0	0	0
A280	1	3	1	0	0	2	0	0	0	0	1	1	0
A360	0	1	4	2	1	1	1	1	0	2	1	2	1
A418	0	0	2	4	1	0	2	2	0	1	0	1	2
A434	0	0	1	1	1	0	1	1	0	1	0	1	1
A440	1	2	1	0	0	2	0	0	0	0	1	1	0
A476	0	0	1	2	1	0	2	2	0	1	0	1	2
A482	0	0	1	2	1	0	2	3	0	1	0	1	3
A608	0	0	0	0	0	0	0	0	0	0	0	0	0
A622	0	0	2	1	1	0	1	1	0	3	0	1	1
A623	0	1	1	0	0	1	0	0	0	0	1	1	0
A670	0	1	2	1	1	1	1	1	0	1	1	2	1
A792	0	0	1	2	1	0	2	3	0	1	0	1	4

Supplementary Table 10 Number of OTUs and corresponding reads of two cultured fungi (A930 and 1022, Muggia *et al.* 2016), found in the complete dataset. The reads found in samples with the same lichen-lichenicolous fungus combination from which culture was isolated are highlighted in bold.

	Cultured fungus	
	A930	**A1022**
Sample		
A032	OTU47 (116)	-
A138	OTU47 (11)	-
A172	OTU47 (57)	-
A194	OTU47 (426)	-
A227	-	-
A229	-	-
A243	-	-
A280	OTU47 (37)	-
A360	OTU47 (246)	OTU9873 (37), OTU3048 (1), OTU10383 (1)
A361	-	-
A368	-	-
A405	OTU47 (3)	-
A418	OTU47 (2)	-
A420	-	-
A434	-	-
A440	**OTU47 (131)**	-
A476	-	-
A482	OTU47 (12)	-
A608	-	-
A622	OTU47 (572), OTU8759 (2)	-
A623	OTU47 (1)	-
A636	-	-
A670	OTU47 (1)	-
A792	-	-
A809	-	-
A832	OTU47 (1)	OTU9873 (57), OTU3048 (1), OTU10383 (1)

CONCLUSIONS

The presented research provides new insights in lichen photobionts stress responses and in the intrathalline fungal diversity. This was achieved through the application of high-throughput-omic technologies transcriptomics and DNA metabarcoding; information acquired from analyses of gene expression, protein quantification and physiological parameters were also integrated.

The outstanding stress tolerance of lichen photobionts was one of the objects of my Ph.D.: the analysis of the photobiont *Trebouxia gelatinosa* allowed the understanding of the stress-related mechanisms in this green alga.

While some mechanisms were found to be stress-specific (i.e. DRPs response to desiccation), common traits in the *T. gelatinosa* responses could be identified, such as the involvement of the photosynthetic apparatus and molecular chaperones.

A fundamental feature of *T. gelatinosa* at molecular level is a conspicuous, powerful and constitutive machinery that gives to the alga the capacity to promptly cope with sudden changes in the external environment, including high oxidative stress and extremely low water content. These results represent further explanations of the reasons why the genus *Trebouxia* occurs as the most common lichen photobiont, adapted to the "life at the extremes" that lichens can have.

In this perspective, further studies could be performed to elucidate some, still unclear aspects of stress tolerance in *T. gelatinosa*.

For instance, the importance of DRPs in *T. gelatinosa* and other lichen photobionts could be investigated, in particular in terms of structural diversification and phylogenetic analysis. The relationship between DRPs and lichenization is intriguing, especially in the view of the hypothesized horizontal gene transfer (HGT) involving the lichen-associated bacteria.

Regarding water stress, different desiccation rates could be tested to understand how gene expression of photosynthesis-related transcripts change, and how it is reflected in terms of decrease and recover of photosynthetic activity after rehydration.

Moreover, given the peculiar behavior of *T. gelatinosa* molecular chaperones (i.e. HSP70), it will be interesting to monitor their response (both at transcript and protein level) when the alga is subjected to a range of other environmental stresses beside the ones already tested (desiccation and oxidative stress), such as heat shock, high light radiation, or combinations of them.

As *T. gelatinosa* mRNA extraction was successfully applied also from lichen thalli (i.e. the epiphytic *Flavoparmelia caperata*, from which it was isolated), the experiments could be performed also *in vivo*, to verify how lichenization influences the molecular and physiological response of the photobiont.

The great intrathalline diversity that was detected in lichens during this Ph.D. showed how the knowledge of these small and complex ecosystems is still at the beginning, and how high-throughput-omics technologies are and will be inestimable tools to assess previously unknown biodiversity. Chaethothyriales are here confirmed as principal component of the lichen mycobiomes. The possibility to investigate and compare symptomatic with asymptomatic thalli proved successful to understand the ecological importance of lichen mycobiomes. The asymptomatic presence of lichenicolous fungi further supports the role of lichen as reservoir of biodiversity.

The lack of representative sequences in databases only allows a shallow taxonomic assignment of most of the lichen-associated fungal taxa, and more efforts are needed to recover this information. The integration with classical techniques, such as cultures and DNA barcoding, is still pivotal to increase the genetic information and make it available. It has been shown that the fungal studies are affected from the choice of the DNA barcode. Also, bioinformatic pipelines developed *ad hoc* for fungi will be helpful to standardize the analyses and favor the integration of data from different studies.

More researches should be conducted for the study of lichen mycobiome, and different research questions could be addressed, including their role in lichen symbioses. For instance, lichens with a wide geographical distribution could own locally differentiated fungal communities. These could present individual responses to local drivers, such as pollutants, humidity, temperature, and likely have a role in the distribution pattern of the lichen species itself.

The interaction between lichen myco- and microbiomes would be also of extreme interest in the view of lichens as microniches, that integrate genetics, physiology and metabolism of different organisms. The composition of lichen myco- and microbiomes could be studied in thalli subjected to different environmental stresses, to evaluate if and how the composition changes.

We know a lot about lichens, but it is even more what we still do not know. Lichens give researchers the possibility to integrate new and classical approaches, different disciplines and expertise. The opportunity to study the lichen thallus in terms of both bi- (mycobiont and photobiont) and multi-partite systems (lichen myco- and microbiomes) is unique and represents a stimulating and exciting challenge in science.

APPENDIX I: DNA METABARCODING UNCOVERS FUNGAL DIVERSITY OF MIXED AIRBORNE SAMPLES

Elisa Banchi[1], Claudio G. Ametrano[1], David Stanković[1,2], Pierluigi Verardo[3], Olga Moretti[4], Francesca Gabrielli[5], Stefania Lazzarin[6], Maria Francesca Borney[7], Francesca Tassan[8], Mauro Tretiach[1], Alberto Pallavicini[1], Lucia Muggia[1*]

[1] University of Trieste, Department of Life Sciences, Trieste, Italy

[2] National Institute of Biology, Marine Biology Station, Piran, Slovenia

[3] Regional Agency for Environmental Protection Friuli Venezia Giulia, Pordenone, Italy

[4] Regional Agency for Environmental Protection Umbria, Terni, Italy

[5] Regional Agency for Environmental Protection Marche, Ascoli Piceno, Italy

[6] Regional Agency for Environmental Protection Veneto, Vicenza, Italy

[7] Regional Agency for Environmental Protection Valle d'Aosta, Saint-Christophe, Italy

[8] Regional Agency for Environmental Protection Friuli Venezia Giulia, Trieste, Italy

* Corresponding author: Lucia Muggia

Main abbreviations

HTS: high-throughput sequencing

ITS: internal transcribed spacer

OTU: operational taxonomic unit

PCoA: principal coordinate analysis

RIF: rock inhabiting fungi

IAS: invasive alien species

Abstract

Fungal spores and mycelium fragments are particles which become and remain airborne and have been subjects of aerobiological studies. The presence and the abundance of certain taxa in aerobiological samples can be very variable and impaired by changeable climatic conditions. Because many fungi produce mycotoxins and both their mycelium fragments and spores are regarded as potential allergens, monitoring the presence of these taxa is of key importance. So far data on exposure and sensitization to fungal allergens are mainly based on the assessment of few, easily

identifiable taxa and focused only on certain environments. This is due in part to the traditional methodologies used to analyze aerobiological samples and the inconspicuous fungal characters which allow only a shallow taxonomical identification. Here we present a first assessment of fungal diversity from airborne samples using a DNA metabarcoding analysis. The region ITS2 was selected as fungal barcode to catch fungal diversity in mixed airborne samples gathered for two weeks in four sites of North-Eastern and Central Italy. We assessed the taxonomic composition and diversity within and among the sampled sites and compared the molecular data with those obtained by traditional microscopy. The molecular analyses provide a tenfold more accurate determination of the taxa than the traditional morphological inspections. Our results prove that the metabarcoding analysis is a promising approach to increases quality and sensitivity of the aerobiological monitoring. The laboratory and bioinformatic workflow implemented here is now suitable for routine, high-throughput, regional analyses of airborne fungi.

Introduction

Fungi are ubiquitous and are among the most important and widespread groups of organisms which play key roles in multiple environments. Fungal spores and mycelium fragments are usually so small, that they belong to the group of particles that becomes and remains airborne (average size of 10 μm) and have been investigated by aerobiologists since the early years of this field [1]. Aerobiology has been acknowledged in the 1930s as the study of biological particles in the air, including the diversity and the processes involved in the movement of microorganisms in the atmosphere between different geographical locations [2]. The long-distance dispersal of fungal spores is especially relevant for many crop plants pathogens, such as the obligatory, biotrophic fungi producing huge numbers of spores and causing rust, blight, powdery and downy mildew diseases. Wind dispersal over hundreds or thousands of kilometers has caused the spread of these severe crop diseases on continental and even global scales [3, 4].

Besides being parasites of plants, fungi with their multiple life styles are also of general interest as they are some of the most common, important and also severe human and clinical pathogens (e.g. [5-11]). Allergenic properties of spores, tissue fragments and metabolites released by fungi have been studied plentifully [5, 12-17].

Researches on aerobiological samples have been performed in indoor and outdoor environments and have focused both on airborne pollen grains and fungal spores [18-23]. Studies on pollen grains have developed into established monitoring networks over several countries worldwide [i.e. Italy (http://www.pollnet.it), United Kingdom (http://www.worc.ac.uk/discover/national-pollen-

and-aerobiology-research-unit.html), USA (http://www.aaaai.org/global/nab-pollen-counts)]. Also, thanks to the established application of DNA barcodes in the identification of organisms, aerobiological analyses of plant diversity based on pollen grains have proceed much further [24-27]. In the past few years studies on pollen diversity have seen a large application of high throughput sequencing (HTS) technologies in palinology, melissopalinology and nutritional biology researches [28-34]. Recently Kraaijeveld et al. [34] accurately identified pollen from mixed airborne samples, including species that could not be recognized microscopically, by sequencing them with the Ion Torrent HTS platform.

On the contrary, the knowledge about fungal diversity in airborne samples is still very poor in comparison to plant data. Limitations to determine airborne fungal diversity are in part due to the very variable daily and seasonal loads of fungal (dia)spores, and to the limitations of the traditional methodologies used in aerobiological analysis [35, 36]. Still, aerobiology mostly employs morphological analyses of volumetric samples (usually spores/m^3) collected with spore trapping and differentiated in non-viable and viable air sampling [18, 36, 37]. The collection of volumetric samples keeps costs low and allows the quantifications of the results. However, it usually provides only a shallow taxonomical identification of the few most abundant and recognizable taxa, as morphological analyses suffer from being highly dependent on human expertise (it needs highly trained personnel). Indeed, routine assessments of fungal spores in pollen bulletin usually report only on a few genera, such as *Alternaria* and *Cladosporium* (e.g. www.pollenwarndienst.at/en/current-data/current-charts.html; www.isac.cnr.it/aerobio/ai/6bulletins.htm; www.arpa.umbria.it/pagine/spore).

In the last decade, molecular approaches (DNA barcoding, RFLP) have also been implemented to assess fungal diversity in airborne samples and have strengthen the perception that the majority of the genera were mostly overlooked by morphological inspections of either viable or non-viable samples [35]. Among the few existing studies, Pashley et al. [35] used PCR amplifications of the ITS and LSU regions coupled with cloning and sequencing of RFLP-types to show that more than three third of all genera sequenced were not detected by morphology, and that the rates were highly variable on daily basis. It was also highlighted that meteorological data, time of year, and length of the sampling period should be taken into account when comparing studies of seasonal fungi [34, 38].

Despite the wide popularity of HTS approaches in monitoring and uncovering microbial fungal diversity from diverse environments [39-44] so far very few researches applied HTS for fungal aerobiological studies. Recently, a DNA sequencing analysis was successfully implemented to identify airborne microorganisms in a hospital to control and supervise hospital infections [22]. Few other studies have assessed the composition of outdoor, aerial microbial communities (including

fungi) with Illumina MiSeq [45-47] or with Roche 454 [14], showing potential for the monitoring of air pollution and human health.

In this study, we assessed the fungal diversity from airborne samples by implementing a DNA metabarcoding analysis using the Ion Torrent technology. We targeted the nuclear internal transcribe spacer region ITS2 and used it as fungal barcode [48-50] in mixed airborne samples gathered from four sites of North-Eastern (NE) and Central Italy (Fig 1).

Fig 1. Geographical location of the sampling sites in the North-Eastern and Central Italy: region and city names are reported (FVG: Friuli Venezia Giulia). The map has been retrieved and modified from http://www.d-maps.com.

With this approach we aimed at *i)* implementing a laboratory and bioinformatic workflow suitable for routine, high-throughput, regional analyses of airborne fungi; *ii)* assessing taxonomic composition and diversity within and among the sampled sites; *iii)* comparing the molecular data with the ones obtained by microscopy determination. We found correspondence between morphological and molecular analyses and provide a much more accurate determination of the taxa in comparison with the traditional morphological inspections.

Materials and Methods

Sampling

The sampling was carried out in four sites of the Italian peninsula (Fig 1) in the following regions (city): Friuli Venezia Giulia (FVG, Pordenone), Marche (Ascoli Piceno), Umbria (Terni) and Veneto (Vicenza). In each site, the sampling was performed on the roof of a building at 15-20 m from the ground using a volumetric sampler (VPPS 2010, Lanzoni) mounted with a sticky tape (Melinex®). The sampling was performed during two whole weeks (starting on Mondays), during the time periods 5^{th}-12^{th} and 19^{th}-26^{th} September 2016.

Microscopy analysis and comparison with molecular data

Eight fragments, corresponding to two incomplete sampled Mondays for each site, were used to screen the presence of fungal spores and perform a taxonomical comparison with the metabarcoding results. The sampling tapes were placed on a glass slide, mounted in water and observed at a light microscope Olympus BH-2. Fungal spore determination was based on the illustration manual [51].

DNA extraction

The tape was detached from the sampling drum under a sterile hood and cut in eight segments. Two segments were the margins of the tape which belonged to two incomplete Mondays of the weeks (the day at which the tape was weekly changed); these pieces were excluded from molecular analyses but were used for microscopy analyses only. The remaining six segments corresponded each to one day of the week (24 h) starting from Tuesday to Sunday. Each segment was further split into two half-day parts, and each of them was fit into a 1.5 ml tube, taking care that the sticky surface with the air samples glued on it was facing the internal part of the tube. The total DNA was extracted using the ZR Fungal/Bacterial DNA MicroPrep™ Kit (Zymo Research), with five minutes of beat-beater processing. The half-day sections were processed individually and pooled at the last step of the protocol to obtain a single DNA extraction for each day. This resulted in 48 samples, 12 for each site.

Molecular analysis and sequencing

The fungal nuclear ribosomal ITS2 region was amplified with the forward primer ITS3 and the reverse primer ITS4 [52]. The amplicons were obtained in two PCR amplifications. The first PCR uses the ITS2 forward and reverse primers modified with GC rich universal tails on the 5'-end [53], which was identical to the tail applied on the 3'-end of the barcodes used in the second PCR. The first

PCR reaction mix contained 3 µl DNA template (10-20 ng), 3 µl HotMasterMix (5PRIME), 0.5 µl BSA 10X (Sigma-Aldrich), 0.75 µl EvaGreen™ 20X (Biotium), 0.5 µl forward primer ITS3 (10 µM), 0.5 µl reverse primer ITS4 (10 µM) in a final volume of 15 µl. The PCR amplification was performed with CFX 96™ PCR System (Bio-Rad) with the following cycling profile: 94 °C for 2 min and 35 cycles at 94 °C for 20 sec, 55 °C for 20 sec, 65 °C for 40 sec followed by a final extension at 65 °C for 2 min. A negative control was used to verify the absence of non-specific amplification products and was carried out for the whole sequencing process. The second PCR (switch PCR) was required for multiplex sequencing through attachment of the barcodes. This amplification used primers modified with an 'A' adaptor and a sample-specific 10 bp barcode to the 5'-end of the forward primer, and a P1 adaptor to the 5'-end of the reverse primer. The reaction was performed in a mix containing 5 µl of the first PCR product, 20 µl HotMasterMix (5PRIME Fisher Scientific), 2.5 µl EvaGreen™ 20X (Biotium), 1.5 µl forward primer (10 µM), and 1.5 µl reverse primer (10 µM) in a final volume of 50 µl. PCR conditions were the same as for the first PCR but were run for 12 cycles. All the amplicons were checked for their quality and length by agarose gel electrophoresis and pooled in equimolar amount. The resulting barcoded library was run on a E-Gel Precast Agarose Electrophoresis System (Thermo Fisher Scientific). The 400 bp product was recovered, measured with Qubit™ Fluorimeter (Thermo Fisher Scientific) and sequenced with an Ion Torrent Personal Genome Machine (PGM, Thermo Fisher Scientific) provided with a 400 bp reads length 314™ chip (Thermo Fisher Scientific).

Sequence data analysis

Data analysis was performed in QIIME 1.9.1 [54]. High quality sequences were demultiplexed, reverse primers and barcodes were removed, and reads that did not pass through the filtering (minimum length 150 bp, minimum average quality score 20, maximum length of homopolymer 8, maximum number of primer mismatches 3) were discarded. The ITS2 region was extracted with ITSx v1.0.11 [55] by selecting the fungal (F) profile option. Chimeric reads were identified and filtered out with UCHIME v4.0 algorithm using the reference dataset updated on 01.12.2016 [50, 56] to obtain the final, high quality dataset. Operational Taxonomic Units (OTUs) were picked at 97% similarity with open reference strategy and UNITE database, updated on November 2016 [57]. The method used for the taxonomic assignment was blast (max E-value $1e^{-30}$). Singletons were removed from the dataset. Statistics and ecological indexes were performed with QIIME [54].

The alpha and beta diversity analyses were conducted on the rarefied dataset. Rarefaction threshold was set at 1284 reads, which corresponds to the number of reads in the first sample over

1000 reads. Alpha diversity in terms of OTUs richness and diversity was calculated using Chao1 [58] and Shannon indexes [59]. A one-way analysis of variance (ANOVA) followed by a Duncan's new multiple range test was applied to verify the significance of differences in alpha diversity among the sites with R version 3.2.0 [60]. The beta diversity was calculated with Bray-Curtis principal coordinate analysis (PCoA); the robustness of the sequencing depth was evaluated with a jackknifing analysis as suggested in qiime1 tutorial for de novo OTU picking. The PCoA was visualized with EMPeror [61].

The sequence data are available at the NCBI short read repository under the accession number SRR6080480.

Results

Traditional microscopy analysis

The morphological analyses of fungal spores resulted in the identification of 22 genera (S1 Table); for the four genera *Alternaria*, *Cladosporium*, *Stemphylium* and *Torula*, morphological and molecular results fully correspond. Also spores of the lichen genus *Caloplaca* and of the lichen family Physciaceae (including the genera *Hyperphyscia*, *Physcia* and *Rinodina* as detected by sequencing, S2 Table) were observed on the tapes. The genus *Caloplaca*, however, was not recovered by sequencing.

Sequencing and data analysis

A total of 328,929 raw reads were generated, 176,054 passed the quality filter and had an average length of 385 bp. After ITS2 extraction and chimera checking a total of 152,418 reads, ranging from 496 to 6,356 reads per sample, were retained and represented the final dataset used for the taxonomic assignment and the statistical analyses (Table 1).

Table 1. Summary of sequencing data and diversity estimation. Sample ID, sampling provenience and number of reads (after ITS2 extraction and chimera removal) are reported. The number of detected OTUs is assessed for the entire sample, values of Chao1 and Shannon diversity indexes are calculated on the dataset rarefied to 1284 reads. (/) Alpha diversity is not calculated due to a number of reads lower than 1284. SD: standard deviation.

ID	Site	Reads	OTUs	Chao1 (SD)	Shannon (SD)
F2	FVG	3,330	379	416 (174)	4.35 (0.22)
F3	FVG	2,074	212	330 (151)	3.57 (0.17)
F4	FVG	2,374	242	353 (166)	3.66 (0.17)

F5	FVG	3,076	289	337 (170)	3.7 (0.19)
F6	FVG	2,959	308	370 (168)	3.81 (0.2)
F7	FVG	3,015	343	428 (184)	3.92 (0.2)
F9	FVG	4,211	323	352 (217)	3.33 (0.17)
F10	FVG	3,066	254	314 (153)	3.42 (0.16)
F11	FVG	4,982	454	408 (188)	3.86 (0.19)
F12	FVG	5,008	403	353 (169)	3.74 (0.18)
F13	FVG	5,749	429	332 (177)	3.57 (0.17)
F14	FVG	6,151	509	379 (173)	3.84 (0.17)
M2	Marche	1,369	312	492 (151)	5.58 (0.3)
M3	Marche	1,284	306	556 (227)	5.67 (0.31)
M4	Marche	2,142	381	472 (172)	5.33 (0.3)
M5	Marche	2,025	266	351 (135)	4 (0.22)
M6	Marche	1,935	307	511 (194)	4.37 (0.23)
M7	Marche	2,303	389	507 (174)	4.64 (0.29)
M9	Marche	1,915	307	502 (187)	4.31 (0.2)
M10	Marche	2,849	401	455 (193)	4.62 (0.27)
M11	Marche	1,847	314	523 (232)	4.42 (0.24)
M12	Marche	2,446	338	432 (172)	4.11 (0.23)
M13	Marche	2,434	331	463 (197)	4.09 (0.22)
M14	Marche	2,664	346	434 (183)	3.95 (0.21)
U2	Umbria	4,549	569	467 (195)	4.68 (0.27)
U3	Umbria	2,998	342	406 (178)	3.77 (0.18)
U4	Umbria	1,886	248	347 (127)	3.93 (0.23)
U5	Umbria	2,919	311	406 (185)	3.64 (0.2)
U6	Umbria	3,671	417	408 (171)	4.01 (0.22)
U7	Umbria	1,627	301	465 (174)	4.84 (0.3)
U9	Umbria	4,270	480	483 (210)	3.85 (0.22)
U10	Umbria	2,519	367	476 (200)	4.2 (0.27)
U11	Umbria	2,047	328	487 (184)	4.31 (0.25)
U12	Umbria	3,218	376	452 (201)	3.68 (0.23)
U13	Umbria	3,585	402	443 (195)	3.99 (0.22)
U14	Umbria	3,871	420	429 (201)	3.88 (0.22)
V2	Veneto	4,278	358	343 (150)	3.57 (0.17)
V3	Veneto	6,356	447	328 (147)	3.34 (0.19)
V4	Veneto	3,435	302	352 (164)	3.48 (0.15)
V5	Veneto	496	120	/	/
V6	Veneto	1,783	183	306 (124)	3.43 (0.17)
V7	Veneto	558	80	/	/
V9	Veneto	5,681	392	386 (204)	2.82 (0.19)

V10	Veneto	3,935	304	324 (158)	2.96 (0.15)
V11	Veneto	4,086	327	320 (152)	3.27 (0.16)
V12	Veneto	5,029	406	378 (174)	3.32 (0.16)
V13	Veneto	4,192	308	305 (150)	3.21 (0.15)
V14	Veneto	4,221	301	275 (129)	3.34 (0.16)

Rarefaction curves showed a large variation in the total number of OTUs among samples. The curves did not reach saturation (S1 Fig), suggesting that an increased sequencing depth would detect additional OTUs.

Comparison within and among sites

Alpha and beta diversity of samples were estimated from the rarified dataset with a minimum value of 1,284 reads. Two samples from Veneto, V5 and V7, resulted in only 496 and 558 reads, respectively, and were therefore excluded (Table 1).

The alpha diversity was estimated using Chao1 and Shannon diversity indexes (Table 1). A significant difference (p-value <0.05) was recorded in comparing the two indexes between sites (Table 1, Fig 2).

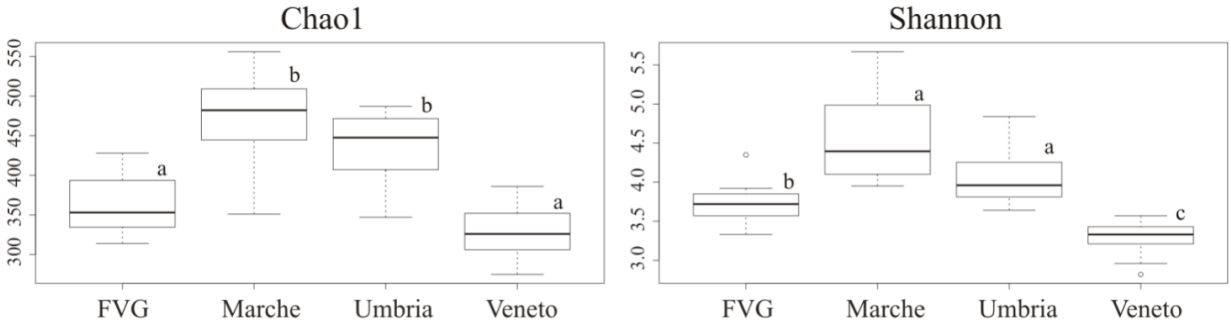

Fig 2. Box plots of Chao1 and Shannon diversity indexes estimated for each site. Significant differences among sites were calculated with Anova and Duncan's new multiple range test and are indicated by different letters (p-value < 0.05).

Both Chao1 and Shannon indices were significantly higher (Duncan's new multiple range test $p < 0.05$) for the two sites from the Central Italy, Marche and Umbria, in comparison with the two sites from the NE Italy, FVG and Veneto. Further, Veneto showed the lowest diversity values (Table 1, Fig 2).

The beta diversity was assessed from Bray-Curtis distance matrices and presented with PCoA plot. The maximum percentage of variation explained by a single PC axis was 35.64% (Fig 3).

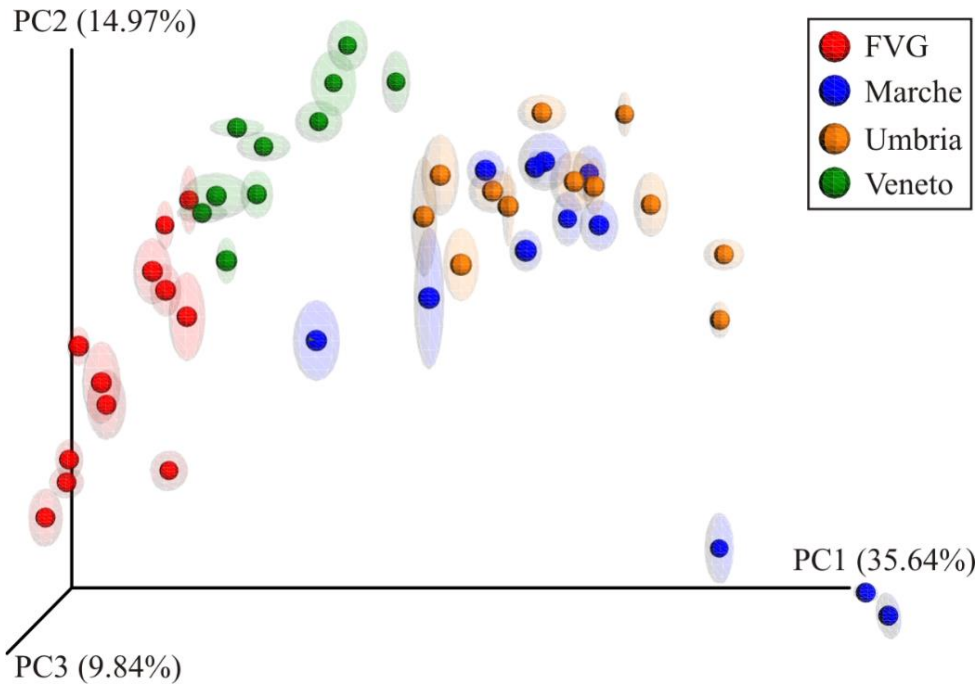

Fig 3. Jackknifed Principal Coordinate Analysis (PCoA) plot of Bray-Curtis distances between the samples of the four sites. Ellipsoids show the statistical confidence of the analysis.

The samples are grouped mostly according to their geography: samples from NE Italy (FVG and Veneto) are well separated between each other and also from the samples from the Central Italy, while these (Marche and Umbria) were clustered together. Within the Central Italian samples, only three samples from Marche (M2, M3 and M4) are distinctly segregated from the others (Fig 3), likely due to a higher presence of Phaeosphaerales and Pleosporales and a lower presence of Capnodiales (S2 Fig).

Taxonomic composition

The ITS2 analysis of airborne fungi allowed a taxonomic assignment for more than the 99% of the reads by clustering them to OTU at 97% similarity (S2 Fig). At division level, in all sampling sites the vast majority of reads belonged to Ascomycetes (Fig 4A).

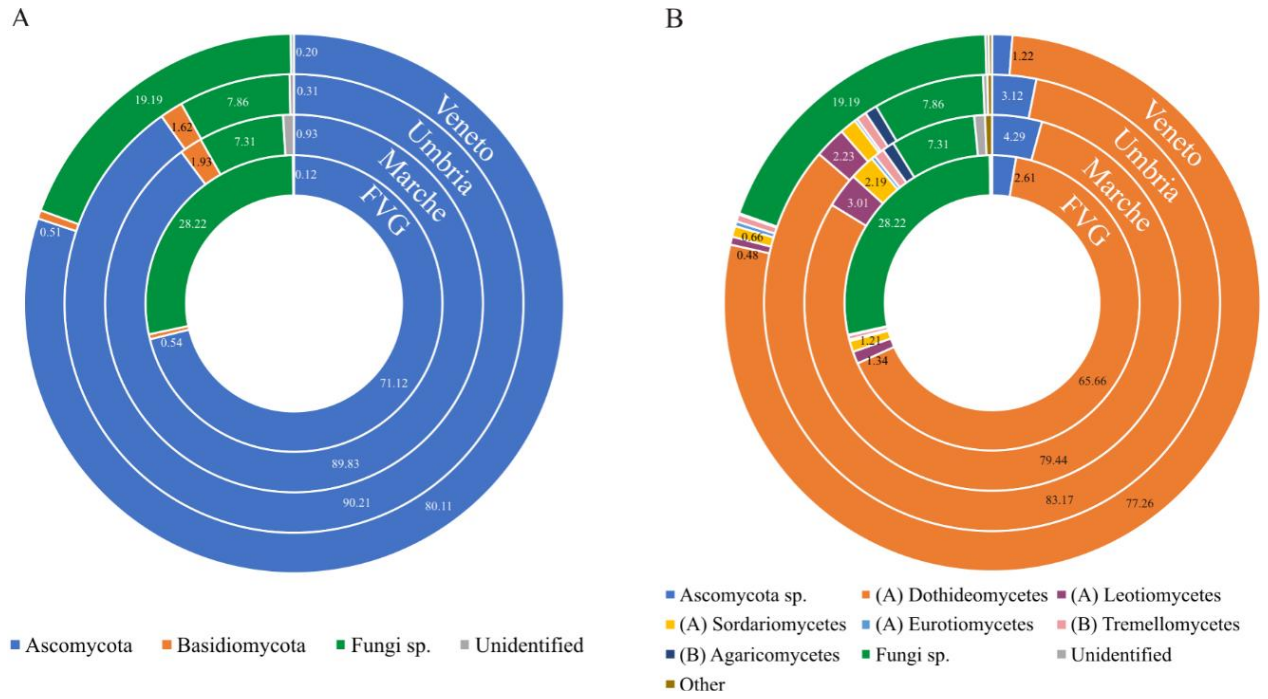

Fig 4. Doughnut charts showing taxonomic composition at division (A) and class (B) level in the four sampling sites. Abundances of taxa are reported with the percentage values of reads. Taxa accounting for <0.1% of reads are grouped as "Other".

However, between the different sites the distribution at division level is not homogenous. The two sites in NE Italy (FVG and Veneto) present a lower proportion of Ascomycetes (71.1 and 80.1%, respectively) but a higher proportion of reads that could be assigned only at kingdom level (Fungi sp. 28.2% and 19.1%, respectively) than the two sites of Central Italy. These latter, Marche and Umbria, are more similar to each other in the amount of Ascomycetes, of which they have 90.2% and 89.8% reads, respectively, and in the amount of Fungi sp., 7.3% and 7.9%, respectively (Fig 4A). Basidiomycetes are present in very low proportions, representing less than 1% in FVG and Veneto and between 1.5% to 2% in Marche and Umbria. The most dominant class is Dothideomycetes, followed by Leotiomycetes, Sordariomycetes and Eurotiomycetes (Fig 4B). Basidiomycetes are represented by Tremellomycetes and Agaricomycetes (Fig 4B).

The order Capnodiales was the most represented order in all the sites, followed by Pleosporales. The most represented genera in all the sites were *Mycosphaerella*, *Alternaria*, *Botrytis* and *Periconia* (Fig 5A).

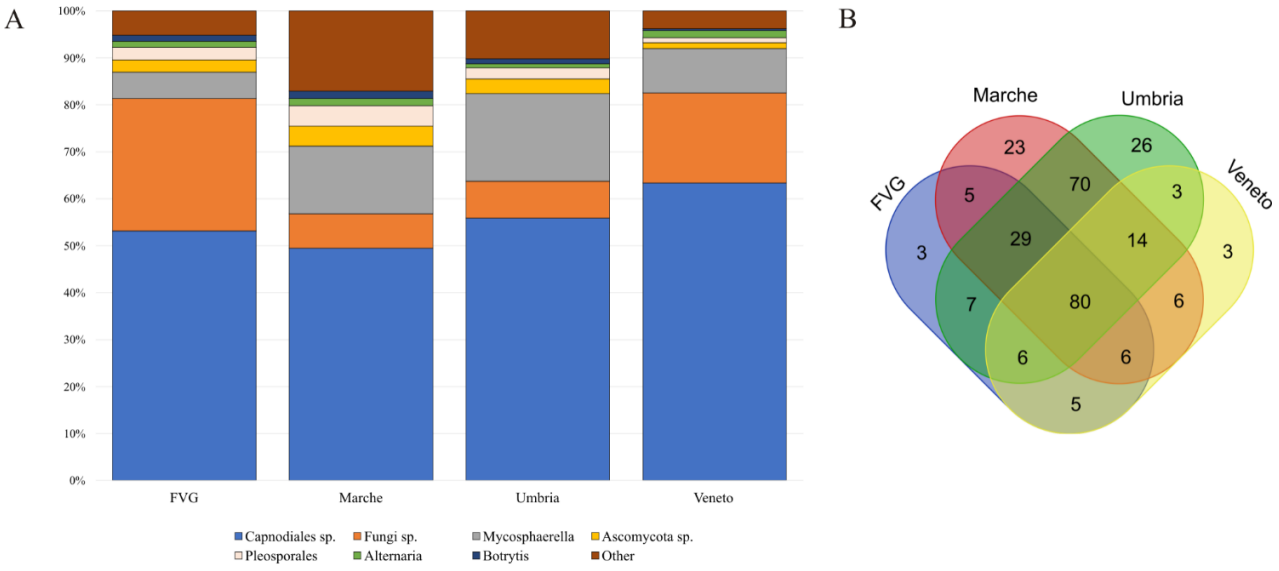

Fig 5. A) Bar charts showing the taxonomic composition up to genus level in the four sampling sites. Abundances of taxa are reported with the percentage values of reads. Taxa accounting for <0.5% of reads are grouped as "Other". B) Venn diagram shows the number of unique and shared taxa identified at the genus level among sites (as in S2 Table).

At species level, in all four sites the most represented species was *Mycosphaerella tassiana* (the teleomorph synonym of *Cladosporium herbarum).* In FVG, *M. tassiana* (5.59%) was followed by *Botrytis cinerea* (1.25%), *Alternaria eichhorniae* (0.64%), *Exserohilum oryzicola* (0.6%), *Periconia pseudobyssoides* (0.46%), *Hannaella luteola* (0.24%), *Alternaria alternata* (0.13%), *Bipolaris sorokiniana* and *Aspergillus intermedius* (0.12% each). In Marche, *M. tassiana* (14.35%) was followed by *B. cinerea* (1.55%), *Stemphylium herbarum* (0.81%), *Phaeosphaeria juncophila* (0.39%), *A. eichhorniae* (0.39%), *Angustimassarina acerina* (0.37%), *Lanzia echinophila* (0.32%), *Lophiostoma macrostomum* (0.27%). In Umbria, *M. tassiana* (18.71%) was followed by *B. cinerea* (1.03%), *Parastagonospora avenae* (0.43%), *P. juncophila* (0.41%), *L. echinophila* (0.33%), *A. eichhorniae* (0.31%), *S. herbarum* (0.31%), *L. macrostomum* (0.22% each). In Veneto, *M. tassiana* (9.46%) was followed by *A. eichhorniae* (0.84%), *B. cinerea* (0.39%), *H. luteola* (0.27%), *Periconia pseudobyssoides* (0.22%), *Aspergillus intermedius* (0.18%), *A. alternata* (0.14%).

Eighty taxa identified up to the genus level, comprising about 99% of the total reads, are shared by the four sites (Fig 5B; being Capnodiales, Fungi sp., *Mycosphaerella*, Ascomycota sp., Pleosporales, *Alternaria*, *Botrytis* and *Periconia* the most abundant). FVG, Marche and Umbria shared 29 taxa (being *Naevala* and *Vuilleminia* the most abundant genera, both representing >0.1% of the reads). Low represented taxa (<0.1% of the reads) are shared among two or three out of four sites (S2 Table). In each site, we also recover unique taxa (<0.1% of the reads) which were otherwise not detected in the other three sites: three for FVG and Veneto, 23 for Marche and 26 for Umbria (S2 Table).

Discussion

Fungal diversity in airborne samples

In this study, we characterized the taxonomic composition of airborne fungi across four Italian sites using the ITS2 region as barcode and the Ion Torrent sequencing platform. The two sites from Central Italy, Marche and Umbria, showed higher species richness and diversity than the two sites in NE Italy, FVG and Veneto. Beta diversity analyses evidenced the tendency of the samples to group on the base of their geography, as a subtle different taxonomic composition was recovered between the sites. This is partially explained by a higher (twice to three times) presence of reads assigned only to kingdom level (Fungi sp.) in the NE Italian sites. Alternatively, the fungal composition during the two sampling weeks remain rather constant within each site (S2 Fig).

The presence and distribution of fungal communities and therefore their spores, are influenced by spatial contexts [62], climatic [63, 64 and reference therein] and meteorological conditions [65-68]. Spatial contexts (such as pedology, land use and vegetation) determine the availability of substrates and plant hosts on which certain fungi can develop [62]. Mean air temperature, relative humidity and wind speed are additional factor shaping the distribution of fungal spores, such as those of *Alternaria*, *Cladosporium*, *Drechslera*-type, *Epicoccum* and *Torula* [69]. Here, we do not correlate the overall diversity observed with the meteorological parameters, as our data were collected over a short period and cannot be generalized in a broader context. However, we do consider that sites in NE and Central Italy are under the influence of different climatic conditions as they are located about 500 km apart from each other on a latitudinal distance. Therefore, the variability of climatic and environmental conditions (e.g. temperatures, precipitations, humidity and elevation) between the sampled sites could partially explain the detected fungal diversity. This expectation is corroborated by a high proportion of *Mycosphaerella/Cladosporium* and *Stemphylium* spores in both sites from the Central Italy as, according to literature [5, 69], these spores require high mean air temperature, low relative humidity and low amount of rain, which are known for these areas.

The main classes of fungi detected by the ITS2 barcode belonged to ascomycetes, whereas basidiomycetes were present in very low proportions. The low proportion of basidiomycetes might be impaired by multiple factors. About 15% of the reads could not be identified (Fungi sp.); these reads might indeed hide further asco- or basidiomycetes taxa as well. In outdoor airborne samples the amounts of the two fungal divisions was often reported to vary during the year, but it can also highly differ within shorter periods of time (i.e. daily; [35, 47]), making the comparison of different surveys difficult. Notwithstanding this bias, the low proportion of recovered basidiomycetes could be attributed to spore dimensions, dispersal ability, weather conditions (as humidity, precipitations), seasonality, availability of substrate or geographical factors. Previous studies report that ascomycetes

are more common than the basidiomycetes during dry days [35, 70]. One other study based on ITS sequencing of airborne fungi captured throughout a year [20] reported that ascomycetes were prevailing (>90%) among larger particles (>9 μm), while the opposite trend was recorded for smaller particles (>3 μm). Among spores, ascomycetes are more often reported in higher abundances than basidiomycetes – e.g. Fierer et al. [71] reported as much as 97% of ascomycetes using cloning and sequencing of the universal marker SSU, while Yang et al. [14] reported abundances reaching over 90% when sequencing fungal ITS1 in a study where haze and non-haze days in Beijing were analyzed based of the particulate matters fraction (PMs). The selection of the barcode primers can also affect the detection of certain taxa [72, 73]; it has been observed that ITS1 barcode captures a higher proportion of basidiomycetes than of ascomycetes [74-76].

Our results also report the presence of eight lichen genera (*Caloplaca*, *Cladonia*, *Flavoparmelia*, *Lecidella*, *Physcia*, *Hyperphyscia*, *Rinodina*, *Umbilicaria*) of which the spores of only two taxa, the genus *Caloplaca* and the family Physciaceae (which includes *Physcia*, *Hyperphyscia* and *Rinodina*), were identified during the morphological inspections of the samples. The majority of the detected taxa are epiphytic lichens commonly distributed in Italy, and can occur also in urban environment if not highly polluted. The only exception is the genus *Umbilicaria* which comprise only epilithic species of montane to alpine environments. This is, however, to the best of our knowledge, the first report of the detection of lichen spores and lichen sequence data in airborne samples.

The genus *Schizoxylon* is one of the 70 genera shared by Marche and Umbria. Interestingly this fungus, known to be both saprotrophic and optionally lichenized [77-79], has been reported only for Scandinavian countries so far [78]. Its presence in our dataset lets us speculate on its possible distribution in the Mediterranean region but further researches are necessary to support this hypothesis.

Surprisingly, also rock inhabiting fungi (RIF) were identified, though in low amounts. Some of them belong to widespread genera, such as *Knufia*, while sequences corresponding to extremophilic genera, such as the *Friedmanniomyces* [80], were also retrieved. It is likely that either their presence in the airborne samples is due to long distance dispersal, or that their identities corresponded to closely related taxa which colonize rock surfaces in or close to the urban environments. The distribution of epilithic and endolithic RIF assemblages is still poorly known, and whether they would be repeatedly recovered in airborne samples should be investigated further.

The sequencing results are characterized by a relatively high percentage of reads here referred as Fungal sp. (about 7% for Central and 25% for Northern sites). These correspond to about 100 OTUs which blasted in NCBI mainly as “Fungal sp.” or “Uncultured fungus” derived from other air

surveys (i.e. FJ820545, KP724985, KF800623), confirming the importance of further studies on this pool of still unknown ecological components.

The genera *Cladosporium*, *Alternaria*, *Epicoccum* and *Stemphylium* of which the sequencing reads represented the highest percentage, were also abundantly found in the samples inspected at the microscope. These genera have their peak of spore dispersal at late summer and early autumn [5, 81, 82] and indeed their spores were spread all over the collecting tapes. Five taxa out of the 22 morphologically identified genera, were detected only by microscopy analyses (S1 Table): *Pithomyces* (soil fungus), *Oidium*, *Peronospora*, *Leptosphaerulina* (it was present only in FVG), and *Polythrincium* (single spores found in Marche and Veneto, respectively). The remaining taxa were detected both by sequencing and morphological analyses.

Fungal pathogens and invasive alien species (IAS)

A number of fungi are known to be the source of allergenic particles in form of spores and/or thallus fragments. Allergenic taxa belong to Ascomycota, Basidiomycota and anamorphic fungi can act as agents for a multiplicity of diseases, such as infections, toxicosis, allergic asthma, allergic rhinitis, allergic sinusitis, broncho-pulmonary mycoses, and hypersensitivity pneumonitis [5, 16, 35, 83]. Because fungal aerosol in indoor environments depends in most cases from outdoor concentrations [18], the presence and distribution of allergenic fungi represents an important issue for public health [16, 84].

In the most frequently detected fungal order Capnodiales (Ascomycota, Dothideomycetes) the main allergenic genus identified in our study was *Cladosporium*; *Alternaria*, *Aspergillus*, *Epicoccum*, *Exserohilum* were found in lower amount. Human and animal pathogens (*Acremonium*, *Candida*, *Cryptococcus*, *Torula*), as well as plant pathogen (*Botrytis*, *Bipolaris*, *Periconia*, *Phaeosphaeria*, *Parastagonospora*, *Ramularia*, *Stemphylium*) have been sequenced from all four sites.

Invasive alien species (IAS) are recognized as a major threat of diverse ecosystems [85]. Due to their inconspicuous nature and the fact that they are still poorly studied also in terms of bio- and phylogeography, fungal reports in IAS databases is still very scarce, with the exception of few important plants and animal pathogen [86]. The DAISIE European Invasive Alien Species Gateway (www.europe-aliens.org) lists about 40 alien fungal species for Italy. Among these, *Discula destructiva* was sequenced from the sampling site in Umbria. This fungus is a pathogenic, causal agent of the dogwood anthracnose, which is one of the major diseases affecting *Cornus* tree species [87]. First observed in North America [88], the disease has been reported also in Germany since 2002 [89] and in Italy since 2003 [90].

HTS technology for the study of airborne fungi

In our survey, species accumulation curves did not reach saturation, indicating an even more remarkable richness and diversity of taxa. A more exhaustive sampling could be obtained if the sequencing depth would be increased, for example by using a larger PGM chips (such as 316^{TM}) Another possibility would be to use other HTS approaches that allow the sequencing of the whole ITS fragment.

The application of HTS technologies is nowadays among the new, standard approaches for environmental studies. Despite the great advantages offered by HTS, e.g. the high taxonomic resolution, reproducibility and short processing time [91], DNA metabarcoding is still affected by some pitfalls. Among them, the possibility to quantify the abundance of the taxa with higher accuracy (stochasticity of the PCR amplifications and also sequencing the HTS results are semi-quantitative at best) and primer bias impair sequencing results at the most [91-93]. Further, the underestimation of species diversity is unpredictable in several fungal taxa, although primers have been designed *ad hoc* for certain groups [93-95]. The low proportion of basidiomycetes (see previous section) detected in this survey might be attributed to the selected primers (ITS3/ITS4), as they were shown to preferentially amplify ascomycetes [74-76]. One of the reasons for this could be that the ITS2 amplicon is longer in basidiomycetes than in ascomycetes (30-50 bp longer, [76]) and therefore the selected primer pair may preferentially amplify the shorter ITS2 in the ascomycetes [75, 76], explaining the higher proportion of ascomycetes reads in our dataset. As the application of HTS to fungal communities studies is increasing, there is a general need to develop primers that minimize the taxonomic biases so far persisting [73, 96].

The identities of the generated sequences are still hardly comparable with reference databases and this represent a drawback in such surveys. We expect that the establishment of site-specific reference databases would implement in the future the identification of airborne fungal particles and further improve the air monitoring.

Conclusions

Intraspecific morphological variation, low quantity and lack of distinctive morphological characters have been the major constraints for the microscopy identification of fungal spores in airborne samples. In the present study we have showed that the great number of taxa identified with DNA metabarcoding is ten-fold higher than the one identified by microscopy analyses (238 vs. 22 genera). This strengthens the perception that HTS analyses are tools of key importance to increase the sensitivity of air biomonitoring and our knowledge on airborne fungal diversity. The

standardization of HTS techniques in aerobiology will make the monitoring of pathogenic fungal agents and their distribution affordable in shorter time and with higher reliability. The prompt identification of new or potential allergenic substances from plant and fungal tissues, as well as invasive species, is essential for an effective prevention and management of diverse environments. A long-scale monitoring extended on a wider geographic area in Italy is taking into account seasonal variation and meteorological conditions (Muggia et al. in prep.). Further, the development of regional database for airborne fungi and the ongoing implementation of existing worldwide fungal database [97, 98] represents a 'must' to reliably asses the identity of new sequence data.

Acknowledgments

We thank Fiorella Florian and Fabrizia Gionechetti (Trieste) for technical help in the laboratory.

References

1. Fernstrom A, and Goldblatt M. Aerobiology and its role in the Transmission of infectious diseases. J Pathog. 2013: 1–13. doi:10.1155/2013/493960.
2. Gregory PH. Microbiology of the atmosphere. Wiley New YorkUSA;1973.
3. Brown JKM, Hovmøller MS, Wyand RA, Yu Z. In: Dispersal, J. M. Bullock, R. E. Kenward, R.S. Hails, Eds. Blackwell Science, Oxford;2002 pp. 395–409.
4. Brown JKM, Hovmøller MS. Aerial dispersal of pathogens on the global and continental scale and its impact on plant disease. Science. 2002; 297(5581): 537–541.
5. Oliveira M, Delgado L, Ribeiro H, Abreu I. Fungal spores from Pleosporales in the atmosphere of urban and rural locations in Portugal. J Environ Monit. 2010; 12(5): 1187-94
6. Horner WE, Helbling A, Salvaggio JE, Lehrer SB. Fungal allergens. Clin Microbiol Rev. 1995;8: 161-179.
7. Dean R, Van Kan JA, Pretorius ZA, Hammond-Kosack KE, Di Pietro A, Spanu P. D et al. The Top 10 fungal pathogens in molecular plant pathology. Mol plant pathol. 2012;13(4): 414-430.
8. Chowdhary A, Khaturia S, Agarwal K, Meis JF. Recognizing filamentous basidiomycetes as agents of human disease: A review. Med. Mycol. 2014; 52: 782-797.
9. O'Donnell K, Ward TJ, Robert VARG, Crous PW, Geiser DM, Kang S. DNA sequence-based identification of *Fusarium*: Current status and future directions. Phytoparasitica. 2015;43: 583-595.
10. De Hoog GS, Queiroz-Telles F, Haase G, Fernandez-Zeppenfeldt G, Angelis DA, Gerrits van den Ende AHG et al. Black fungi: clinical and pathogenic approaches. Med Mycol. 2000;38: 243-250.
11. De Hoog GS, Dukik K, Monod M, Packeu A, Stubbe D, Hendrickx M et al. Towards a novel multilocus phylogenetic taxonomy for dermatophytes. Mycopathologia. 2016;doi: 10.1007/s11046-016-0073-9.
12. Green BJ, Tovey ER, Sercombe JK, Blachere FM, Beezhold DH, Schmechel D. Airborne F. fungal fragments and allergenicity. Med Mycol. 2006;44: S245–55. doi:10.1080/13693780600776308.
13. Pringle Anne. Asthma and the diversity of fungal spores in air. PLoS Pathog. 2013;9(6): 1–4. doi:10.1371/journal.ppat.1003371.
14. Yang CS, Eckardt J, De-Wei L. Airborne fungi and mycotoxins. Manual of Environmental Microbiology. 2016. doi:10.1128/9781555818821.ch3.2.5.
15. Kurup V, Shen H, Banerjee B. Respiratory fungal allergy. Microbes Infect. 2000; 2:1101-10.
16. Khan, AA, Karuppayil SM. Fungal pollution of indoor environments and its management. Saudi J of Biol Sci. 2012;19(4): 405–26. doi:10.1016/j.sjbs.2012.06.002.
17. Twaroch TE, Curin M, Valenta R, Swoboda I. Mold allergens in respiratory allergy: from structure to therapy. Allergy Asthma Immunol Res. 2015;7(3): 205–20. doi:10.4168/aair.2015.7.3.205.
18. Shelton BG, Kirkland KH, Flanders WD, Morris GK. Profiles of airborne fungi in buildings and outdoor environments in the united states. J Appl Environ Microbiol. 2002;68(4): 1743–53. doi:10.1128/AEM.68.4.1743.

19. Amend AS, Seifert KA, Samson R, Bruns TD. Indoor fungal composition is geographically patterned and more diverse in temperate zones than in the tropics. Proc Natl Acad Sci USA. 2010;107: 13748–13753.
20. Yamamoto N, Bibby K, Qian J, Hospodsky D, Rismani-Yazdi H, Nazaroff WW, Peccia J. Particle-size distributions and seasonal diversity of allergenic and pathogenic fungi in outdoor air. ISME J. 2012;6(10): 1801–11. doi:10.1038/ismej.2012.30.
21. Pavan R, Manjunath K. Qualitative analysis of indoor and outdoor airborne fungi in cowshed. J of Mycol. 2014;1–8. doi:10.1155/2014/985921.
22. Tong X, Xu H, Zou L, Cai M, Xu X, Zhao Z, Xiao F, Li Y. High Diversity of airborne fungi in the hospital environment as revealed by meta-sequencing-based microbiome analysis. Scientific Reports. 2017;7: 1-8 39606. doi:10.1038/srep39606.
23. Pusz W, Weber R, Dancewicz A, Kita W. Analysis of selected fungi variation and its dependence on season and mountain range in southern Poland—key factors in drawing up trial guidelines for aeromycological monitoring. Environ Monit and Assess. 2017;189(10): 526.
24. Hebert PDN, Cywinska A, Ball SL, deWaard JR. Biological identifications through DNA barcodes. Proc R Soc Lon. 2003;270: 313–321.
25. Kress WJ, Wurdack KJ, Zimmer EA, Weigt LA, Janzen DH. Use of DNA barcodes to identify flowering plants. Proc Nat Acad Sci of the USA. 2005;102(23): 8369–74. doi:10.1073/pnas.0503123102.
26. Hajibabaei M, Singer GAC, Hebert PDN, Hickey DA.DNA Barcoding: How it complements taxonomy, molecular phylogenetics and population genetics. Trends Genet. 2007;23(4): 167–72. doi:10.1016/j.tig.2007.02.001.
27. Joly S, Davies TJ, Archambault A, Bruneau A, Derry A, Kembel SW, Peres-Neto P, Vamosi J, Wheeler TA. Ecology in the age of DNA barcoding: the resource, the promise and the challenges ahead. Mol Ecol Resour. 2014;14(2): 221–32. doi:10.1111/1755-0998.12173.
28. Longhi S, Cristofori A, Gatto P, Cristofolini F, Grando MS, Gottardini E. Biomolecular identification of allergenic pollen: a new perspective for aerobiological monitoring? Ann Allergy, Asthma Immunol. 2009;103(6): 508–14. doi:10.1016/S1081-1206(10)60268-2.
29. Galimberti A, De Mattia F, Bruni I, Scaccabarozzi D, Sandionigi A, Barbuto M, Casiraghi M, and Labra M. A DNA barcoding approach to characterize pollen collected by honeybees." PLoS ONE. 2014;9(10).
30. Hawkins J, De Vere N, Griffith A, Ford CR, Allainguillaume J, Hegarty MJ, Baillie L, Adams-Groom B. Using DNA metabarcoding to identify the floral composition of honey: a new tool for investigating honey bee foraging preferences. PLoS ONE. 2015;10(8): 1–20. doi:10.1371/journal.pone.0134735.
31. Keller A, Danner N, Grimmer G, Ankenbrand MVD, Ohe KVD., Ohe W, Steffan-Dewenter I. Evaluating multiplexed next-generation sequencing as a method in palynology for mixed pollen samples. Plant Biol. 2015;17(2): 558-566.
32. Richardson RT., Lin CH, Sponsler DB, Quijia JO, Goodell K, Johnson RM. Application of ITS2 metabarcoding to determine the provenance of pollen collected by honey bees in an agroecosystem. Appl Plant Sc. 2015; 3(1): 1400066. doi:10.3732/apps.1400066.
33. Prosser SWJ, Hebert PDN. Rapid identification of the botanical and entomological sources of honey using dna metabarcoding. Food Chem. 2017;214: 183–91. doi:10.1016/j.foodchem.2016.07.077.

34. Kraaijeveld K, de Weger LA, Ventayol García M, Buermans H, Frank J, Hiemstra PS, den Dunnen JT. Efficient and sensitive identification and quantification of airborne pollen using next-generation DNA sequencing. Mol Ecol Resour. 2015;15(1): 8–16. doi:10.1111/1755-0998.12288.
35. Pashley CH, Fairs A, Free RC, Wardlaw AJ. DNA analysis of outdoor air reveals a high degree of fungal diversity, temporal variability, and genera not seen by spore morphology. Fungal Biol. 2012; 116(2): 214–24. doi:10.1016/j.funbio.2011.11.004.
36. Anurag S, Clark E, McGlothlin JD, Mittal SK. Efficiency of airborne sample analysis platform (ASAP) bioaerosol sampler for pathogen detection. Front Microbiol. 2015; 6.
37. Portnoy JM, Barnes CS, Kennedy K. Sampling for indoor fungi. J All and Clin Immunol. 2004;113(2): 189-198.
38. Sabariego S, Díaz De La Guardia C, Alba F. The effect of meteorological factors on the daily variation of airborne fungal spores in Granada (southern Spain). Int J Biometeorol. 2000;44:1–5. doi:10.1007/s004840050131.
39. U'Ren JM, Lutzoni F, Miadlikowska J, Laetsch AD, Arnold AE. Host and geographic structure of endophytic and endolichenic fungi at a continental scale. Am J Bot. 2012;99: 898–914.
40. Fort T, Robin C, Capdevielle X, Delière L, Vacher C. Foliar fungal communities strongly differ between habitat patches in a landscape mosaic. PeerJ. 2016;4: e2656. doi:10.7717/peerj.2656.
41. Li W, Wang MM, Wang XG, Cheng XL, Guo JJ, Bian XM, Ca L. Fungal communities in sediments of subtropical Chinese seas as estimated by DNA metabarcoding. Scie Rep. 2016; 6.
42. Durand A, Maillard F, Foulon J, Gweon HS, Valot B, Chalot M. Environmental metabarcoding reveals contrasting belowground and aboveground fungal communities from poplar at a Hg phytomanagement site. Microb Ecol. 2017 doi:10.1007/s00248-017-0984-0.
43. Fernándes-Mendoza F, Fleischhacker A, Kopun T, Grube M, Muggia L. Taxonomically informed amplicon sequencing of lichens and lichenicolous fungi highlights the low specificity of the mycobiomes at a local scale. Mol Ecol. 2017
44. Malacrinò A, Schena L, Campolo O, Laudani F, Mosca S, Giunti G, Strano CP, Palmeri V. A metabarcoding survey on the fungal microbiota associated to the olive fruit fly. Microb Ecol. 2017;73(3): 677–84. doi:10.1007/s00248-016-0864-z.
45. Bowers R M, Lauber CL, Wiedinmyer C, Hamady M, Hallar AG, Fall R, Fierer, N. Characterization of airborne microbial communities at a high-elevation site and their potential to act as atmospheric ice nuclei. Applied and Environmental Microbiology. 2009;75(15): 5121-5130.
46. Cao C, Jiang W, Wang B, Fang J, Lang J, Tian G et al. Inhalable microorganisms in Beijing's PM2.5 and PM10 pollutants during a severe smog event. Environ Sci Technol. 2014;48: 1499–1507. 10.1021/es4048472.
47. Oh SY, Fong JJ, Park MS, Chang L, Lim YW. Identifying airborne fungi in Seoul, Korea Using Metagenomics. J Microbiol. 2014;52(6): 465–72. doi:10.1007/s12275-014-3550-1.
48. Schoch CL, Seifert KA, Huhndorf S, Robert V, Spouge JL, Levesque CA, Chen W, et al. Nuclear ribosomal internal transcribed spacer (ITS) region as a universal DNA barcode marker for fungi. Proc Natl Acad Sci USA. 2012;109(16): 1–6. doi:10.1073/pnas.1117018109.
49. Nilsson RH, Ryberg M, Abarenkov K, Sjökvist E, Kristiansson, E. The ITS region as a target for characterization of fungal communities using emerging sequencing technologies. FEMS Microbiol Lett. 2009;296: 97-101.

50. Nilsson RH, Tedersoo L, Ryberg M, Kristiansson E, Hartmann M, Unterseher M, et al. A comprehensive, automatically updated fungal ITS sequence dataset for reference-based chimera control in environmental sequencing efforts. Microbes Environ. 2015;30: 145-150.
51. Smith EG. Sampling and identifying pollens and molds. An illustrated identification manual for air samplers. Sat Antonio, Texas: Blewston Press; 2000.
52. White TJ, Bruns T, Lee SJWT, Taylor JW. Amplification and direct sequencing of fungal ribosomal RNA genes for phylogenetics. In: Innis MA, Gelfand DH, Sninsky JJ, White TJ. editors. PCR protocols: a guide to methods and applications. New York: Academic Press; 1991. pp. 315-322.
53. Carew ME, Pettigrove VJ, Metzeling L, Hoffmann A. Environmental monitoring using next generation sequencing: rapid identification of macroinvertebrate bioindicator species. Front Zool. 2013;10: 45.
54. Caporaso GJ, Kuczynski J, Stombaugh J, Bittinger K, Bushman FD, Costello EK, et al. QIIME allows analysis of high-throughput community sequencing data. Nat Methods. 2010;7: 335-336.
55. Bengtsson-Palme J, Ryberg M, Hartmann M, Branco S, Wang Z, Godhe A, et al. Improved software detection and extraction of ITS1 and ITS2 from ribosomal ITS sequences of fungi and other eukaryotes for analysis of environmental sequencing data. Methods Ecol Evol. 2013;4: 914-919.
56. Edgar RC, Haas BJ, Clemente JC, Quince C, Knight R. UCHIME improves sensitivity and speed of chimera detection. Bioinform. 2011;27: 2194-2200.
57. Kõljalg U, Nilsson RH, Abarenkov K, Tedersoo L, Taylor AFS, Bahram M, et al. Towards a unified paradigm for sequence-based identification of fungi. Mol Ecol. 2013;22: 5271-5277.
58. Chao A, Colwell RK, Lin CW, Gotelli NJ. Sufficient sampling for asymptotic minimum species richness estimators. Ecology. 2009;90: 1125-1133.
59. Spellerberg IF, Fedor PJ. A tribute to Claude Shannon (1916–2001) and a plea for more rigorous use of species richness, species diversity and the 'Shannon–Wiener' Index. Glob Ecol Biogeogr. 2003;12: 177-179.
60. R Development Core Team. R: a language and environment for statistical computing, 2.15.1. Vienna, Austria: R Foundation for Statistical Computing; 2012.
61. Vazquez-Baeza Y, Pirrung M, Gonzalez A, Knight R. EMPeror: a tool for visualizing high-throughput microbial community data. Gigascience. 2013;2: 16.
62. Peay KG, Bruns TD. Spore dispersal of basidiomycete fungi at the landscape scale is driven by stochastic and deterministic processes and generates variability in plant-fungal interactions. New Phytol. 2014;204(1): 180-191.
63. Favero-Longo SE, Sandrone S, Matteucci E, Appolonia L, Piervittori R. Spores of lichen-forming fungi in the mycoaerosol and their relationships with climate factors. Sci. Total Environ. 2014;467: 26-33.
64. Fröhlich-Nowoisky J, Kampf CJ, Weber B, Huffman JA, Pöhlker C, Andreae MO, et al. Bioaerosols in the earth system: climate, health, and ecosystem interactions. Atmos Res. 2016;182: 346-376.
65. Hjelmroos M. Relationship between airborne fungal spore presence and weather variables: Cladosporium and Alternaria. Grana. 1993;32: 40-47.

66. Hernàndez Trejo FH, Rodríguez AFM, Molina RT, Palacios IS. Airborne ascospores in Mérida (SW Spain) and the effect of rain and other meteorological parameters on their concentration. Aerobiologia. 2014;28(1): 13-26.
67. El Haskouri F, Bouziane H, Trigo MdM, Kadiri M, Kazzaz M. Airborne ascospores in tetouan (NW Morocco) and meteorological parameters. Aerobiologia 2016;32(4): 669-681.
68. Grinn-Gofroń A, Bosiacka B, Bednarz A, Wolski T. A comparative study of hourly and daily relationships between selected meteorological parameters and airborne fungal spore composition. Aerobiologia. 2017 doi:10.1007/s10453-017-9493-3.
69. Grinn-Gofroń A, Bosiacka, B. Effects of meteorological factors on the composition of selected fungal spores in the air. Aerobiologia. 2015;31(1): 63-72.
70. Elbert W, Taylor PE, Andreae MO, Poschl U. Contribution of fungi to primary biogenic aerosols in the atmosphere: wet and dry discharged spores, carbohydrates, and inorganic ions. Atmos Chem Phys. 2007;7: 4569e4588.
71. Fierer N, Liu Z, Rodríguez-Hernández M, Knight R, Henn M, Hernandez MT. Short-term temporal variability in airborne bacterial and fungal populations. Appl Environ Microbiol. 2008;74(1): 200-207.
72. Tedersoo L, Anslan S, Bahram M, Polme S, Riit T, Liiv I, et al. Shotgun metagenome and multiple pair-barcode combinations of amplicons reveal biases in metabarcoding analyses of Fungi. MycoKey. 2015;10: 1-43.
73. Tedersoo L, Lindahl B. Fungal identification biases in microbiome projects. Environ Microbiol Rep. 2016;8: 774-779.
74. Schoch CL, Seifert KA, Huhndorf S, Robert V, Spouge JL, Levesque CA, et al. Nuclear ribosomal internal transcribed spacer (ITS) region as a universal DNA barcode marker for Fungi. Proc Natl Acad Sci USA. 2012;109: 1-6.
75. Bellemain E, Carlsen T, Brochmann C, Coissac E, Taberlet P, Kauserud H. ITS as an environmental DNA barcode for fungi: an *in silico* approach reveals potential PCR biases. BMC microbiol. 2010;10(1): 189.
76. Bokulich NA, Mills DA. Improved selection of internal transcribed spacer-specific primers enables quantitative, ultra-high-throughput profiling of fungal communities. Appl Environ Microbiol. 2013;79(8): 2519-2526.
77. Wedin M, Döring H, Gilenstam G. Saprotrophy and lichenization as options for the same fungal species on different substrata: environmental plasticity and fungal lifestyles in the *Stictis–Conotrema* complex. New Phytol. 2004;164: 459-465.
78. Wedin M, Döring H, Gilenstam G. *Stictis* s. lat. (Ostropales, Ascomycota) in northern Scandinavia, with a key and notes on morphological variation in relation to lifestyle. Mycol Res. 2006;110: 773-789.
79. Muggia L, Baloch E, Stabentheiner E, Grube M, Wedin M. Photobiont association and genetic diversity of the optionally lichenized fungus *Schizoxylon albescens*. FEMS Microbiol Ecol. 2010;75(2): 255-272.
80. Onofri S, Pagano S, Zucconi L, Tosi S. *Friedmanniomyces endolithicus* (Fungi, Hyphomycetes), anam. - gen. and sp. nov. from continental Antarctica. Nova Hedwigia. 1999;68: 175-181.
81. Li DW, Kendrick B. A year-round study on functional relationships of airborne fungi with meteorological factors. Int J Biometeorol. 1995;39(2): 74-80.
82. Gómez de Ana S, Torres-Rodríguez JM, Alvara-do-Ramírez E, Mojal-García S, Belmonte-Soler J. Seasonal distribution of *Alternaria*, *Aspergillus*, *Cladosporium* and *Penicillium* species

isolated in homes of fungal allergic patients. J Investig Allergol Clin Immunol. 2007;16: 357-363.
83. Piecková E, Wilkins K. Airway toxicity of house dust and its fungal composition. Ann Agric Environ Med. 2004;11(1): 67-73.
84. Samet JM, Spengler JD. Indoor environments and health: moving into the 21st century. Am J Public Health. 2003;93(9): 1489-1493.
85. Pejchar L, Mooney HA. Invasive species, ecosystem services and human well-being. Trends Ecol Evol. 2009;24(9): 497-504.
86. Desprez-Loustau, ML. Alien fungi of Europe. Handbook of alien species in Europe. 2009: 15-28.
87. Miller S, Masuya H, Zhang J, Walsh E, Zhang N. Real-Time PCR detection of dogwood anthracnose fungus in historical herbarium specimens from Asia. PloS ONE. 2016;11(4): e0154030.
88. Byther RS, Davidson RM Jr. Dogwood anthracnose. Orn NW Newsletter. 1979;3: 20–21.
89. Stinzing A, Lang K. Dogwood anthracnose. Erster Fund von *Discula destructive* an *Cornus florida* in Deutschland. Nachrichtenbl. Deut. Pflanzenschutzd. 2003;55: S1-S5.
90. Tantardini A, Calvi M, Cavagna B, Zhang N, Geiser D. Primo rinvenimento in Italia di antracnosi causata da *Discula destructive* su *Cornus florida* e *C. nuttallii*. Informatore Fitopatologico. 2004;12: 44-47.
91. Elbrecht V, Vamos EE, Meissner K, Aroviita J, Leese F. Assessing strengths and weaknesses of DNA metabarcoding-based macroinvertebrate identification for routine stream monitoring. Methods Ecol Evol. 2017 10.1111/2041-210X.12789.
92. Piñol J, Mir G, Gomez-Polo P, Agustí N. Universal and blocking primer mismatches limit the use of high-throughput DNA sequencing for the quantitative metabarcoding of arthropods. Mol Ecol Resour. 2014;15: 1-12.
93. Elbrecht V, Leese F. Can DNA-based ecosystem assessments quantify species abundance? Testing primer bias and biomass – sequence relationships with an innovative metabarcoding protocol. PLoS ONE, 2015;10: e0130324-16.
94. Tedersoo L, Nilsson RH, Abarenkov K, Jairus T, Sadam A, Saar I, et al. 454 Pyrosequencing and Sanger sequencing of tropical mycorrhiza fungi provide similar results but reveal substantial methodological biases. New Phytol. 2010;188: 291-301.
95. Schmidt PA, Bálint M, Greshake B, Bandow C, Römbke J, Schmitt I. Illumina metabarcoding of a soil fungal community. Soil Biol Biochem. 2013;65: 128-132.
96. Toju H, Tanabe AS, Yamamoto S, Sato H. High-coverage ITS primers for the DNA-based identification of ascomycetes and basidiomycetes in environmental samples. PloS ONE. 2012;7(7): e40863.
97. Nilsson RH, Ryberg M, Kristiansson E, Abarenkov K, Larsson KH, Kõljalg U. Taxonomic reliability of DNA sequences in public sequence databases: a fungal perspective. PloS ONE. 2006;1(1): e59.
98. Hibbett D, Abarenkov K, Kõljalg U, Öpik M, Chai B, Cole, J, et al. Sequence-based classification and identification of Fungi. Mycologia. 2016;108(6): 1049-1068.

Supporting information

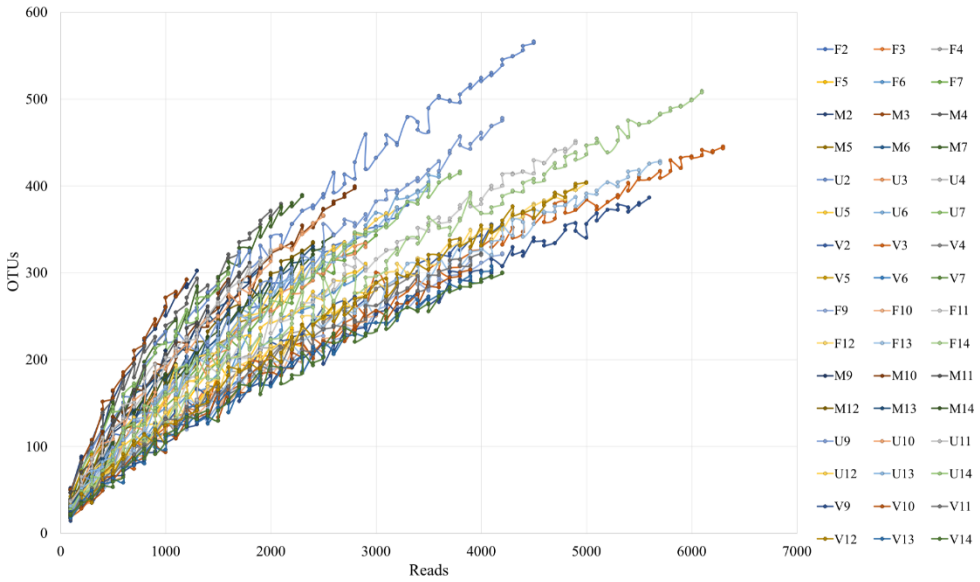

S1 Fig. Rarefaction curves of the complete dataset.

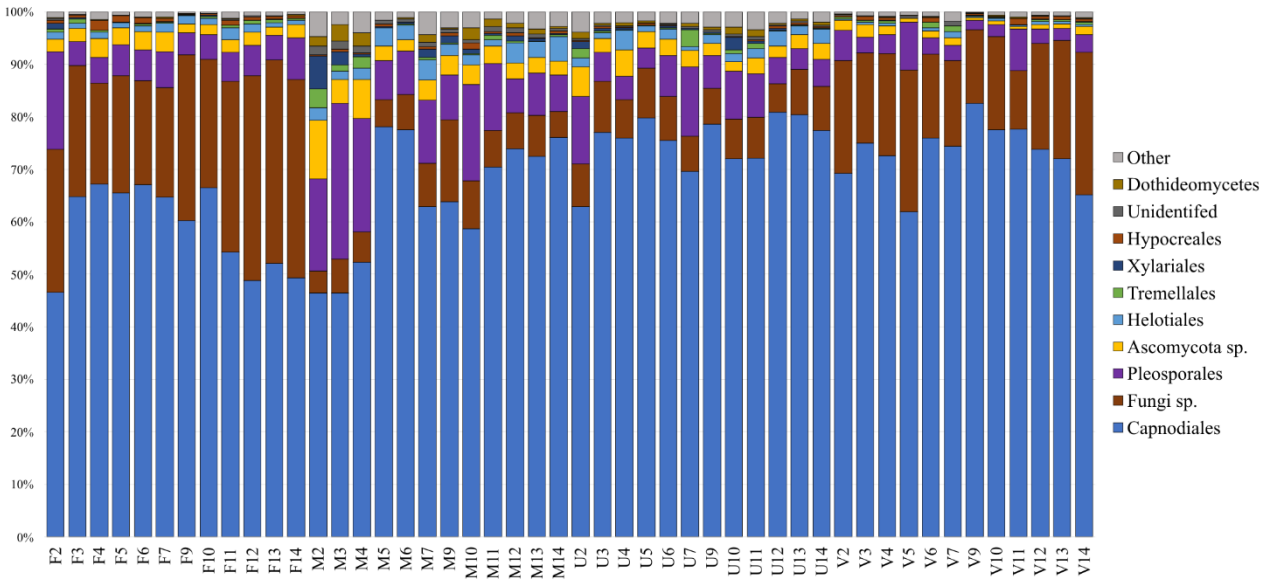

S2 Fig. Bar charts showing the taxonomic composition up to class level in the 48 samples. Abundances of taxa are reported with the percentage values of reads. Taxa accounting for <0.1% of reads are grouped as “Other”.

S1 Table. List of the taxa recovered by microscopy analysis in the sampling sites. For each taxon, presence (√) or absence (-) in each sampling sites is shown for both microscopy (micr) and amplicon sequencing (DNA).

	FVG		Marche		Umbria		Veneto	
	Micr	DNA	Micr	DNA	Micr	DNA	Micr	DNA
Alternaria	√	√	√	√	√	√	√	√
Amphisphaeria	-	√	√	√	-	-	-	-
Bipolaris	√	√	-	√	√	√	√	√
Caloplaca	-	-	√	-	-	-	-	-
Cladosporium	√	√	√	√	√	√	√	√
Curvularia	√	√	-	√	-	√	√	√
Drechslera	√	√	-	-	√	√	√	-
Epicoccum	√	√	√	√	√	√	√	-
Exserohilum	√	√	-	√	√	√	√	√
Keissleriella	-	√	-	√	-	√	√	√
Leptosphaeria	√	√	√	√	√	√	-	√
Leptosphaerulina	√	-	-	-	-	-	-	-
Lophiostoma	√	√	√	√	√	√	-	√
Massarina	-	√	√	√	√	√	√	√
Oidium	-	-	-	-	√	-	-	-
Periconia	√	√	-	√	-	√	√	√
Peronospora	√	-	√	-	-	-	√	-
Pithomyces	√	-	-	-	-	-	√	-
Pleospora	√	√	√	√	-	√	-	√
Polythrincium	-	-	√	-	-	-	√	-
Stemphylium	√	√	√	√	√	√	√	√
Torula	√	√	√	√	√	√	√	√

S2 Table. List and presence of taxa down to genus level in the Venn diagram of Fig. 5B. The letters before the taxon name indicate the taxonomic level: "k": kingdom, "p": phylum, "c": class, "o": order, "f": family, "g": genus. The taxa represented by more than 0.1% of the reads are highlighted in bold.

FVG	Marche	Umbria	Veneto	Nr. taxa	Taxa (up to genus level)
√	√	√	√	80	**k_Fungi sp.**, **p_Ascomycota**, **c_Dothideomycetes**, c_Sordariomycetes, c_Tremellomycetes, **o_Capnodiales**, o_Helotiales, **o_Pleosporales**, o_Xylariales, **f_Diatrypaceae**, f_Leptosphaeriaceae, **f_Nectriaceae**, **f_Phaeosphaeriaceae**, f_Pleosporaceae, f_Pleosporales_fam_Incertae_sedis, f_Pseudeurotiaceae, f_Xylariaceae, g_*Acremonium*, **g_*Alternaria***, **g_*Angustimassarina***, g_*Arthrinium*, g_*Ascochyta*, **g_*Aspergillus***, g_*Aureobasidium*, g_*Biatriospora*, g_*Bipolaris*, **g_*Botrytis***, **g_*Bullera***, g_*Candida*, **g_*Cercospora***,g_*Chalastospora*,g_*Ciboria*, **g_*Cladosporium***,g_*Coprinellus*,g_*Cryptococcus*,g_*Curvularia*,g_*Dendryphion*, g_*Didymella*, **g_*Dioszegia***, **g_*Exserohilum***, g_*Fusarium*, g_*Ganoderma*, g_*Gibberella*, **g_*Hannaella***, g_*Hansfordia*, g_*Hymenoscyphus*, g_*Hyphodermella*, g_*Hyphodontia*, **g_*Hypoxylon***, g_*Keissleriella*, **g_**L***anzia***, g_*Leptosphaeria*, g_*Leptospora*, **g_*Lophiostoma***, g_*Massarina*, g_*Monographella*, **g_*Mycosphaerella***, g_*Myrmecridium*, g_*Nigrospora*, g_*Paraconiothyrium*, **g_*Parastagonospora***, **g_*Passalora***, g_*Penicillium*, **g_*Periconia***, **g_*Phaeosphaeria***, **g_*Phoma***, g_*Pleospora*, g_*Podosphaera*, g_*Pseudodidymosphaeria*, g_*Sawadaea*, g_*Septoria*,

					g_*Setophaeosphaeria*, g_*Sordaria*, **g_*Stagonospora***, **g_*Stemphylium***, g_*Teichospora*, g_*Torula*, **g_*Xenobotryosphaeria***, g_*Xylaria*, **Unidentified**
√	√	√		29	p_Basidiomycota, o_Agaricales, o_Rhytismatales, f_Pyronemataceae, f_Rhytismataceae, g_*Bulleribasidium*, g_*Cladophialophora*, g_*Comoclathris*, g_*Coniothyrium*, g_*Epicoccum*, g_*Eutypa*, g_*Extremus*, g_*Lachnum*, g_*Lentithecium*, **g_*Naevala***, g_*Neoascochyta*, g_*Neodevriesia*, g_*Neofusicoccum*, g_*Neokalmusia*, g_*Phialocephala*, g_*Plectania*, g_*Pleurophragmium*, g_*Pyrenochaetopsis*, g_*Rinodina*, g_*Sphaerellopsis*, g_*Sporobolomyces*, g_*Truncatella*, **g_*Vuilleminia***, g_*Xylodon*
	√	√	√	14	c_Agaricomycetes, f_Corticiaceae, g_*Basidiodendron*, g_*Coriolopsis*, g_*Dactylaria*, g_*Incrucipulum*, g_*Lophodermium*, g_*Preussia*, g_*Pyrenophora*, g_*Rachicladosporium*, g_*Rutstroemia*, g_*Schizopora*, g_*Scirrhia*, g_*Umbilicaria*
√		√	√	6	o_Botryosphaeriales, f_Polyporaceae, g_*Endoconidioma*, g_*Peniophorella*, g_*Phaeodactylium*, g_*Pilidium*
√	√		√	6	o_Sporidiobolales, f_Capnodiales_fam_Incertae_sedis, g_*Cladonia*, g_*Coprinopsis*, g_*Golovinomyces*, g_*Physisporinus*
√	√			5	f_Amphisphaeriaceae, g_*Annulohypoxylon*, g_*Blumeria*, g_*Datronia*, g_*Uwebraunia*
	√	√		70	c_Leotiomycetes, o_Auriculariales, o_Chaetothyriales, o_Diaporthales, o_Polyporales, f_Acarosporaceae, f_Peniophoraceae, g_*Acicuseptoria*, g_*Auricularia*, g_*Botryosphaeria*, g_*Byssomerulius*, g_*Cadophora*, g_*Capnobotryella*, g_*Chalara*, g_*Ciborinia*, g_*Clathrosphaerina*, g_*Cryptosphaeria*, g_*Cryptovalsa*, g_*Cyphellophora*, g_*Diaporthe*, g_*Diatrypella*, g_*Dichomitus*, g_*Discosia*, g_*Dissoconium*, g_*Exidia*, g_*Exidiopsis*, g_*Friedmanniomyces*, g_*Fuscoporia*, g_*Glarea*, g_*Gloeophyllum*, g_*Gnomoniopsis*, g_*Graphostroma*, g_*Hypholoma*, g_*Knufia*, g_*Laetiporus*, g_*Lenzites*, g_*Melanconium*, g_*Mollisia*, g_*Mycoacia*, g_*Nemania*, g_*Neocladophialophora*, g_*Neosetophoma*, g_*Noosia*, g_*Penidiella*, g_*Peniophora*, g_*Perenniporia*, g_*Pezicula*, g_*Phaeosphaeriopsis*, g_*Phlebia*, g_*Phlebiella*, g_*Physcia*, g_*Plenodomus*, g_*Populocrescentia*, g_*Pringsheimia*, g_*Protodontia*, g_*Ramularia*, g_*Resupinatus*, g_*Reticulascus*, g_*Schizoxylon*, g_*Sclerotinia*, g_*Seimatosporium*, g_*Sistotremastrum*, g_*Spiroplana*, g_*Toxicocladosporium*, g_*Tremella*, g_*Trichopezizella*, g_*Valdensinia*, g_*Volucrispora*, g_*Xenasma*, g_*Xeropilidium*
		√	√	3	o_Hypocreales, g_*Clohesyomyces*, g_*Hysterium*
√			√	5	g_*Hyphopichia*, g_*Paraphoma*, g_*Pichia*, g_*Setosphaeria*, g_*Xenodidymella*
√		√		7	g_*Adisciso*, g_*Camarosporium*, g_*Drechslera*, g_*Fomes*, g_*Fomitopsis*, g_*Neophaeomoniella*, g_*Phaeomollisia*
	√		√	6	f_Halosphaeriaceae, g_*Abortiporus*, g_*Catenulostroma*, g_*Menispora*, g_*Radulidium*, g_*Sclerostagonospora*
√				3	g_*Colletotrichum*, g_*Lecidella*, g_*Paramycosphaerella*
	√			23	o_Sordariales, f_Sporormiaceae, g_*Allophaeosphaeria*, g_*Austroafricana*, g_*Calycina*, g_*Cylindrium*, g_*Derxomyces*, g_*Dinemasporium*, g_*Eutypella*, g_*Hirsutella*, g_*Inocybe*, g_*Leuconeurospora*, g_*Mycena*, g_*Periconiella*, g_*Phialemoniopsis*, g_*Physalospora*, g_*Pluteus*, g_*Psathyrella*, g_*Roseodiscus*, g_*Sydowia*, g_*Torrendiella*, g_*Trametes*, g_*Trichopeziza*
		√		26	o_Sebacinales, o_Tremellales, f_Ceratobasidiaceae, f_Russulaceae, f_Sclerotiniaceae, f_Teratosphaeriaceae, g_*Ampelomyces*, g_*Candelariella*, g_*Celosporium*, g_*Ceriporia*, g_*Cordyceps*, g_*Discostroma*, g_*Discula*, g_*Flavoparmelia*, g_*Gregarithecium*, g_*Helicoma*, g_*Hexagonia*, g_*Hyperphyscia*, g_*Letendraea*, g_*Neurospora*, g_*Pestalotiopsis*, g_*Phacidium*, g_*Podospora*, g_*Stereum*, g_*Terana*, g_*Tetracladium*
			√	3	g_*Kodamaea*, g_*Lentinus*. g_*Wallemia*

APPENDIX II: SCIENTIFIC PRODUCTION

PAPERS WITH IF * equally contribution

PUBLISHED

Candotto Carniel F*, Gerdol M*, Montagner A, **Banchi E**, De Moro G, Manfrin C, Muggia L, Pallavicini A, Tretiach M. (2016) New features of desiccation tolerance in the lichen photobiont *Trebouxia gelatinosa* are revealed by a transcriptomic approach. *Plant Molecular Biology* 91(3): 319-339.

UNDER REVIEW

Banchi E, Ametrano CG, Stankovic D, Verardo P, Moretti O, Gabrielli F, Lazzarin S, Borney MF, Tretiach M, Pallavicini A, Muggia L. DNA metabarcoding uncovers fungal diversity of airborne samples (under review in *PLoS ONE*).

Banchi E, Candotto Carniel F, Montagner A, Petruzzellis F, Giarola V, Bartels D, Pallavicini A, Tretiach M. Relation between water status and desiccation-affected genes in the lichen photobiont *Trebouxia gelatinosa* (under review in *Plant Physiology and Biochemistry*).

Banchi E, Stankovic D, Fernàndez-Mendoza F, Gionechetti F, Pallavicini A, Muggia L. ITS2 metabarcoding analysis complements data of lichen mycobiomes (under review in *Mycological Progress*).

Montagner A*, **Banchi E***, Candotto Carniel F, Bosi S, Martìn C, Pallavicini A, Vázquez E, Tretiach M, Prato M. Effects of Graphene-Based Materials on the aeroterrestrial microalga *Trebouxia gelatinosa*: focus on internalization and oxidative stress (under review in *Environmetal Microbiology*).

REFEREED PROCEEDINGS AND OTHER PUBLICATIONS

Banchi E, Stankovic D, Fernàndez-Mendoza F, Pallavicini A, Muggia L. (2017) ITS2 metabarcoding analysis complements data of lichen mycobiomes. Lichen Genomics Workshop II. *Fritschiana (Graz)* 85: 10-11 ISSN 1024-0306.

Banchi E, Montagner A, Bertuzzi S, Candotto Carniel F, Gerdol M, Muggia L, Pallavicini A, Tretiach M. (2017) Relation between water status and desiccation affected genes in the lichen photobiont *Trebouxia gelatinosa*. *Notiziario della Società Lichenologica Italiana* 30: 35 ISSN 1121-9165.

Banchi E and Borsato V. (2017) Nuova segnalazione per l'Italia Nord-Orientale (Foresta del Cansiglio, Veneto, NE-Italia) di *Campanula bertolae* tramite la tecnica del DNA barcoding. *Lavori della Società Veneziana di Scienze Naturali* 42-2017: 131-133 ISSN 0392-9450.

Banchi E, Stankovic D, Fernàndez-Mendoza F, Pallavicini A, Muggia L. (2016) Intrathalline diversity of lichen-inhabiting fungi assessed by metabarcoding of ITS region. *Notiziario della Società Lichenologica Italiana* 29: 25 ISSN 1121-9165.

Banchi E. (2016) Intrathalline diversity of lichen-inhabiting fungi assessed by metabarcoding analysis. *Notiziario della Società Lichenologica Italiana* 29: 152-156 ISSN 1121-9165.

Banchi E and Montagner A. (2016) Lichens and the "omics". *Notiziario della Società Lichenologica Italiana* 29: 66-75 ISSN 1121-9165.

Banchi E, Gerdol M, Montagner A, Candotto Carniel F, Muggia L, Pallavicini A, Tretiach M. (2015) The desiccation-related proteins in *Trebouxia*: a family to discover. *Notiziario della Società Lichenologica Italiana* 28: 34 ISSN 1121-9165.

FUNDED PROJECTS

Muggia L, Pallavicini A, **Banchi E**, Ametrano CG, Stankovic D, Ongaro S, Tordoni E, Tretiach M. (2017-2018) Finanziamento di Ateneo per la Ricerca Scientifica (FRA - UNITS) "Development of DNA metabarcoding for the characterization of aerobiological samples".

GRANTS AND AWARDS

- Ph.D. scholarship funded by Italian Government with "Fondo Trieste"
- Travel Grant for International Association of Lichenology Symposium 2016 Helsinki, Finland
- International "Gaggi Award" for the best Ph.D. thesis offered by Italian Lichen Society (2016)